SORPTION STUDIES

OF CAESIUM

BY COMPLEX HEXACYANOFERRATES

by

DAVID LOUIS JACOBI

Thesis submitted for the degree of
Doctor of Philosophy
(University of London)
and
The Diploma of Imperial College

Nuclear Technology Group
Department of Chemical Engineering
Imperial College
London SW7 2BY

August 1991

ABSTRACT

The research contract was part of a larger work programme at UKAEA, Harwell for the treatment of radioactive waste and was sponsored by the Department of the Environment. The work was primarily concerned with the removal of caesium by sorption with complex hexacyanoferrates which are known to be highly selective for caesium in high salt content solutions. Inorganic ion exchange materials are of special interest in the nuclear industry due to their excellent radiation and thermal stability and general suitability for long term immobilisation and storage.

A comprehensive literature review was carried out on the preparation of complex hexacyanoferrates in a granular form suitable for use in a packed column. The nickel complex in particular has been found to have exceptionally good sorption properties compared to the use of other transition metals such as copper, cobalt, zinc and titanium.

The preparation of sodium nickel hexacyanoferrate using a freeze-thaw method was studied in detail and a method developed to produce a consistent and reproducible granular product. The chemical and physical stability of the products was assessed over a wide range of experimental conditions.

The equilibrium and sorption kinetics were studied using a series of batch and column tests, and the process modelled to predict performance under various conditions. It was found that the caesium could be removed down to very low levels with an extremely favourable adsorption isotherm. Mathematical models were developed and found to fit the experimental breakthrough curves enabling the effect of various parameters to be predicted with some precision.

ACKNOWLEDGEMENTS

The major part of the work described in this thesis was carried out in the Nuclear Technology Group of the Department of Chemical Engineering and Chemical Technology at Imperial College, London, under the supervision of Dr. M. Streat(now Professor at Loughborough University of Technology). Part of the work was also carried out in the Chemistry Division of AEA Technology, Harwell, under the direct supervision of Mr. E. W. Hooper.

I am especially indebted to both Professor M. Streat and Mr. E. W. Hooper for their invaluable help, advice, and many suggestions during the course of the work.

Funding for this research was provided by Her Majesty's Inspectorate of Pollution and their support is gratefully acknowledged.

I would like to thank Dr. D. White and Dr. P. Clay, along with the other members of the Nuclear Technology Group, for the many discussions and assistance during the work, and especially the friendly atmosphere always present within the group. My thanks also to Mr. M Dix and Mr. R. Wood for the design and construction of the controlled freezer unit.

My sincere thanks also to my parents who have always given me wonderful support and encouragement throughout my studies, and also, along with my sister Margaret, for their great help in enabling me to complete this thesis.

TABLE OF CONTENTS

	Abstract	1
	Acknowledgements	2
	Table of Contents	3
	List of Figures	8
	List of Tables	10
1.	**Introduction**	
1.1	The Nuclear Industry worldwide and in the UK	12
1.2	Radioactive waste in the nuclear industry	14
	1.2.1 The sources and classification of radioactive waste	14
	1.2.2 The treatment of radioactive waste and discharge requirements	17
1.3	The treatment of medium (MA) and low active (LA) liquid effluents	18
	1.3.1 Methods used in the treatment of MA and LA liquid effluents	18
	1.3.2 Commercial processes for the treatment of liquid effluents	20
1.4	The use of inorganic ion exchange for the treatment of liquid effluents	21
	1.4.1 The development of inorganic ion exchangers	21
	1.4.2 Types of inorganic ion exchangers	23
	1.4.3 The removal of caesium by inorganic exchange	26
2.	**Review of the literature on the preparation of complex hexacyanoferrates in a granular form for the removal of radiocaesium from waste streams**	
2.1	The required criteria for granular hexacyanoferrates	30
2.2	General assessment of hexacyanoferrates	31
	2.2.1 General review	31
	2.2.2 General preparation	32
2.3	Granulation methods	32
	2.3.1 Gel method	32
	2.3.2 Freeze-thaw method	32
	2.3.3 Supported hexacyanoferrates	33

2.3.4 Use of binding materials 34
2.3.5 Sol-gel method 34
2.3.6 Slow growth 35
2.4 Review of granular metal hexacyanoferrates 36
2.4.1 Chromium 36
2.4.2 Cobalt 37
2.4.3 Copper 40
2.4.4 Nickel 42
2.4.5 Tin (IV) 45
2.4.6 Titanium 46
2.4.7 Zinc 48
2.4.8 Zirconium 51
2.5 Conclusions from survey 53

3 The Preparation of sodium nickel hexacyanoferrate (NaNiHCF)

3.1 Selection of preparative method 55
3.2 Preparative methods 56
3.1.1 Precipitation 56
3.2.2 Heating precipitate in the mother liquor 56
3.2.3 Washing 56
3.2.4 Freezing and thawing 57
3.2.5 Filtration 57
3.2.6 Drying 57
3.2.7 Measurement of yield and particle size distribution 57
3.3 Preliminary preparations 58
3.3.1 Experimental 58
3.3.2 Discussion 63
3.4 Investigation of Ni:Fe ratio in the preparation of NaNiHCF 63
3.4.1 Experimental 63
3.4.2 Discussion 64
3.5 Effect of heating and washing freshly formed precipitates of NaNiHCF 70

3.5.1 Experimental 70

3.5.2 Discussion 71

3.6 Investigation of the freeze-thaw method 75

3.6.1 Initial assessment of the freeze-thaw method 75

3.6.2 Fundamental aspects of the freeze-thaw method 77

3.6.3 Set-up of controlled freezer unit 83

3.6.4 Results from controlled preparations 87

3.6.5 Discussion 99

4. **Characterisation of prepared samples of nickel hexacyanoferrate**

4.1 General chemical stability of the hexacyanoferrate complex 100

4.2 Conditioning of NaNiHCF and KNiHCF at various pH 101

4.2.1 Experimental 101

4.2.2 Discussion 101

4.3 Mechanical strength of prepared granules of NaNiHCF and KNiHCF 103

4.4 Chemical analysis 104

4.4.1 Chemical decomposition 104

4.4.2 Experimental 104

4.4.3 Analysis of solutions 104

4.4.4 Discussion 105

4.5 Measurement of surface area 109

4.6 Measurement of pore size distribution by mercury porosimetry 112

4.7 Use of electron microscope to observe granular samples 116

5. **The sorption of caesium by granular NiHCFs**

5.1 Introduction 119

5.2 The assessment of sorption properties 119

5.2.1 Percentage removal and distribution coefficient 119

5.2.2 Sorption capacity and uptake 120

5.2.3 Sorption isotherm 121

5.3 Use of caesium-134 tracer and counting equipment 123

5.4 The removal of trace levels of caesium 124

5.4.1 Preliminary tests 124

5.4.2 Effect of pH, particle size and drying temperature on caesium sorption 125

5.5 The uptake of caesium and determination of the sorption isotherm 127

5.5.1 Caesium uptake tests 127

5.5.2 Determination of the caesium adsorption isotherm 131

5.6 Removal of a variety of radionuclides from a simulated waste effluent 134

5.6.1 Set-up of batch tests 134

5.6.2 Results 135

5.6.3 Discussion 143

6 The Performance of NaNiHCF in a packed column and the prediction of breakthrough curves

6.1 Introduction 146

6.2 Experimental methods 146

6.2.1 Column set-up 146

6.2.2 Set-up of counting equipment for analysis of the column effluent 147

6.2.3 Calculation of working capacity 151

6.2.4 Determination of bed voidage 151

6.2.5 Prediction of mass transfer mechanism 151

6.3 Prediction of column performance 153

6.3.1 The development of a suitable model 153

6.3.2 Numerical solution with a Freundlich type isotherm 156

6.3.3 Analytical solution with an assumed rectangular isotherm 160

6.4 Results 164

6.5 Discussion 177

7 Conclusions 179

8 Recommendations for future work 181

9 **Nomenclature** 182

10 **References** 184

Appendix A - Listing of BBC Basic program for controlled freezer unit 197

Appendix B - Listing of Fortran program 'Freund' 202

Appendix C - Paper 205
Sorption of caesium by sodium nickel hexacyanoferrate(II):
column performance and prediction of breakthrough curves
Jacobi, D. L. and Streat, M.
I. Chem. E. Symp. Series No 119 (Extraction '90) 107-118, 1990

LIST OF FIGURES

Figure 1.1	Classification of inorganic ion exchange materials	24
Figure 3.1	Sieve analyses of NaNiHCF samples from batches 20 P and 21P	61
Figure 3.2	Sieve analyses of KNiHCF samples from batches 20 P and 21P	62
Figure 3.3	Ni:Fe ratio of the products against Ni:Fe ratio of the reactants	68
Figure 3.4	Product yield against Ni:Fe ratio of the product	69
Figure 3.5	An ideal cooling curve for a pure liquid	78
Figure 3.6	A less ideal cooling curve for a pure liquid	79
Figure 3.7	Design of controlled freezer unit	84
Figure 3.8	Aluminium casing for 50 mL centrifuge tube (channels 1&2)	85
Figure 3.9	Aluminium casing for 150 mL plastic bottle (channels 3 &4)	86
Figure 3.10	Sieve analyses of samples to show the reproducibilty of granulation	89
Figure 3.11	Sieve analyses of samples to show the effect of insulation on granulation	90
Figure 3.12	Sieve analyses of samples to check complete freezing	91
Figure 3.13	Cooling curves for NaNiHCF-NJ9 A2 (−10 °C with insulation)	92
Figure 3.14	Cooling curves for NaNiHCF-NJ9 A3 (−8 °C with no insulation)	93
Figure 3.15	Sieve analyses of samples NJ9 A2 and NJ9 A3	94
Figure 3.16	Cooling curves for NaNiHCF-NJ9 B1 (− 10°C with insulation)	95
Figure 3.17	Cooling curves for NaNiHCF-NJ9 B2 (− 10°C with no insulation)	96
Figure 3.18	Cooling curves for NaNiHCF-NJ9 B3, (− 7 °C with insulation)	97
Figure 3.19	Sieve analyses of samples NaNiHCF-NJ9-B1,-NJ9-B2 and -NJ9-B3	98
Figure 4.1	Measured isotherm plot for NaNiHCF-NJ7 B1	110
Figure 4.2	BET plot from measured isotherm plot	110
Figure 4.3	Cumulative pore volume from mercury penetration method for samples of NaNiHCF-NJ3 A1	114
Figure 4.4	Cumulative pore volumes from mercury penetration method for samples of NaNiHCF-NJ9 B2	115
Figure 4.5	Picture of sample NaNiHCF-NJ3 A1 at magnification × 50	117
Figure 4.6	Picture of sample NaNiHCF-NJ7 B1 at magnification × 50	117

Figure 4.7	Picture of sample NaNiHCF-NJ3 A1 at magnification × 2000	118
Figure 4.8	Picture of sample NaNiHCF-NJ7 B1 at magnification × 2000	118
Figure 5.1	Uptake of caesium onto NaNiHCF-NJ3 A3	129
Figure 5.2	Uptake of caesium onto NaNiHCF-NJ5 A1	130
Figure 5.3	Adsorption isotherm for NaNiHCF - NJ3 A1	132
Figure 5.4	Adsorption isotherm for NaNiHCF - NJ5 A2	133
Figure 5.5	Sorption from simulated waste solution, Cs-134 removal	138
Figure 5.6	Sorption from simulated waste solution, Sr-85 removal	139
Figure 5.7	Sorption from simulated waste solution, Am-241 removal	140
Figure 5.8	Sorption from simulated waste solution, Np-237 removal	141
Figure 5.9	Sorption from simulated waste solution, Ru-106 removal	142
Figure 6.1	Column test rig	148
Figure 6.2	Arrangement of counting equipment for column tests	149
Figure 6.3	Response of the counting equipment to a step change with an empty column	150
Figure 6.4	Mesh used in the numerical solution using implicit method	157
Figure 6.5	Flow diagram of program FREUND.FOR	159
Figure 6.6	Equations used in Lotus spreadsheet to give analytical solution	163
Figure 6.7	Breakthrough curve for column test 12	166
Figure 6.8	Breakthrough curve for column test 16	167
Figure 6.9	Breakthrough curve for column test 18	168
Figure 6.10	Lotus spreadsheet to give analytical solution for column test 12	169
Figure 6.11	Printout of Fortran program FREUND numerical solution for column test 12	170
Figure 6.12	Breakthrough curves for column tests 20 and 21 (on basis of BV)	172
Figure 6.13	Breakthrough curves for column test 20 and 21 (on basis of feed volume)	173
Figure 6.14	Breakthrough curve for column test 9 Showing a restart after an interuption	174
Figure 6.15	Breakthrough curves for column tests 12 and 13 - To show the effect of feed concentration with all other parameters constant	175

LIST OF TABLES

Table 1.1	Sources of radioactive waste and main contaminants	15
Table 1.2	Liquid waste classification	16
Table 1.3	Solid waste classification	16
Table 2.1	Summary of the preparation and properties of granular hexacyanoferrates	54
Table 3.1	Preparation of NaNiHCF and KNiHCF Batches 20P and 21P	60
Table 3.2	Series B, Preparation of samples of NaNiHCF with various Ni:Fe ratios	65
Table 3.3	Release of nickel from precipitates of NaNiHCF prepared in Series B	66
Table 3.4	Details of precipitates of NaNiHCF which were repeatedly washed (Series D)	72
Table 3.5	Investigation of the effect of heating time on the release of nickel from precipitates of NiNaHCF (Series E)	73
Table 3.6	Investigatation of repeated heating and washing of NaNiHCF precipitates(Series F)	73
Table 3.7	Preliminary study of the effect of freezing time on the granulation of NaNiHCF	76
Table 4.1	Conditioning of NaNiHCF in 1 M $NaNO_3$ at various pH	102
Table 4.2	Conditioning of KNiHCF in 1 M $NaNO_3$ at various pH	102
Table 4.3	Chemical analysis of solutions from decomposition of hexacyanoferrates	106
Table 4.4	Stoichiometry of hexacyanoferrates from chemical analysis	107
Table 4.5	Comparison of Ni:Fe ratios calculated from preparation and analysis	108
Table 4.6	Characterisation from measured adsorption and desorption isotherms	111
Table 4.7	Total pore volume of samples measured by mercury porosimetry	113
Table 5.1	Effect of pH on the sorption of caesium onto NaNiHCF	126
Table 5.2	Effect of NaNiHCF particle size on the sorption of trace amounts of caesium	126
Table 5.3	Effect of KNiHCF particle size on the sorption of trace amounts of caesium	127

Table 5.4	Caesium uptake onto NaNiHCF and KNiHCF in the absence of competing ions	128
Table 5.5	Measured activity of solution from sorption tests with simulated waste	136
Table 5.6	Percentage removal of radionuclides from simulated waste	137
Table 5.7	Caesium distribution coefficients from tests with simulated waste	143
Table 6.1	Experimental details of column tests	164
Table 6.2	Details of column tests which were modelled as examples	176
Table 6.3	Parameters used to fit models	176

CHAPTER 1

INTRODUCTION

1.1 The Nuclear Industry worldwide and in the United Kingdom

The use of Nuclear Power is now well established as a means of producing electricity with over forty years of operating experience within the United Kingdom Atomic Energy Authority (UKAEA). Nuclear power is an efficient and stable source of energy with low operating costs and allows savings of valuable coal and oil reserves which may then be used as more general raw materials. Under normal operating conditions, nuclear reactors are generally environmentally clean compared to those of coal and oil which are now increasingly causing concern due to acid rain and global warming. However, the accident at Chernobyl in 1986 indicated the vast geographical area that could be affected by a major accident, and also showed the vital need for international cooperation within the nuclear industry. In addition, the problems associated with the discharge of effluents from nuclear installations and the disposal of radioactive wastes have now become key issues of public concern.

The recent state of nuclear power generation and the associated fuel cycle around the world is described in an IAEA report(1), and detailed statistics for 1990 are given in the World Nuclear Industry Handbook(2). There are presently around 500 nuclear power reactors in operation worldwide, with a further 97 under construction in July 1990. The total generating capacity is expected to grow from 400 to 500 GW(e) by the year 2005. The evolution of nuclear power is now continually influenced by the Chernobyl accident leading to a vastly increased awareness of safety, although there have been no significant changes in the acceptance of nuclear power. Those countries with major programmes are continuing their commitment, while others with strong opposition are either proceeding with slowed down programmes or have stopped further expansion.

In the UK, the role of nuclear power within the CEGB in 1988 is described by Marshall (3), with a general overview of the UK nuclear industry given in a text by Cole (4). In July 1990 there were 22 Magnox reactors and 14 Advanced gas cooled reactors (AGRs) operating in the UK with a combined capacity of 14.8 GWe(2). The Magnox reactors use a fuel of natural uranium with < 1 % fissile uranium and the AGRs a fuel enriched with 2-3 % uranium. The only reactor currently under construction in the UK is the pressurised water reactor (PWR) at Sizewell which saw a change in policy in the use of American technology. The project was controversially only given the go-ahead in 1988 after the longest public enquiry in the UK(5).

The first generation Magnox reactors, which are continuing to supply electricity after about 25 years operation, are now beginning to come to the end of their life with four units already shut down in July 1990. The problems of decommissioning and decontamination of these sites are having to be tackled with the development of appropriate technologies.

The reprocessing of nuclear fuel is currently carried out in nine countries with the largest installations in France(La Hague), America, India, Japan and in the UK. Since 1954, the Purex Process, or variants of it, have been used in all the reprocessing plants around the world. The fuel is dissolved in nitric acid and then tri-butyl phosphate (TBP) is used as a solvent, to first remove both uranium and plutonium from the fission products, and then separate the plutonium and uranium.

In the UK, reprocessing is carried out at two sites, Dounreay and Sellafield. Dounreay is operated by the UKAEA and treats 8 tonne heavy metal p.a.(tHM/y) of waste from the experimental fast breeder reactor. Sellafield is operated by British Nuclear Fuels Limited (BNFL) and has been the main reprocessing facility in the UK since 1952 when the reprocessing operations were begun. In total over 25,000 tonnes of Magnox fuel (Uranium metal) were treated in the first 30 years and present capacity is 1500 tHM/y of Magnox fuel. The fuels from LWRs and

AGRs (uranium oxide) are presently stored in pond stocks at Sellafield and will be treated by the Thermal Oxide Reprocessing plant (Thorp). This plant, detailed by Bennett(6), is now due to start up in 1992, with a capacity of 1200 tonnes/year with two thirds of this coming from abroad. The capacity is already taken up for the first ten years with fuel from the UK and imported from other countries not having their own reprocessing facilities.

It is the reprocessing operations which are responsible for most of the radioactive waste streams produced in the nuclear industry, and with which the main applications of inorganic ion exchange are required.

1.2 Radioactive waste in the Nuclear Industry

1.2.1 The sources and classification of radioactive waste

A wide variety of radioactive wastes are formed in each stage of the nuclear fuel cycle which vary widely in the amount of activity, and may be in either the solid, liquid or gas phases. The range of wastes produced is shown in the inventory of the wastes arising in the UK which was given in 1982 by Duncan and Brown(7) which listed the wastes arising from commercial power reactors, fuel reprocessing and other general uses. An outline of the liquid effluents from the nuclear industry and general methods of waste management is given by Carley-Macauley(8). A summary of the wastes produced from different operations and the main active contaminants involved are listed in Table 1.1

The wide range of wastes produced in terms of both the chemical and physical forms demands different techniques and processes for treatment and consequently the wastes are generally classified into categories according to the amount of activity and the physical state. Hooper et al.(9) give the classifications that are used by the UKAEA, which are shown in Table 1.2 for liquid wastes, and in Table 3 for solid wastes.

The bulk of the activity in wastes arises as a direct consequence of nuclear fission, as the fission products, and the effect of neutron activation on materials in

the reactor. Due to the resultant changes in the properties of the fuel and the loss in reactivity due to the build-up of the fission by-products there is a need to reprocess the fuel periodically. In addition to the uranium being reprocessed there is also a need to recover the plutonium which is a valuable by-product of fission. A detailed review of the fission products arising from different types of power reactors and the methods used for their separation from liquid effluents has been given by Kourim and Vojtech(10) and Carley-Macauley(8). The application of these methods, to low and medium active wastes is described in Section 1.3.1

Table 1.1 Sources of radioactive waste and main contaminants

Operation	Source	Main Contaminants
Uranium Processing		^{235}U, ^{238}U and decay products (Th and Pu,) very low levels
Power Reactors		Tritium Activation products of steel(^{60}Co,^{54}Mn) Fission Products escaped from fuel (^{90}Sr, ^{137}Cs), low levels,
Reprocessing		Tritium
	Fuel Dissolution	Fission products, (eg. ^{90}Sr, ^{137}Cs, ^{106}Ru, ^{95}Zr and ^{95}Nb)
	U & Pu Separation	Pu, U and Am
Pu fuel Fabrication		Pu, Am (α)

Table 1.2 Liquid waste classification

Category	Activity Ci m^{-3}
Highly Active (HA)	$> 10^3$
Medium Active (MA)	10^3 - 10^{-3}
Low Active (LA)	$< 10^{-3}$

Table 1.3 Solid waste classification

Category	$\beta\ \gamma$ Activity	α Activity
High $\alpha\beta\gamma$	$> 10^3$ mR	>25 μCi g^{-1} >20 mCi m^{-3}
Low α High $\beta\gamma$	10^3-10^{-3} mR	<25 μCi g^{-1} <20 mCi m^{-3}
High α Low $\beta\gamma$ (PCM)*	$< 10^{-3}$ mR	>25 μCi g^{-1} >20 mCi m^{-3}
Low $\alpha\beta\gamma$	$< 10^{-3}$ mR	<25 μCi g^{-1} <20 mCi m^{-3}

* PCM plutonium contaminated material.

1.2.2 The treatment of radioactive waste and discharge requirements.

Although fuel processing operations involve the use of strong acids and toxic reagents, for which the standard precautions are taken, it is the radioactive material that is unique to the nuclear industry and that requires the most stringent of precautions. The special problems that are posed by the need to dispose of radioactive wastes were already clearly recognised in the UK from the earliest developments of the nuclear industry in the 1940's. The responsibility was placed with central government in contrast to the disposal of other wastes which was placed locally.

In 1977, the responsibility was passed from the Department of Energy to the Department of the Environment (DoE) and in 1982, policies for radioactive waste management were outlined in a government white paper. In order to provide new waste disposal facilities, the main waste producers (BNFL, the UKAEA and the CEGB) set up the UK Nuclear Industry Radioactive Waste Executive (NIREX).

An outline of the strategy adopted in 1982 was given by Duncan and Brown(7) which included examples of the various treatment processes which were being developed. The options available in the UK for radioactive waste disposal in 1988 have also been given by Ginniff and Monckton(11). The techniques mentioned include those for volume reduction, decontamination, and testing the inertness and compatibility with immobilization matrices.

Radiological protection is based on the recommendations made by the International Commission on Radiological Protection (ICRP) which are accepted in most countries of the world. The recommendations include radiation dose limits for workers in the nuclear industry and for the general public. Presently the ICRP recommendsthat members of the public should not be exposed to > 5 mSv in any one year with a lifetime dose of < 1 mSv/year.

In the UK absolute limits are fixed by the Radiochemical Inspectorate of the Department of the Environment although British Nuclear Fuels Limited (BNFL) also formulates its own standards and objectives. These have been outlined by

Jones(12) and are based on the control of the collective dose to the environment and the public. In 1977 its plants have been designed such that the collective dose to the public is limited to <0.5 MSv/year. In addition to the absolute control of the collective dose, the ALARA (as low as reasonably achievable) principle is also applied in which a monetary value is placed on the dose which accounts for any expected detriment to health and relevant social factors.

In order to maintain the discharges from its Sellafield site below the required low levels which are to be permitted in the 1990's, BNFL has had to introduce new facilities. These being the Site Ion Exchange Process (SIXEP) and the Enhanced Actinide Removal Process (EARP) which are described in Section 1.3.2.

1.3 The treatment of medium (MA) and low active (LA) liquid effluents

1.3.1 Methods used in the treatment of MA and LA liquid effluents

In the treatment of radioactive liquid effluents, it is required to separate the activity from the bulk water and concentrate it into a solid form. In order to achieve these aims several methods have been adopted which are based on either physical or chemical phenomena. These methods have been outlined in the reviews by Carley-Macauley (8) and by Kourim and Vojtech (10).

Filtration is used for a variety of effluents with the filters usually backwashed to recover the activity either under gravity or by centrifugal force. Pressurised deep-bed filters are the main type usually used and in many cases as a pre-treatment before ion exchange. The use of filtration with streams at a pH > 3-4 will usually remove most of the α activity which will be in a suspended form.

Evaporation is a very effective method to concentrate activity in the absence of volatile dissolved activity such as iodine. The method is relatively expensive in both energy and equipment costs and so is generally used as a final process prior to immobilisation. High and medium active waste streams from reprocessing plants with low salt contents are generally treated by evaporation,

although the degree of concentration may be limited by precipitation of some of the salts.

Membrane processes, such as reverse osmosis, ultrafiltration or electrodialysis have been found to be suitable for the removal of ions, large molecules or suspended matter. Reverse osmosis is used for the treatment of low level effluents but is not suitable for high salt or acid wastes due to the limitations of the membrane. Ultrafiltration is particularly useful when colloidal particles already exist in the stream or have been induced by the addition of small quantities of precipitating agents. The application of ultrafiltration in the EARP process is described in section 1.3.2. The application of finely divided ion exchangers (eg. hydrous titanium oxide) as additives during ultrafiltration has been recently studied by Hooper and Cross at Harwell (13). Electrodialysis is not favoured as a method of concentration due to the complexity of the equipment, but has been used as a means of recycling valuable components such as D_3BO_3.

The use of precipitation and flocculation is now well established for a variety of waste streams containing Na, K, Mg and Ca from fuel reprocessing operations. Selective precipitation can be used to remove nearly all the actinides with further removal of α activity achieved by the addition of Fe to form ferric hydroxide. This application of flocculation is used in the EARP process at Sellafield as described in Section 1.3.2. Other materials such as Sr have been removed by co-precipitation with calcium phosphate as hydroxyapatite at pH 10 or with $BaSO_4$ at pH > 8.5. Precipitation methods for the removal of caesium include the addition of divalent ferrocyanides while ruthenium is removed by reducing compounds such as ferrous hydroxide. These precipitates are generally formed in-situ in a highly dispersed state and are therefore very effective absorbers.

The use of ion exchange processes is well suited to many waste streams as the chemical composition of active species is often very low and selective removal of the species is often required. Ion exchange could be used to remove most radioactive species but in practice it is best suited to the complete demineralisation

of low salt content streams or to the selective removal of one species in preference to the bulk species. The use of ion exchange materials for the treatment of radioactive effluents is classified as being either organic or inorganic, and as either cationic or anionic as discussed in Section 2.1. Two detailed reviews of the use of ion exchange processes in the atomic industry have been compiled by Jenkins for the period of October 1972 to April 1978(14) and the period April 1978 to April 1983(15). The reviews show the variety of ion exchange applications in the atomic energy industry and in particular give reference to use of ion exchange for actinide and fission product separation. The application of inorganic ion exchangers based on the metallic complexes of hexacyanoferrate(II) for the selective removal of caesium is the subject described in this thesis.

1.3.2 Commercial process for the treatment of LA and MA liquid effluents

As detailed in Section 1.2.2, there is an increasing need for the reduction in levels of activity in effluents which has led to the development of commercial processes for the treatment of liquid effluents. At Sellafield in particular, two processes have been developed for the treatment of liquid effluents.

The Site Ion Exchange Process (SIXEP) is used to treat the corrosion products in purge water from the cooling ponds which are used for the storage spent Magnox fuel. The background to the Process and details of the design which was completed in 1985 have been detailed by Howden(16). The sludge present in the water is removed by pressurised sand filtration and then the pH reduced before removal of caesium and strontium by ion exchange in pressurised columns. An important part of the process is the removal of magnesium in the first stage, as this would then go into solution and compete with the caesium and strontium in the ion exchange. The choice of a Californian deposit of clinoptilolite as the ion exchanger is described in a separate paper by Howden(17), and is discussed in more detail in Section. 1.4.4.

The Enhanced Actinide Removal Process (EARP) at Sellafield, which is described by Heathfield and Howden(18), is due to be completed by 1992 and will be used to treat both low and medium active streams. The plant will be required to treat 5 low active streams totalling 250 m^3/d containing 5 TBq/year of α activity, and 1000 m^3/d of medium active waste containing between 0.04 and 0.8 TBq/m^3. In the case of the MA waste, the capacity exceeds the present arising to allow for future reprocessing plants. Both the feeds result directly from the reprocessing operations which means that they are acidic streams containing nitrates and significant amounts of iron (up to 4 tonnes/year in the bulk streams). From a study of the methods outlined in Section 1.3.1, flocculation was found to be the most suitable followed by ultrafiltration to remove the floc. Sodium hydroxide is added to the acidic streams to increase the pH from 0.5 to 9.5 to form the ferric hydroxide floc. Most of the α activity is removed from the solution by coprecipitation along with the floc. This floc is then removed from the solution by ultrafiltration in which the liquor is pumped at pressure and at a relatively high velocity ($4.5\ ms^{-1}$) through a tubular membrane. After dewatering to an appropriate level, the floc can be solidified in cementitious material without further treatment.

1.4 The use of Inorganic Ion Exchange for the treatment of liquid effluents

1.4.1 The development of inorganic ion exchangers

The historical developments of ion exchange are covered in many of the standard ion exchange texts, such as those by Kunin(19), Helfferich(20), Dorfner(21), and in the text on inorganic ion exchange by Amphlett(22).

The earliest observations of ion exchange were made by Thomson and concerned the exchange of calcium and ammonium ions in soils(23). Way made the first systematic study of these phenomena and among the conclusions it was stated that the exchange involved equivalent quantities of ions and that aluminium silicates were responsible for the exchange(24).

The earliest synthetic ion exchange materials were also inorganic materials, the synthetic zeolites or permutites developed by Gans(25). Both synthetic and natural aluminium silicates were used for water softening and for the treatment of sugar solutions which constituted the first industrial use of ion exchange. Two principal types of permutites were distinguished, the fusion permutites, which were similar to natural zeolites, and gel permutites, which were prepared under closely controlled conditions to produce an irregular gel resembling silica gel in appearance. Synthetic zeolites were also extensively made by slow hydrothermal crystallisation at elevated temperatures from solutions of silica, alumina and alkali.

The early synthetic zeolites were subsequently replaced by organic resins, especially after the development of condensation resins and later emulsion polymers based on polystyrene. These materials enabled spherical beads to be produced with a well defined particle size, composition, and ion exchange properties. The ion exchange was also more rapid and the resins could be converted to acid forms in contrast to the aluminosilicates which were unstable in acids.

The organic resins, however, are unstable at high temperatures, in ionizing radiation and can be explosive in the presence of nitric acid as detailed by Calmon(26). These limitations made organic resins most unsuitable for the treatment of radioactive wastes. As a result, there was renewed interest in inorganic materials which offer the following advantages for the treatment of radioactive waste:-

a) many inorganic materials offer little or no change in chemical or physical properties when subjected to high radiation doses.
b) most inorganic exchangers are not decomposed in the presence of HNO_3 which is a component of many waste effluents from fuel reprocessing plants.
c) inorganic materials are more compatible than organic resins with matrix materials such as concrete or glass which are used for the immobilisation of nuclear waste.
d) in general, inorganic materials have a higher exchange capacity than organic materials which implies that a smaller volume of exchanger would be

required to treat the same volume of waste. In some cases the high capacity will not be of any practical use as the heating effects of the loaded nuclides would be excessive.

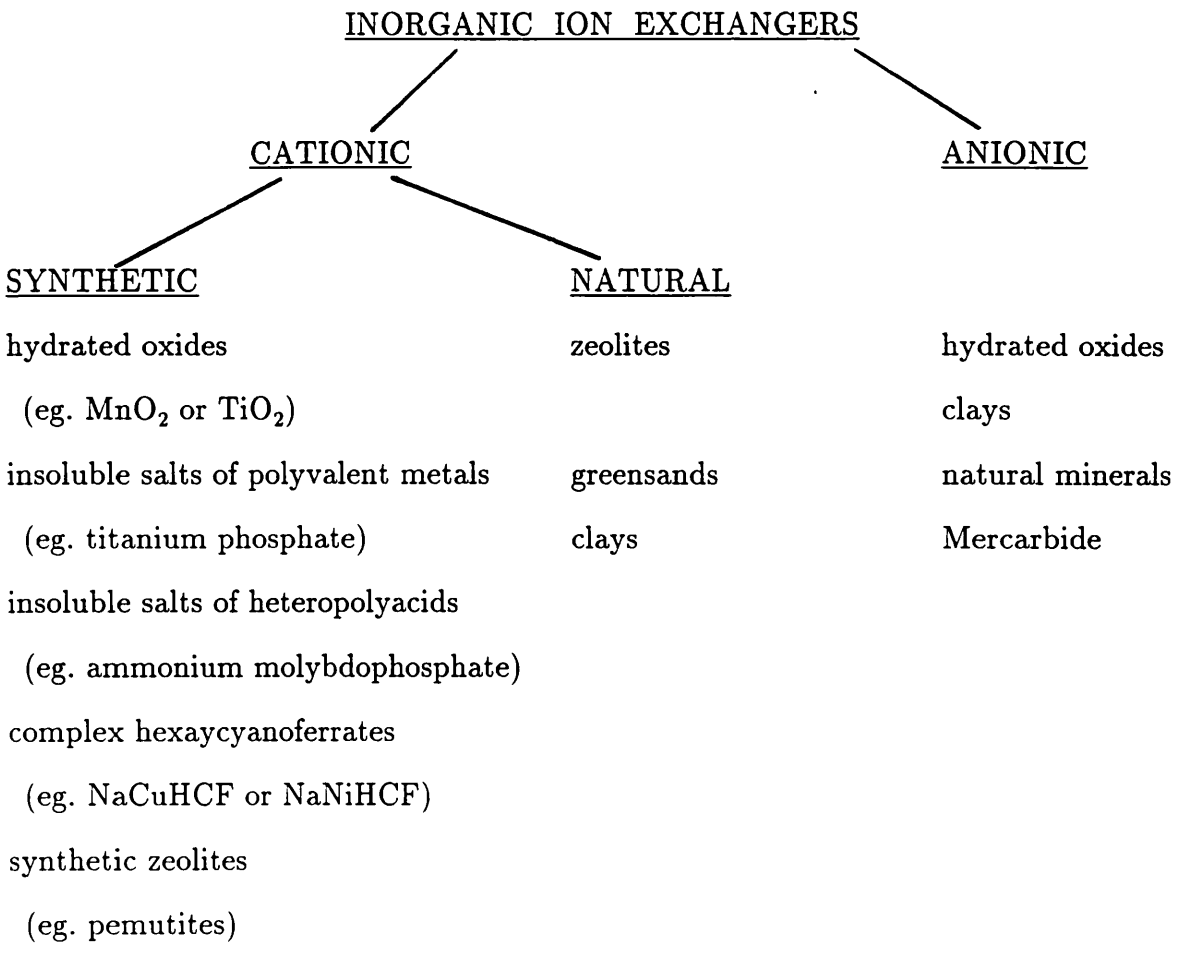
e) many inorganic materials can exhibit a high degree of selectivity for certain ions. Ion exchangers usually show the greatest affinity for ions with the highest charge or charge density, the removal of an ion from a mixture when this is not the case is possible only if a selective ion exchanger is used. This selectivity is of great importance in the present work as the main reason for studying complex hexacyanoferrates is their selectivity for caesium.

1.4.2 Types of inorganic ion exchangers

A description of the variety of inorganic ion exchange materials which have been used has been given in the text by Amphlett(22). A detailed assessment of their application to the treatment of intermediate level waste was made by Hooper et al.(9) and a review of inorganic ion exchangers for the separation of fission products from liquid wastes has been made by Kourim and Vojtech(10).

Inorganic ion exchange materials are generally classified as either anionic or cationic exchangers and then further into either synthetic or natural materials as shown in Figure 1.1. The majority of ions in waste streams which need to be removed are cations, as is the case in the present work on the removal of caesium. An initial assessment of inorganic anionic materials has been made by Dyer and Jemil(27) with particular reference to the removal of TcO_4^-, I^- and SO_4^{2-}.

Figure 1.1 Classification of inorganic ion exchange materials



The following categories of ion exchangers have been used for the removal of specific ions from various waste streams in the nuclear industry and are discussed more fully in the references mentioned above.

Clay minerals

Clay materials are composed of alternate layers of silicate tetrahedra and aluminate octahedra in a variety of arrangements. Ion exchange is due to isomorphous substitution within the layers which will show wide variations for different types of clays. Some ions, such as the alkali metals are very strongly adsorbed at room temperature but the materials are not generally used as there is a lack of reproducibility due to variations in the composition.

Zeolites

Zeolites are crystalline aluminosilicates having a layered structure enclosing cavities which occur naturally or can be synthesised. The materials can occur in several structures although zeolites with a rigid three dimensional structure are usually used as ion exchangers. The channels within the structure have a uniform dimension which means that the lattice cannot accommodate ions above a certain size.

Zeolites can show a degree of selectivity for certain ions such as mordenite and clinoptilolite which are selective for Sr^{2+} and Cs^{+}. The use of clinoptilolite in SIXEP at Sellafield is discussed in Section 1.4.4.

The use of zeolites is limited to the decontamination of only weakly acidic or alkaline solutions due to their lack of stability in stronger acidic or alkaline solutions.

Hydrous metal oxides

Much work has been carried out on the use of hydrous titanium oxide and manganese dioxide to treat nuclear effluents. Both these oxides can be prepared in a variety of forms with either a crystalline or amorphous structure. Hydrous metal oxides are generally amphoteric with the ion exchange behaviour depending on the pH of the solution. In acid solutions they act as anion exchangers and in alkaline solutions as cation exchangers.

Hydrous titanium oxide has a high capacity for most fission products, in particular ^{137}Cs, ^{106}Ru and ^{90}Sr which would make it suitable for the treatment of alkaline waste. Manganese dioxide has also been found suitable for absorbing both anions and cations, but many variations in the ion exchange properties have been observed which are probably due to variations in the composition and structure.

Insoluble salts of acids with multivalent metals

A large number of synthetic exchangers have been made of this type

including arsenates, antimonates, phosphates, molybdates vanadates and tungstates of metals such as Zr, Cr, U and Sn. The exchangers are generally made by precipitation to give either crystalline or amorphous forms with varying composition depending on the preparative conditions. It is generally found that the form of the exchanger has an important effect on the ion exchange properties.

Zirconium and titanium phosphates have both been extensively studied as ion exchange materials for the treatment of nuclear effluents. The saturation capacities of the phosphates increase with increasing pH; for zirconium phosphate the capacity in acids is ~ 0.5 meq/g and upto 5-6 in alkaline solutions. The materials also show a marked selectivity for caesium and rubidium compared to other alkali metals. The materials could be used in acidic and weak alkaline solutions, and can often be prepared from readily available and cheap materials. It is generally difficult to make granular materials for column use which have reproducible properties.

Complex hexacyanoferrates

A large number of transition and p-block metals form insoluble salts with the hexacyanoferrate complex. Many of these have good ion exchange properties for a number of cations and are particularly selective for caesium as described in Section 1.4.3. The materials have been extensively studied in both finely divided and granular forms, and are the basis for the present work.

1.4.3 The removal of caesium by inorganic ion exchange

There are 13 isotopes of caesium formed during fission of U-235 of which two are sources of hard gamma radiation with relatively long half lives that need to be removed and isolated from other fission products in waste effluents. These isotopes are ^{134}Cs with a half life of 2.02 years and ^{137}Cs with a half life of 30 years. From the earliest developments in the nuclear industry, the significance of removing these isotopes, especially the ^{137}Cs, has been realised and considerable effort made

to develop suitable methods.

The first large scale removal of caesium from waste effluents did not involve ion exchange and was achieved by the co-crystallisation of caesium with aluminium sulphate. The process, which was developed at Oak Ridge in the late 1940s, was used for slightly acidic wastes and was well proven despite its relative complexity.

For the removal and isolation of caesium on a large scale, the advantages of using ion exchange were soon realised and in particular the use of inorganic materials due to their advantages which have been given in Section 1.4.1. The use of ion exchange is relatively simple in terms of equipment and could be used to remove caesium with a high degree of selectivity.

A wide variety of materials have been developed for the removal of caesium, many of which have been mentioned in the summaries by Kourim and Vojtech(10), and Jenkins(14,15). Depending on the materials which are used, the caesium may be retained on the materials and directly immobilised, or the caesium eluted and further processed in a second stream. Few of the materials developed have been used in large scale operations.

Synthetic aluminosilicates have been used for the removal of caesium from alkaline wastes as they have sufficient capacity and selectivity, and the caesium can be easily eluted. The use of these materials is limited to only slightly acidic or slightly alkaline materials. Caesium was removed from alkaline solutions at Hanford using beds of aluminosilicates with decontamination factors of caesium from sodium of over 300 obtained. The loaded beds were transported to Oak Ridge where the caesium were eluted using ammonium nitrate solution, and then the beds returned for reuse(10).

The natural aluminosilicate mineral clinoptilolite was chosen by BNFL for selective removal of caesium and strontium in SIXEP at Sellafield as described in Section 1.3.2. A material was required with a high selectivity at low caesium and strontium concentrations from a liquor with a high sodium content, and with lower but significantly competitive levels of calcium and magnesium(17). In order to

avoid further processing, a non-regenerative system was to be used which precluded the use of organic materials as these would not be compatible with vitrification or encapsulation in concrete. The only materials which were found to meet these requirements were aluminosilicates either as natural zeolites or synthetic permutites. From a three year programme of work carried out by the Industrial Chemistry Group at Harwell, the performance of various materials was tested in small columns. The choice was reduced to two materials, the natural zeolite clinoptilolite and the synthetic permutite Decalso Y. Finally, taking into account the availability of the materials or production, any further development work required, geological recommendations and cost, a Californian deposit of clinoptilolite was selected. In using this material, a pH adjustment stage was used to operate the ion exchange stage at pH 8 ± 1 as leaching of the clinoptilolite occurred at pH 11 or above.

Recent work by Marrocchelli et al.(28) and Robinson et al.(29) shows that there is still considerable interest in the use of zeolites which are selective for caesium in solutions containing sodium salts. From batch and column tests it was found that the zeolite Union Carbide IE 96 had an isotherm which could be represented as a very slightly favourable Freundlich type, and could be used in alkaline solutions although the presence of sodium severely reduced the caesium adsorption(28).

The use of insoluble salts of heteropolyacids is well established for the removal of caesium from acidic waste solutions(10). Some of the methods for using ammonium molybdophosphate and zirconium phosphate in columns for the selective removal of caesium have been summarised by Amphlett(22). It was found that the molybdophosphate in particular had a high selectivity for caesium while zirconium phosphate had the advantage it could be easily eluted. With both these materials, it was found difficult to produce a stable granular form which could be used in column tests and attempts were made to mount the materials on a support of either silica gel or asbestos.

For the selective removal of caesium from high concentrations of alkali metals, the hexacyanoferrates are found to be almost unique in terms of their very high selectivity. Depending on the metal used to make the complex, there are wide variations in the sorption properties, selectivity, stability, and the extent to which the caesium can be eluted. A considerable amount of work has been carried out in the study of these materials, particularly in the development of methods to make these materials in a granular form as described in Chapter 2.

The separation of caesium from Acid Intermediate Waste-Purex solutions by sorption on inorganic ion exchangers was recently investigated by Faubel and Sameh(30). Seven ion exchange materials were studied including ammonium molybdophosphate(AMP), hydrated oxides, phosphates and hexacyanoferrates (CoHCF and NiHCF). The AMP was selected as being most suitable, showing a high selectivity for caesium in salt-free and 3.5 M $NaNO_3$ solutions, and its applicability over a broad range of pH, particularly in very strong nitric acid. The hexacyanoferrates were found to be suitable at pH 7 and pH 10, and the NiHCF had the fastest kinetics of the materials studied, and was the only material not to suffer a heavy loss in capacity with solutions of 300 g/L $NaNO_3$.

In the present work, a comprehensive survey is presented of the methods which have been used to make granular hexacyanoferrates, and the use of the nickel complex for the removal of caesium is studied in detail.

CHAPTER 2

REVIEW OF THE LITERATURE ON THE PREPARATION OF COMPLEX HEXACYANOFERRATES IN A GRANULAR FORM FOR THE REMOVAL OF RADIOCAESIUM FROM WASTE STREAMS

2.1 The required criteria for granular hexacyanoferrates

The use by the nuclear industry of complex hexacyanoferrates (HCF) for the selective removal of ^{137}Cs and ^{134}Cs from waste streams is now well established due to their excellent radiation and thermal stability. Over the last thirty years there has been considerable effort to prepare and study the HCFs of many bi, tri, and tetravalent metals, and, in particular, to produce these materials in a hard granular form suitable for column use.

The aim of the review was to survey the methods which have been used to prepare granular HCFs and compare the properties which would make them suitable for the removal of caesium from various streams. The relatively suitability of the materials requires consideration of the following criteria:-

i) solubility and stability under the expected operating conditions.

ii) caesium sorption properties - selectivity, sorption capacity and kinetics.

iii) mechanical strength of the granules.

iv) ease and reproducibility of preparation using low cost reagents

The hexacyanoferrate complex may be either the Fe(II) or Fe(III) form and for convenience these have been abbreviated. In a specific complex, HCF, or HCF(II) for greater clarity in some cases, refer to the Fe(II) form, and HCF(III) refers to the Fe(III) form. The general use of HCF or HCFs may refer to either form.

2.2 General assessment of hexacyanoferrates

2.2.1 General review

The preparation and properties of HCFs have been reviewed by Pederek and Vesely(31), Lowenschuss(32), Lee(33) and Hooper et al.(9). Loos-Neskovic et al.(34) recently carried out a detailed review of NiHCF and ZnHCF which have been found to have exceptionally strong affinities for caesium.

A study of the sorption properties and general characteristics of HCFs has been made by Vol'khin et al.(35,36). The affinities of the ammonium and alkali metal ions for various HCFs have been studied by Dolezal et al.(37,38) who compared the exchange isotherms for each case directly. Of the alkali metals, caesium was found to have the largest affinity, which has been explained by its charge density being the most compatible with the HCF lattice. The affinity of univalent ions for the complex HCF decreases with the increasing stability of the complex. Of the complexes studied manganese had the greatest affinity and zinc the least.

Bellomo(39) studied the formation of several HCFs and compiled data on the solubilities, K_{sp}, and the thermodynamic properties of the complexes. The zinc complex was found to be the least soluble, and those of manganese and cobalt the most. Hendrickson and Riel (40) compiled lists of the distribution coefficients and capacities for various HCFs from different sources. A list of caesium K_d values for several HCFs is also given by Krylov(41)

From a computer search of the more recent literature and previous work described above, it appears that 8 metal HCFs (Cr, Co, Cu, Ni, Sn(IV), Ti, Zn and Zr) are most suitable according to the criteria listed in section 2.1. Other metals which have been used to make HCFs include W, Sn(II), Mo, Cd, Mn, and V, although these have found limited use due to either a low capacity, slow exchange kinetics or limited stability (9,31-33), and are therefore not included in this review.

2.2.2 General preparation

Hexacyanoferrates are generally prepared by mixing a solution of the transition (or p block) metal salt with a solution of either $Fe(CN)_6^{4-}$ or $Fe(CN)_6^{3-}$; usually the sodium, potassium, or ammonium salt, or ferrocyanic acid. The products are generally sparingly soluble precipitates with a small particle size and may even be colloidal depending on the transition metal used, the concentration and molar ratio of the reactants, and the temperature. The precipitates may be aged, washed, filtered and dried, but rarely give a granular product. In order to improve the granular strengths of the materials, different preparative methods have been used for each transition metal. These methods, which are detailed in Section 2.3, include drying (gel method), freezing and thawing, use of a support, use of a binding material, and more recently, using a sol-gel method, or by slow growth on crystals of sodium or potassium hexacyanoferrate.

2.3 Granulation methods

2.3.1 Gel method

The reactants are mixed to form a precipitate which is then washed, filtered and dried. It was found that the concentration and molar ratio of the reactants are important factors and an excess of one of the reactants may be required(42). For some hexacyanoferrates, coagulation of the precipitate may be increased by heating and/or aging the precipitate(43). The filtration rate is usually slow and the drying conditions are found to have a significant effect on the hardness and sorption properties of the product.

2.3.2 Freeze-thaw method

Granulation of a finely divided precipitate may be achieved by freezing at a set temperature and subsequent thawing. The freeze-thaw method was developed in the 1960s by Vol'khin and co-workers (44-49) who made a series of HCFs. It was found that CuHCF and NiHCF were the most suitable for column use and

their preparation was studied in more detail.

Egorova et al.(50) found that ZrHCF prepared by the freeze-thaw method had much better mechanical properties than the gel product and they developed an optimal method for the preparation.

Sharygin et al.(51,52) studied the effect of temperature and various electrolytes on the extent of granulation achieved by this method when used to prepare zirconyl phosphate. It was generally found that the granulated products had a larger ion exchange capacity than the original gels.

2.3.3 Supported hexacyanoferrates

In order to produce a granular HCF absorber with good mechanical properties, several investigators have resorted to the use of a support. These include a charcoal for NiHCF (53), a zeolite for CuHCF (54) or silica gel for NiHCF (53-56), CoHCF (57), and ZnHCF, CuHCF, CdHCF, and FeHCF (58). An organic cation exchange resin has also been used for TiHCF (59) and an anion resin for NiHCF (30,60). Hendrickson and Riel (39), prepared granular HCFs using several of these supports and found them to be easier to prepare and provide better flow characteristics than other products made earlier by the authors.

Supported HCFs are generally made by impregnating the support sequentially with a solution of the ferrocyanide ions followed by a salt of the transition metal. The product is then washed and dried. The order of the impregnation may be reversed but may affect the final form of the exchanger. In some cases the materials have been subjected to repeated impregnation to increase the loading of the HCF.

The advantage of using a support is the ease of preparation of hard granules with a specific size determined by the size of the support. However the presence of the support usually reduces the capacity of the exchanger per unit volume (or mass). For example the silica supported CoHCF made by Terada (57) had an effective capacity of < 0.02 meq/g while the gel CoHCF made by Prout (42) had

an effective capacity of 0.5 meq/g. In contrast, Kozlova et al. (60) found that when silica gel is precipitated in the presence of a preformed precipitate of NiHCF, there is an increase in the sorption capacity compared to pure NiHCF. Dave and Indusaker(61) found that 50% silica ZnHCF made by repeated impregnation had a caesium capacity comparable with that of the gel ZnHCF, implying that the ZnHCF has twice the capacity when on the silica gel. This observed increase in capacity has been attributed to the increased surface area.

Roginskii et al.(62) used cement as a support for NiHCF. The preparation differed from the normal use of a support in that the freshly formed precipitate was added to the cement grout which was left to set to give cubes and then crushed. Very durable granules of the required size were obtained with good sorption properties.

2.3.4 Use of binding materials

The HCF is generally prepared by the gel method to obtain a granular form which is then mixed with a binding material to improve the mechanical strength of the granules. Kourim and co-workers (63,64) used organic binding materials to improve the strength of materials, notably CoHCF made by the Prout method (42). A series of polymers were tried which are insoluble in water but soluble in an organic solvent; polyvinyl alcohol was found to be the most suitable. Nott (65) recently selected the CoHCF made by this method for the sorption of caesium from the decontamination of spent organic ion exchange resins.

2.3.5 Sol-gel method

The use of a sol-gel method for the preparation of inorganic ion exchangers was first considered by Tympl and co-workers (66-68). Hard spherical particles can be made with good resistance to disintegration, peptization and abrasion, making these products very suitable for use under dynamic conditions in a packed column.

The method involves the preparation of hard spherical particles of the metal

hydroxide (hydrogel) which are then converted to the hexacyanoferrate by contact with a solution of ferrocyanide. The preparation of Zr, Ti and Sn hydrogels was investigated by Calekta and Tympl(68). Zirconyl oxychloride, titanium oxychloride or tin(IV) chloride was mixed with organic reagents and then particles, with sizes of the order 1mm, obtained in a semi-continuous gelation column. The column contained silicone oil at 95 °C into which the solutions were injected via capillaries; the particle size being dependent on the internal diameter of the capillaries. The uptake of several inorganic acids onto the hydrogel was measured as a function of the acid concentration and found to be highest on the Zr hydrogel and lowest on the Sn.

Sharygin et al.(69) describe the preparation of Zr hydrogel from an anion deficient solution of zirconyl oxychloride which was dispersed in a gelation column containing concentrated ammonia. The diameter of the particles was 0.40-1.0 mm with a crushing strength of 780 ± 160 kg/cm^2. ZrHCF was then obtained by treating the hydrogel with a hydrochloric acid solution of potassium ferrocyanide(70), and the effect of the preparative conditions on the composition, structure and sorption properties were determined. The use of an X-ray microprobe by Vizzachi et al.(71) showed that the sol-gel products possess a high degree of homogeneity.

2.3.6 Slow growth

In the search for a new preparative process to control the particle size and produce a HCF suitable for column use, Zouad et al.(72) developed a slow growth method. NiHCF and ZnHCF were prepared by slow growth on sodium or potassium ferrocyanide crystals placed in a concentrated nickel or zinc solution. The products prepared in this way are in the form of hollow spheres with a diameter related to that of the starting crystals. It was claimed to be easy to prepare particles between 0.1 and 0.5 mm, and that the yields of size > 0.2 mm reach 95 %. The products did not react with water or lithium borate solution.

A drawback of this method is the slight elution of cations from the HCF making them unsuitable for the continuous treatment of PWR circuits. However it is claimed that they are still well adapted for use with all effluents before final disposal.

2.4 Review of granular transition metal hexacyanoferrates

2.4.1 Chromium

Chromium hexacyanoferrate(II) (CrHCF) was prepared in a granular form by Malik et al.(73) using a gel method. The preparative route was optimised by studying the pH of the solutions, reactants used, drying time and the Cr:Fe ratio. The product $K_6Cr_2[Fe(CN)_6]_3.16H_2O$ had a maximum capacity of 3.65 meq/g and was obtained with a mixing ratio of Cr:Fe = 0.327 at pH 2. The reactants were heated to 80 °C, mixed and then held at this temperature for 6-8 hours during which gel formation took place. The gel was then left in the mother liquor for 48 hours, washed and dried at 90 °C. The exchanger was then converted to the hydrogen form by immersion in 1-2 M nitric or hydrochloric acid for 48 hours and then in deionised water. The product was stable in salt solutions and 1-3 M mineral acids but decomposed in alkali. The solubility was measured to be 0.0002 g Fe/L in water and 0.05 g Fe/L in acid.

Saraswat and co-workers(74-78) studied the kinetics and mechanism of uptake onto this material. Particle sizes of 100-300 mesh were used in the batch tests and 50-100 mesh in the column tests. It was found that 1 hour was sufficient for equilibration. The dependence of the Cs^+, Rb^+ and Tl^+ K_d values on pH and the concentrations of ammonium nitrate and nitric acid showed that the mechanism was normally pure ion exchange, except in the case of caesium sorption for which it was found that a mechanism other that ion exchange was involved.

CrHCF(III) was selected in preference to CoHCF by Jain et al.(79,80) for the separation and estimation of ^{137}Cs in active waste. The advantages of the CrHCF(III) were the specific sorption of only monovalent ions and that the caesium was easily eluted using 10 M nitric acid.

2.4.2 Cobalt

Prout et al.(42) prepared granular $K_2CoFe(CN)_6$ using a gel method and it was found that it was necessary to add to the HCF a 40 % excess of $Co(NO_3)_2$ to avoid a colloidal product. The granular particles were hard and physically stable in boiling concentrated nitric and hydrochloric acid but dissolved in boiling sulphuric acid. Sodium hydroxide solutions greater than 0.01 M caused peptization unless sodium nitrate was present. The material had an effective capacity of 0.5 meq/g and was used to remove 99.9 % of the ^{137}Cs from 40 000 bed volumes of waste containing 850 Bq ^{137}Cs/ml. In the batch contact tests, equilibration took 1 hour and it was demonstrated that most of the caesium was adsorbed on the surface of the granules.

The exchange of caesium and rubidium on KCoHCF made by the Prout method was studied by Nagy and Madi(81). The number of active centres was determined by the application of the Langmuir-Hückel isotherm. With a particle size of 0.15-0.25 mm, the kinetics of caesium exchange were measured as a function of temperature, and the distribution coefficients determined as function of HNO_3 and HCl concentrations.

Lehto et al.(82) also made granular CoHCF using a gel method by mixing 0.5M $K_4Fe(CN)_6$ with 0.5M $Co(NO_3)_2$ in the same Co:Fe ratio of 1.43 as Prout(42), and additionally with ratios of 1.0 and 2.0. With the ratio of Co:Fe=1.43 a product of composition $K_{1.7}Co_{1.12}Fe(CN)_6.1H_2O$ was formed after drying at 110 °C. From the stoichiometry of the ion exchange for potassium and cobalt, the product was found to be heterogeneous, consisting of two phases, $K_2[CoFe(CN)_6]$ (85-88%) and $Co[CoFe(CN)_6]$ (12-15%). The effective capacity from the batch contacts and from breakthrough curves gave the same values of 0.33-0.35 meq/g. This is only 6% of the theoretical capacity suggesting that caesium is probably absorbed as a monolayer on the surface.

Boni(83) used the Prout CoHCF for the rapid ion exchange analysis of biological and environmental samples. It was found that pretreatment was not

necessary for most of the samples and that caesium exchange was not affected by sample pH.

Kourim et al.(64) improved the mechanical stability of the Prout KCoHCF by using polyvinyl alcohol with negligible loss of the sorption properties as described in Section 2.3.4. Nott(65) recently selected this product as the caesium selective sorbent in the bench scale process for the electrodialytic decontamination of spent ion exchange resins.

Arino and Kramer(84) found that the Prout KCoHCF was not stable, showing a greenish-yellow colour in water. However, when the product was treated with cupric ions, it was found to be more chemically and physically stable. The compound, cupric-cobalt-hexacyanoferrate(CuCoHCF) was prepared by adding 20g of KCoHCF (a commercial product from BioRad Laboratory, 20-50 mesh) to 150 ml of 12% copper sulphate in 0.1 M HCl, heating the slurry at 80 °C for 30 minutes and then cooling to room temperature. The solution was then decanted and the slurry washed with water. The product was found to be stable over the temperature range 20-80 °C and inert over the pH range 1-10.

Lehto and Harjula(85) made a detailed comparison of the sorption performance of the Prout KCoHCF, the Arino KCuCoHCF, and a commercial ammonium phosphomolybdate. The caesium distribution coefficient was measured as a function of pH, sodium and potassium concentrations, and the batch factor (ratio of solution volume to exchanger mass). The ion exchange kinetics were also determined for the three grain sizes (0.007-0.14, 0.14-0.32, and 0.32-0.85 mm) and at temperatures of 20, 40, and 60 °C. For both KCoHCF and KCuCoHCF, high K_d values of 10^4-10^5 were obtained with a linear dependence on the batch factor. Neither pH nor a high salt content had a significant effect on the caesium retention for KCuCoHCF, while for KCoHCF it was reduced by a factor of ten from pH 8.5 to 12.5 when there was a high salt content. The exchange rate increased with decreasing particle size and increasing temperature, however raising the temperature also caused break-up of the particles. It was generally found that

KCoHCF had the better sorption properties but KCuCoHCF was more physically and chemically stable making it the favoured product.

Vol'khin et al. (48,49) prepared a granular product with the composition $K_{1.1}Co_{1.44}Fe(CN)_6$ using a freeze-thaw method. The product had a capacity of 0.71 meq/g but was not studied further since it was found to be inferior to the HCFs of nickel and copper.

Terada et al.(57) describe the preparation and characteristics of KCoHCF supported on silica gel and its application to the determination of ^{137}Cs in natural water. The exchanger, with 0.029 g of KCoHCF per g of exchanger, had a capacity of 0.019 meq/g which was considered large enough for caesium removal from natural water, but would limit its use for waste streams with higher levels of caesium.

Lee and Streat (86,33) compared the capacities, stability, sorption mechanism and kinetics of caesium exchange of KCoHCF and KCuHCF samples which were prepared by the authors using gel methods, and commercial products from Applied Research, Brussels, Belgium. The commercial KCoHCF was found to have poor mechanical stability in agitated solutions and also fragmented in acidic solutions. The sorption kinetics were faster with CoHCF although the caesium capacity (0.6-0.8 meq/g) was less than that of CuHCF. The exchange of caesium involved contributions from both potassium and cobalt.

Faubel and Sameh(30) studied the sorption properties of a commercial NH_4CoHCF from Formitalia Carlo Erba, Milan, Italy, and compared it with KNiHCF and other inorganic exchangers. The caesium capacity was about 0.6 meq/g in neutral and alkali (pH 12) solutions, but was significantly reduced at higher H^+ and salt concentrations.

2.4.3 Copper

Kourim et al.(64) prepared copper hexacyanoferrate(II) (CuHCF) as a stable product using a gel method. A 50 % excess of $Cu(NO_3)_2$ (assuming a product with Cu:Fe=2) was added to $K_4Fe(CN)_6$ and the reaction mixture boiled for two hours to improve coagulation. To improve the mechanical properties of the product ($0.1 - 0.5$ mm) for column use, it was impregnated with 4% polyvinyl alcohol as described in Section 2.3.4. The caesium capacity from the batch tests was 1.9 meq/g. About 60 % of the caesium could be eluted with 6 M HNO_3 which also caused some oxidation of the product to CuHCF(III).

Kawamura (87) prepared gel CuHCF in a similar way with Cu:Fe ratios of 10:1, 3:1, 2:1, 1:1 and 1:10. It was found that the slurries other than that with Cu:Fe=10:1 were finely dispersed.

Shahbandeh(43,88) examined a range of HCFs made by gel methods and selected CuHCF as the most suitable for caesium removal. An optimum preparative method was developed to give a product $Na_{0.47}Cu_{1.67}Fe(CN)_6$ which was in a suitable granular form for column use. The product had good sorption properties and a capacity of 1.35 meq/g. Bennett et al.(89) studied the X-ray diffraction patterns and Mössbauer spectra of this product before and after the incorporation of caesium. It was found that NaCuHCF has a cubic lattice structure which remains cubic as the caesium atoms enter. The isomer shift data from the Mössbauer spectroscopy suggest that the sorption mechanism is not simple ion exchange and involves a chemisorption step.

Lee and Streat studied the sorption properties(90) and ion exchange kinetics(91) of a commercial KCuHCF from Applied Research, Brussels, Belgium. The product had a composition $K_2Cu_3[Fe(CN)_6]_2.4H_2O$ with an effective caesium capacity of 2.15 meq/g and was highly selective for caesium in high salt content solutions. However the product was found to be unstable below pH 3. The properties of this product were also compared with those of a commercial KCoHCF also from Applied Research, and products made by the authors using gel

methods(86). Granular particles used in the tests were confined to the size $0.355 - 0.420$ mm. The two copper forms $Cu_2Fe(CN)_6.2.5H_2O$ and $K_2Cu_3[Fe(CN)_6]_2.4H_2O$ had the larger capacities (1.5 and 2.15 meq/g), while the sorption kinetics were faster for KCoHCF. The CuHCF products made by the authors were the most attrition resistant in agitated test solutions.

Vol'khin and co-workers (48,49) prepared a granular product with a composition $M_{0.33}Cu_{1.83}Fe(CN)_6$ ($M = K^+$ or Na^+) using a freeze-thaw method. The caesium capacity was found to be 0.33 meq/mg atom Fe (1.7 meq/g) corresponding to complete ion exchange of the alkali metal. The copper and nickel HCFs were found to be more suitable than other materials for column use and were studied in more detail(92). The capacity and distribution coefficients were measured as a function of composition and loading of the sorbent, and it was found that CuHCF was more suitable for the removal of caesium from solutions of rubidium salts.

Konecny and Calekta(56) impregnated CuHCF onto silica gel and prepared a product with a capacity of 0.24 meq/g. The product was found to be stable in 6M HNO_3 although the retention of caesium fell 30 %.

Watari et al.(93) precipitated CuHCF onto a strongly basic amine type ion exchange resin. No exchange capacity was quoted, but K_d values of 3×10^3 were obtained in $0.1 - 1$ M HNO_3 and HCl.

Kawamura and Motojima(54) used a CuHCF impregnated zeolite (molecular sieve, 13X, 60-80 mesh, Nikka Seiko Co.) for the removal of caesium from waste streams of sodium salts. The exchanger was prepared by repeated impregnation with aqueous $CuSO_4$ followed by $K_4Fe(CN)_6$. A range of other HCFs (Mn, Fe, Co, Ni and Zn) were also prepared in a similar way and those of Co and Ni found to be preferable. CuHCF-zeolite was found to have excellent stability over a range of pH 1.5-10, but its use may be limited due to the low capacity of 0.08 meq/g.

The use of CuHCF(III) for the separation of caesium has been investigated by Jain et al.(94). The exchanger was made by a gel method to give a product

$K[CuFe(CN)_6].5H_2O$ which was sieved to a mesh size of 50-100. The solubility of CuHCF(III) was measured in a range of solutions and found to be very low (<0.001 g/L). The maximum sorption capacity was 2.8 meq/g which was due to complete exchange of potassium, partial exchange of copper and additional adsorption of caesium. The exchanger was used in ^{137}Cs separations in preference to CoHCF and NiHCF from which the elution of caesium is difficult.

The characterisation of CuHCF(II) and CuHCF(III) and their use as caesium adsorbers has been described by Ganzerli Valentini et al.(95). The products were prepared using a gel method with an excess of ferrocyanide or ferricyanide ions to promote the formation of $Cu_2Fe(CN)_6.H_2O$ and $Cu_3[Fe(CN)_6]_2.14H_2O$. The products were washed with 95% ethanol and ether, and then air dried. CuHCF(III) could only be dried at room temperature as decomposition begins at 80 °C. From comparison of the isotherms, it was found that caesium adsorption was stronger on CuHCF(III) and in both cases the distribution coefficients were significantly reduced in concentrations of K^+ and NH_4^+ above 10^{-2} M. However the prepared HCF(III) lacked good mechanical properties and the possibility of loading columns with CuHCF(II) and oxidising to HCF(III) without loss of mechanical strength was suggested.

2.4.4 Nickel

Nickel hexacyanoferrate(II) (NiHCF) has a very high affinity for caesium and its use in a finely divided form is generally preferred to other HCFs (62). Its use in a packed column has been limited by the difficulty of producing it in a suitable granular form (43,47).

A detailed review of the preparation, composition and structure of NiHCF has been made by Loos-Neskovic et al.(34). Preparative methods from 26 references by various authors are listed, but there are few details on the stability of the products and extent to which they are granular. In contrast to some of the HCFs (eg. Zn), NiHCF does not appear to have a definite formula and may be

represented by the general formula $M_{2x}Ni_{2-x}Fe(CN)_6.nH_2O$, where M is an alkali metal. The range of values for x is usually 0.1-0.8 for sodium and 0.5-1.1 for potassium. No specific value for n has been found and in all cases the product has a cubic(fcc) structure.

Precipitates of NiHCF are always very finely divided particles which may even be colloidal. The colloidal character has been found to depend on the reactant ratio and decreases when the Ni:Fe ratio increases from 1.0 to 1.5 (96). The zeta potential of the precipitate was measured by Pottier and Chauvet (97) and found to be negative when Ni:Fe < 1.09.

Many authors have used a gel method in an attempt to obtain a granular product. Shabandeh compared the methods of Prout(42), Kawamura(98) and Kourim(64), and found the product to be either finely divided or a dark crystalline solid which broke up on contact with aqueous solutions. Roginskii(62) investigated the sorption properties of gel NiHCF and found that in batch tests caesium extraction was largely independent of the NiHCF composition over a wide range of pH. To prepare NiHCF in a granular form, Roginskii concluded that it was necessary to use an inert carrier of charcoal or silica gel, or to put it in cement as described in Section 2.3.3.

Products supported on silica gel have been studied by Baranovskii et al.(55), Konecny and Calekta(56) and Kozlova et al.(60,99). These were made by impregnation except for the Kozlova product which was made by precipitation of the silica gel in a slurry of the NiHCF precipitate. The details of these methods have already been given in Section 2.3.3. The capacities of the supported materials are generally less than the gel products but Kozlova and Vol'khin(60) found that with a product $KNi_{1.5}Fe(CN)_6.mSiO_2$, when 2<m<5, the rate of caesium sorption is increased even though the capacity is reduced by approximately 50 %. This was attributed to the increased surface area of the NiHCF on the silica gel.

Vol'khin and co-workers(44-48) prepared granular NiHCF using a freeze thaw method as described in Section 2.3.2. This method, in contrast to the use of

binding agents and drying gave a product suitable for use in a packed column(47). A product with the composition $Rb_{3.79}K_{0.05}Na_{0.2}Ni_{4.04}[Fe(CN)_6]_3$ was made with a caesium capacity of 1.57 meq/g (44), while a second product $K_4Ni_4[Fe(CN)_6]_3$ had a capacity of 2.16 meq/g, consisting of exchange of both the alkali metals and nickel(46). With these products, there was exchange of sodium with the other alkali metals to give $Na_6Ni[NiFe(CN)_6]_4$. The effect of various competing ions on the sorption of Rb^+ and Cs^+ has been studied and their presence generally causes a slight reduction in the capacity (45,46). NiHCF, together with CuHCF, was found to be more suitable for column use than other HCFs made using the freeze-thaw method (48,49).

Faubel and Sameh(30) compared the use of NiHCF, CoHCF, and other inorganic ion exchangers for the sorption of caesium. Two samples of KNiHCF were used in the tests, made by the authors using an organic anion exchange resin as a support, and commercial KNiHCF from Applied Research, Belgium. The retention of caesium (%) was correlated against the loading (g Cs/g exchanger) and it was found that KNiHCF was appropriate for the separation of caesium from neutral or alkaline (pH 10) solutions. Of the exchangers studied, only KNiHCF did not suffer a heavy loss of caesium capacity at higher salt loadings (300 g $NaNO_3$/L).

Loos-Neskovic and Federoff (100,101) investigated the recovery of silver from solutions, and from column tests chose NiHCF as the most suitable from a range of commercial HCFs from Applied Research. The NiHCF had the highest silver capacity (1 g Ag/g) and it was found that the silver displaced all the cations from the exchanger to give a final product $Ag_4Fe(CN)_6$. The presence of competing ions which form very insoluble HCFs, such as caesium and iron, reduced the silver capacity of the NiHCF.

Zouad et al.(72) prepared granular NiHCF by slow growth on either sodium or potassium ferrocyanide crystals placed in a concentrated nickel salt solution as described in Section 2.3.6. A sample with the composition $Ni_{1.25}Na_{1.7}Fe(CN)_6.nH_2O$

was made which gave a decontamination factor of 1000 for caesium in a column test, a working capacity of 2.04 meq/g, and a maximum capacity of 3.07 meq/g. It was found that the product could be used over a large range of pH (0-11) without any influence on caesium retention. However, $K_2Zn_2[Fe(CN)_6]_2$ made by the same slow growth method had a larger capacity and decontamination factor than the NiHCF.

A detailed study of different samples of NiHCF (and also ZnHCF), and the mechanism of caesium fixation has also been carried out by Loos-Neskovic and Federoff(102). The samples of NiHCF were obtained from Applied Research, Belgium, Alpha Inorganics,USA, and, for column tests, samples made using the slow growth method(103). The influence of the hexacyanoferrate composition and structure, retention kinetics and capacity and changes in the solid were studied by different methods - radioactive tracers, atomic absorption, infra-red spectroscopy, X-ray diffraction and potentiometric measurements. For all the NiHCF samples the composition was expressed as $M_{2x}Ni_{2-x}Fe(CN)_6.nH_2O$, as mentioned above, but it was stated that in all cases the NiHCF also contained hydrogen mixed with the alkaline metal, M. All the X-ray diffraction patterns could be indexed with a fcc structure with a mean lattice parameter of 10 Å. It was found that caesium exchange occurs with the hydrogen and alkali metals, and that at higher caesium concentrations small amounts of nickel are also released. The exchange was non-reversible and did not lead to any change in the structure of the solid.

2.4.5 Tin (IV)

The preparation of tin(IV)hexacyanoferrate(II) (SnHCF) by a gel method has been studied by Qureshi et al.(104). A product with a ratio of Sn:Fe=4.5 was found to have the highest capacity, but they preferred to use a material with the composition $(SnO_3)(OH)_3.HFe(CN)_6.3H_2O$ which was granular. The use of a gel method was also studied by Gill and Tandon(105) who found that a ratio of Sn:Fe=10.9 gave the best material in the form of hard semi-transparent granules. It was also found that the Sn:Fe ratio had little effect on the capacity. The

capacity of this material was less than that of Qureshi, but was found to be greater when used in a packed column. Both these materials were stable in nitric, sulphuric, formic and acetic acids at all concentrations, in HCl<3 M, and in 10% oxalic acid. Both materials were unstable in even dilute alkalis and Qureshi also found degradation in metal chloride solutions. Gill and Tandon found the solubility to be 0.03 g Fe/L in 6M HNO_3 and 0.02 g Fe/L in water.

Gill and Tandon found that SnHCF had a higher exchange capacity and better chemical stability than the HCFs of other quadrivalent metals(105), and also studied the stoichiometric uptake of cations onto SnHCF, ZrHCF and some other exchangers(106). It was found that the plots of $\log(K_d)$ vs. pH were linear but the slopes did not correspond to the valency of the exchanged ion, except for Cs^+ which approximated to unity suggesting that only for univalent ions was there an ion exchange mechanism. The K_d values for SnHCF were higher than those of ZrHCF by approximately a factor of ten.

Calekta and Tympl(68) prepared SnHCF using the sol-gel method by studying the uptake of $H_4Fe(CN)_6$ on $Sn(OH)_4$ hydrogel as described in Section 2.3.5. However only the sorption properties of TiHCF and ZrHCF were studied in further work.

2.4.6 Titanium

Granular samples of titanium hexacyanoferrate(II) (TiHCF) were prepared by Bastian and Lieser(107,108) using a gel method with Ti:Fe ratios varying from 1:10 to 10:1. An optimum product was made corresponding to $(TiO)_2(OH)HFe(CN)_6.4H_2O$ by mixing $H_4Fe(CN)_6$ and $TiCl_4$ in 2M HCl. It had good mechanical properties with a capacity of 1.4-1.5 meq/g and was resistant to 2M H_2SO_4, but was soluble in more concentrated acids.

The chemistry of TiHCF precipitates was discussed by Kourim(109) who found that with a ratio of Ti:Fe=2 a relatively stable compound was formed with a composition $(TiO)_2Fe(CN)_6$. It was found that 2 equivalents of caesium exchanged

with 1 equivalent of titanium which was explained by the exchange of Cs^+ with TiO^{2+}. The capacity of TiHCF was found to be 1.88 meq/g which was higher than prepared samples of ZrHCF and ThHCF.

The preparation of TiHCF by the gel method was also investigated by Narbutt and co-workers(110,110). Solutions of 0.01 or 0.1M $TiCl_4$ with various amounts of HCl (pH 0.7-1.7) were treated with given amounts of $K_4Fe(CN)_6$ to obtain a ratio of Ti:Fe=8 (110), or Ti:Fe=10 (111). The samples obtained had good sorption and mechanical properties and were used in small chromatographic columns. The properties of TiHCF were found to depend strongly on the conditions of precipitation. By changing the pH between identical samples, the Ti:Fe ratio was found to vary from 2:1 (pH<0.9) to 8:1 (pH>1.2). At pH 1.7 titanium hydrolysis is observed and hence samples with a high Ti:Fe ratio may be regarded as a mixture of TiHCF and hydrous TiO_2. A strong correlation was also found between the composition of TiHCF, affinity for caesium and solubility. Black crystalline samples, prepared at pH 1.2 and pH 1.5, had a high affinity for caesium (K_d of the order 10^5) and a low solubility. The solubility of samples with Ti:Fe ratios of 8:1 and 4:1 was small, while those with ratios of 2:1 and 1:1 were somewhat soluble in water. In column tests TiHCF was found to have a very high caesium affinity and no loss was observed due to its solubility.

In further work by Narbutt et al.(58), attempts were made to overcome the slow kinetics and relatively poor mechanical properties of the gel TiHCF by implanting TiHCF onto activated charcoal and organic polymers. Five samples were prepared in different ways and directly compared in terms of their chemical and mechanical stability, and sorption properties. A product with good mechanical strength was only obtained when a cation exchange resin was used as the support. Spherical particles of diameter $0.5 - 1.0$ mm were formed with a very low solubility and excellent sorption properties despite the exchanger only being composed of 23% TiHCF.

The preparation and properties of TiHCF made by the sol-gel method were

investigated by Caletka and Konecny(112). TiHCF(II) and TiHCF(III) were obtained by treating spherical particles of $Ti(OH)_4$ hydrogel with $H_4Fe(CN)_6$ $H_3Fe(CN)_6$ or acidified solutions of $K_4Fe(CN)_6$, as described in section 2.3.5. A series of products were made using different concentrations of either HCl or HNO_3 with $K_4Fe(CN)_6$. The caesium sorption properties were measured in batch tests and values of K_d given as a function of the phase contact time and concentrations of HCl, NH_4NO_3 and HNO_3 in the test solutions. The uptake of caesium was also measured as a function of the $Fe(CN)_6^{4-}$ content of the TiHCF samples and compared to other transition metal HCFs. The maximum uptake was 2.62 meq/g with a TiHCF sample prepared by repeated treatment of the hydrogel with 0.7M $K_4Fe(CN)_6$ in 1M HCl for 12 hours. The samples of TiHCF(II) were found to oxidise easily to the more water soluble TiHCF(III) which may limit their applicability.

The sorption of caesium onto TiHCF was also studied by Krylov et al.(113) A product $H_2[Ti(OH)_3]_2Fe(CN)_6$ was made using a gel method by mixing $TiCl_4$ and $K_4Fe(CN)_6$ in 1 M acetic acid. The precipitate was allowed to stand for 10 hours, the solution decanted, and the precipitate washed with water until the solution reached pH 3-4. The product was then air dried. The product had a caesium capacity of 301 mg/g (2.1 meq/g) and, from batch sorption tests, found to have a Langmuir adsorption isotherm.

2.4.7 Zinc

A detailed review of the preparation, composition and structure of zinc hexacyanoferrate (ZnHCF) has been made by Loos-Neskovic at al.(34). Preparative methods from 33 references are listed, but there are few details of the stability and the extent of granulation. ZnHCF has an exceptionally large affinity for caesium which may be easily eluted under suitable conditions, and its solubility is lower than other HCFs (114-116).

Zinc hexacyanoferrate(II) (ZnHCF) is usually either in the form $Zn_2Fe(CN)_6$

or $M_2Zn_3[Fe(CN)_6]_2$ (M = Na or K); the composition depending on the ratio of Zn^{2+} and $Fe(CN)_6^{4-}$ used in the preparation. These two forms differ markedly in the rate of caesium uptake; $Na_2Zn_3[Fe(CN)_6]_2$ reached equilibrium within 15 minutes, while $Zn_2Fe(CN)_6$ in batch tests took over 10 hours to reach equilibrium(32). The exchange of caesium for potassium on $K_2Zn_3Fe(CN)_6$ has been shown to be pure ion exchange(117-119) with a plot of $\log(K_d)$ vs. $\log[K^+]$ giving a line of slope -1.

ZnHCF made using gel methods gave finely divided products which were generally unsuitable for column use (32,120). Vlasselaer et al.(117,118) prepared fine particles of ZnHCF using a gel method and then mixed them with silica gel in a ratio of 1:4 to provide increased flowrates through a column.

Kourim et al.(64) succeeded in making granular particles (0.1-0.5 mm) using a gel method in which a 50% excess of zinc nitrate was used to improve coagulation of the precipitate. The reaction mixture was boiled for 2 hours and then washed with 0.3M $NaNO_3$. After slow drying over 4 hours, a product was formed which was mechanically stable on contact with water. In order to make the product suitable for column use the mechanical stability had to be improved by using 4% polyvinyl alcohol as a binder, as described in section 2.3.4. The caesium capacity of the product was found to be 6.1 meq/g. The product was used in sorption-elution cycles under dynamic conditions for separations of Cs-Rb, Rb-K and K-Na(120).

Stejskal et al.(63) used organic binding materials to improve the mechanical strength. Granules with a size 0.1-0.5 mm were made which were used in a packed column and had a capacity of 1.5 meq/g.

Vol'khin and Shulga(49,50) prepared a product with the composition $M_{0.5}Zn_{1.75}Fe(CN)_6$ (M = Na or K) using the freeze-thaw method. However, in contrast to other HCFs, ZnHCF could not be readily obtained in a granular form using this method and was found to only selectively remove caesium in the absence of high concentrations of competing ions.

Konecny and Calekta(56) impregnated ZnHCF onto silica gel as described in section 2.3.3. Several granular products were prepared with capacities ranging from 0.4 to 1.0 meq/g depending on the ZnHCF content of the exchanger. Dave and Indusaker(61) prepared $K_2Zn_3[Fe(CN)_6]_2$ by both the gel method and using silica gel as a support. Only the supported material produced hard granules. The gel ZnHCF had a caesium capacity of 2.85 meq/g while that of the 50% silica ZnHCF was 2.32 meq/g which means that the pure ZnHCF had almost twice the capacity when mounted on the support.

Ganzerli Valentini et al.(114) prepared ZnHCF(III) by oxidation of $Zn_2[Fe(CN)_6]$ in $HNO_3 > 0.2$ M and measured its caesium sorption properties. However it has increased solubility and is also attacked by concentrated HNO_3 with partial decomposition.

Zouad et a1.(72) prepared granular ZnHCF by slow growth on sodium or potassium ferrocyanide crystals placed in concentrated nickel salt solutions as described in section 2.3.6. Two forms, $K_2Zn_3[Fe(CN)_6]_2.nH_20$ and $Zn_2Fe(CN)_6.2H_20$, were prepared and both were found to have a caesium capacity of 5.5 meq/g. However only the first of these had a large decontamination factor (10^3) in a column test, and was found to be better than a material $Ni_{1.15}Na_{1.7}Fe(CN)_6$ prepared using the same slow growth method.

The structure of samples of ZnHCF (and NiHCF), and the mechanism of caesium fixation were also studied by Loos-Nescovic and Federoff(102) as detailed in Section 2.4.4. Both the mixed product $M_2Zn_3[Fe(CN)_6]_2$ (M = H, Na or K) with a rhombohedric R$\bar{3}$C structure, and the simple $Zn_2Fe(CN)_6.2H_2O$ with a triagonal structure, were studied. For the mixed ZnHCF, it was found that there was exchange of caesium with the alkali metal with very fast kinetics, whereas for the simple ZnHCF, the caesium was only incorporated into the hexacyanoferrate with a structural change and much slower kinetics.

2.4.8 Zirconium

The use of ZrHCF for the selective extraction of caesium from seawater is described by Egorova et al.(50). It was found that ZrHCF was more selective and sorbs caesium more effectively than samples of CoHCF. ZrHCF made by the gel method was found to be difficult to prepare in a granular form due to the need to wash the precipitate completely free of potassium which reduces the mechanical strength of the particles and increases their solubility in water. The precipitate also had to be dried over a long period since increasing the temperature promoted partial oxidation to HCF(III). In an attempt to produce a granulated ZrHCF lacking these shortcomings, $H_4Fe(CN)_6$ was used instead of $K_4Fe(CN)_6$ and the freeze-thaw method used for granulation. Mechanically very strong particles were obtained by mixing 0.3M $ZrOCl_2$ containing 1M HCl, with 0.15M $H_4Fe(CN)_6$ also containing 1M HCl, in a ratio of Zr:Fe=2. The coagulum was washed to pH 2.5-3 and then placed in an air-filled refrigerator at −16 deg.C for 24 hours. After thawing the particles were filtered and dried. The product was found to have reproducible caesium sorption characteristics with K_d values of $6.5 \pm 0.6 \times 10^4$ for particles of 0.25−0.5mm.

Gill and Tandon(121) made hard semi-transparent particles of ZrHCF (100-300 mesh) using the gel method. $ZrOCl_2$ was mixed with either $K_4Fe(CN)_6$ or $H_4Fe(CN)_6$ in various Fe:Zr ratios ranging from 0.40−6. The use of $Zr(NO_3)_4$ gave a product which broke up in neutral solutions.

Kawamura et al.(122) found that for the preparation of mechanically stable ZrHCF (by the gel method), it was necessary to initially dissolve $ZrOCl_2$ in 3M HCl and mix this with $Na_4Fe(CN)_6$ in a ratio of Fe:Zr = 1.25. After allowing the precipitate to stand for 24 hours before washing and drying, a granular material was obtained with the ratio Fe:Zr = 1.0. Using this method definite mesh sizes were readily obtained and were used in columns for the determination of ^{137}Cs and other nuclides in seawater.

The preparation of spherical particles of ZrHCF using a sol-gel method was

first developed by Caletka and Tympl(68). Moist spherical particles of $Zr(OH)_4$ hydrogel were treated with $Fe(CN)_6^{4-}$ ions as described in section 2.3.5.

Sharygin and co-workers studied the effect of the preparative conditions of the sol-gel ZrHCF on its properties(70), and the homogeneity of the products(71) as described in section 2.3.5. Spherical particles were obtained with diameters of 0.6–1.0 mm which were light to dark blue in colour, with a violet tinge depending on the fraction of $Fe(CN)_6^{4-}$ in the particles. The exchangers were stable in neutral and acidic solutions up to 3M, while treatment in alkaline solutions led to a complete removal of $Fe(CN)_6^{4-}$ ions from the solid. Samples of sol-gel ZrHCF and zirconium phosphate (d=0.5-0.9mm) were directly compared in column tests using 1M NaCl solutions and active sewage containing Cs^+ and Co^{2+}(120). The exchangers were found to have high mechanical strength in contrast to the weaker products made by the traditional gel method. The caesium capacity of sol-gel ZrHCF (Fe:Zr=0.28) was found to be 0.38 meq/g in 1M NaCl and 2.87 meq/g in the waste sewage.

2.5 Conclusions from survey

A summary of the preparation and properties of granular metal hexacyanoferrates is given in Table 2.1. The table provides a convenient reference to the important parameters in selecting a particular adsorbent for a specific application. The methods which have been used for each complex are indicated and the important parameters summarised. This should facilitate the selection of a particular hexacyanoferrate for a set of required conditions, although few of the materials are available in large scale commercial production.

The most well studied materials appear to be the Co, Cu, Ni and Zn complexes, which have all been prepared in granular forms by a variety of methods. Only the Co material made by the Prout method has been used to any extent in later work, although even this has been found unsuitable in some cases without further treatment. In particular, the Co and Cu complexes in a granular form have been widely used and the commercial samples well studied.

There appear to be distinct advantages in using the Ni complex compared to other HCFs, notably in terms of its sorption of caesium over a comparative wide range of pH and its selectivity for caesium in high concentrations of competing ions. This is reflected in the extent to which the Ni complex has been studied, although it appears that no granulation method has been well proven, and the granular products available have only found limited use.

Table 2.1 Summary of the Preparation and Properties of Granular Hexacyanoferrates

		Chromium	Cobalt	Copper	Nickel	Tin(IV)	Titanium	Zinc	Zirconium
form of	gel method	hard granular	granular	hard granular	finely divided	hard granular	granular	finely divided	granular
products made	freeze-thaw	NI	granular	hard granular	hard granular	NI	NI	finely divided	hard granular
using the	supported	NI	hard granular	hard granular	hard granular	NI	NI	hard granular	NI
different	use of binder	NI	hard granular	hard granular	hard granular	NI	NI	NI	NI
granulation	sol-gel	NI	NI	NI	NI	hard spherical	hard spherical	NI	hard spherical
methods	slow growth	NI	NI	NI	hollow spheres	NI	NI	hollow spheres	NI
stoichiometry of product		definite	mixture of two definite forms	variable	variable	definite	variable	definite (two forms)	definite
particle size (largest)		50-300 mesh	0.5 mm	0.5 mm	0.5-1.0 mm	NI	0.5-1.0 mm	0.1-0.5 mm	0.5-1.0 mm
caesium	Log(Kd) ml/g	4 - 5	4 - 5	3 - 4	4 - 5	NI	4 - 5	3 - 4	4 - 5
sorption properties	capacity meq/g (quoted values)	3.65	0.5 - 0.8	2.1 - 4.5	2.5 - 5.8	2.0 - 2.5	1.4 - 1.9	6.1	2.87
	mechanism	not solely ion exchange	pure ion exchange at surface	chemisorption	chemisorption	not pure ion exchange	NI	pure ion exchange	not pure ion exchange
solubility	acid	5.0 (5M HNO3)	NI	0.4 (6M HNO3)	NI	30 (6M HNO3)	low, Ti:Fe > 4	NI	2.7
ppm Fe	water	0.0	0.7 (0.012)	0.3 (0.0051)	0.6 (0.01)	15	NI	0.4 (0.076)	0.4
(mmol/l)	alkali	20 (0.1M NaOH)	NI	NI	NI	NI	NI	NI	NI
pH range of chemical stability		0 - 13	1 - 12	3 - 10	4 - 10	0 - 11	0 - 11	0 - 11	0 - 11
mechanical strength		good	good	good	good	good	very good	moderate	very good
cost of transition metal		moderate	moderate-high	low	moderate	high	low	low	high
order of decreasing toxicity of trans. metal compounds		1 (0.05 ppm)	3 (NI)	4 (1.0-1.5 ppm)	2 (0.05 ppm)	8 (NI)	7 (NI)	5 (5-15 ppm)	6 (NI)
elution		100% with 10M nitric acid	97% with 6M nitric acid	70% with 6M nitric acid	very difficult	NI	NI	>99% with 6M nitric acid	NI
mention of HCF(III) in survey		yes	no	yes	no	no	yes	yes	no
comments		easily eluted, CrHCF(III) is selective for monovalent ions.	found use in several small scale applications	good product obtained using gel method	best freeze-thaw product; best for Cs sorption when finely divided	found to be better than other quadrivalent materials	recently used to remove Cs from PWR cooling water	slow growth product better than that of nickel	used for Cs removal from sea water and power station waste sludge

NI = not investigated

CHAPTER 3

THE PREPARATION OF SODIUM NICKEL HEXACYANOFERRATE IN A GRANULAR FORM

3.1 Selection of preparative method

Nickel hexacyanoferrates are formed by precipitation on mixing a nickel salt with a ferrocyanide solution. The ratio of nickel to ferrocyanide (Ni:Fe) may be varied, and for the reaction between nickel sulphate and sodium hexacyanoferrate may be represented by the following general equation:-

$$(2\text{-}x)\ Ni(SO_4)_2 + Na_4Fe(CN)_6 \rightarrow Na_{2x}Ni_{2-x}Fe(CN)_6 + (2\text{-}x)Na_2SO_4 \qquad (3.1)$$

The various methods which have been used to granulate precipitates of NiHCF have been outlined in Section 2.4.4. One of the methods which appeared to be promising was the freeze-thaw method used by Vol'khin and co-workers(46). It was stated that this method, as opposed to the addition of binding agents and drying, was the only way that gave a granular product which would meet the requirements of column chromatography. Potassium ferrocyanide was mixed with nickel nitrate to give $K_4Ni_4[Fe(CN)_6]_3$, which is formed as a finely divided precipitate, and aqueous potassium nitrate according to the reaction (3.2).

$$4\ Ni(NO_3)_2 + 3\ K_4Fe(CN)_6 \rightarrow K_4Ni_4[Fe(CN)_6]_3 + 8\ KNO_3 \qquad (3.2)$$

The precipitate was washed and then frozen at a temperature not below $-10^{\circ}C$. The freezing and thawing was found to compact the precipitate into a granular form which could be easily filtered, and then after drying gave a product suitable for column use.

In some preliminary preparations, this method was initially assessed and certain aspects of the preparation identified for further study.

3.2 Preparative methods

3.2.1 Precipitation

In all of the preparations, the following concentrations were used for precipitation of the complex:-

The nickel salt, $NiSO_4$ or $Ni(NO_3)_2$ - 0.3 M

The ferrocyanide, $Na_4Fe(CN)_6$ or $K_4Fe(CN)_6$ - 0.5 M.

The volume of the reagents were selected to give a specified ratio of nickel to ferrocyanide (Ni:Fe ratio), and to give the quantity of product that was required. In the preliminary preparations a ratio of Ni:Fe=1.33 was used. After the investigation of this ratio described in Section 3.4, a ratio of Ni:Fe = 1.3 was selected, and then used in all the subsequent preparations.

With the concentration of the reagents used for the precipitation, the reaction liquor will contain approximately either 0.4 M of the alkali metal nitrate or 0.2 M of the sulphate.

The reactants were mixed either in small centrifuge tubes, or for the larger preparations, in 1 L centrifuge bottles, which allowed direct centrifuging of the reaction mixture. In all cases the addition was made instantaneously, and the order of mixing or addition of one of the reagents over a period of time were not investigated.

3.2.2 Heating of the precipitate in the mother liquor

In some of the preparations the precipitate was heated in the mother liquor. This was achieved by placing the reaction mixture in a water bath, which was generally set to 80 °C for a fixed period of time.

3.2.3 Washing

Samples were washed by centrifuging the reaction mixture, decanting the supernate, and replacing it with a set volume of the wash liquor. The mixture was

agitated by hand until it appeared homogeneous, and then the procedure repeated if required.

3.2.4 Freezing and thawing

Samples of the nickel hexacyanoferrate were initially frozen in the freezer compartment of a domestic fridge, which was set at −8 °C, and also using a domestic chest freezer, which was set at −18 °C. In order to study the freezing process in more detail, a controlled freezer unit was constructed as described in Section 3.6.3.

In all cases the samples were allowed to thaw at room temperature. The thawing conditions were not varied as it was not thought to affect the granulation.

3.2.5 Filtration

The samples were filtered using a Buchner funnel under vacuum. The time required for the filtration was found to be greatly reduced after freezing and thawing the mixture under the correct conditions, and was used as a parameter in the investigation of the freeze-thaw method. The volume of the filtrate was measured and when required analysed for nickel.

3.2.6 Drying

After filtration, the samples were left to dry at room temperature, or on a warm surface (30-40 °C) for several hours after which they could be easily removed from the filter paper. The samples were then dried at 110 °C for 4 hours. Some of the samples were additionally dried at 170 °C to investigate whether this improved the granular form or the sorption properties.

3.2.7 Measurement of yield and particle size distribution

The product yields were measured by direct weighing and were compared to theoretical yields based on some assumptions in the preparation. The particle size

distribution was measured using small sieves which were shaken by hand. In order to compare the size distribution of different samples, the particle diameter d_p was plotted against the cumulative mass % < d_p.

3.3 Preliminary preparations

3.3.1 Experimental

The feasibility of using the freeze-thaw method was initially assessed with some preliminary preparations of KNiHCF and NaNiHCF. 26 mL of 0.3 M $Ni(NO_3)_2$ was mixed with 12 mL of 0.5 M $K_4Fe(CN)_6$ to form a precipitate according to Reaction 3.2. Samples of NaNiHCF were prepared in the same way except that $Na_4Fe(CN)_6$ was used in place of $K_4Fe(CN)_6$. In some cases $NiSO_4$ was used in place of the $Ni(NO_3)_2$ to check if any differences were observed. In some of the preparations, the precipitates were heated in the mother liquor.

The precipitates were subsequently washed, frozen and thawed, filtered and dried to give the product. For different samples, the conditions used in each of these stages were varied to initially find the best methods to give a granular product. The effect of various ions in solution on the precipitate was initially investigated by washing with the following solutions:-

1) Distilled water
2) Potassium nitrate was used with KNiHCF, and sodium nitrate with NaNiHCF. Solutions with concentrations of 0.01 M, 0.1 M, 1 M, and 4M were used in different batches.
3) Nickel nitrate solutions with concentrations 0.01 M and 0.1 M.

It was found that when distilled water was used the mixture could not be separated in a centrifuge, indicating that the sample had become very finely divided. There was no change in the appearance of the product when the washing was with nickel nitrate, or either sodium or potassium nitrate. A more consistent product was made when the more dilute solutions were used in the washing, but a small salt content was found necessary to prevent the precipitate becoming finely

divided.

The appearance, consistency, and possible breakup of these preliminary products in aqueous solutions were observed. The better granular products were also contacted with trace levels of caesium in simple batch tests and the percentage caesium removal and the distribution coefficients (K_d) after a contact time of 24 hours were determined as described in Section 5.3.

From these preliminary preparations, a method was found which appeared to give a consistent granular product:-

1. 0.5 M of sodium or potassium ferrocyanide was mixed with 0.3 M of either nickel sulphate or nickel nitrate in the molar ratio of Ni:Fe = 1.33
2. The precipitate was washed three times with 0.01 M sodium or potassium nitrate in a batch manner with the liquor being separated by centrifuging.
3. The mixture was frozen at −8 °C in the freezer compartment of a domestic fridge for a period of over 20 hours during which the colour is seen to darken.
4. The sample was then thawed at room temperature and the product filtered in a Buchner Funnel.
5. The product is dried on a warm surface (30-40 °C) until the sample becomes dark brown and can be removed from the filter paper. It is then dried at 110°C for 4 hours.

Two larger batches (P20 and P21) were made of both NaNiHCF and KNiHCF using this method. The preparation of these materials is detailed in Table 3.1 and the sieve analyses given in Figures 3.1 and 3.2. These products were used as a benchmark for comparison with the subsequent preparations.

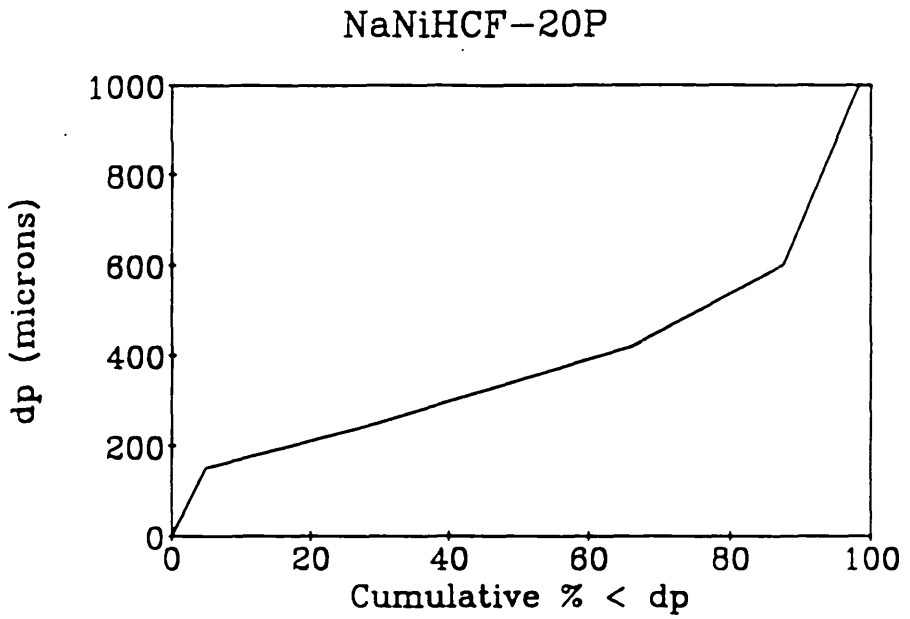
Table 3.1 Preparation of NaNiHCF and KNiHCF batches 20P and 21 P

	NaNiHCF				KNiHCF			
	20P		21P		21P		21P	
Reactants	120 mL 0.5M $Na_4Fe(CN)_6$ 226.8mL 0.3M $Ni(NO_3)_2$		225 mL 0.5M $Na_4Fe(CN)_6$ 500 mL 0.3M $NiSO_4$		120 mL 0.5M $K_4Fe(CN)_6$ 266.8 mL0.3M $Ni(NO_3)_2$		450 mL 0.5M $K_4Fe(CN)_6$ 1000 mL 0.3 M $NiSO_4$	
Particle size (microns)	mass (g)	%	mass (g)	%	mass (g)	%	mass (g)	%
< 90	1.19	4.9	0.75	1.9	1.87	7.8	2.63	3.0
90 - 250	6.12	25.0	2.95	7.4	6.26	26.2	12.67	14.6
250 - 420	8.85	36.2	6.29	15.7	7.38	30.8	18.15	21.0
420 - 600	5.29	21.6	9.37	23.4	5.39	22.5	16.19	18.7
600 - 1000	2.58	10.5	17.65	44.2	2.66	11.1	31.49	36.4
> 1000	0.44	1.8	2.96	7.4	0.37	1.6	5.42	6.3
Total mass	24.47	100	39.97	100	23.93	100	86.55	100
	g	%*	g	%*	g	%*	g	%*
Theoretical yield (assuming $M_4Ni_4[Fe(CN)_6]_3$)	19.25	127.1	36.09	110.8	20.52	116.3	77.01	112.4

M = Na or K

* percentage of theoretical yield

Figure 3.1 Sieve analyses of NaNiHCF samples from batches 20 P and 21P



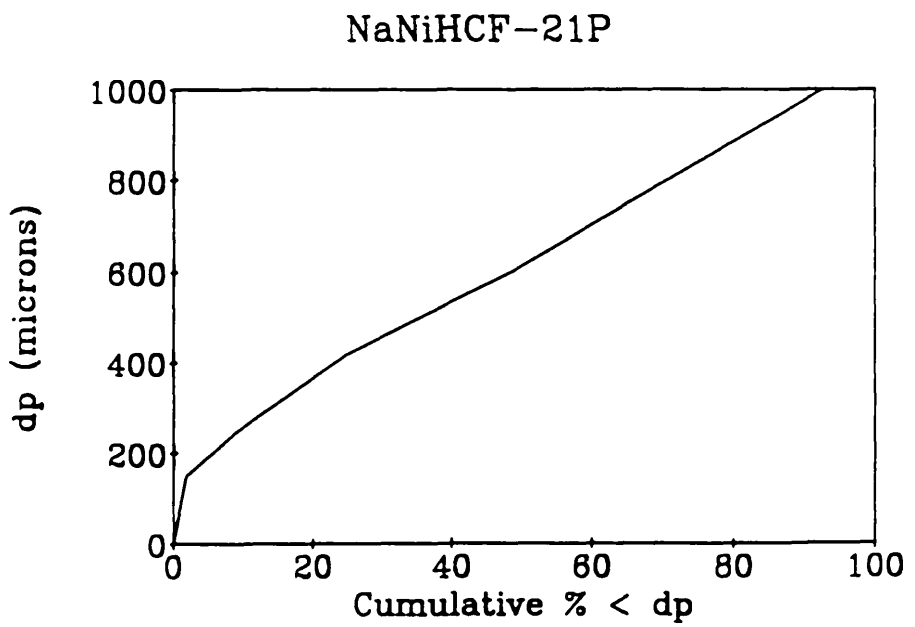
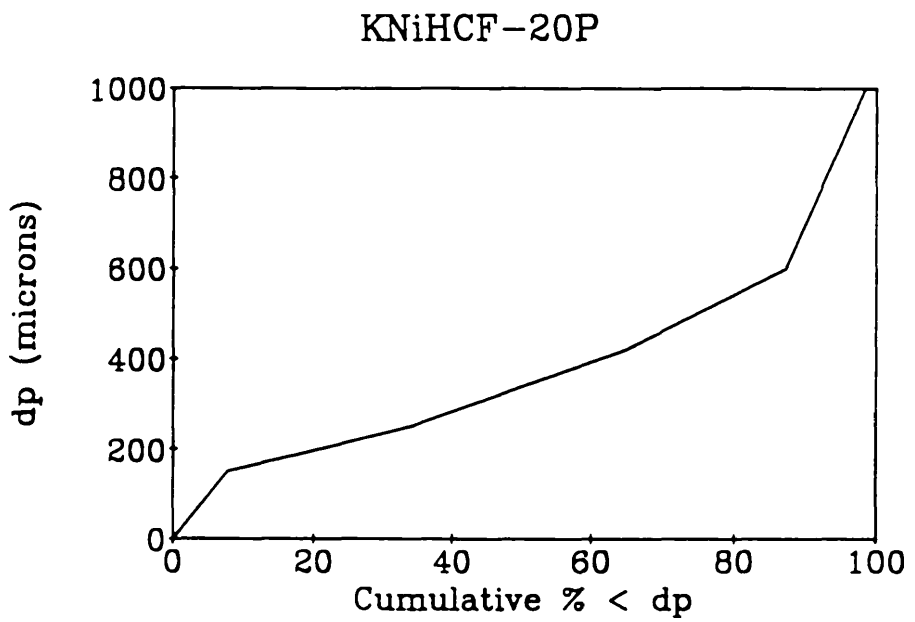
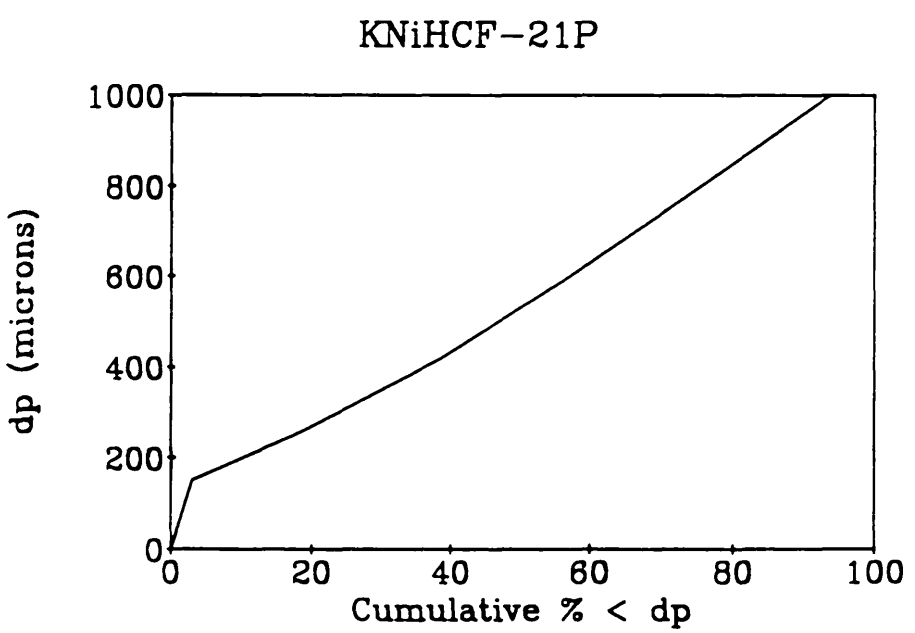


Figure 3.2 Sieve analyses of KNiHCF samples from batches 20 P and 21P





3.3.2 Discussion

From the preliminary preparations, it was found that a suitable granular material could be made which also had excellent sorption properties. A product with a large percentage of the yield being of a suitable size(> 250 microns) could be made, although considerable difficulties were found in reliably reproducing the granulation.

In order to develop a preparative method for a product having the required properties and with a consistent granular form, some key variables were identified for further study:-

i) The Ni:Fe ratio of the reactants.

ii) Heating of the precipitate in the mother liquor and the release of Ni into solution.

iii) Washing of the precipitate.

iv) The freezing and thawing conditions required for granulation.

v) The chemical and physical stability of the products.

3.4 Investigation of the effect of the Ni:Fe ratio in the preparation of NaNiHCF

3.4.1 Experimental

In Series B (Table 3.2), preparations were carried out to make NaNiHCF using volumes of reagents such that the Ni:Fe ratio in the system varied from 1.0 to 1.5. In each preparation, 12mL of 0.5M $Na_4Fe(CN)_6$ were mixed with the volume of 0.3M $NiSO_4$ to give the required Ni:Fe ratio.

For each Ni:Fe ratio, four samples were prepared; A and B were washed directly after precipitation, while C and D were put in a hot water bath (80°C) for two hours and then washed. The precipitates were washed once using 15mL of 0.1 M $NaNO_3$ as the wash liquor and then placed in the freezer compartment of a domestic fridge set at approximately −8 °C for 24 hours. The samples were left to thaw at room temperature until the solid had completely settled out leaving a clear solution, and were then filtered and dried.

The details of each individual preparation in the series are given in Table 3.2. From analysis of the wash liquors and filtrate, the amount of nickel in the final product was calculated. Assuming complete reaction of the hexacyanoferrate, the actual ratios of Ni:Fe in the products were calculated and are listed in Table 3.3. In Figure 3.3 the calculated ratio of Ni:Fe in the product is plotted against that of the reactants, and in Figure 3.4, the yield is plotted against the calculated Ni:Fe ratio of the product.

3.4.2 Discussion

It was found that with a Ni:Fe ratio of 1.0 no granulation was achieved using the freeze-thaw method. The samples in which the reaction liquor was not heated could only be filtered very slowly giving a thick mud which formed shiny black granules on drying, and which broke up on contact with water. When the reaction liquor was heated (Ni:Fe = 1.0) it was found that after freezing and thawing the products could not be filtered and so were not examined further.

With a Ni:Fe of 1.1 or above, finely divided products were formed which could be filtered quickly but on drying did not produce a hard granular solid. This may be due to the conditions during the freezing of the sample although work carried out by Pottier and Chauvet(97) showed that with a ratio of Ni:Fe<1.09 the zeta potential of the precipitate is negative which would result in a poorly formed product. No direct measurements of this were made in the present work.

In Figure 3.3, it is seen that for Ni:Fe ratios up to 1.4, the product formed when the reaction liquor was not heated had essentially the same Ni:Fe ratio as that in which the reactants had been mixed. At higher ratios, significant amounts of nickel were present in the wash liquor. It should be noted that trace levels (10-15 ppm) of nickel were always present in solution, even at lower Ni:Fe ratios.

Table 3.2 Series B - Preparation of samples of NaNiHCF with various Ni:Fe ratios

No.	Na4HCF (0.5M) mL	NiSO4 (0.3M) mL	Ni:Fe	Heat *	Reaction Liquor			Freeze		Filtration	Filtrate			Drying		Yield		Appearance of Final Product
					vol. mL	pH	Ni ppm	deg.C	hrs.		vol. mL	pH	Ni ppm	deg.C	hrs.	g	% **	
B1A	12	20	1.0	NA	14.5	8.8	13	-8	24	very slow	18.5	7.2	14	110	4	1.58	83	shiney black granules
B1B	12	20	1.0	NA	15.0	8.1	14	-8	24	very slow	15.5	7.1	12	110	4	1.82	96	shiney black granules
B1C	12	20	1.0	2 hrs.	3.0	7.4	14	-8	24	impossible	-	-	-	110	4	-		green mud - dried to solid cake
B1D	12	20	1.0	2 hrs.	4.5	7.4	20	-8	24	impossible	-	-	-	110	4	-		green mud - dried to solid cake
B2A	12	22	1.1	NA	17.5	7.3	9	-8	24	fast	24.0	6.2	10	110	4	2.06	109	grey finely divided particles
B2B	12	22	1.1	NA	17.0	7.1	10	-8	24	fast	24.0	6.4	3	110	4	2.02	106	black granules
B2C	12	22	1.1	2 hrs.	15.5	7.0	16	-8	24	very fast	20.5	6.0	7	110	4	2.05	107	green finely divided particles
B2D	12	22	1.1	2 hrs.	15.5	7.1	25	-8	24	very fast	21.5	7.0	8	110	4	1.97	103	green finely divided particles
B3A	12	24	1.2	NA	16.0	7.2	12	-8	24	very fast	31.0	6.1	6	110	4	2.15	112	grey finely divided particles
B3B	12	24	1.2	NA	16.5	7.2	10	-8	24	very fast	31.0	6.8	6	110	4	2.20	115	grey finely divided particles
B3C	12	24	1.2	2 hrs.	15.0	7.1	65	-8	24	very fast	26.0	6.6	30	110	4	1.92	100	green finely divided particles
B3D	12	24	1.2	2 hrs.	15.5	7.5	100	-8	24	very fast	21.0	6.7	47	110	4	1.95	102	green finely divided particles
B4A	12	26	1.3	NA	15.0	7.3	10	-8	24	very fast	36.0	6.4	5	110	4	2.27	118	green finely divided particles
B4B	12	26	1.3	NA	17.0	7.4	10	-8	24	very fast	32.0	6.1	8	110	4	2.29	119	green finely divided particles
B4C	12	26	1.3	2 hrs.	21.0	8.2	165	-8	24	very fast	24.0	6.5	105	110	4	1.97	103	green finely divided particles
B4D	12	26	1.3	2 hrs.	19.5	7.6	152	-8	24	very fast	25.0	6.3	100	110	4	2.08	109	green finely divided particles
B5A	12	28	1.4	NA	20.0	6.8	9	-8	24	very fast	28.0	7.0	9	110	4	2.30	119	green finely divided particles
B5B	12	28	1.4	NA	19.0	6.8	12	-8	24	very fast	28.0	6.1	10	110	4	2.30	123	green finely divided particles
B5C	12	28	1.4	2 hrs.	20.0	7.3	1060	-8	24	very fast	24.0	6.7	500	110	4	2.13	111	green finely divided particles
B5D	12	28	1.4	2 hrs.	21.0	7.3	1000	-8	24	very fast	25.0	6.6	520	110	4	2.13	111	green finely divided particles
B6A	12	30	1.5	NA	22.0	6.8	56	-8	24	very fast	32.0	6.3	62	110	4	2.36	122	green finely divided particles
B6B	12	30	1.5	NA	18.0	6.8	39	-8	24	very fast	30.0	6.3	40	110	4	2.32	120	green finely divided particles
B6C	12	30	1.5	2 hrs.	24.0	7.4	1400	-8	24	very fast	24.5	6.7	760	110	4	2.18	113	green finely divided particles
B6D	12	30	1.5	2 hrs.	23.5	7.4	1640	-8	24	very fast	24.5	6.5	720	110	4	2.11	109	green finely divided particles

All samples were washed with 15 ml 0.1 M sodium nitrate.
* Heated on a hot water bath at approximately 80 deg.C.
** Based of a theoretical yield as calculated in section 2.4.2
NA Not applicable

Table 3.3 Release of nickel from precipitates of NaNiHCF prepared in Series B

No.	Ni in wash liquor mmol	Ni in final product mmol	Ni:Fe in final product mol/mol
1A	0.008	5.992	0.999
1B	0.007	5.993	0.999
1C	0.002	5.998	1.000
1D	0.002	5.998	1.000
2A	0.007	6.593	1.099
2B	0.004	6.596	1.099
2C	0.007	6.593	1.099
2D	0.007	6.593	1.099
3A	0.006	7.194	1.199
3B	0.006	7.194	1.199
3C	0.030	7.170	1.195
3D	0.043	7.157	1.195
4A	0.006	7.794	1.299
4B	0.007	7.793	1.299
4C	0.102	7.698	1.283
4D	0.093	7.707	1.285
5A	0.007	8.393	1.399
5B	0.009	8.391	1.399
5C	0.566	7.834	1.306
5D	0.578	7.821	1.304
6A	0.023	8.977	1.496
6B	0.032	8.968	1.495
6C	0.890	8.110	1.352
6D	0.957	8.043	1.341

When the precipitate was heated in the reaction liquor, significant amounts of nickel were released when the Ni:Fe ratio was >1.2. If it is assumed that all the hexacyanoferrate remains in the product, the release of nickel will result in a large discrepancy between the product Ni:Fe ratio and that of the reactants. The release of nickel on heating the precipitate in the reaction liquor was also observed in the preliminary preparations as discussed in Section 3.3.

The release of nickel on heating the precipitates in the reaction liquor was compared with the release of nickel from the final product when it was conditioned with a solution below pH 4 as described in Section 4.2.

The product yields were compared to a theoretical yield assuming that there was no loss of hexacyanoferrate in the preparation. The amount of nickel is set by the Ni:Fe ratio, and the balance to ensure charge neutrality assumed to be made up of sodium - eg. NaNiHCF with a Ni:Fe ratio of 1.3 would have a theoretical product $Na_{1.4}Ni_{1.3}Fe(CN)_6$. The percentage of these theoretical yields are listed in Table 3.3 and the actual yields plotted against the product Ni:Fe ratio in Figure 3.4

With the exception of a Ni:Fe ratio of 1.0, the yields were all above the theoretical. For the products in which the precipitates were not heated, there is a consistent increase in the actual yield as the Ni:Fe ratio increased and as a result the percentage yield based on the assumed theoretical composition also increased from 108% with Ni:Fe = 1.2 to 121% with Ni:Fe = 1.5. When the precipitates had been heated no trend was observed in the actual yields, except that all yields were in the range 100-110% of the theoretical.

The results suggest that heating the precipitates changes the structure of the products and may also vary the amount of water of crystallisation. To clarify this point further chemical analysis of the products needs to be carried out as described in Section 4.3.

Figure 3.3 Ni:Fe ratio of the products against Ni:Fe ratio of the reactants

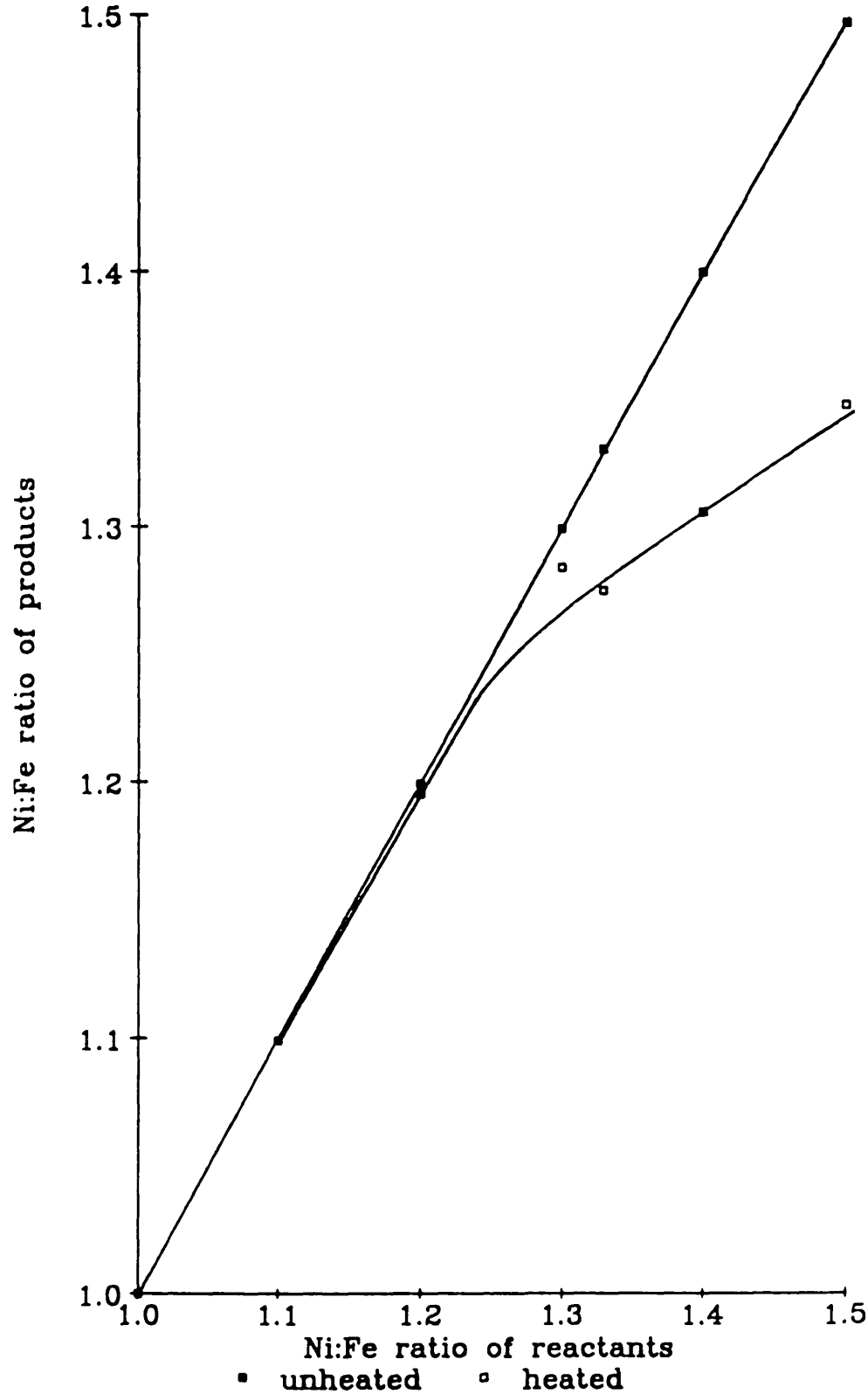
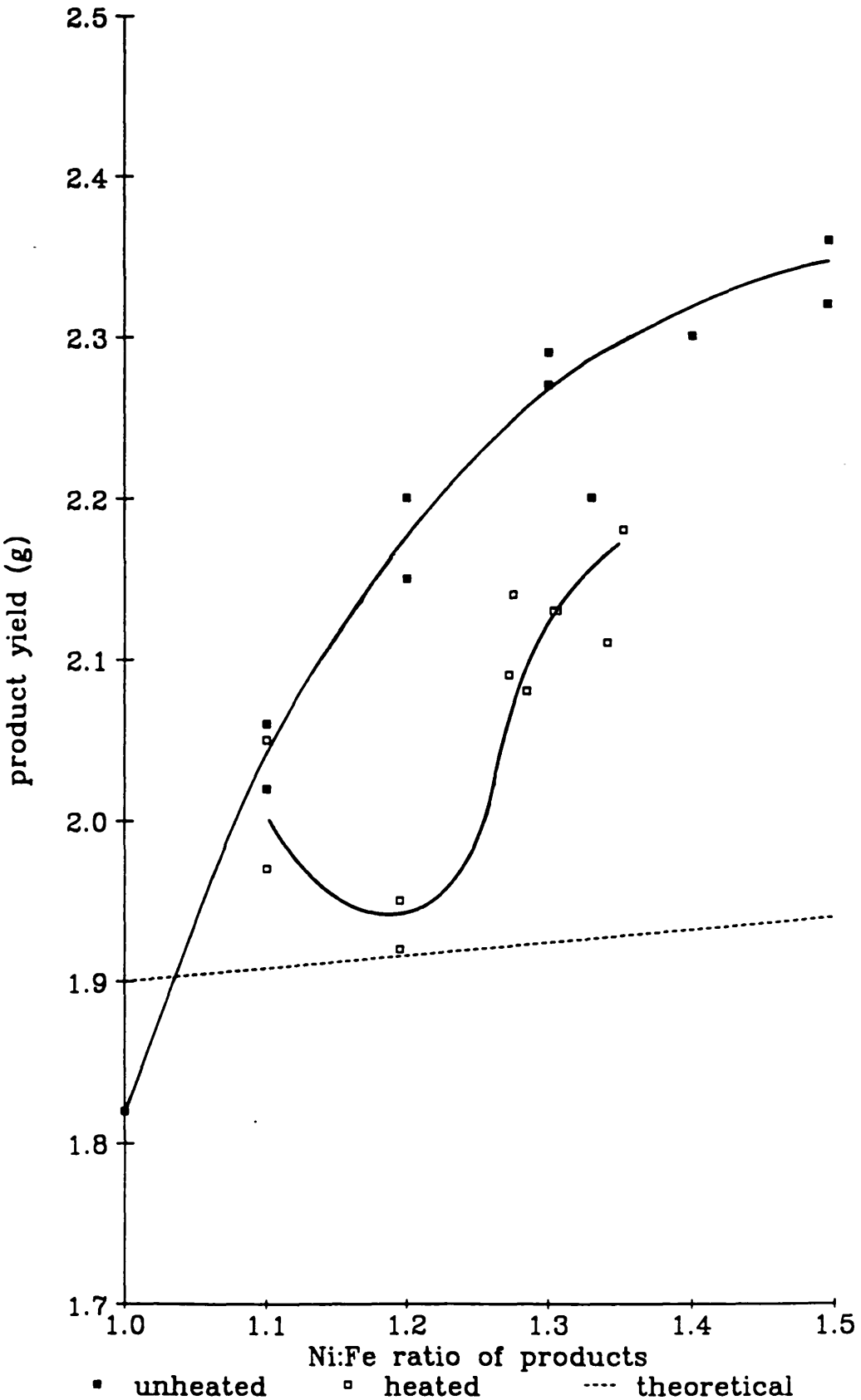


Figure 3.4 Product yield against Ni:Fe ratio of the product



The measured pH of the wash liquors are listed in Table 3.2 and show that when the Ni:Fe = 1.0, the reaction liquors which had not been heated had higher pH values than those which were heated, whereas for a ratio of 1.1 and 1.2 the pH is the same (7.0-7.5). With a Ni:Fe of 1.3 and above the pH was higher in the heated reaction liquor.

From the results, it appears that the optimum range of the Ni:Fe ratio is $1.2 - 1.3$. With smaller ratios a stable product cannot be formed and with larger ratios excess nickel is present. In order to fix the optimum ratio it was felt necessary to determine the exact composition of the products and their stability over a range of conditions which is discussed in Section 4.3.

From consideration of the physical stability it appeared that the NaNiHCF was better suited than the KNiHCF, and with consideration of both the granular form and chemical stability, a ratio of Ni:Fe=1.3 was selected as the most suitable. This Ni:Fe ratio was used in all the subsequent preparations of NaNiHCF in which the effect of heating, washing and the freeze-thaw conditions were studied in more detail.

3.5 Effect of heating and washing freshly formed precipitates of NaNiHCF

3.5.1 Experimental

Three series (D, E and F) of NaNiHCF preparations were carried out using a ratio of Ni:Fe = 1.3. In each individual preparation 12 mL $Na_4Fe(CN)_6$ was mixed with 26 mL 0.3 M $Ni(N0_3)_2$ or $NiS0_4$ in a centrifuge tube and stirred. Some of the samples were heated in a controlled water bath (80 °C), and washed with a known volume of the wash liquor. The reaction and wash liquors were analysed for nickel by atomic absorption. The use of the ferrous sulphate test indicated an absence of $Fe(CN)_6^{4-}$ ions in the solutions.

In Series D, precipitates were formed and heated at 80 °C for 2 and 4 hours or at 90 °C for 2 hours, and compared with unheated precipitates. The volume and nickel content of the reaction liquor obtained after centrifuging the mixtures are

listed in Table 3.4. Four of these precipitates (heated at 80 °C for 4 hours) were repeatedly washed with 25 mL 0.1 M $NaNO_3$ at room temperature, and then frozen, thawed, filtered and dried according to the procedures described in Section 3.2. The analysis of the wash liquors and yield of products obtained are also listed in Table 3.4.

In Series E, the kinetics of the release of nickel were further investigated with precipitates heated for varying periods of time (1/2, 1, 3, 5 and 6 hours). The volume and nickel content of the reaction liquors are listed in Table 3.5.

In Series F, precipitates were formed and heated at 80 °C for periods of 2 hours with the precipitates washed with 25 mL 0.1 M $NaNO_3$ after each period of heating. In each case the mixtures were centrifuged directly after heating without leaving them to cool. The volumes and analyses of the reaction and wash liquors are listed in Table 3.6.

3.5.2 Discussion

From the results from Series D (Table 3.4), it is suggested that the release of nickel from the precipitates is kinetically controlled since the nickel concentration in the reaction liquor increases both with time and with the temperature at which the precipitate was heated. This is further suggested by the results from Series E (Table 3.5) where the nickel concentrations after 6 hours of heating increased over 500 % from those after 1/2 an hour of heating. This trend was found for both the nitrate and sulphate systems, but for the sulphate system, there was a significantly larger release of nickel from the precipitates. This difference was still observed after heating the precipitates for 6 hours.

Table 3.4 Details of precipitates of NaNiHCF which were repeatedly washed (Series D)

Reactants :- 26 mL 0.3 M nickel sulphate of nickel nitrate
12 mL 0.5 M sodium ferrocyanide
Initial ratio Ni:Fe = 1.3

	D 5 A Nitrate		D 5 B Nitrate		D 6 A Sulphate		D 6 B Sulphate	
	vol. mL	Ni ppm	vol. mL	Ni ppm	vol. mL	Ni ppm	vol. mL	Ni ppm
1 reaction liquor	21.2	405	19.5	360	18.5	650	21.0	875
2 wash liquor	24.5	228	24.5	201	27.0	290	26.0	282
3 wash liquor	25.0	91	24.5	78	25.5	122	25.5	115
4 wash liquor	25.0	41	25.0	34	25.0	107	25.0	74
5 wash liquor	23.5	23	23.5	20	25.0	68	25.0	49
6 wash liquor	24.5	16	25.0	19	25.0	49	25.5	46
7 wash liquor	25.0	12	25.0	11	25.0	41	25.0	37
8 wash liquor	25.0	8	25.0	9	-	-	-	-
9 wash liquor	25.0	6	25.0	7	-	-	-	-
10 wash liquor	25.0	9	25.0	6	-	-	-	-
11 filtrate	14.0	5	8.0	6	15.5	10	12.0	5
Yield g	2.34		2.36		2.23		2.23	
Calc. Ni:Fe ratio	1.25		1.25		1.21		1.20	

Table 3.5 Investigation of the effect of heating time on the release of nickel from precipitates of NiNaHCF (Series E)

Reactants :- 26 mL 0.3 M nickel sulphate of nickel nitrate
12 mL 0.5 M sodium ferrocyanide
Initial ratio Ni:Fe = 1.3

NITRATE				SULPHATE			
No.	time heated hours	vol. mL	Ni ppm	No.	time heated hours	vol. mL	Ni ppm
E 1 A	1/2	19	70	E 2 A	1/2	19	187
E 1 B	1	17	150	E 2 B	1	15	600
E 1 C	2	16	220	E 2 C	2	15	640
E 1 D	4	15	370	E 2 D	4	13	700
E 1 E	5	14	430	E 2 E	5	14	940
E 1 F	6	14	460	E 2 F	6	13	1230

Table 3.6 Investigation of repeated heating and washing of NaNiHCF precipitates (Series F)

Reactants :- 26 mL 0.3 M nickel sulphate of nickel nitrate
12 mL 0.5 M sodium ferrocyanide
Initial ratio Ni:Fe = 1.3

	F1 A Sulphate		F 1 B Sulphate		F 2 A Nitrate		F 2 B Nitrate	
	vol. mL	Ni ppm	vol. mL	Ni ppm	vol. mL	Ni ppm	vol. mL	Ni ppm
1 reaction liquor	24.0	640	23.5	510	22.6	190	24.0	250
2 wash liquor	29.2	405	30.0	360	29.6	215	29.5	260
3 wash liquor	26.2	245	26.5	230	25.0	150	25.0	160
4 wash liquor	25.6	170	25.7	160	24.8	110	25.5	120
5 wash liquor	25.5	130	25.0	120	25.0	90	25.0	100

With the precipitates formed in series D, which were washed repeatedly at room temperature, it is suggested that the release of nickel only takes place when the precipitate is initially heated, the presence of nickel in the subsequent wash liquors is due to the solution retained with the solid phase after the mixture is centrifuged. This is supported by the observed reduction in the nickel concentrations in successive wash liquors and the low levels of nickel found in the latter wash liquors. The final yields of the products formed from these repeatedly washed precipitates (also listed in Table 3.5) are slightly lower for the products from the sulphate system which may be expected due to the greater quantity of nickel released during the preparation.

With the precipitates formed in Series F (Table 3.6), which were repeatedly heated and washed, there was a reduction in the quantity of nickel in each successive wash liquor. However it is clear that in each case more nickel is released from the precipitate since the amount of nickel in solution is greater than that found in Series D as discussed above. In Series F, the amount of nickel in the reaction liquors of the sulphate system was approximately twice as much as that in the nitrate system, but in the 5th wash liquors the difference between the two systems was only 20 %.

3.6 Investigation of the freeze-thaw method

3.6.1 Initial assessment of the freeze-thaw method

The formation of granules using the freeze-thaw method was initially investigated in the preliminary preparations which were described in Section 3.2. The samples were placed in the freezer compartment of a domestic fridge set at −8°C. After freezing for 16 hours, the precipitates were seen to be compacted and the colour changed from a pale to a dark green. The samples were allowed to thaw at room temperature and left a clear liquor above the granules. Washing with the various salt solutions described above did not appear to affect the appearance of the product from the freeze process except that with the 1M nitrate solution the mixture was not completely frozen at −8 °C.

Some of the batches in the preliminary preparations were placed in a domestic freezer set at −18 °C. The samples appeared to be completely frozen after 2 hours and even after a prolonged period of 16 hours in the freezer granulation did not occur. In other batches the samples were washed with 1 M or 4 M nitrate solutions to lower the melting point of the solution and thus reduce the rate that the mixture freezes. It was found that this resulted in the formation of finely divided particles.

For the formulation of granular NaNiHCF, the progress of the freeze process was investigated with a series of identical preparations. The reactants were mixed in 50 mL centrifuge tubes and washed 3 times with 0.1M sodium nitrate. The samples were then placed in the freezer compartment of a domestic fridge set at −8°C. The samples were removed after varying periods of time and thawed at room temperature. The settled height of the product, time required for filtration, appearance of the product, and the volume and Ni analysis of the filtrate are recorded in Table 3.7.

Table 3.7 Preliminary study of the effect of freezing time on the granulation of NaNiHCF

Products prepared by:- i. mixing 13 mL 0.5 M $Na_4Fe(CN)_6$ with 26 mL 0.3 M $NiSO_4$
ii. washed three times with 25 mL 1 M $NaNO_3$
iii. frozen in freezer compartment of domestic fridge, approx -8 °C

Time hr	Appearance of mixture	Settled height cm *	Filtration Time s (approx)	Filtrate		Appearance of the Product		Yield	
				vol (mL)	Ni (ppm)	Before Drying	After Drying	g	% **
3.5	first indication of freezing	2.1	200	26	14	finely divided green mud	fine brown powder	1.77	92
4.0	partly frozen	2.2	600	29	30	finely divided green mud	fine brown powder	1.96	102
4.5	surface completely frozen	1.6	600	23	6	finely divided green mud	dark brown powder	1.86	97
5.5	layers formed stratified appearance	1.9	600	27	14	finely divided green mud	dark brown powder	1.92	100
6.5	stratified appearance	1.5	120	26.5	23	finely divided green mud	dark brown powder	1.92	100
8.0	slightly darker colour uniform appearance	1.3	< 10	27	4	bright green granules	finely divided black granules	2.14	111
16	darker colour uniform appearance	1.0	< 10	28	7	darker green granules	black granules (some fines)	2.08	108
22.5	darker colour uniform appearance	0.9	< 10	26.5	9	dark green granules	black granules (some fines)	2.03	105
30	darker colour uniform appearance	0.8	< 10	26.5	42	dark green granules	black granules	1.89	98

* settled height approximately measured in a 25 mL plastic bottle
** theoretical yield calculated assuming a product $Na_4Ni_4[Fe(CN_6]_3$

During period of freezing, three stages with indistinct transitions were observed:- An initial period when freezing begins (0-4 hrs.), followed by the formation of layers giving a stratified appearance (4-8 hrs.), and then on complete freezing (>8 hrs.), a darkening of the colour with the occurrence of granulation.

3.6.2 Fundamental aspects of the freeze-thaw method

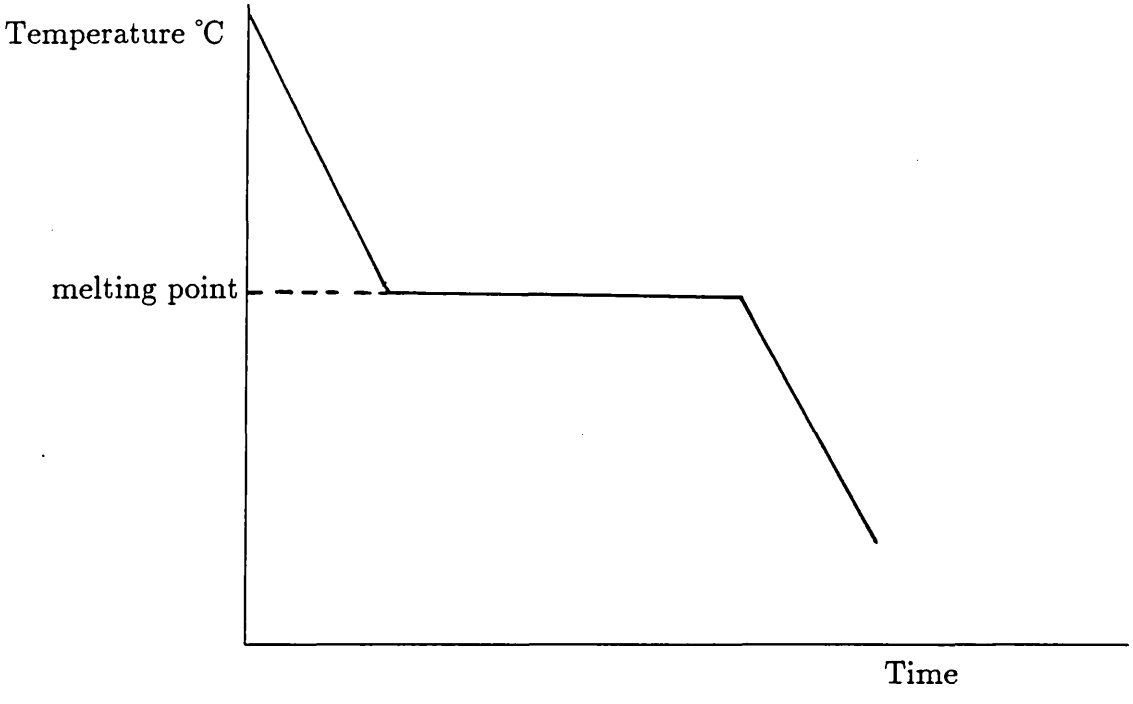
In order to achieve a consistent granular form of NaNiHCF, especially on a larger scale, an understanding is required of the underlying phenomena which lead to granulation during the freeze-thaw process. On freezing samples of NiHCF, the phenomena which lead to granulation are clearly complicated as the mixture comprises both liquid and solid phases and additionally dissolved salt in the liquid phase.

In the literature concerning the use of the freeze-thaw method mentioned in Section 2.3.2, few details are given concerning the preparation of granular HCFs, except that the temperature is usually stated and in some cases it is specified that the freezing process should be slow. For the preparation of ZrHCF, Egorova et al.(50) froze the sample in an air-filled refrigerator at -16 °C for 24 hours, during which two processes were found to occur simultaneously: dehydration(freezing out of water) and granulation of the sample. It was additionally found that the granular strength of the material was only satisfactory with a ratio of Zr:$Fe(CN)_6$ ≥ 2. A similar freeze-thaw method was investigated by Smyth(124) and, although a detailed study of the mechanism was not carried out, it was found that the same two processes occurred. It was additionally found that the rate of freezing should be slow and that the thawing rate did not affect granulation. The only rate of heat removal found in the literature was specified by Sharygin et al.(51,52) as 5-10 cal/mL.h for the preparation of granular zirconyl phosphate(ZrP). Sharygin et al.(52) also studied the effect of temperature and different electrolytes on the freeze granulation of the ZrP. After thawing, the effect of the freezing was quantified by measurement of the sedimentation volume, the rate of passage of water through the filtrate, and the moisture content of the ZrP. It was found that the freezing

represents an irreversible dehydration process with the precipitate volume being reduced 10-20 fold and the moisture content decreasing by 21-33%. The freezing also improved the filtration 250-500 fold, and increasing the concentration of the electrolyte caused a deterioration in the filtration properties.

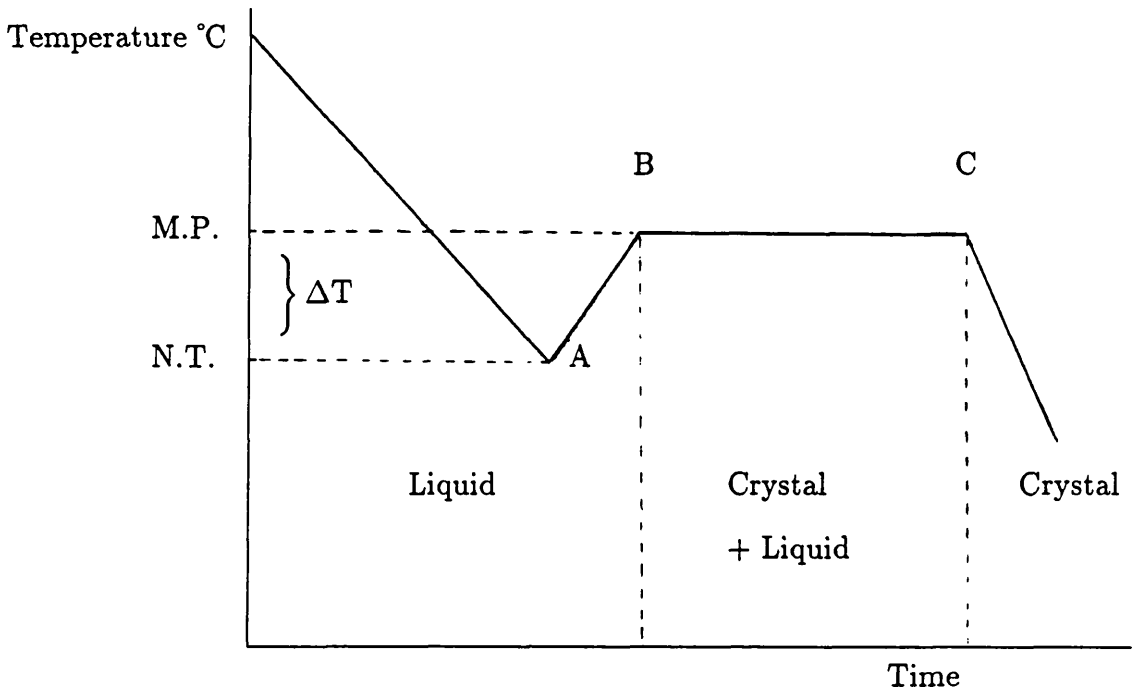
The freezing of a pure liquid is well understood and is described in detail in the text by Knight(125). An ideal cooling curve, as shown in Figure 3.5, consists of three distinct stages, the cooling of the liquid to the melting point, freezing of the liquid at constant temperature and then cooling of the completely formed solid.

Figure 3.5 An ideal cooling curve for a pure liquid (constant rate of heat removal)



In reality, as the liquid is cooled it may deviate from this ideal behaviour by cooling to below the melting point before the onset of freezing. Below the normal melting point the liquid is supercooled which is metastable, moving only to a more stable state as freezing begins at the onset of nucleation. The experimental cooling curve for a pure liquid at a constant rate of heat removal is shown in Figure 3.6.

Figure 3.6 A less ideal cooling curve for a pure liquid (constant rate of heat removal)



In Figure 3.6, nucleation occurs at point A with crystal growth occurring between points A and B, and also between points B and C. It is found that the nucleation temperature (N.T.) is always lower than the melting point (M.P.), with the temperature difference ΔT termed the nucleation supercooling. From experimental work, it is found that there is a correlation between the type of material and the nucleation supercooling, although from repeated freezing of the same material, it is found that the nucleation temperature is not totally reproducible.

A thorough investigation of the water-ice system was made in 1948 by Dorsey(126) who examined water of different purity. It was found that the purest water then available had a nucleation temperature of between -20 and -25 °C, while tap water had a nucleation temperature of between -5 and -10 °C. Furthermore, it was found that the cooling rate had no effect whatever on the nucleation temperature. From these and other experiments it was proved that normally with water there is heterogeneous nucleation due to presence of foreign particles in the water. Heterogeneous nucleation in other materials has been

studied, although not as thoroughly as water, and it is well established that the nucleation behaviour of any substance is the same in principle as that of water.

If there are no impurities present in a substance, homogeneous nucleation will occur. This has been extensively studied although it is generally difficult to obtain pure materials completely free of foreign particles. For the samples of HCF, since the solution contains dissolved salts and the HCF precipitate, the nucleation will clearly be heterogeneous.

After nucleation has occurred, crystal growth takes place at a rate which is dependent on many factors including the degree of supercooling(temperature), the rate of heat removal, the geometry, and the presence of impurities. For a pure liquid, the crystal growth may be characterised by a linear crystallisation velocity which is a direct function of the degree of supercooling as outlined by Knight(125). In the case of a salt solution with solid particles present, the growth process becomes complicated and consideration must be given to each factor depending on the system.

A physical model has been presented by Wollhöver et al.(127) for the coupled transient transport of heat and mass in a freezing solution of NaCl of finite extent. Due to total rejection of salt particles at the phase boundary, it was found that very steep concentration profiles developed in front of the solid-liquid interface. This resulted in reaching the eutectic salt concentration after a certain time of freezing which is dependent on the imposed freezing conditions. The increase in the salt concentration at the boundary resulted directly in a slowing down of the velocity of the liquid-solid interface.

A detailed study of the diffusion of both heat and solute during the freezing of salt solutions has been given by Grange et al.(128). In general, the solidification process is determined by heat and mass transfer as well as interface kinetics. The controlling rate may be either nucleation or growth depending on the system, although in many situations the rate of growth is controlled by the rate at which the latent heat of fusion generated in the process can be removed from the freezing

front. If this last case is occurring, knowledge of the temperature distribution is required in addition to the heat and mass transfer. Both experimental and analytical investigations were made on the redistribution of salt during the one-dimensional freezing of NaCl solution with concentrations of 0.4–4.0M. The temperature and concentration distributions, as well as the rate of phase change, were determined both experimentally and from a model. This model was solved both numerically and with an approximate analytical solution. The solute distribution was found to be an important parameter which could be used to indicate solute rejection at the interface. Initially, the interface velocity was relatively large, and little or no salt rejection was observed. This was due to the concentration layer formed being so thin that it was entrapped by the advancing ice crystals on a microscopic level. Subsequently, the interface velocity became very small and solute rejection became significant. As a result of this, the liquid interface concentration was not constant but increased with time due to increased salt rejection. The majority of the solute in the solid was attributed to bulk entrapment at the interface, although it was found that the model could not be used to predict the amount of entrapment. In order to explain the phenomenon of salt rejection at the interface, it was concluded that a description of the microscopic effects occurring at the interface was required. Also the effects of concentration, gravity, temperature gradients and crystal orientation must be fully understood.

Several specific freezing phenomena, which have important practical implications, have been studied in some detail and may provide an insight into the freezing of HCF samples. Two such phenomena are the migration of brine in the freezing of sea water, and the frost heaving of soil.

Kingery and Goodnow(129) discuss the freezing of salt water and the mechanisms by which brine migration occurs. The structure of sea ice is very much dependent on its salinity as salt has almost no solubility in the solid ice. The salt is thus found in highly concentrated pockets of liquid brine in a matrix of salt free ice. Two mechanisms have been proposed for the elimination of the salt brine.

Firstly, brine drains out along grain channels under the influence of gravity, and secondly brine trapped inside a grain moves under the influence of gravity. It was found that when a block of frozen NaCl was stored at -20 °C for a long period a puddle of highly concentrated brine was formed under the block which was attributed to gravity drainage. From direct measurements of the brine migration velocity, it was found that gravity drainage is the primary mechanism of salt elimination whereas temperature gradients contribute to a lesser extent. It was also stated that the migration velocity was limited by solute diffusion although in some cases it may be limited by the flow of heat.

The phenomenon of frost heaving of wet soil is known to be very complex and has been outlined by Knight(125). Due to the variety of natural soils there is a large variation in observed frost heaving. The heaving may be several hundred percent when a a pan containing soil is placed in a pan of water and frozen from the top. Expansion in water can only account for about 10 % of this and it is clear another factor is involved in the migration of freezing water. This has been explained by a 'crystallisation pressure' which is exerted when the freezing interface passes between small solid particles.

3.6.3 Set-up of controlled freeze unit

Objective

For the preparation of NaNiHCF and KNiHCF, the freeze-thaw method was found to provide a relatively hard granular form. However, it was difficult to reproduce results using a conventional domestic freezer or fridge and therefore not possible to elucidate the exact conditions at which granulation occurs.

In order to study the effect of temperature, composition, and time on the freezing process it was decided to construct an accurately controlled unit. The unit must be able to maintain samples at uniform temperature over a long period, or allow the freezing to be carried out to a specified programme. The expected temperature for the process was found from previous work to be in the range 0 to -10 °C. No commercial unit could be found to operate in this range and so it was decided to construct a unit using the facilities at Imperial College. In the design of the unit, provision was made for easy scale-up.

Design of the unit

The sample is enclosed in an aluminium casing which is to be maintained at the required temperature. The high thermal conductivity of aluminium allows fast heat transfer resulting in a uniform temperature over the unit. The casing is placed in a conventional chest freezer at approx. -25°C and then heated to the required temperature by means of a coil wound around the casing. The temperature of the casing is measured by a thermistor embedded in its base which is connected via an analog to digital converter to a BBC microcomputer. Using a conventional PID control algorithm the BBC micro manipulates the power input to the coil maintaining the required temperature. Provision was made to enter either a constant set point temperature or a constant rate of change of temperature between two specified temperatures. A full listing of the control program, which was written in BBC Basic, is given in Appendix A.

Four independent units can be operated using the four channels of the BBC

micro. Scale-up of the sample size is achieved by increasing the size of the aluminium casing with no changes required to the computer hardware or software.

Two aluminium cases were made for 50 mL centrifuge tubes and two for plastic bottles which could hold 120 mL of solution. A block diagram of the complete system controlled freezer unit is shown in Figure 3.7 and the drawings for the two sizes of aluminium cases shown in Figures 3.8 and 3.9

Figure 3.7 Design of controlled freezer unit

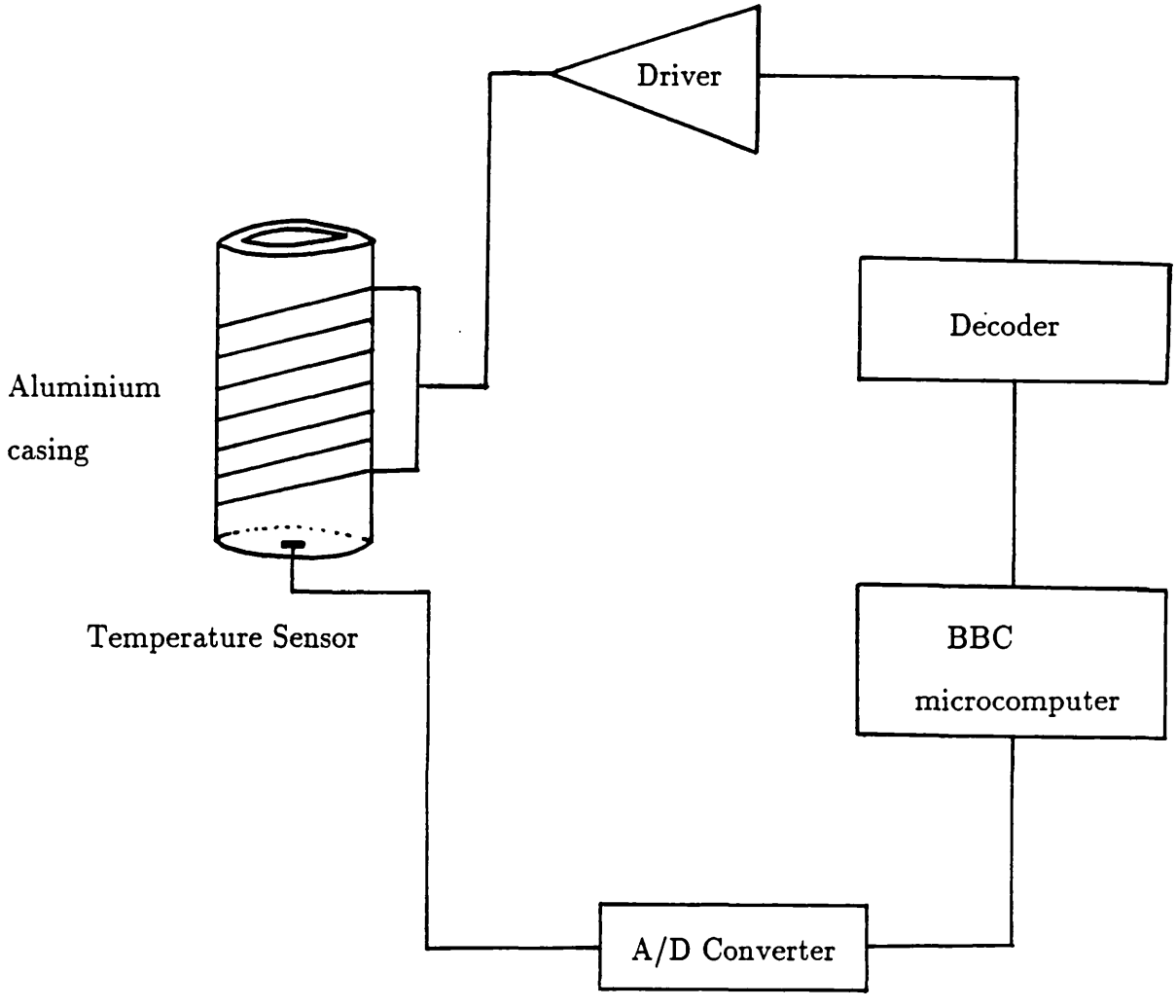


Figure 3.8 Aluminium casing for 50 mL centrifuge tube (channels 1&2)

(all dimensions mm)

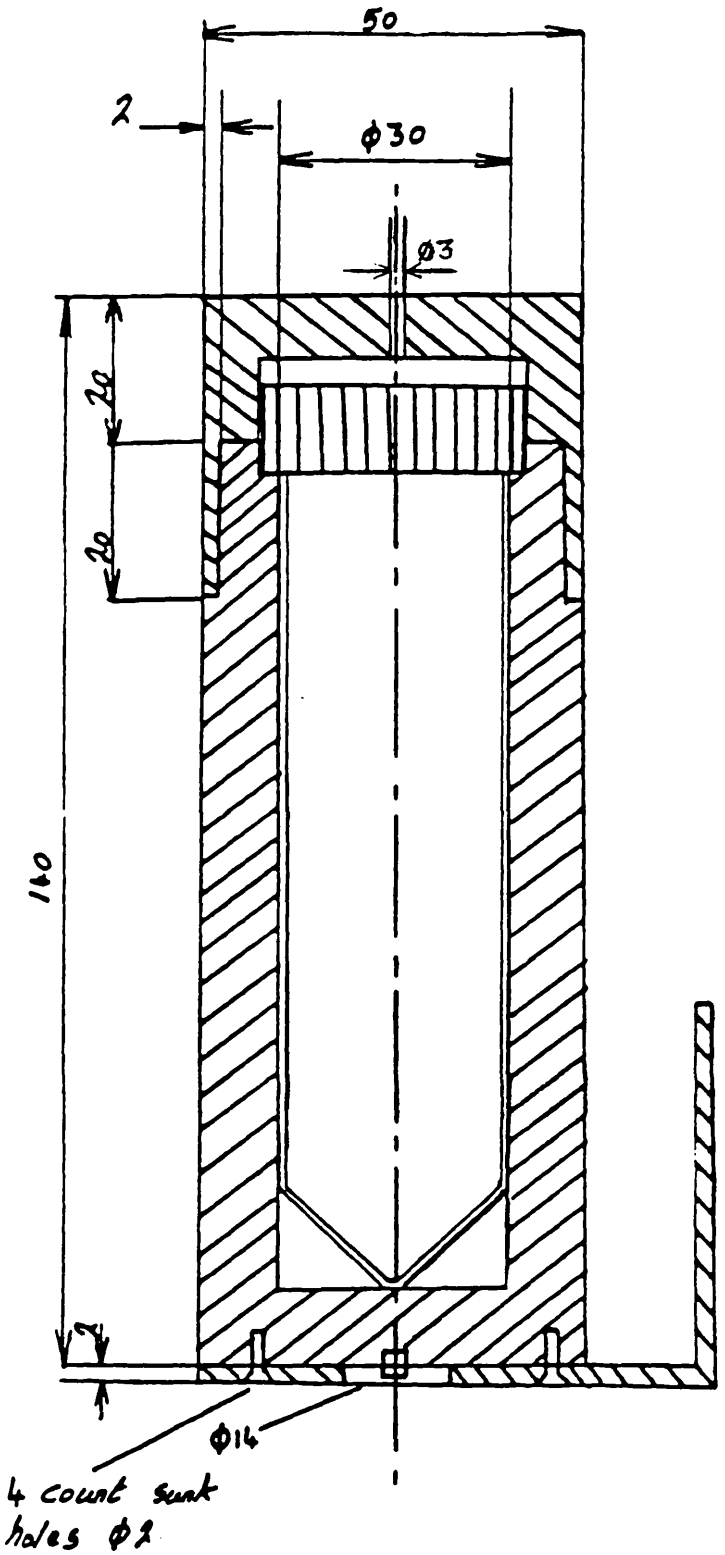
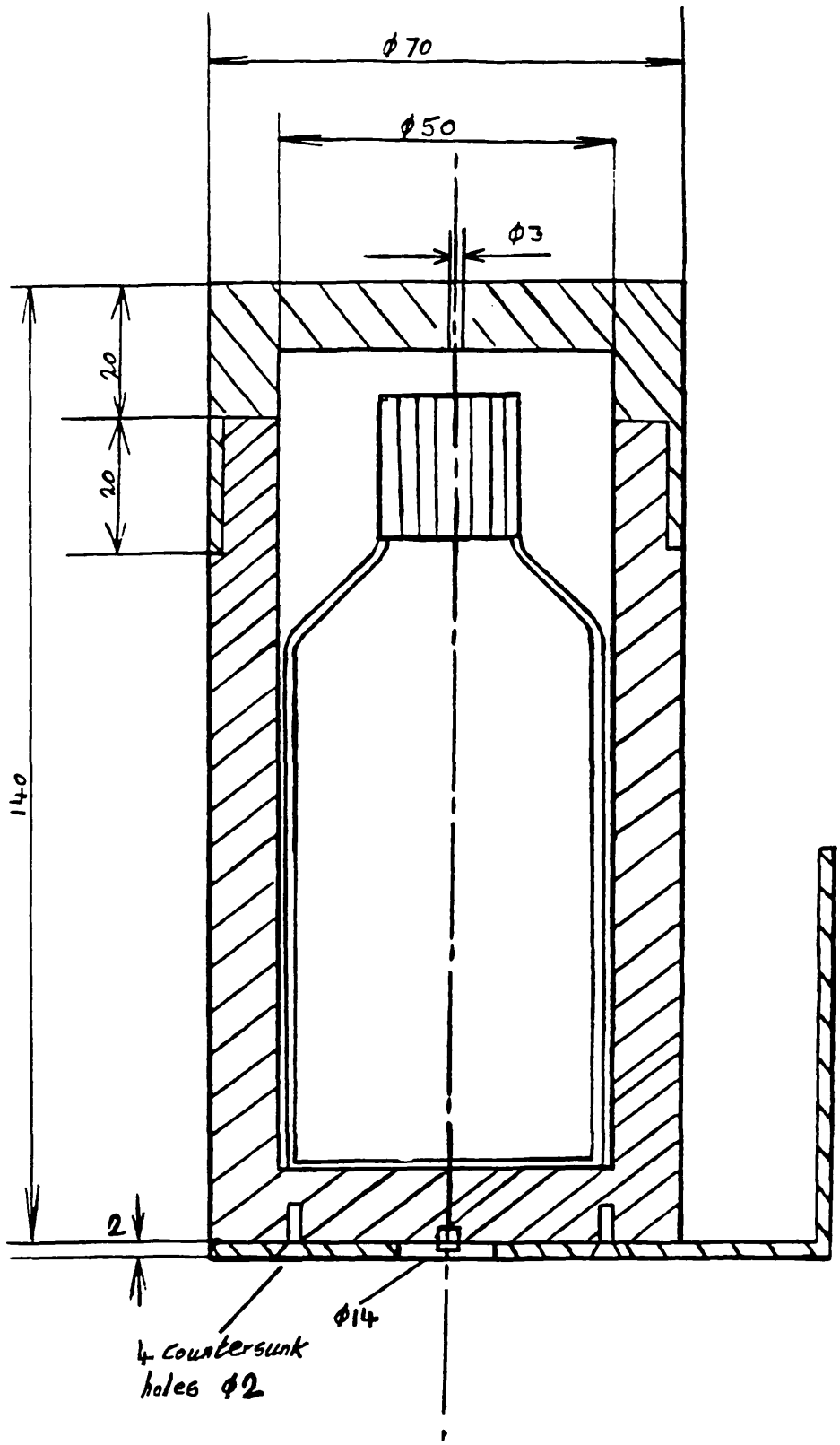


Figure 3.9 Aluminium casing for 150 mL plastic bottle (channels 3 &4)

(all dimensions mm)



3.6.4 Results from controlled preparations

Initially, some samples of NaNiHCF prepared in 50 mL centrifuge tubes were frozen in the controlled freezer unit. The precipitates were formed with a Ni:Fe ratio of 1.3 and washed with 1M $NaNO_3$. Using the casings shown in Figure 3.8, which were connected to channels 1 and 2 of the freezer control unit, the precipitates were frozen at temperatures of −7, −8 and −10 °C for varying periods of time. In all the cases, granulation only occurred to a limited extent with the products having a fast filtration time but only a small particle size. It was observed that the samples froze over a shorter period than was found with the samples frozen at the same temperature in a domestic fridge. It was suggested in Section 3.6.2 that the rate of heat transfer from the samples is an important factor. The controlled samples are in contact with the aluminium case which may give rise to higher heat transfer than contact with air, which was the case in the domestic fridge. In both cases, though, the base of the samples is in contact with a metal surface.

Using the larger 150 mL sample bottles, larger batches of NaNiHCF were prepared by applying the same preparative method; i.e. 108 mL of 0.5 M $Na_4Fe(CN)_6$ was added to 234 mL of 0.3 M $NiSO_4$. The precipitates were formed and washed in 1 L centrifuge bottles and then the mixture was split into equal amounts to fill three of the 150 mL sample bottles. The samples were initially also frozen at −7, −8 and −10 °C for varying periods of time. It was found that in each case a degree of granulation occurred, although not to the same extent as was found in the preliminary preparations, 20P and 21P. As with the smaller centrifuge tubes, it was thought that the rate of heat transfer was likely to be an important factor.

In order to decrease the rate at which the samples froze, some polystyrene discs were placed in the aluminium freezing units to insulate the base. To investigate reproducibility, the effect of the insulation, the effect of temperature, and to check the completion of freezing, a series of controlled preparations was

carried out. Samples were prepared in the 150 mL sample bottles as before and then frozen under the required conditions. After thawing, filtering and drying the products, the particle size distribution was used to quantify the extent of granulation.

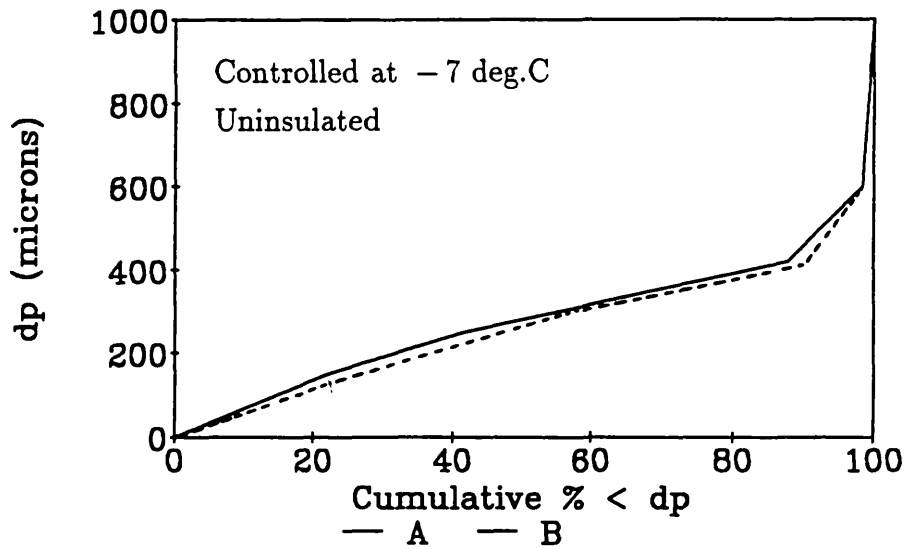
The reproducibility of the freezing method was checked with two samples frozen under the same conditions. Figure 3.10 shows the size distribution of two samples which were frozen at -7 °C for 15 hours without insulation, and two samples which were frozen at -8 °C for 15 hours with insulation.

The effect of the insulation at the base of the samples was investigated at three temperatures which were all frozen for 15 hours. The size distributions for these samples are shown in Figure 3.11.

In order to check the extent of completeness of the freezing process at the three different temperatures. Figure 3.12 shows the size distribution of products after freezing for 15 and 22 hours, with each sample being insulated at the base.

To gain a better indication of the freezing process, and in particular the degree of supersaturation and existence of temperature gradients within the samples, some cooling curves of the samples were obtained. Two thermocouples were placed directly in the sample mixture via the top of the sample bottle. One of the thermocouples was arranged to be at the bottom of the sample while the other was located near the top. During the freezing process, these two temperatures and the controlled temperature were logged manually at regular intervals. The cooling curves for two samples of NaNiHCF - NJ9A frozen under different conditions are shown in Figures 3.13 and 3.14 with the corresponding sieve analyses of the products shown in Figure 3.15. In a similar way three cooling curves for samples of NaNiHCF-NJ9 B(1 to 3) are shown in Figures 3.16-3.18, with the corresponding sieve analyses shown in Figure 3.19.

Figure 3.10 Sieve analyses of samples to show the reproducibilty of granulation



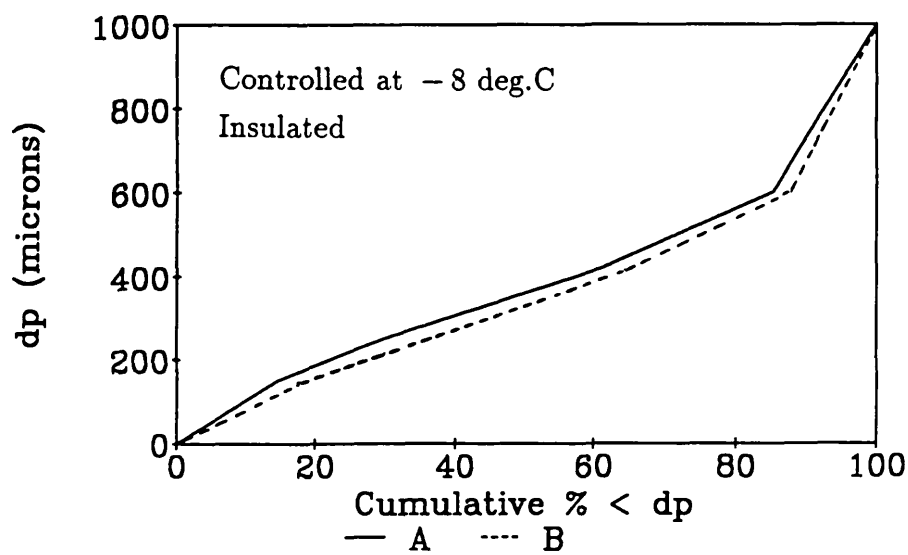
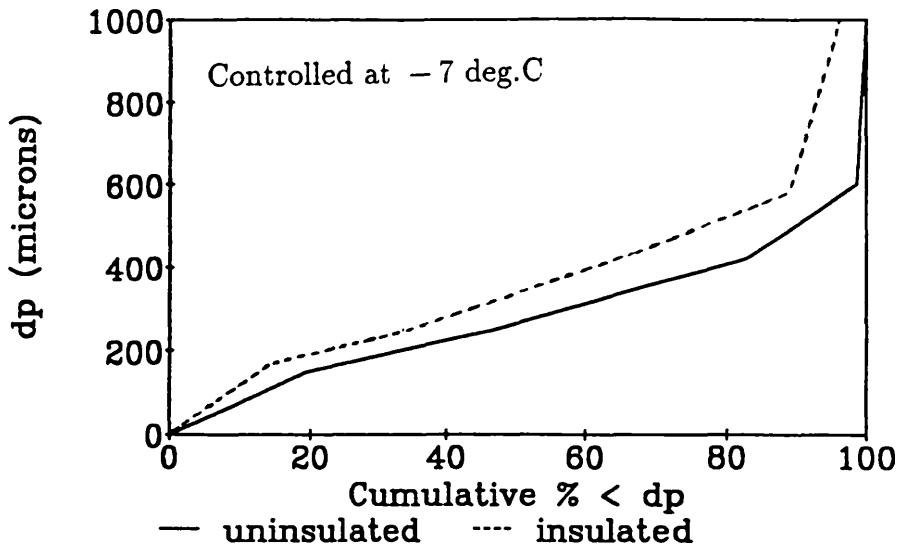
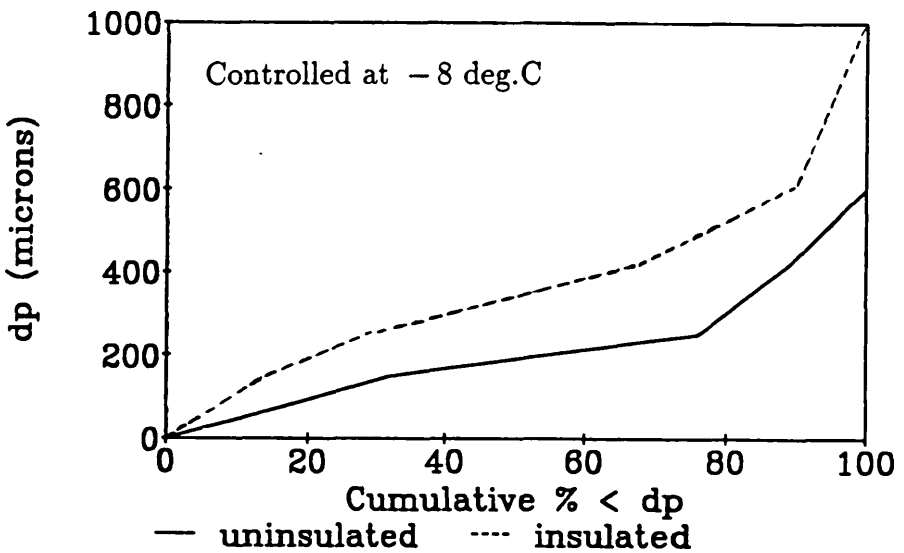


Figure 3.11 Sieve analyses of samples to show the effect of insulation on granulation





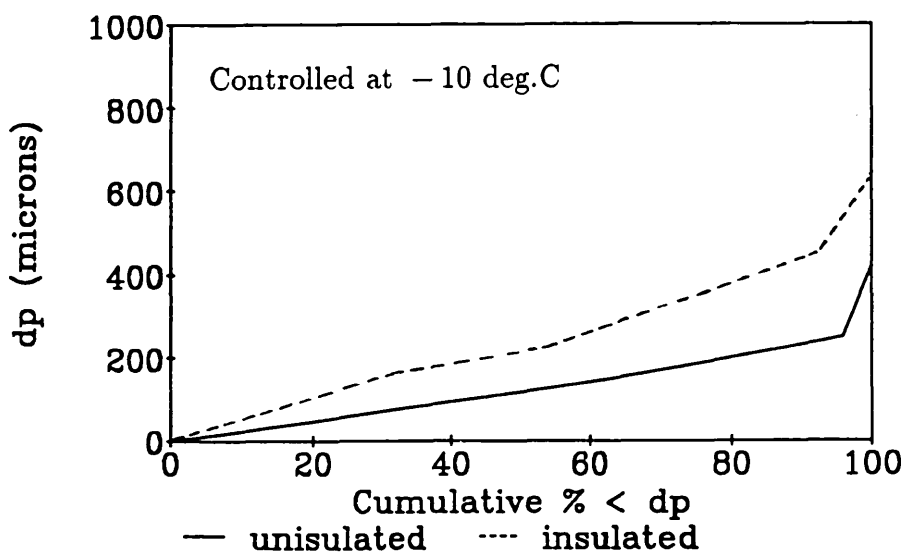
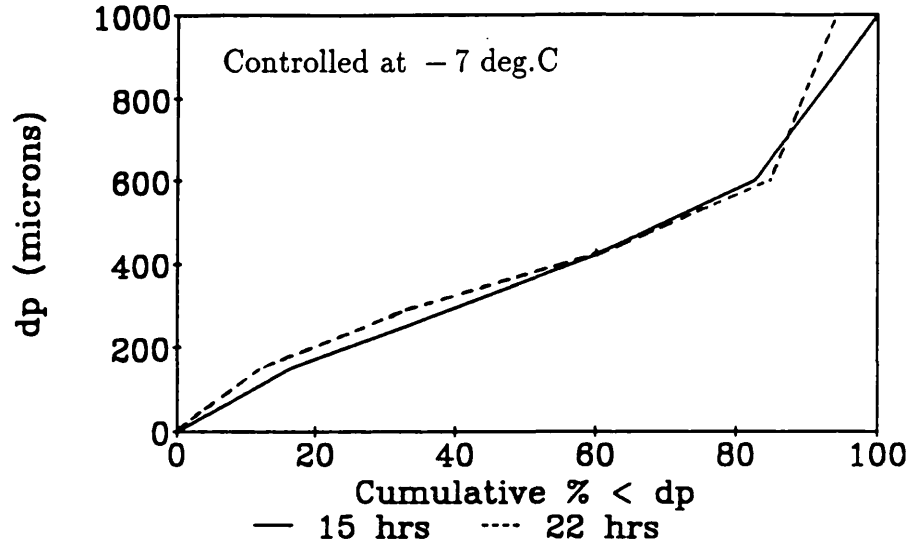
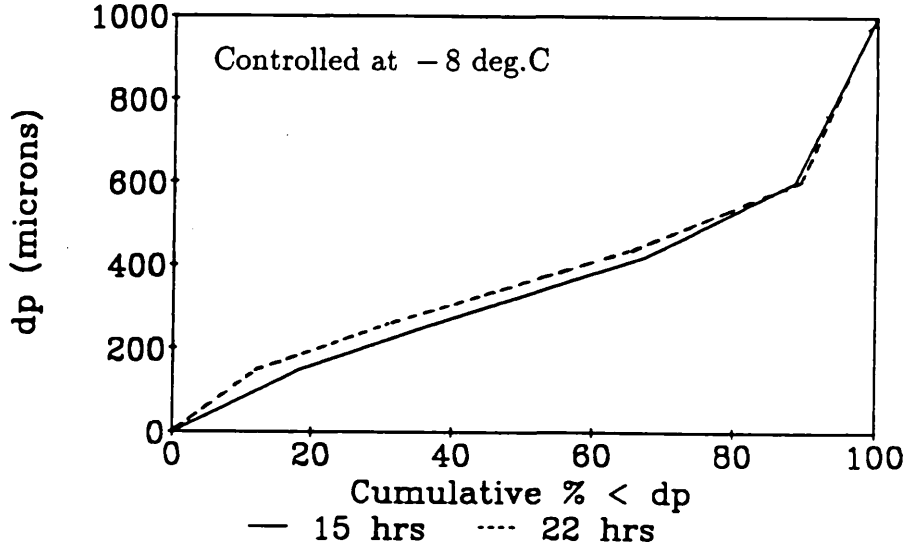


Figure 3.12 Sieve analyses of samples to check complete freezing





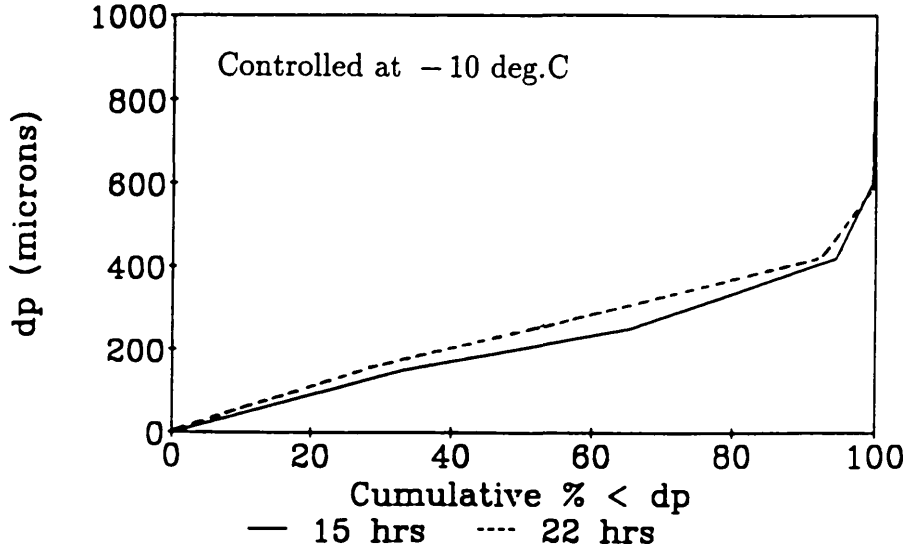


Figure 3.13 Cooling curves for NaNiHCF - NJ9 A2

controlled at −10 °C with insulation at base of sample

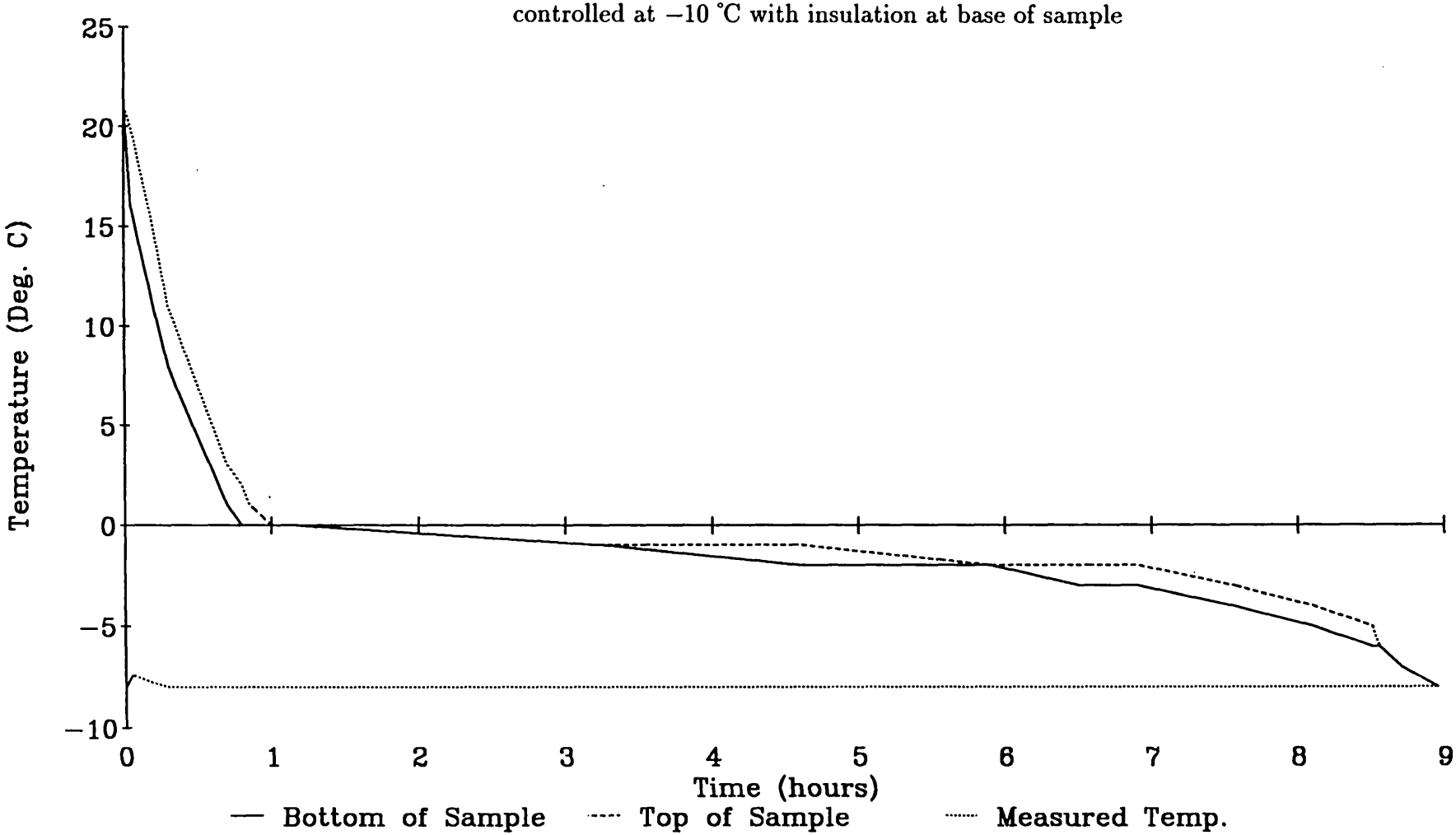


Figure 3.14 Cooling curves for NaNiHCF - NJ9 A3

controlled at −8 °C with no insulation

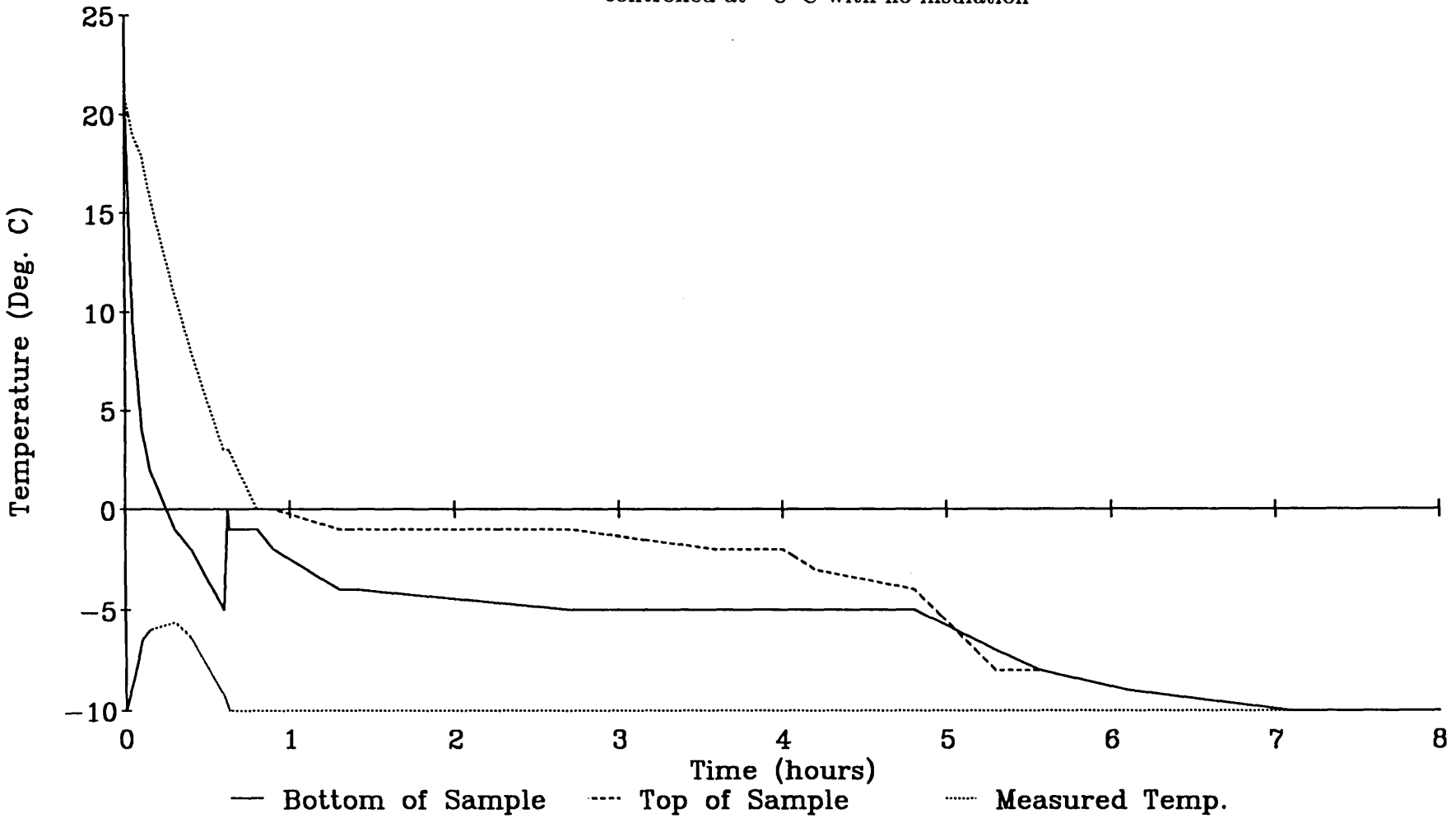
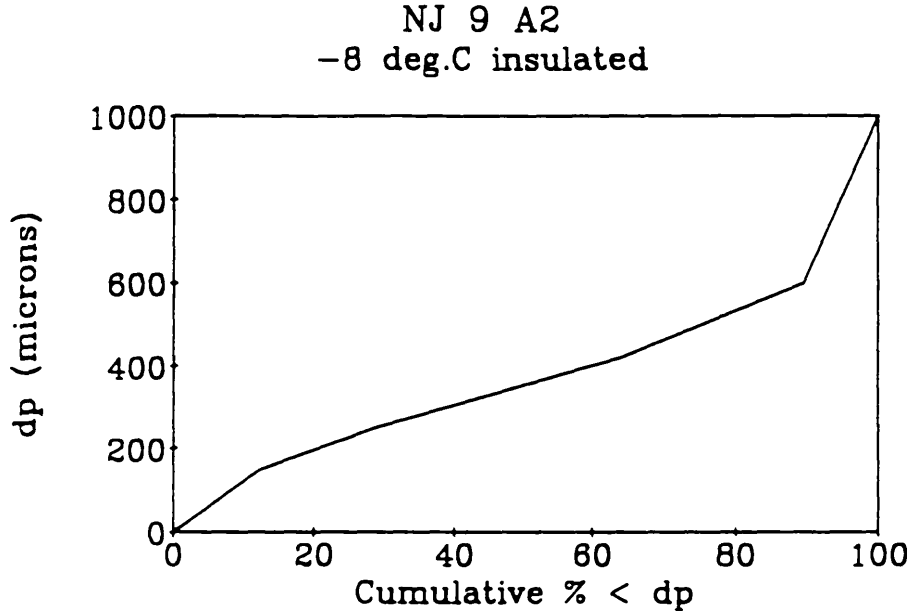


Figure 3.15 Sieve analyses of samples NJ9 A2 and NJ9 A3



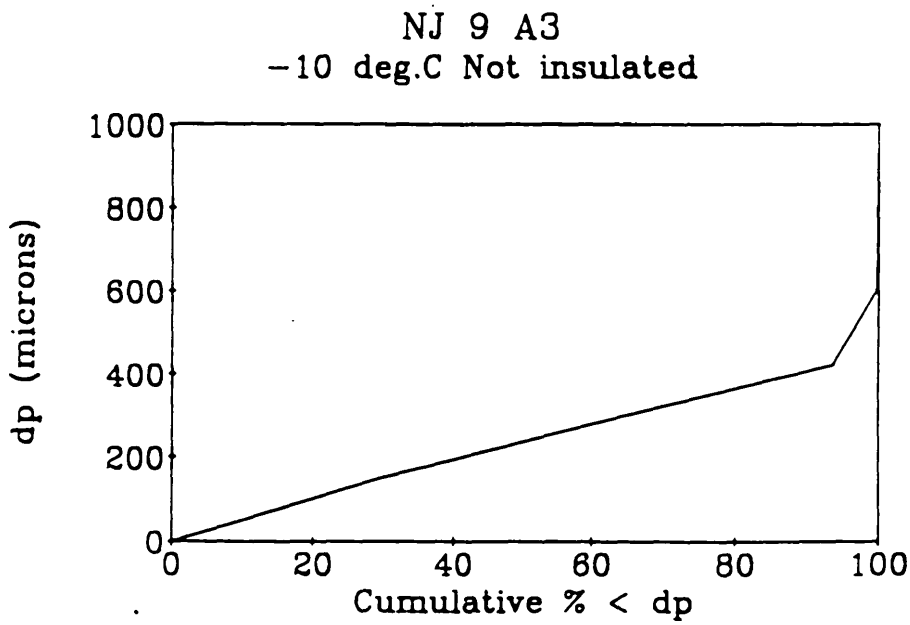


Figure 3.16 Cooling curves for NaNiHCF - NJ9 B1

controlled at −10 °C with insulation at base of sample

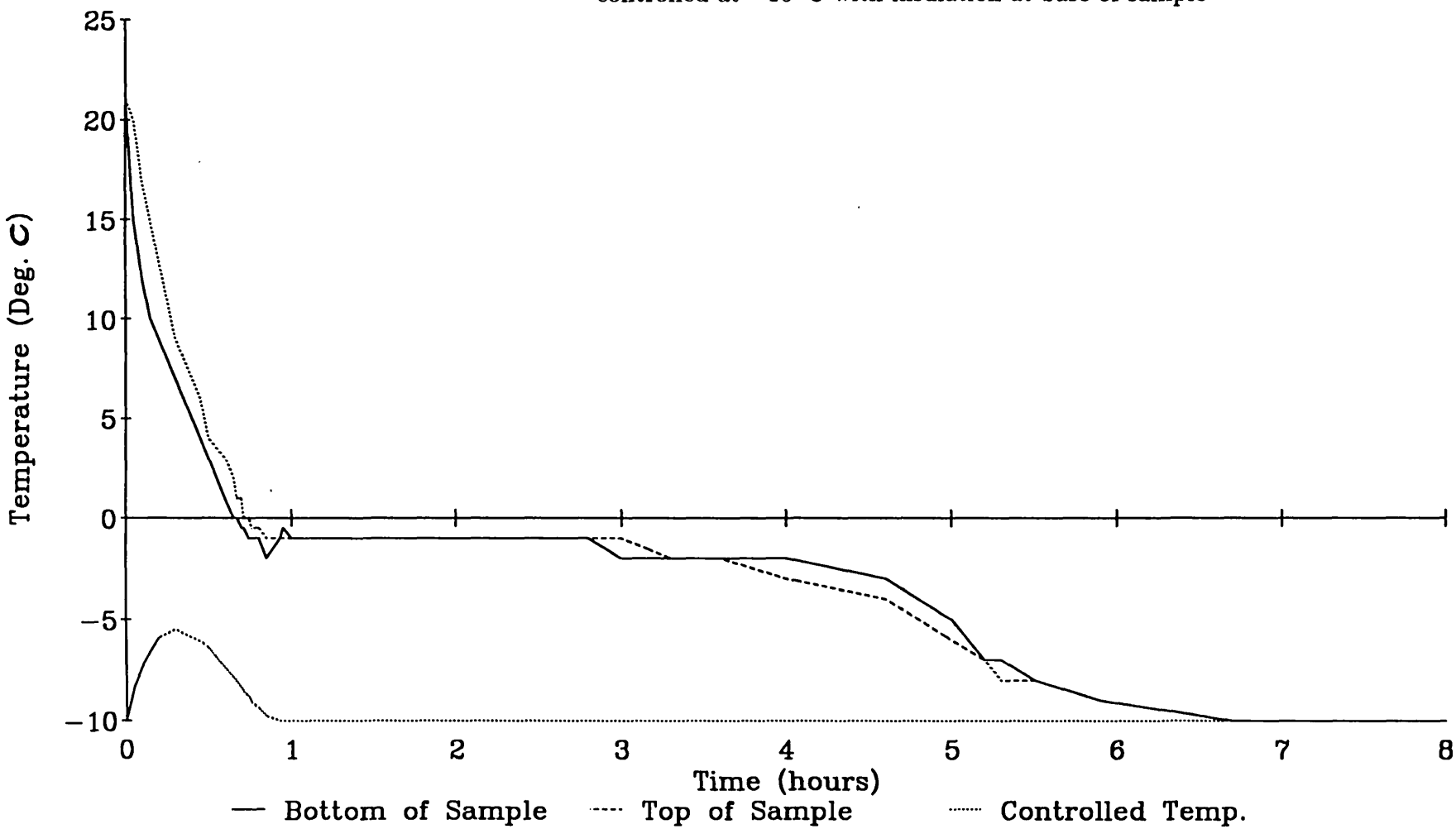


Figure 3.17 Cooling curves for NaNiHCF - NJ9 B2

controlled at −10 °C with no insulation

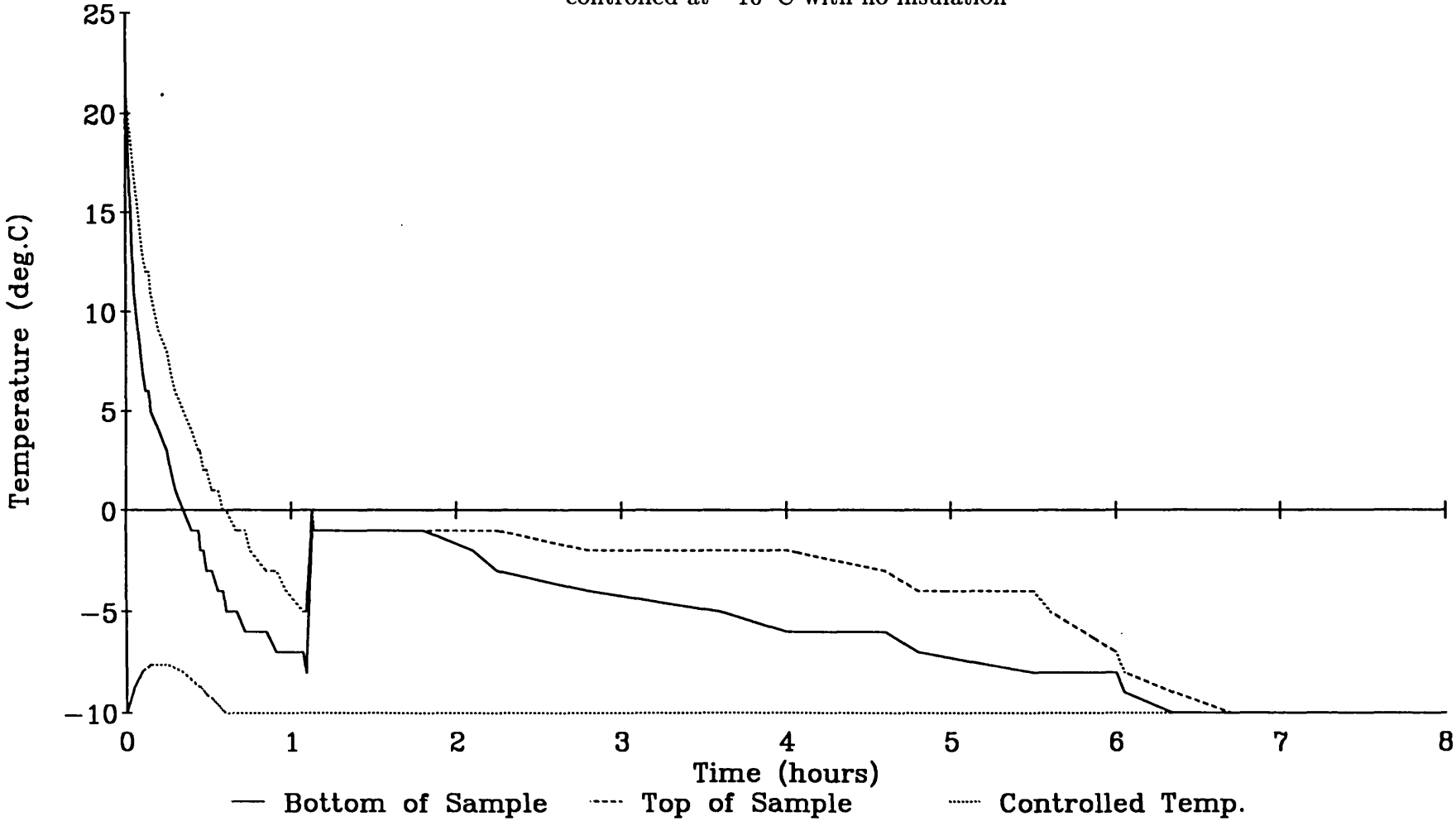


Figure 3.18 Cooling curves for NaNiHCF - NJ9 B3

controlled at −7 °C with insulation at base of sample

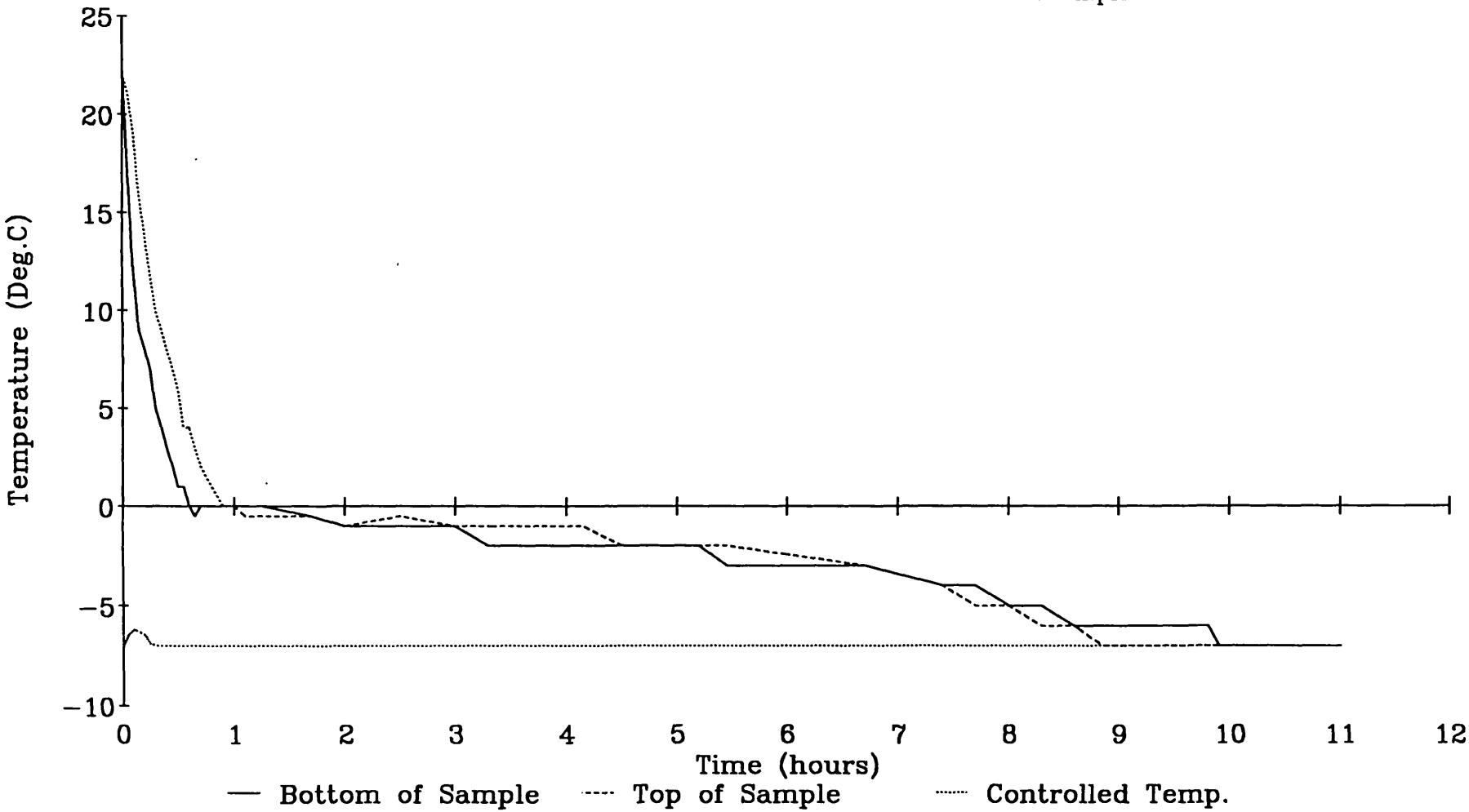
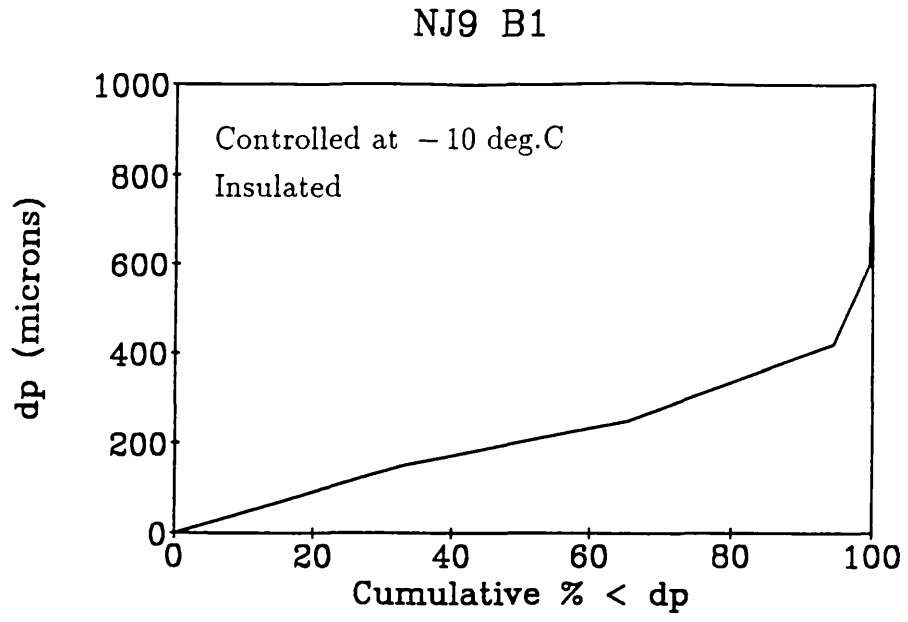
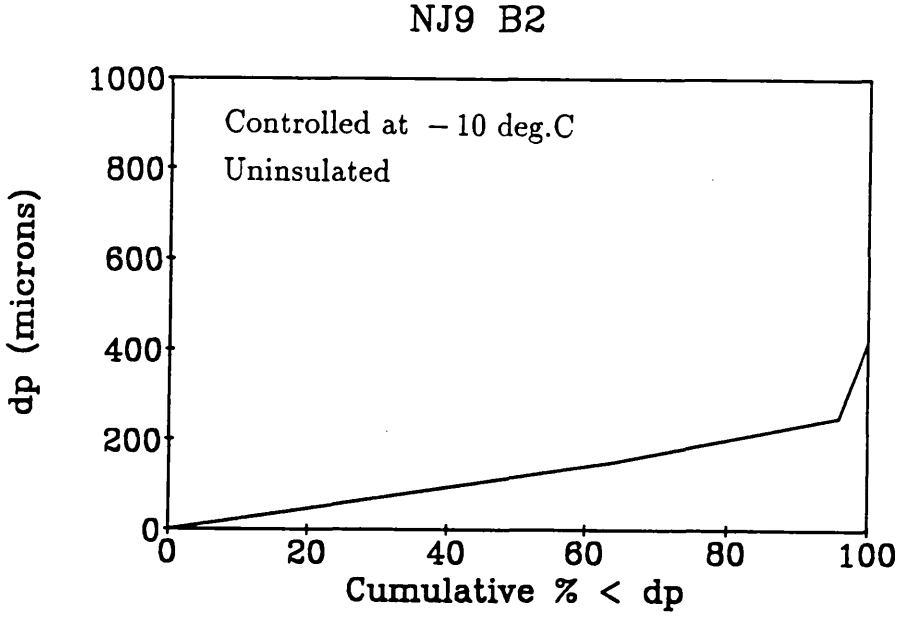
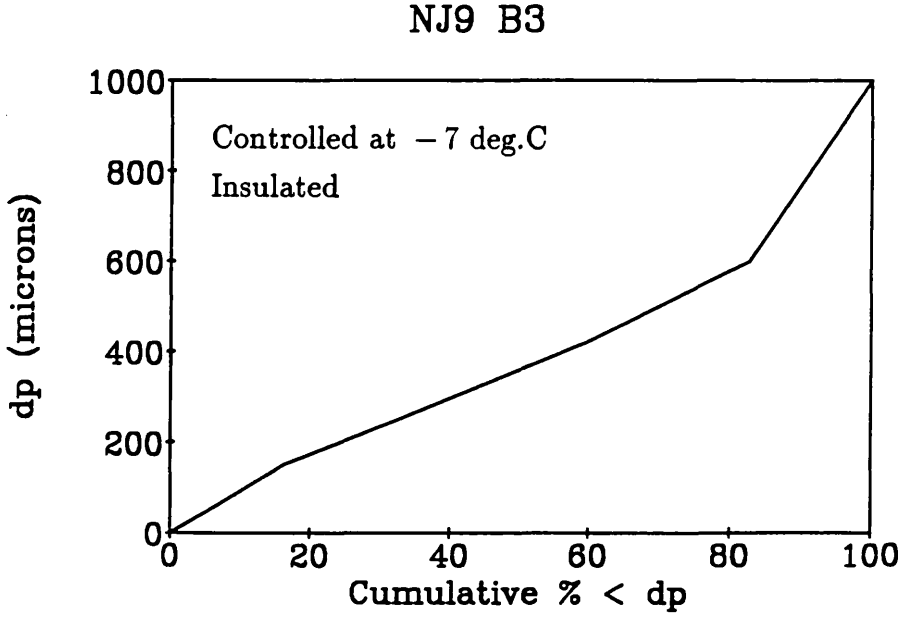


Figure 3.19 Sieve analyses of samples NJ9 B1, NJ9 B2 and NJ9 B3







3.6.5 Discussion

The results from the controlled freezer unit clearly show that the process is reproducible and that a crucial factor is the rate of heat removal from the samples. The samples which were frozen with insulation were found to have a significantly better granular form than those which were not. The improvement was seen at each of the three temperatures studied. Very little difference was seen in the particle size of the samples which were frozen for 15 hours and those frozen for 22 hours, except for the samples at -7 °C for which there was a slight improvement with the extra time.

The cooling curves for the samples provide a good indication of the difference between the samples which were, or were not insulated. In the cases which were not insulated there were significant differences between the temperatures at the top and bottom of the samples, and a high degree of supercooling was observed. This high supercooling is due to rate of heat removal being significantly faster than the rate at which nucleation occurs.

From the sieve analyses of the products, it is evident that the lower heat transfer rate as a result of the insulation is the prime factor for successful granulation. A good indication of the relative rate of heat transfer from the samples is given by the degree of supercooling which is observed in the temperature profiles. A small degree of supercooling was observed when the rate of heat loss from the samples was relatively slow and granulation was achieved.

CHAPTER 4

CHARACTERISATION OF PREPARED SAMPLES OF SODIUM NICKEL HEXACYANOFERRATE

4.1.1 General chemical stability of the hexacyanoferrate complex

The general chemistry of the hexacyanoferrates is detailed by Vogel(130). The transition metal hexacyanoferrates are insoluble in water and cold dilute acids but decompose in alkalis to give the hexacyanoferrate ion and the transition metal hydroxide. Complete decomposition of the hexacyanoferrate to carbon monoxide only occurs when boiled with concentrated sulphuric acid while partial decomposition liberating hydrogen cyanide occurs when boiled with dilute sulphuric acid. It can be assumed that similar reactions occur with nitric acid although these are not mentioned by Vogel. In addition nitric acid will also tend to oxidise the hexacyanoferrate.

Lee(33) investigated the stability of KCuHCF and found that it completely dissolved in hot concentrated sulphuric acid (which was used in analysis) and strong alkali, while partial dissolution also occurred even at moderate alkali concentrations.

From these findings it appears that the stability of the hexacyanoferrates of nickel and copper are similar in that decomposition only occurs at under extreme conditions and under the normal expected operating conditions of pH 2 - 10 the exchangers are stable.

4.2 Conditioning of granular NaNiHCF and KNiHCF at various pH

4.2.1 Experimental

The exchangers (batch 21: 600-1000 microns) were conditioned at a range of pH. A known mass of the exchanger (0.5 g) was contacted with 50 mL of 1 M sodium nitrate solution. The pH of the solution initially adjusted to the correct value by adding drops of either nitric acid or sodium hydroxide and then regularly corrected over a long period (several weeks) until no further change was observed. The solution was then decanted off, the volume measured, and the Ni concentration determined using an ion chromatograph. These results are shown in Table 4.1 for NaNiHCF and in Table 4.2 for KNiHCF.

4.2.2 Discussion

During the conditioning there were significant deviations in the pH of the contact solution from the required value. At low pH there was an observed rise in the pH value and above pH 10, the pH fell. The deviations from the required value were least in the range pH 9 - 10 and the solutions stabilised quickly. These changes in pH may be caused by ion exchange of hydrogen with the alkali metal ions on the exchanger at low pH, or by the dissolution of the exchanger at high pH to give the aqueous hexacyanoferrate ion and nickel hydroxide as discussed below.

At pH 2 there was considerable physical break-up of KNiHCF and slight break-up of NaNiHCF with the formation of a large number of fines. After a period of several days the liquor gained a green tint suggesting the release of nickel from the exchangers. This was confirmed from the analyses of the liquor which are listed in Tables 4.1 and 4.2. The release of nickel under these conditions is similar to that which was found when the precipitates were heated during preparation and this has already been discussed in section 3.3.2. Vol'khin and Kosheeva(46,47) also found that in addition to the exchange of nickel by either sodium or potassium, when KNiHCF is contacted with a sodium solution there is exchange of potassium by the sodium resulting in the formation of $Na_6Ni[NiFe[CN]_6$ as in the case of NaNiHCF.

Table 4.1 Conditioning of NaNiHCF in 1 M $NaNO_3$ at various pH

(NaNiHCF-P21: 600-1000 microns)

pH	Mass of NaNiHCF	Liquor		comments	Final form of exchanger	moles Ni released / moles $Na_4Ni_4(HCF)_3$	Ni:Fe final
		Ni ppm	volume mL				
2	1.5 g	1440	24	liquor has green tint after few days, some fines produced	black granules	0.38	1.207
3	0.5 g	88	63	liquor had green tint after few days no observed breakup of granules	black granules	0.17	1.277
4	0.5 g	3	62	no observed breakup of granules	black granules	0.01	1.330
5	0.5 g	0	61	no observed breakup of granules	black granules	0.00	1.333
8	0.5 g	0	25	no observed breakup of granules	dull black granules	0.00	1.333
10	0.5 g	0	67	no observed breakup of granules	dull black granules	0.00	1.333
12	0.5 g	0	50	liquor brown after few days indications of breakup of granules	brown granules	0.00	1.333

Table 4.2 Conditioning of KNiHCF in 1 M $NaNO_3$ at various pH

(KNiHCF-P21: 600-1000 microns)

pH	Mass of NaNiHCF	Liquor		comments	Final form of exchanger	moles Ni released / moles $Na_4Ni_4(HCF)_3$	Ni:Fe final
		Ni ppm	volume mL				
2	1.5 g	1200	22	liquor has green tint after few days granules broke up into fines	fine black granules	0.30	1.234
3	0.5 g	114	63	liquor had green tint after few days slight breakup of granules	brown granules	0.24	1.253
4	0.5 g	13	59	no observed breakup of granules	brown granules	0.03	1.323
5	0.5 g	6	58	no observed breakup of granules	brown granules	0.01	1.330
8	0.5 g	0	27	no observed breakup of granules	brown granules	0.00	1.333
10	0.5 g	0	59	no observed breakup of granules	brown granules	0.00	1.333
12	0.5 g	0	54	liquor brown after few days indications of breakup of granules	brown granules	0.00	1.333

4.3 Mechanical strength of prepared granules of NaNiHCF and KNiHCF

The mechanical strength of particles was measured in the Industrial Chemistry Division at AEA Technology, Harwell using an Instron Compression Tester. This was calibrated using a weight of 100g to give a full scale reading on the pen recorder.

About 20 individual granules were placed on a microscope slide with a drop of water on each granule. The slide was lined up so that one of the granules was under the weight which was slowly increased until the two peaks were observed. The first peak indicates the point at which the particle structure begins to deform and the second the point when the particle shatters. The test was carried out for about 20 particles to obtain a statistically significant result. As the area of the particles was not known, the result was expressed as a mass supported by an individual particle.

It was found that the prepared NaNiHCF(21 0.42–0.6mm) had a strength of 61 ± 43 g normally, and 65 ± 46 g after they had been heat treated (150°C for 10 mins) which was stronger than the sample of NaNiHCF from Applied Research in Belgium. For KNiHCF the strengths were 47 ± 33 g normally and 42 ± 34 g after the same heat treatment. It can be concluded that the strengths appear to be independent of the heat treatment which is in contrast to increased stability of the heat treated particles in aqueous solutions. The strengths of all the nickel cyanoferrates were appreciably better than that of the copper cyanoferrate from Applied Research which was 29 ± 13 g.

In all of the samples there was a large spread in the results with the error being as large as two thirds of the mean value in some cases.

4.4 Chemical analysis

4.4.1 Chemical decomposition

The composition of prepared hexacyanoferrates can be determined by dissolving them in boiling concentrated sulphuric acid and analysing the resulting solution after dilution. The reaction for the decomposition is given by Vogel(130) and yields the sulphates of all the cations generated (Ni^{2+},Na^{+}, Fe^{3+} and NH^{+}) and carbon monoxide.

On dilution, if the reaction is not complete, some ferrous sulphate will react with undecomposed ferrocyanide yielding $Na_2Fe[Fe(CN)_6]$ which gradually oxidises to Prussian Blue(s). Hence, complete decomposition in the concentrated acid is confirmed if the solution remains clear after dilution.

4.4.2 Experimental

0.1 g of the sample was accurately weighed out and added to 20mL concentrated sulphuric acid in a small beaker. This was then placed on a hot plate, brought to the boil and simmered for at least half an hour. The sample is seen to dissolve and the solution become clear. The solution was allowed to cool and then added slowly to approximately 50 mL distilled water in a 100 mL volumetric flask. The solution was then made up to 100 mL by slowly adding distilled water.

4.4.3 Analysis of solutions

Nickel, iron and copper were determined by atomic absorption on a spectrometer (in the analytical laboratory of the Department of Chemical Engineering and Chemical Technology, Imperial College). The samples were diluted to be within the linear range of the instrument. It was found more reliable to use the wavelengths with a sensitivity of about one tenth that of the most sensitive for each metal. In this way the linear range was extended up to about 40 ppm and more consistent readings could be taken. Sodium was determined by atomic emission after diluting samples by a factor of 100 to obtain clear and

consistent readings. Analysis of potassium could not be obtained using the available spectrometer.

The measured concentrations of the samples are listed in Table 4.3. The total amount of each element in the samples and the molar ratio based on 2 moles iron were calculated. The discrepancy in mass between that of the sample and the combined mass of sodium, hexacyanoferrate (measured as iron) and nickel was assumed to be that of the water of crystallisation. The calculated stoichiometry of the samples are given in Table 4.4.

4.4.4 Discussion

The ratio of Ni:Fe obtained from the analyses are in general agreement with the ratios that were calculated from the preparations. However for samples 20 Na, 21 Na and 21K (described in Section 3.3) the Ni:Fe ratio from the analysis and that of the reactants show significant differences. In the case of 20 Na the ratio from the analysis is 1.5 while the remaining samples are in the range 1.20-1.25. For these 4 samples the Ni:Fe ratio of the reactants was 1.33.

There is much better agreement with the analysis of Series B where the Ni:Fe ratio from the analysis is within10% of the reactant ratio of 1.3.

There appears to be large variations in the amount of sodium in the samples, this may be the case, or the determination of sodium by atomic emission may have been unreliable: this needs to be clarified in future work.

Table 4.3 Chemical Analysis of Solutions from Decomposition of Hexacyanoferrates

0.1 g of the hexacyanoferrate was dissolved into 15ml conc. H_2SO_4 and 15 ml HNO_3 and made upto 100 ml.

Sample		Nickel			Hexacyanoferrate			Sodium			Water	
	mass mg	ppm	mg	mmol	ppm (Fe)	mg (HCF)	mmol	ppm	mg	mmol	mg	mmol
B4A1	100	160	16	0.27	130	49.39	0.23	111	11.1	0.48	23.51	1.31
B4A2	100	160	16	0.27	126	47.87	0.23	110	11	0.48	25.13	1.40
B4C1	100	160	16	0.27	124	47.11	0.22	101	10.1	0.44	26.79	1.49
B4C2	100	155	15.5	0.26	128	48.63	0.23	96	9.6	0.42	26.27	1.46
B6A1	100	174	17.4	0.30	118	44.83	0.21	63	6.3	0.27	31.47	1.75
B6A2	100	172	17.2	0.29	118	44.83	0.21	65	6.5	0.28	31.47	1.75
B6C1	100	163	16.3	0.28	124	47.11	0.22	82	8.2	0.36	28.39	1.58
B6C2	100	168	16.8	0.29	133	50.53	0.24	84	8.4	0.37	24.27	1.35
D5A1	100	160	16	0.27	133	50.53	0.24	93	9.3	0.40	24.17	1.34
D5A2	100	164	16.4	0.28	130	49.39	0.23	87	8.7	0.38	25.51	1.42
D5B1	100	160	16	0.27	135	51.29	0.24	91	9.1	0.40	23.61	1.31
D5B2	100	160	16	0.27	137	52.05	0.25	101	10.1	0.44	21.85	1.21
D6A1	100	165	16.5	0.28	133	50.53	0.24	104	10.4	0.45	22.57	1.25
D6A2	100	172	17.2	0.29	126	47.87	0.23	106	10.6	0.46	24.33	1.35
D6B1	100	168	16.8	0.29	132	50.15	0.24	85	8.5	0.37	24.55	1.36
D6B2	100	157	16.7	0.28	120	45.59	0.22	87	8.7	0.38	29.01	1.61

Table 4.4 Stoichiometry of hexacyanoferrates from chemical analysis

Summary of the results listed in Table 4.3.

Sample	Nickel	Iron	Ni:Fe ratio	Sodium	Water
B4A1	2.34	2.00	1.17	4.14	11.21
B4A2	2.41	2.00	1.20	4.24	12.37
B4C1	2.45	2.00	1.23	3.95	13.39
B4C2	2.30	2.00	1.15	3.64,	12.72
B6A1	2.80	2.00	1.40	2.59	16.53
B6A2	2.77	2.00	1.39	2.67	16.53
B6C1	2.50	2.00	1.25	3.21	14.19
B6C2	2.40	2.00	1.20	3.06	11.31
D5A1	2.29	2.00	1.14	3.39	11.27
D5A2	2.40	2.00	1.20	3.25	12.17
D5B1	2.25	2.00	1.13	3.27	10.84
D5B2	2.22	2.00	1.11	3.58	9.89
D6A1	2.36	2.00	1.18	3.79	10.52
D6A2	2.60	2.00	1.30	4.08	11.97
D6B1	2.42	2.00	1.21	3.12	11.53
D6B2	2.65	2.00	1.32	3.52	14.99

Table 4.5. Comparison of Ni:Fe ratios calculated from preparation and analysis

Sample	Ni : Fe of reactants	Ni : Fe calculated from preparation (mean values)	Ni : Fe from analysis
B2A	1.10	1.10	NA
B2C	1.10	1.10	NA
B3A	1.20	1.20	NA
B3C	1.20	1.20	NA
B4A	1.30	1.30	1.19
B4C	1.30	1.28	1.19
B5A	1.40	1.40	NA
B5C	1.40	1.31	NA
B6A	1.50	1.50	1.40
B6C	1.50	1.35	1.23
D5A	1.30	1.25	1.17
D5B	1.30	1.25	1.12
D6A	1.30	1.21	1.24
D6B	1.30	1.21	1.28

NA - Analysis not carried out

There were particularly large variations in the mass balances of the samples which was assumed to be the water content. It is generally found that water is present in HCFs both as water of crystallisation and as interstitial water. In some HCFs, it has been found that there is a fixed amount of water, for example Shahbandeh(43,88) found KCuHCF to have 8-10 molecules of water. The present results suggest that this is not the case with the nickel hexacyanoferrate with the water varying from 7 to 20 molecules based on 2 molecules of $Fe(CN)_6$). In the

survey of NiHCF preparations carried out by Loos-Nescovic et al.(34), it was found that there were few cases in which the water content was measured and that no fixed amount had been found.

4.5 Measurement of surface area

The surface area of material is expected to be proportional to the sorption capacity and the pore size, as was found by Shahbandeh and Streat(43,88) in a study of the sorption of caesium by CuHCF.

The standard method of measuring the surface area of a solid is based on the physical adsorption of a gas on the surface. Usually the amount of nitrogen is measured at its normal boiling point and the amount adsorbed to give a covering of one molecular layer is determined to give the surface area. The classical 'static volumetric method', developed by Brunnauer Emmett and Teller(131), requires measurement of the volume of N_2 adsorption over a range of pressures and is generally laborious. A discussion of this method and other methods developed more recently is given by Gregg and Sing(132) and Smith(133). The traditional method has also been automated by the use of pressure transducers and direct analysis of data which has considerably improved its usefulness.

The surface area of some of the prepared samples of sodium nickel hexacyanoferrate was measured in such a way using a Micromeretics ASAP 2000 surface area analyser which was available in the Department of Chemical Engineering and Chemical Technology at Imperial College. The adsorption and desorption isotherms were measured and tested for the fit with the BET isotherm. A typical output of the adsorption isotherms is shown in Figure 4.1 and the fit of the BET Isotherm is shown in Figure 4.2. From the adsorption and desorption isotherms at higher pressures when capillary condensation occurs, a measurement of the micropore size distribution can be obtained using the Kelvin equation and a correction for the thickness of adsorbed layers(132,133). These calculations are carried out directly by the surface area analyser and are included in the printout.

Figure 4.1 Measured Isotherm Plot for NaNiHCF-NJ7 B1

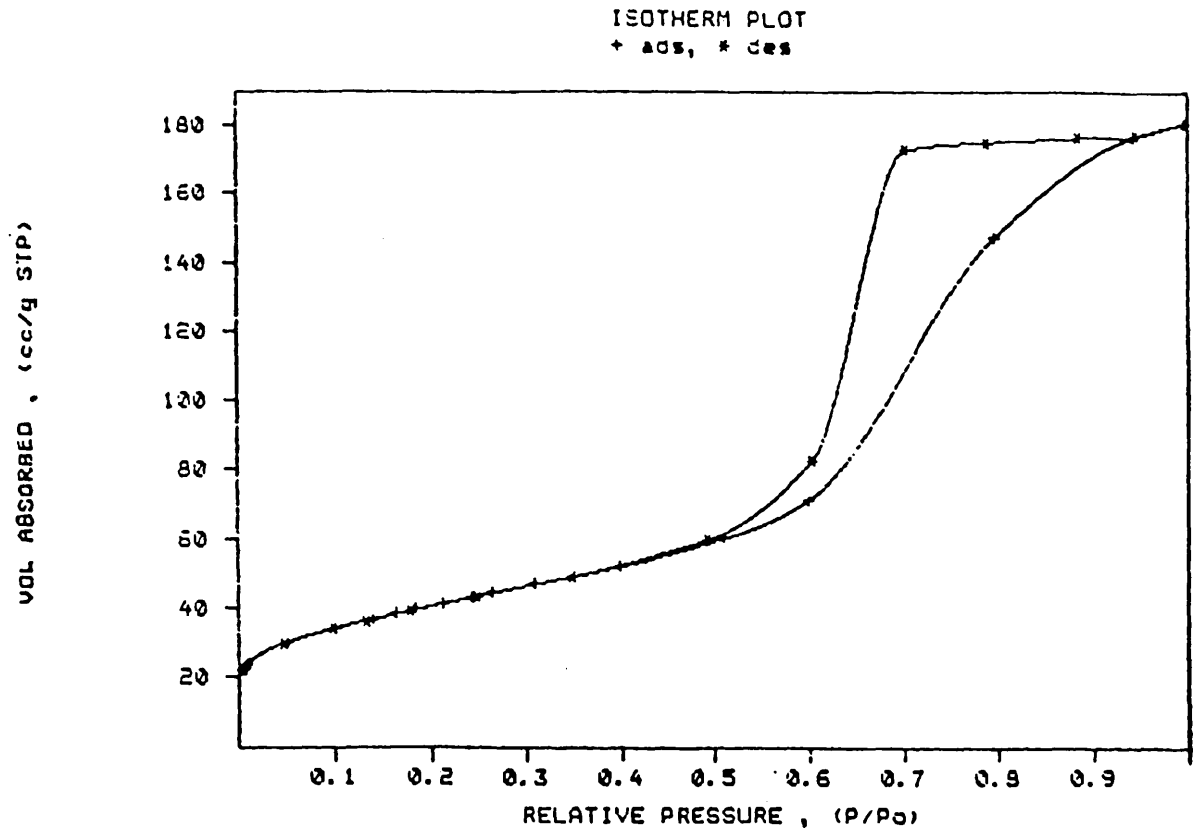
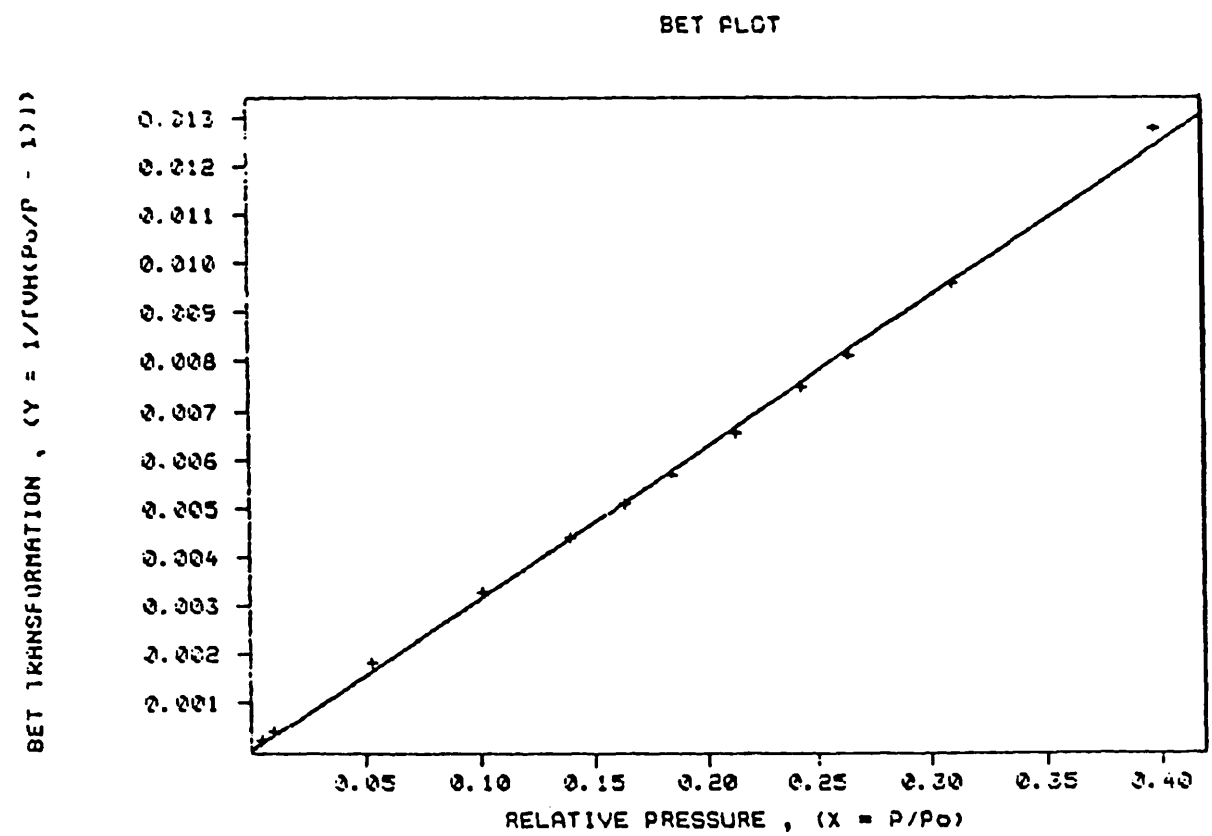


Figure 4.2 BET Plot from Measured Isotherm Plot



The measured values of the surface area, pore volume and pore size for the samples of NaNiHCF which were analysed are given in Table 4.6.

Table 4.6 Characterisation from measured adsorption and desorption isotherms

SAMPLE	NJ3 B2	NJ3B2	NJ7 B1	NJ7B1
PARTICLE SIZE (microns)	150-250	150-250	250-420	250-420
DRYING TEMPERATURE	110 °C	170 °C	110 °C	170 °C
AREA (m^2/ g)				
BET Surface area	88	89	139	134
Langmuir Surface Area	154	169	-	-
Single point Adsorption S.A at p/p_0 = 0.3096	90	92	140	135
BJH Cum. Adsorption surface area of pores 1.7 to 300 nm diam.	106	108	211	170
BJH Cum. Desorption surface area of pores 1.7 to 300 nm diam.	140	133	178	224
Micropore Area	76.6	86	0.267	1.82
VOLUME (cc/g)				
Single point total pore volume < 2.64 nm at p/p_0= 0.3096	0.047	0.047	0.072	0.070
BJH Cum. Adsorption pore volume of pores 1.7 to 300 nm diam.	0.260	0.277	0.277	0.289
BJH Cum. Desorption pore volume of pores 1.7 to 300 nm diam.	0.261	0.275	0.281	0.295
Micropore volume	0.0073	0.0056	0.0018	0.0023
PORE SIZE (nm)				
Average pore diameter (4V/A by BET)	1.22	1.13	2.068	2.07
BJH Adsorption average pore diameter (4V/A)	9.8	10.3	6.23	6.78
BJH Desorption average pore diameter (4V/A)	7.4	8.3	5.33	5.27

The results show a marked difference in the surface area, pore volume and pore size between the sample which was heated in the mother liquor(NJ3 B2), and the sample which was not(NJ7 B1). The values follow the expected increase which is also seen in the measured caesium uptake of the products which is detailed in Chapter 5.

There is was a large difference in the micropore area which was close to the total BET surface area for the samples of NJ3 B2 (76.6 and 86 m^2/g), while for the samples of NJ7 B1 (0.267 and 1.82 m^2/g) the micropore area was only a small

fraction of the total area.

There were only very slight changes in all of the measured parameters for the both samples after drying at 110 or 170 °C. This indicates that there is little of no change in the structure of the materials after they are dried at the higher temperature.

4.6 Measurement of pore size distribution by mercury porosimetry

The macropore size distribution of the prepared samples, (pore sizes generally larger than 200 Å), was measured using the usual mercury penetration method which is outlined by Smith(133). A Carlo Erba Mercury Pressure Porosimeter Model 70-H was used which was available in the Department of Chemical Engineering and Chemical Technology at Imperial College. A pressure range of 0 to 1000 bar was used. The pore diameter is obtained by equating the force due to the surface tension, preventing the mercury from entering a pore, with the applied force. Ritter and Drake(134) obtained the expression given in equation 4.1 which was used to calculate the pore radius, a. Any set of consistent units may be used to calculate a.

$$a = \frac{-2\,\sigma\cos\theta}{p} \tag{4.1}$$

For mercury, a contact angle of $\theta = 130^{\circ}$ and the surface tension of $\sigma = 485$ dyne cm^{-1} are usually used.

The pore size distribution was measured for two samples of NaNiHCF which were dried at temperatures of 110 and 170 °C. The cumulative pore volume(cc) is plotted against the pore size(Å) for samples NJ9 B2 (not heated in the preparation) in Figure 4.5, and for samples of NJ3-A1(heated in the preparation) in Figure 4.6. The total pore volumes of the samples are given in Table 4.7.

Table 4.7 Total pore volume of samples measured by mercury porosimetry

Sample	drying temperature °C	measured pore volume cc/g
NJ3 A1	110	0.0791
NJ3 A2	170	0.1017
NJ9 B2	110	0.0975
NJ9 B2	170	0.0848

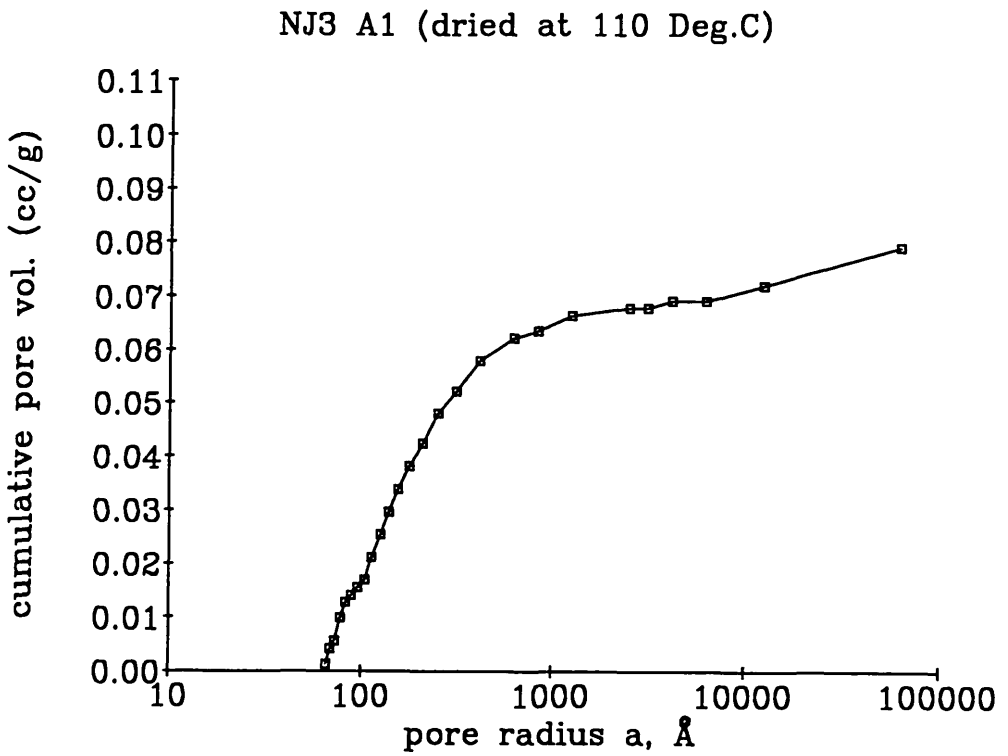
From the measured shapes of the cumulative pore volumes it is found that the pore radius of the samples is within the range of 80 to 2000 Å for all the samples. There is a discontinuity in the curve for sample NJ9-B2 which was dried at 110 °C which is most likely due to the sample shattering under the applied pressure. The shapes of the curves are very similar indicating little change in the macropore (intraparticle) volume.

These results, together with the values for the area, volume and pore size obtained from the N_2 isotherm, suggest that the samples are composed of individual particles which are compressed together in the freeze-thaw process to form a granular product. The relative large differences measured in the micropores imply that heating the sample in the mother liquor during the preparation has an important effect on the structure within the individual particles. In contrast, the comparatively small changes in the macropores suggest that there is no changein the way that the different samples are compacted together as a result of the freeze-thaw process.

Figure 4.3 Cumulative pore volume from mercury penetration method for samples of NaNiHCF-NJ3 A1

(Sample with the precipitate heated in mother liquor at 80 °C for 2 hours)

(Particle Size 250-420 microns)



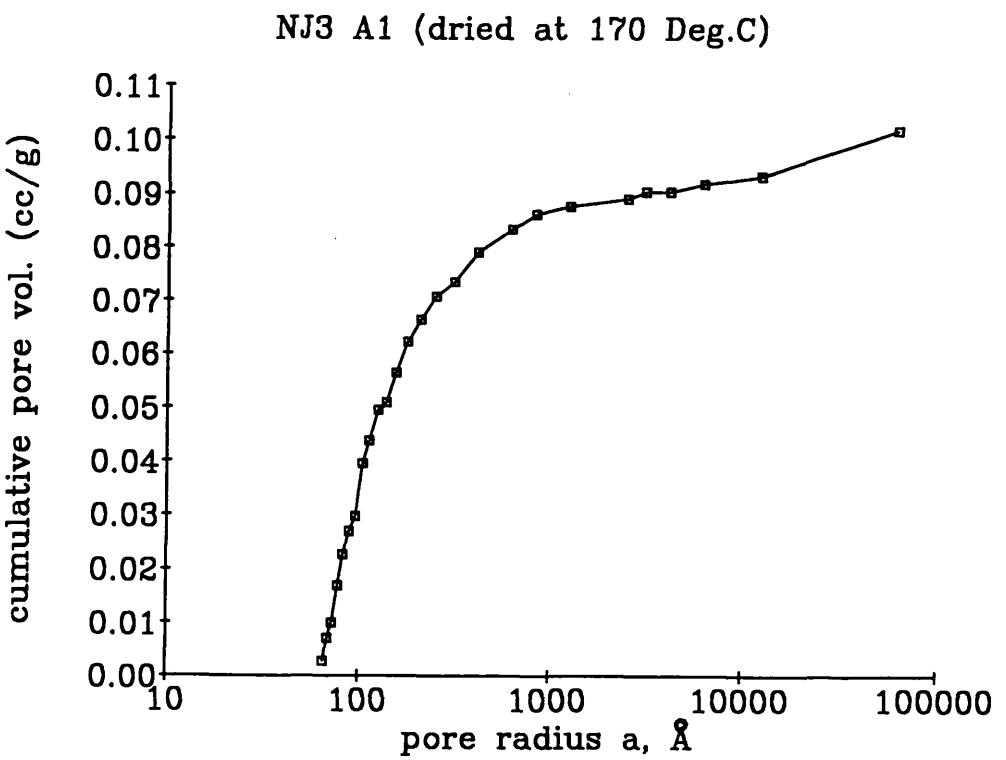
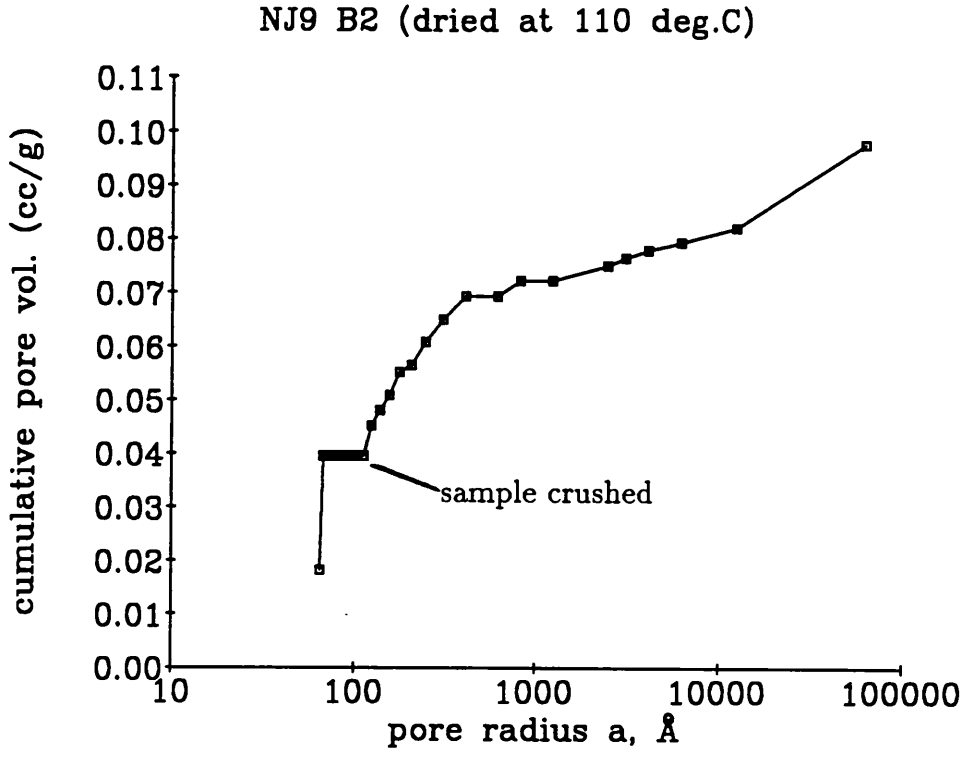


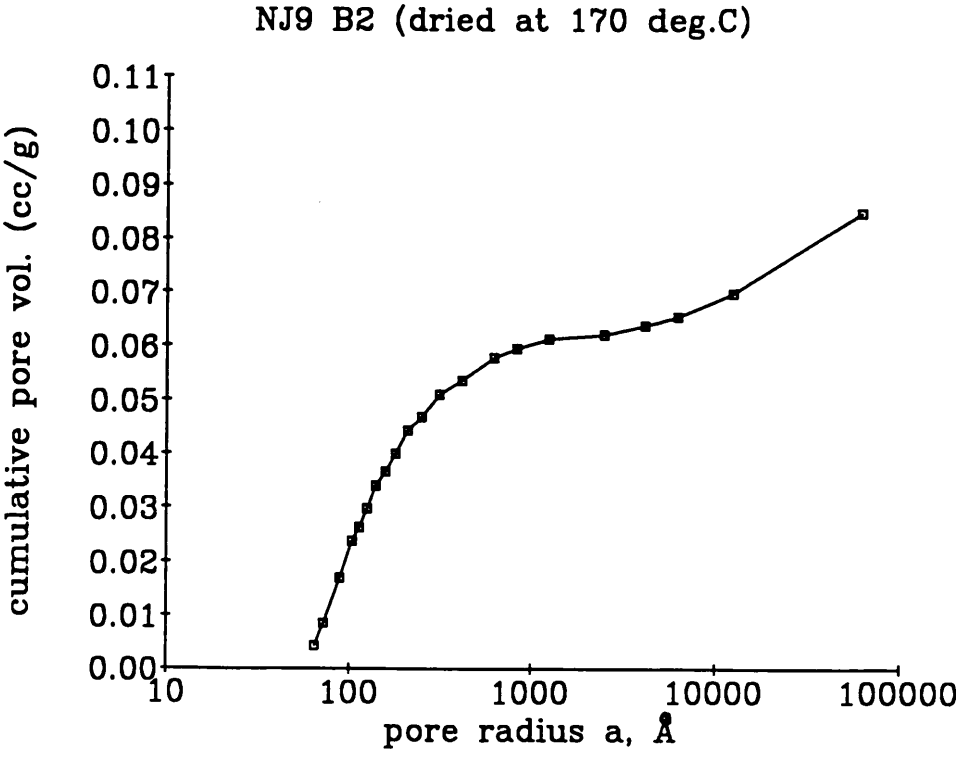
Figure 4.4 Cumulative pore volumes from mercury penetration method

For samples of NaNiHCF-NJ9 B2

(Sample for which the precipitate was not heated in mother liquor)

(Particle Size 250-420 microns)





4.7 Use of electron microscope to observe granular samples

Using a Jeol JSM-T220A electron microscope, some pictures were taken of two of the prepared samples of NaNiHCF. The appearance of both samples which either were heated in the preparation or not heated during the preparation was assessed. A range of magnifications from $\times 50$ to $\times 20000$ was used.

The particles were mounted onto the microscope stubs and gold coated with a E.M. gold splutterer. The pictures were taken with an exposure time of 70 seconds with an applied voltage of 10 kV, except at higher magnification when the voltage was increased to 15 or 20 kV. Four pictures of prepared samples are shown in Figures 4.5 to 4.8.

Two pictures at a magnification of $\times 50$ are shown, in Figure 4.5 of a sample of NaNiHCF(NJ3 A1) which was heated in the mother liquor during the preparation and in Figure 4.6 of a sample(NJ7 B1) which was not heated in the preparation. The granular form of both is clearly seen and there appears to be distinct differences in the shape of the granules. There are indications of curved surfaces in Figure 4.5 which may be due to the presence of air bubbles in the samples during the freezing process.

Two pictures at a magnification of $\times 2000$ are shown in Figure 4.7 for sample NJ3 A1(heated) and in Figure 4.8 of sample NJ7 B1(unheated). The picture in Figure 4.8 was zoomed in onto a crack to observe it more closely. The cause of the cracking may be due to the sample being dried at 170°C rather than 110°C which was generally used. With both samples the surface appears to be fairly uniform though there are small particles attached to the surface. It is not easy to draw any positive conclusions from the pictures with regard to whether the particles are crystalline or composed of an array of small particles which have been compacted together as was suggested in Section 4.6

Figure 4.5 Picture of sample NaNiHCF-NJ3 A1 at magnification $\times 50$

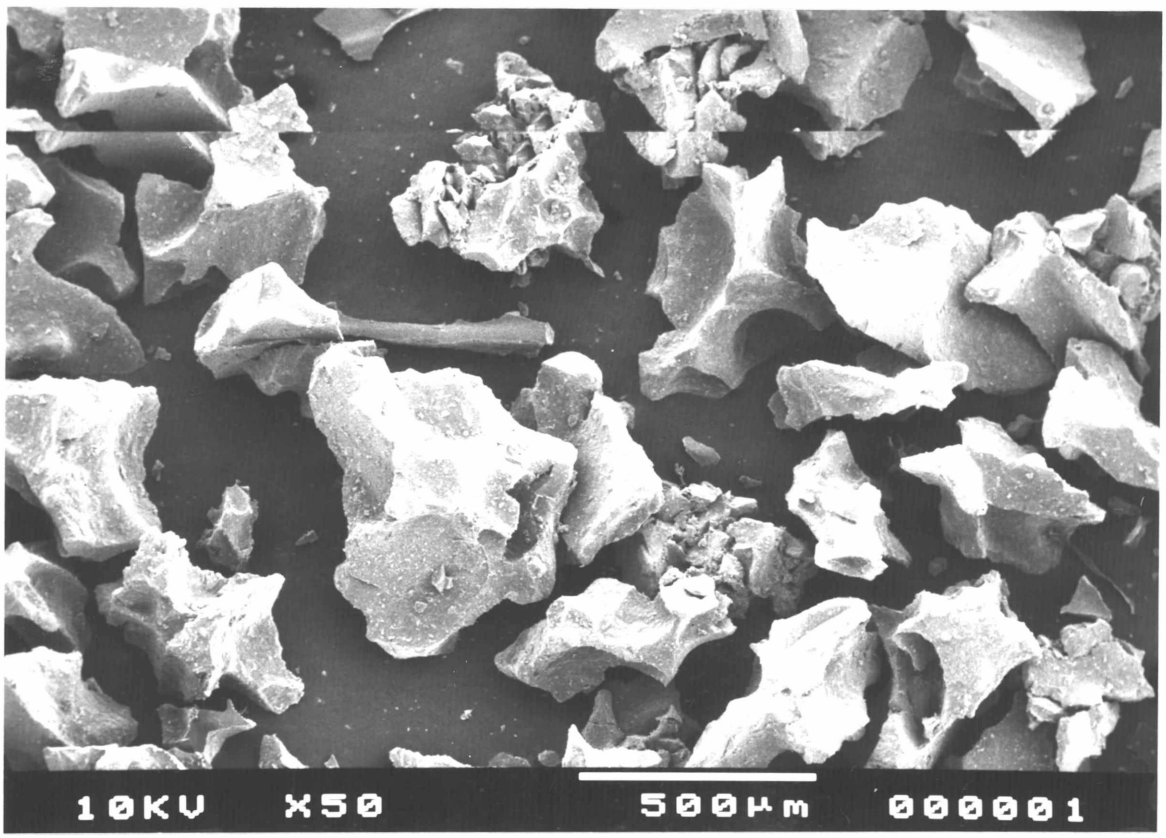


Figure 4.6 Picture of sample NaNiHCF-NJ7 B1 at magnification $\times 50$

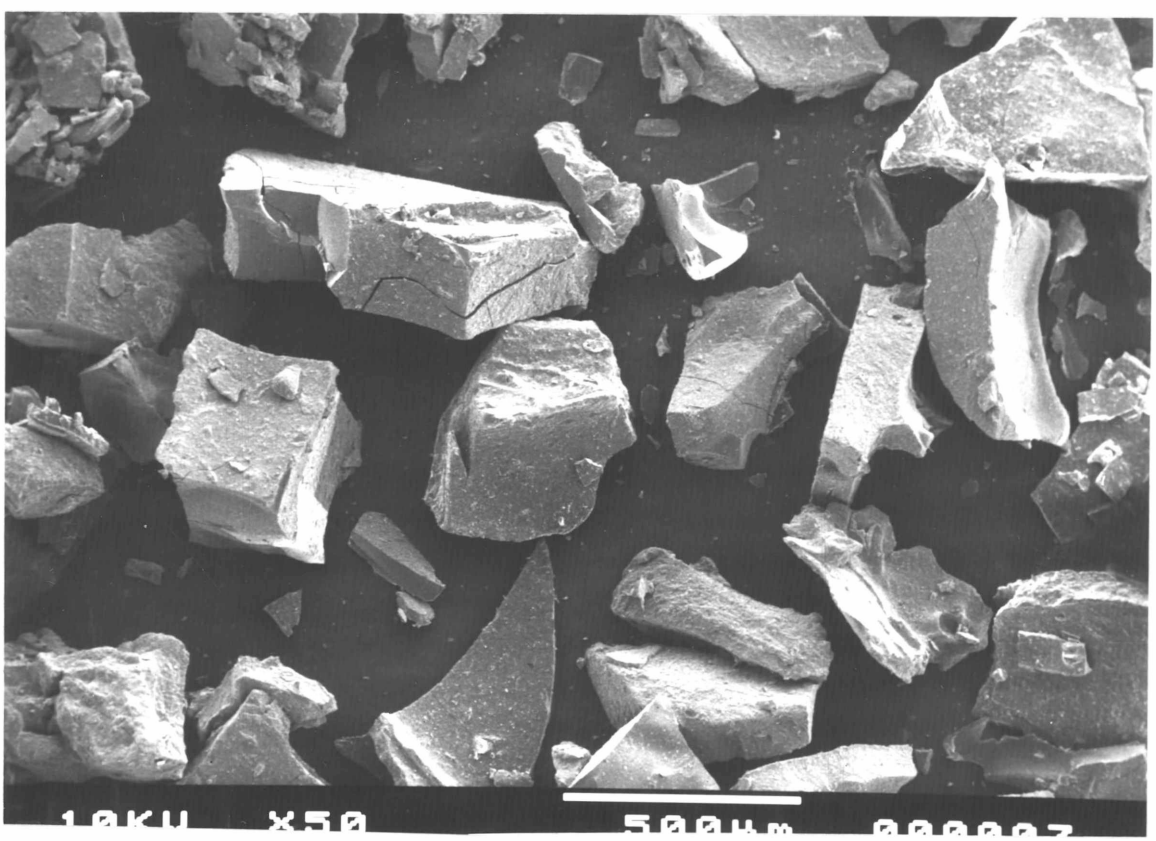


Figure 4.7 Picture of sample NaNiHCF-NJ3 A1 at magnification × 2000

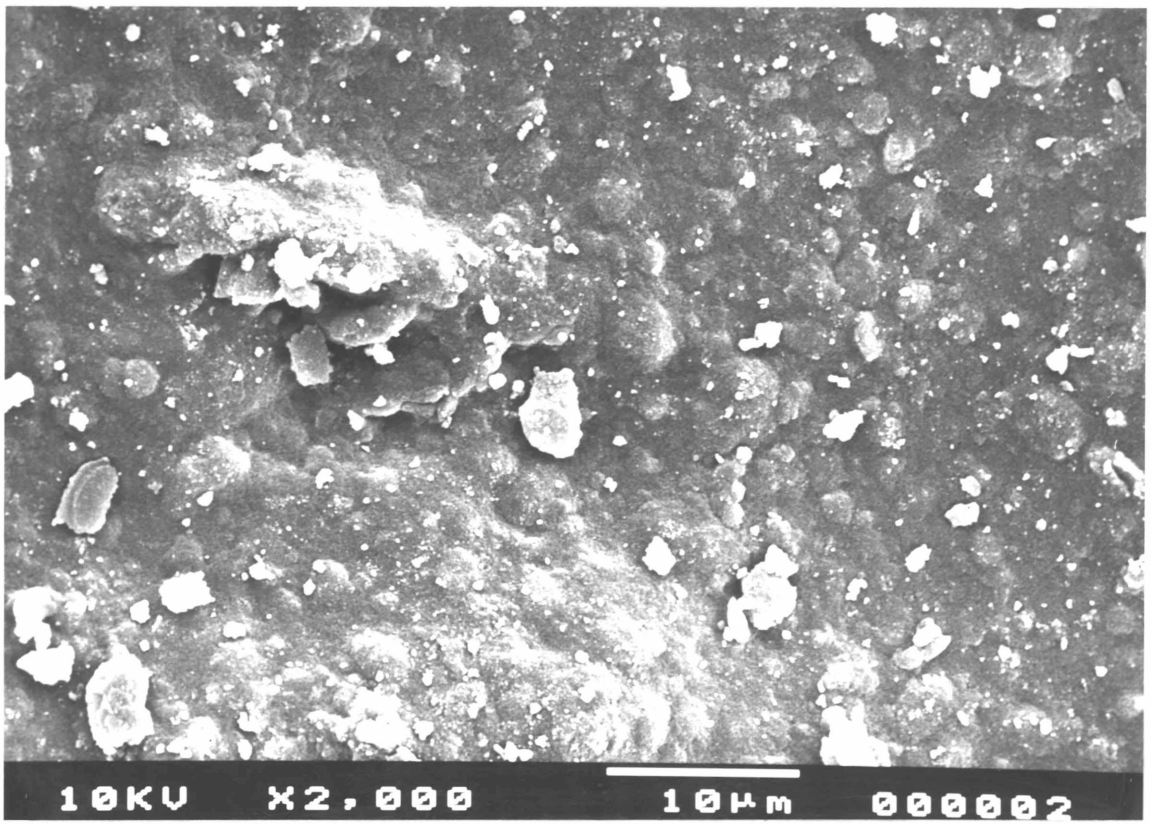
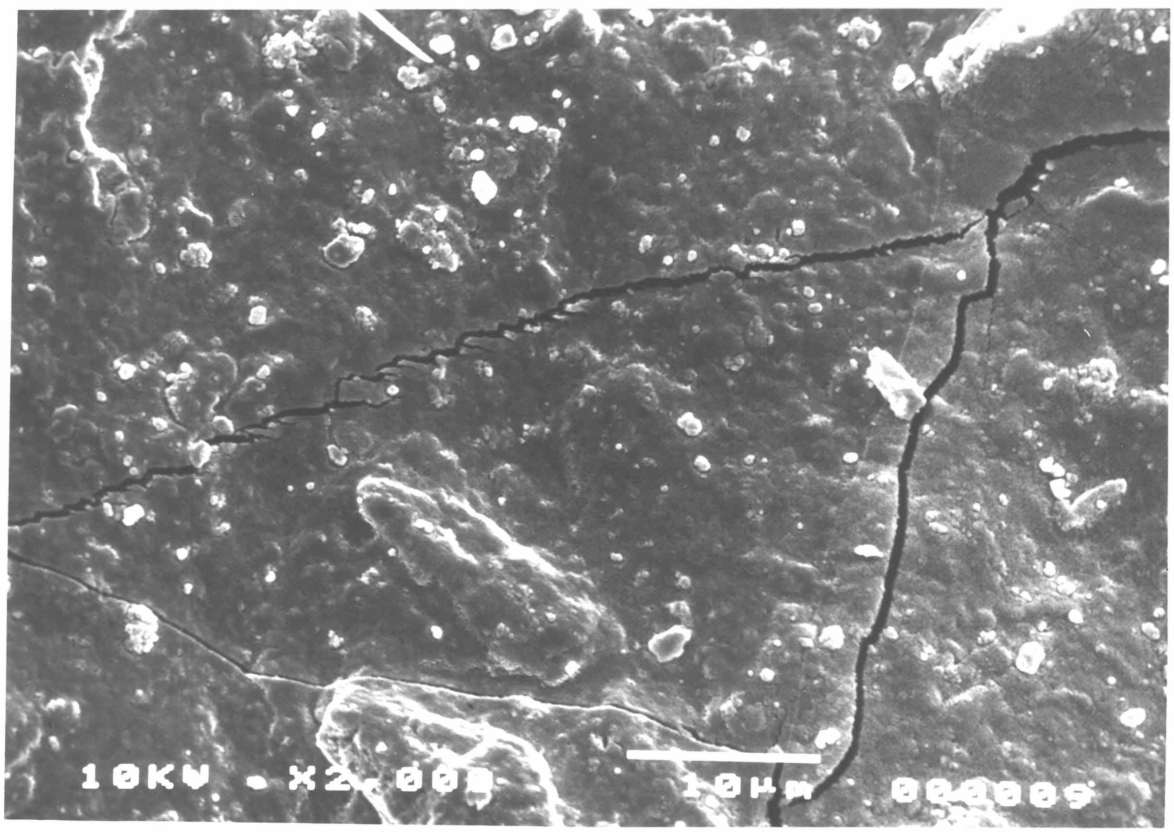


Figure 4.8 Picture of sample NaNiHCF-NJ7 B1 at magnification × 2000



CHAPTER 5

THE SORPTION OF CAESIUM BY GRANULAR NICKEL HEXACYANOFERRATES

5.1 Introduction

The term 'sorption' is used to describe phenomena which involve the transfer of molecules between a solid and fluid. The most common of these phenomena being physical sorption, chemisorption, ion exchange and capillary condensation. The occurrence, specific characteristics and differences between each of these are covered in the standard texts such as that by Ruthven(135), and the review of separation by adsorption methods given by Vermeulen(136).

The sorption of caesium by the nickel HCF, is generally irreversible except for elution by silver which itself becomes irreversibly attached to the HCF(100, 101). Caesium sorption is found to be largely due to direct exchange of the alkali metal although a contribution from exchange of nickel is also found(46).

In the present work, the mechanism of the sorption has not been studied in any detail, and only direct measurements of the performance of the prepared samples for the removal of caesium was assessed.

5.2 The assessment of sorption properties

5.2.1 Percentage removal and distribution coefficient

The percentage removal of a solute, and the distribution coefficient are widely used for an initial assessment of the sorption properties of a material. A known mass of the material is contacted with a volume of solution for a period of time, t. For the removal of radionuclides, the concentration is conveniently measured by counting a sample of the solution, and the percentage caesium removal(P) and the distribution coefficient(R_d) are calculated directly as defined in

Equations 5.1 and 5.2 respectively.

$$P = \frac{A_0 - A_t}{A_0} \times 100\ \% \qquad (5.1)$$

$$R_d = \frac{A_0 - A_t}{A_t} \cdot \frac{V}{m} \qquad mL\ g^{-1} \qquad (5.2)$$

The use of a distribution coefficient, R_d, which is defined after a specified contact time, is more applicable assessing the removal of radionuclides than the equilibrium distribution coefficient, K_d, when the final approach to equilibrium is very slow.

5.2.2 Sorption capacity and uptake

The capacity is a measure of the amount of solute which is taken up by a specified amount of adsorbent. It is important in the characterisation of a material and is also required for numerical calculation of adsorption processes. The sorption capacity is usually defined specifically as the amount of solute taken up by adsorption rather than ion exchange, although the term is often used in a broader sense to measure the amount of a species which can be taken up by a solid.

The capacity has been defined in a variety of different ways, and with a variety of units, depending on the nature of the sorption mechanism and the experimental conditions. A detailed discussion of the most common of these definitions is given by Helfferich(20). If possible the capacity should be defined such that it is a characteristic constant of a material, although in practice it is more usual to use a definition based on experimental conditions.

The maximum, or ion exchange capacity, refers to the total number of ionogenic groups per specified amount of exchanger. For example, a sample of nickel hexacyanoferrate with the formula $Na_{1.4}Ni_{1.3}Fe(CN)_6$ which allowed total exchange of Na with Cs would give a total capacity of 4.37 meq/g (581mg Cs/g). However, in practice it has been found that partial exchange of the Ni also takes

place as described above, and additionally there is variable amount of water associated with the material as described in Sections 2.4.4 and 4.3.4. These factors lead to a large degree of uncertainty in the stated value of the maximum capacity for the nickel hexacyanoferrate, resulting in the value having little practical significance.

For a given set of experimental conditions such as pH, concentration, and temperature, an apparent capacity can be defined as the number of ionogenic groups which are available, or a useful capacity defined when equilibrium is not attained. A breakthrough capacity can also be defined as that utilised in a column test under specific conditions.

In the present work, only a direct assessment of the performance of the prepared samples for the removal of caesium is required, and it is convenient to consider only the measured uptake over a fixed period of time. The uptake can be conveniently expressed as the amount of caesium per unit mass of the dry exchanger, using units of either meq/g or mg Cs/g, for a given set of conditions. The uptake was measured in batch tests by analysis of the solution and calculating the uptake by mass balance. Measurement of the breakthrough capacity was also made in column tests as described in Section 6.

5.2.3 Sorption isotherm

The sorption isotherm gives the equilibrium concentration of a solute in the solid phase as a function of the concentration in the fluid phase at constant temperature. Three major classes of isotherms are characterised according to their effects on column performance, a favourable case in which the shape is convex upward, an unfavourable case which is concave upward, and an intermediate case which is a linear function. Additionally, a fourth class of isotherm can be characterised when the equilibrium is extremely favourable and the sorption considered irreversible. In fixed bed operation, a favourable isotherm leads to relatively sharp concentration gradients in the direction of flow, while an

unfavourable isotherm leads to more diffuse boundaries.

For gas-solid systems, the classical definition of five types of isotherms was given by Brunauer et al.(137). These types being entirely favourable at all concentrations, entirely unfavourable at all concentrations, and types having a point of inflection with ranges of both favourable and unfavourable equilibrium.

The Brunauer-Emmett-Teller(BET) equation(131) is widely used for the measurement of surface area as described in Section 4.5 and can be used to fit two of the isotherm types. When the adsorption is restricted to a monolayer, the BET equation for the isotherm reduces to the familiar Langmuir equation. Both of these equations are based on the assumption that the enthalpy of adsorption does not change when the concentration of the solute in each phase changes. The Tempkin isotherm is derived from the Langmuir isotherm by assuming that the heat of adsorption drops linearly with increasing loading, and the Freundlich isotherm is derived by assuming a logarithmic decrease(133). The Freundlich isotherm was originally used empirically to fit experimental data for the sorption of organic from aqueous solution by charcoal(138), and due to its flexibility can usually be used to fit data over a wide range of concentrations.

Other forms of isotherms have been developed empirically by Kobble and Corrigan(139), or by Sipps(140) assuming a particular enthalpy distribution. At low concentrations, both these forms reduce to the Freundlich relationship.

In adsorption from the liquid phase, it is assumed that the solid is fully wetted by the liquid and, by using the liquid phase solute concentration in place of the partial pressure, the same approach can be used in an empirical way(136). In the liquid phase, the Freundlich relationship is usually expressed in the following form:-

$$q^* = a\, c^b \tag{5.3}$$

If $b < 1$, the isotherm is favourable, and if $b > 1$, the isotherm unfavourable. A limitation of using a Freundlich expression is that the isotherm is

open ended, with no account being made for saturation of the solid phase. This may be avoided by restricting the expression to a specified concentration range and expressing the isotherm in dimensionless form:-

$$y^* = x^b \tag{5.4}$$

where $x = \frac{C}{C_0}$

and $y^* = \frac{q^*}{q_0}$

If the adsorption is irreversible the isotherm can be described by a rectangular isotherm:-

$$\begin{aligned} q^* &= 0 \quad \text{for } c=0 \\ q^* &= q_0 \quad \text{for } c>0 \end{aligned} \tag{5.5}$$

and in dimensionless form:-

$$\begin{aligned} y^* &= 0 \quad \text{for } x = 0 \\ y^* &= 1 \quad \text{for } x > 0 \end{aligned} \tag{5.6}$$

In cases when the isotherm is very favourable, Vermeulen(141) describes the use of the assumption that the behaviour approaches that of a rectangular isotherm. The use of this assumption allows considerable simplification of the prediction of the sorption performance in a packed column as detailed in Chapter 6.

5.3 Use of caesium-134 tracer and counting equipment

Test solutions were prepared using stable caesium-133 and caesium-134 tracer to enable efficient and accurate analysis of caesium in the samples. The tracer caesium-134 used in this work was purchased from Amersham International (29/3/79) and was supplied in the form of caesium chloride with a specific activity of 1-10 mCi/mg. Allowing for decay and successive dilutions, adequate tracer (0.4-

0.6 nCi/mL) was added to the test solutions to give about 7000 counts in 4000 secs for a sample of 5 mL. It was calculated that the tracer caesium concentration in the test solutions was negligible.

Gamma counting was carried out on either an EG&G Ortec computer based gamma detector system which was coupled to a Gamma-X detector, or a Phillips NaI counter. A known volume of the sample was pipetted into a glass vial to ensure a consistent geometry for all the counts in one set of tests. The Gamma-X detector has a relatively low efficiency but enables the counting of specific isotopes in any solution, while the NaI had a higher efficiency but could only be used when one isotope was present.

The main error in using the tracer technique is due to the activity measurement. The standard deviation of the number of counts recorded(A) is given by its square root($\sqrt{A}$). From this an estimate can be made of the errors in any calculated value.

5.4 The removal of trace levels of caesium

5.4.1 Preliminary tests

The granular exchangers prepared in the small scale preparations were initially tested for caesium sorption using a test similar to that used by Lee (33). 0.2 g of the unconditioned exchanger was contacted with 15 mL of test solution containing 10 ppm Cs, 0.3 M $NaNO_3$, 0.2 M HNO_3, and 15 g/L Fe(III). The contact time was 24 hours with continual shaking. Samples of the solution were then taken, centrifuged, and counted.

The percentage caesium removal(P) and the distribution coefficient after 24 hours contact(R_d) were calculated as defined in Section 5.2.1. All the exchangers removed 97-100 % of the caesium and gave R_d values of above 3000 mL/g. The effect of various parameters on the sorption of caesium is discussed below.

5.4.2 Effect of pH, particle size and drying temperature on caesium sorption

The effect of pH on the sorption of caesium was initially investigated in a series of tests with a solution of 3M sodium nitrate with 10 ppm caesium. The pH of the solution was adjusted by adding nitric acid or sodium hydroxide as appropriate. It was found that between pH 2 and pH 12 there was 98-100% removal of the caesium but below pH 1 or above pH 12 this was significantly reduced. Below pH 1, it was observed that the exchangers broke up into fine particles and the solution turned green suggesting that Ni was in solution. At pH 12 no physical break-up of the exchangers was observed but very fine brown particles were seen suspended in the solution. These effects have already been discussed with regard to the conditioning of the exchangers in Section 4.2. The percentage Cs removal and calculated Rd values for NaNiHCF at various pH are given in Table 5.1.

The effect of particle size on the sorption of caesium was investigated in a series of tests with the same solution which was set at pH 2. The tests were carried out on both KNiFC and NaNiFC in a form which had been dried only on a warm surface, and also one which had been heated to 150 °C for 10 minutes. This heat treatment was found to increase the strength of the granular forms during the tests. The percentage caesium removal and calculated R_d values from these tests are given in Table 5.2 for NaNiHCF and Table 5.3 for KNiHCF. About 98% of the caesium is removed with largest particle size (>600 mics) and this increased to 100% with the smallest size (<90 mics). The Rd values were larger for NaNiHCF compared to those for KNiHCF, and also with the exchangers that were heat-treated (150 °C for 10 mins.).

Table 5.1 Effect of pH on the sorption of caesium onto NaNiHCF

0.2 g of the exchanger (NaNiHCF-P18A) in contact with 15 mL of 3M $NaNO_3$ with 10 ppm Cs. Contact time of 24 hours.

pH	% Caesium Removal	R_d (mL/g)
1	96.8	2386 ± 250
2	99.8	53000 ± 1000
3	99.7	28100 ± 9000
5	99.9	79800 ± 10000
7	99.9	51000 ± 10000
9	99.9	107000 ± 20000
11	100	*
12	98.9	6100 ± 300

* no count detected above background

Table 5.2 Effect of NaNiHCF particle size on the sorption of trace amounts of caesium

0.2 g NaNiHCF-P18A contacted with 15 mL 3 M $NaNO_3$ with 10 ppm Cs for 24 hours. (NaNiHCF was not heated during preparation)

	dried at 110 °C		dried at 170 °C	
particle size (microns)	% Cs removed	Rd mL/g	% Cs removed	R_d mL/g
< 90	99.9	69000 ± 15000	100	*
90 - 250	99.6	17800 ± 5000	100	*
250 - 420	99. 5	16300 ± 5000	99.8	34000 ± 10000
420 - 600	99.0	7620 ± 900	99.3	10300 ± 2000
> 600	98.3	4600 ± 400	100	*

* no count detected above background

Table 5.3 Effect of KNiHCF particle size on the sorption of trace amounts of caesium

0.2 g NaNiHCF-P19A contacted with 15 mL 3 M $NaNO_3$ with 10 ppm Cs for 24 hours. (KNiHCF was not heated during preparation)

	dried at 110 °C		dried at 170 °C	
particle size (microns)	% Cs removed	Rd m/g	% Cs removed	R_d mL/g
< 90	99.3	11200 ± 2000	100	*
90 - 250	99.3	11200 ± 2000	99.9	64300 ± 15000
250 - 420	99.7	22400 ± 3000	99.4	11600 ± 2000
420 - 600	99.4	11600 ± 2000	97.8	3300 ± 200
> 600	98.6	530 ± 600	98.9	7000 ± 900

* No count detected above background

5.5 The uptake of caesium and determination of the sorption isotherm

5.5.1 Caesium uptake tests

To determine the caesium uptake for a range of particle sizes, in the absence of any competing ions, a series of batch tests were carried out in which a fixed mass of exchanger was contacted with a fixed volume of solution. 0.2 g of the exchanger was contacted with 15mL of solution containing 26 g $CsNO_3$/L for a period of 24 hours with continual shaking at room temperature. The 15 mL of solution contains 2 meq. of caesium and hence uptake is given directly from the percentage caesium removal, 100% removal giving an uptake of 10 meq./g. It was found that the samples which were not heat-treated broke up on contact with the caesium solution, while the samples that were heat-treated (150 °C for 10 mins.) remained in a granular form during the test. The measured uptake for both NaNiHCF and KNiHCF after a contact time of 24 hours is given in Table 5.4. The uptake was found to increase as the particle size is reduced which is to be expected as the specific surface area is increased. The uptake of the sodium form was found to be greater than that of the potassium by up to 20 %.

Table 5.4 Caesium uptake onto NaNiHCF and KNiHCF in the absence of competing ions

0.2 g of exchanger contacted with 15 mL solution containing 26g Cs/L, contact time 24 hour

	NaNiHCF - P20 dried at 170 °C		KNiHCF - 20P dried at 170 °C	
particle size (microns)	% Cs removed	uptake meq./g	% Cs removed	uptake, q meq./g
< 90	23.8	2.38 ± 0.01	19.8	1.98 ± 0.01
90 - 250	22.6	2.27 ± 0.01	16.3	1.63 ± 0.01
250 - 420	19.1	1.93 ± 0.01	17.8	1.75 ± 0.01
420 - 600	15.8	1.59 ± 0.01	13.8	1.38 ± 0.01
> 600	11.8	1.16 ± 0.01	12.2	1.23 ± 0.01
Theoretical maximum*		4.16		3.90

* assuming 4 exchangeable Na or K atoms

The uptake of caesium onto samples of NaNiHCF in the presence of 1 M $NaNO_3$ was investigated in a further series of batch tests. The tests were carried out both with samples that were heated in the mother liquor during the preparation, and with samples which were not heated. A sample of the contact solution was taken after contact times of 1, 24 and 48 hours, and the caesium uptake calculated by mass balance. Four ranges of particle sizes were used in the tests.

The uptake onto NaNiHCF-NJ3 A3 (precipitate heated in mother liquor) is shown in Figure 5.1 and NaNiHCF-NJ5 A1 (precipitate not heated) is shown in Figure 5.2.

Figure 5.1 Uptake of caesium onto NaNiHCF-NJ3 A3

(precipitate heated in mother liquor during preparation)

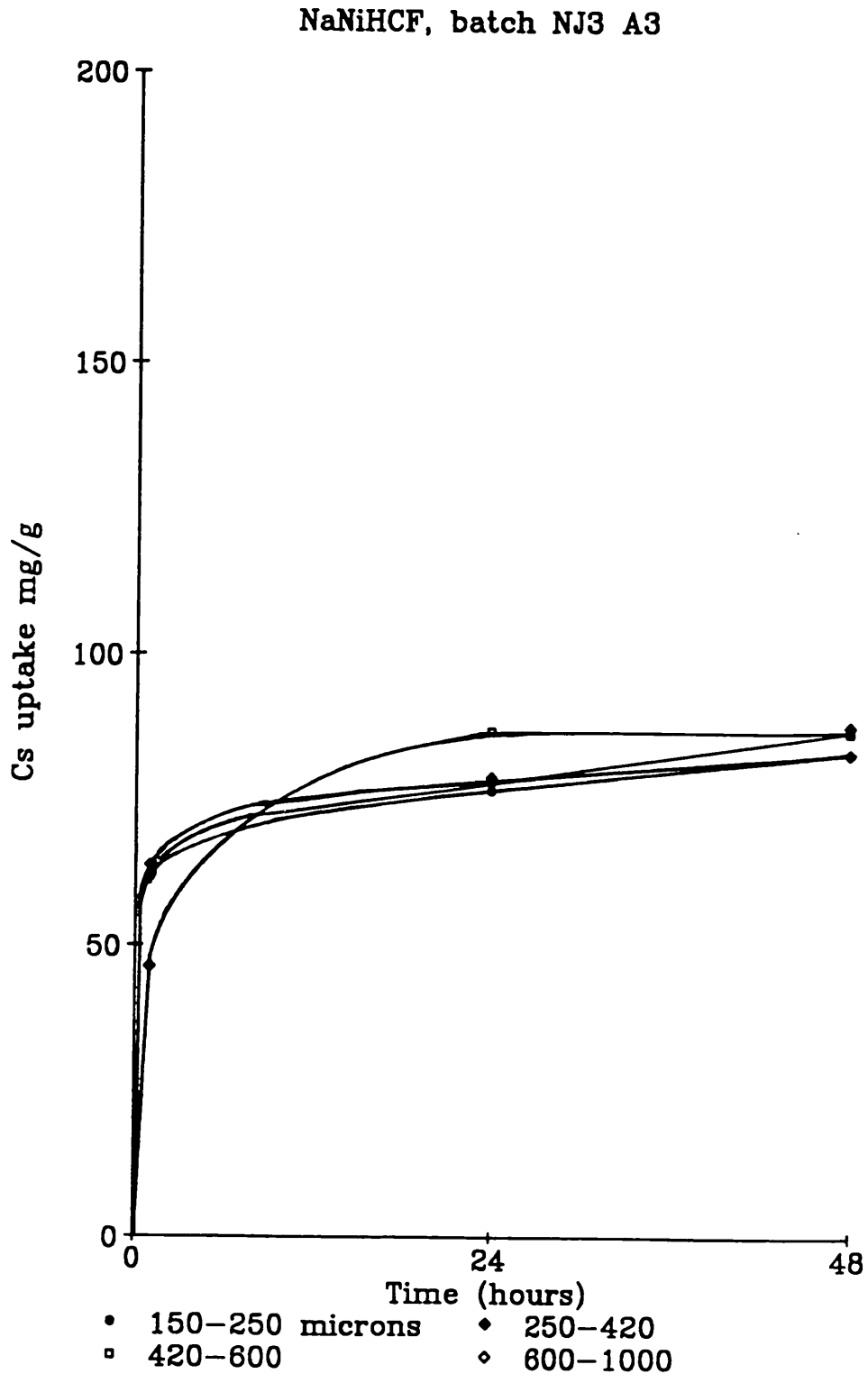
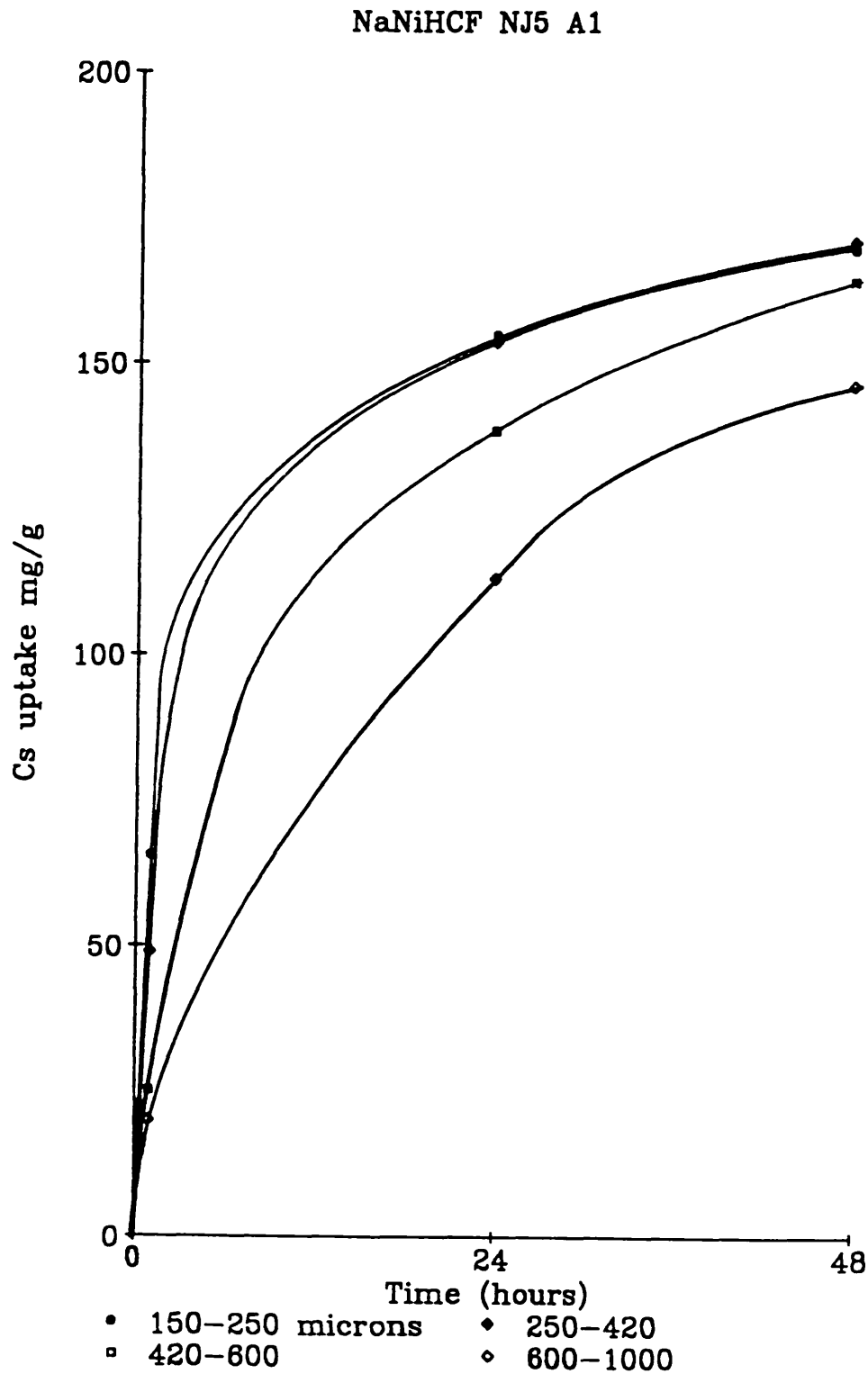


Figure 5.2 Uptake of caesium onto NaNiHCF-NJ5 A1

(precipitate not heated in mother liquor during preparation)



It is clearly seen that there is a substantial difference in the uptake for the two samples both in terms of the final uptake and the rate at which the materials become loaded. With the sample NJ3 A3, the total caesium uptake was 92 mg/ g which was essentially complete after 1 hour, and the effect of particle size is not so significant. In the case NJ5 A1, though, caesium sorption was slow and the uptake was about 182 mg/g after 48 hours which was still not complete after 48 hours. A clear difference is also seen in this case in the uptake for different particle sizes.

5.5.2 Determination of the caesium adsorption isotherm

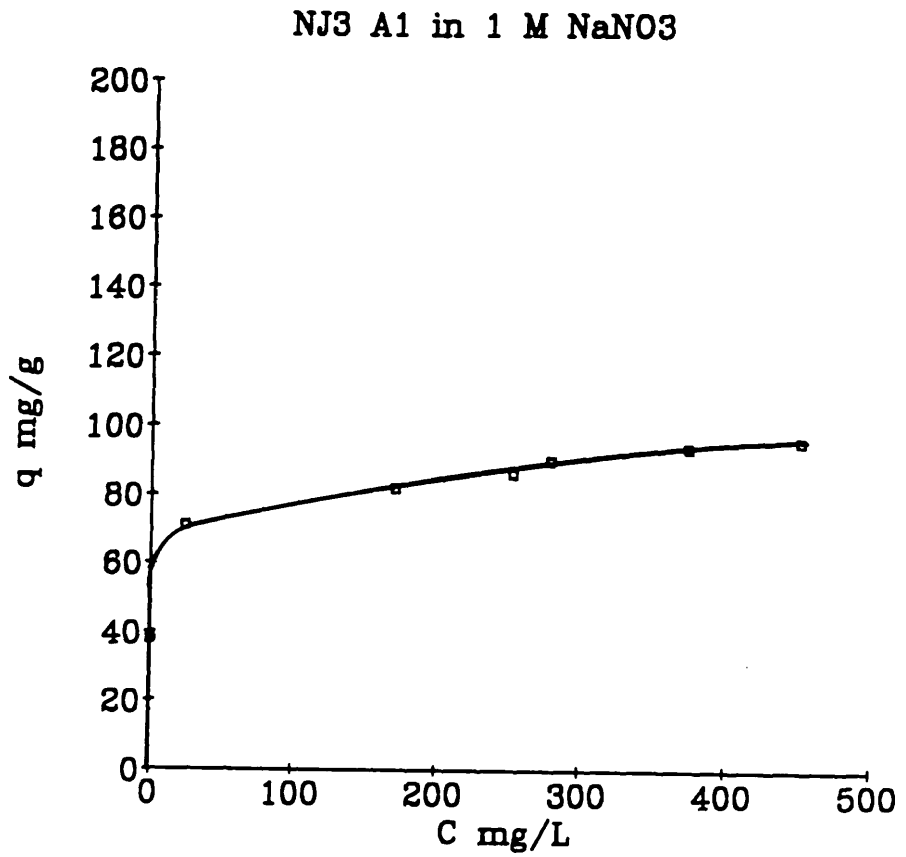
The adsorption isotherm for NaNiHCF was determined in a series of batch contact tests. Each individual test was carried out as described in the previous section. By varying the mass of exchanger or the volume of solution the adsorption isotherm was determined. The samples were shaken over a period of 72 hours which was assumed sufficient for equilibrium to be reached. The caesium concentration of the solution, c, was determined by a count of the solution and the solid phase concentration, q^*, determined by mass balance. The solid phase concentrations were expressed as mg Cs per g of dry mass of exchanger.

The caesium adsorption isotherms for two samples of NaNiHCF in contact with 1 M $NaNO_3$ are shown in Figures 5.3 and 5.4. As with uptake tests described above, NJ3 A1 was a sample which was heated in the mother liquor, while sample NJ5 A2 was not heated.

It was found that both isotherms were very favourable although the sample which was heated in the preparation, NJ3 A1, had a capacity of 92 mg/g while that which was not heated, NJ5 A2, had a capacity of 182 mg/g. The plots of $\log y$ against $\log x$ shown in Figures 5.3 and 5.4 give straight lines showing that a Freundlich type isotherm applies. The Freundlich coefficient for sample NJ3 A1 was 0.13, and for NJ5 A2 the coefficient was 0.25. Due to the very favourable nature of these isotherms it can be assumed that they are effectively irreversible as used in chapter 6.

Figure 5.3 Adsorption isotherm for NaNiHCF - NJ3 A1

(precipitate heated in mother liquor during preparation)



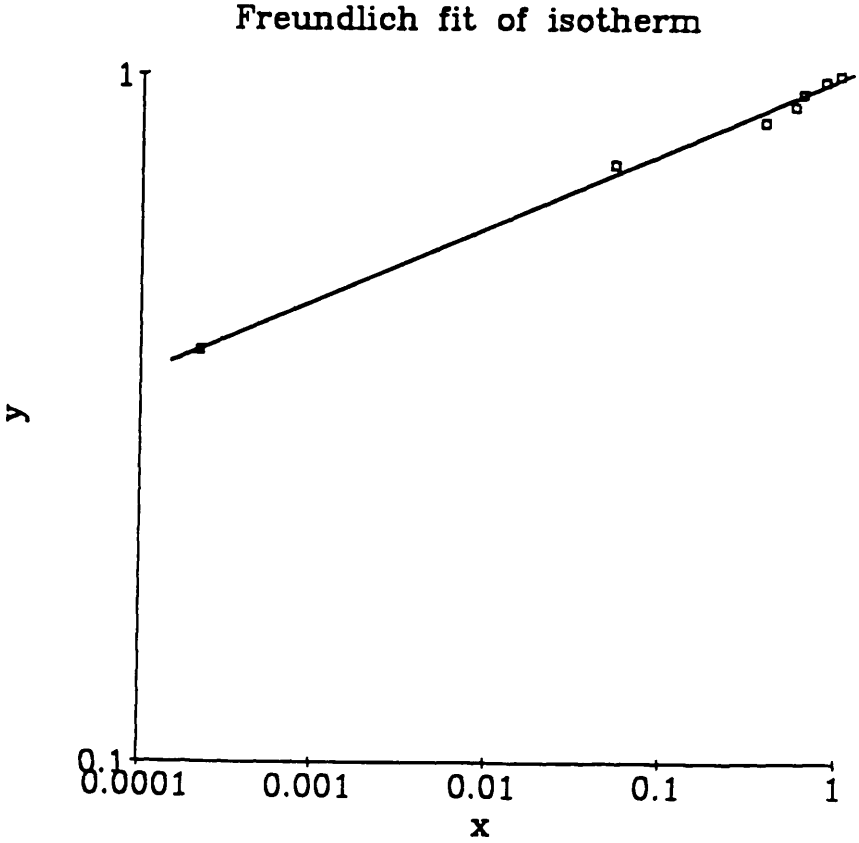
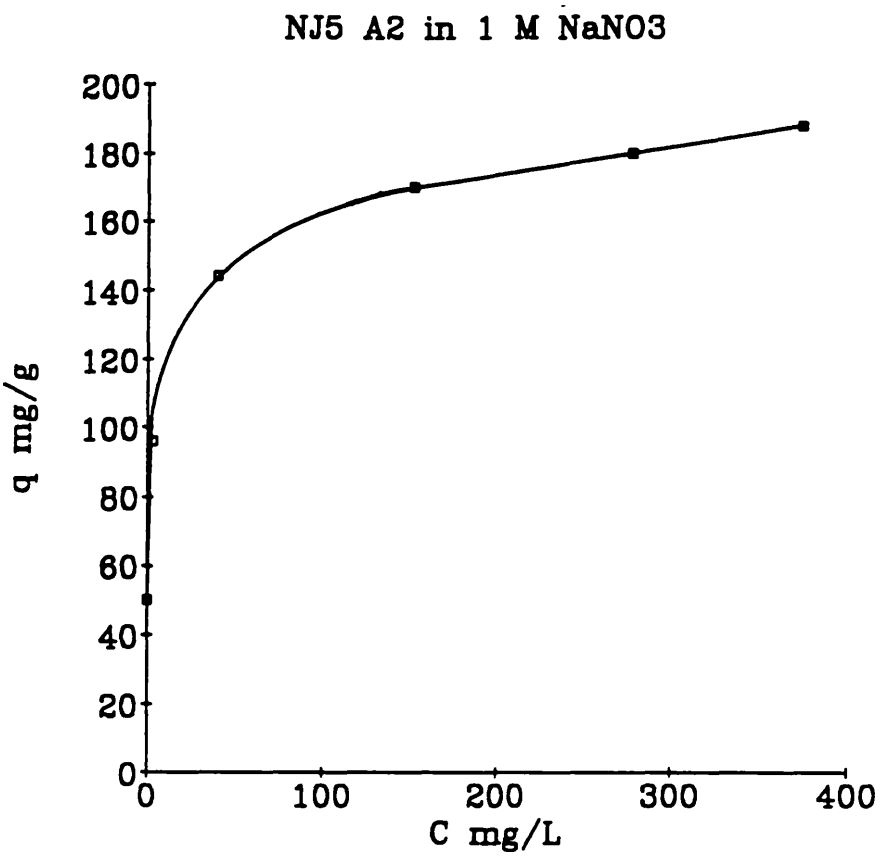
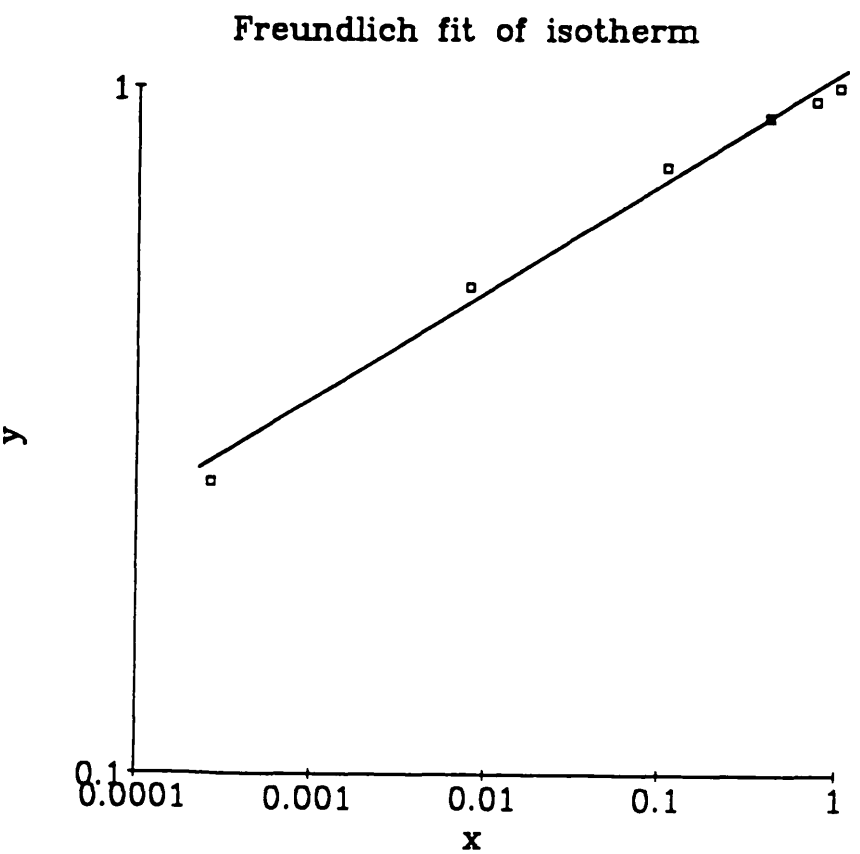


Figure 5.4 Adsorption isotherm for NaNiHCF - NJ5 A2

(precipitate not heated in mother liquor during preparation)





5.6 Removal of a variety of radionuclides from a simulated waste effluent

5.6.1 Set-up of batch tests

The granular samples NaNiHCF-20P and KNiHCF-20P which were prepared using the freeze-thaw method (batch 21: 600-1000 microns) and two silica based exchangers [(SBM2) and (SBM3)] (supplied by the Chemistry Divison, Harwell) were tested in batch contact experiments with a simulated waste solution. The solution was spiked with a solution of irradiated fuel and also some shorter lived radionuclides. The ratio of stable ^{133}Cs to active ^{137}Cs in the solution was approximately 3:1. The effectiveness of the exchangers in removing the wide range of radionuclides from the solution was assessed.

The exchangers were conditioned to pH 2 and pH 8 with 1 M sodium nitrate solution as described in section 4.2. The following procedure was used :-

1. 50 mL of 1 M $NaNO_3$ was adjusted to the appropriate pH by adding either NaOH or HNO_3
2. 1.5 g of the exchanger was contacted with 50 mL of the conditioned 1M sodium nitrate solution, the pH being adjusted at regular intervals.
3. After 24 hours the solution was decanted and replaced with a fresh conditioned 1M $NaNO_3$ solution. The pH was again adjusted at regular intervals over a prolonged period (several weeks) until there was no further change in the pH.
4. The solution was decanted off and replaced with a fresh conditioned 1 M sodium nitrate solution and allowed to stand for 24 hours. Minor corrections were made to the pH as required.

At pH 2 there was appreciable break-up of KNiHFC and slight break-up of NaNiHFC. After the long period of conditioning at pH 2 the solution was found to contain greater than 1000 ppm nickel which had been released from the exchanger. This has already been discussed in Section 5.1.2. After the fines had been removed in the decanted liquor, granules of both the NaNiHCF and KNiHCF remained

which did not break-up in the batch contact tests. At pH 8 there was no observed break-up of the exchangers and nickel was not detected in the conditioning solution.

In each batch contact test 0.5 mL of the conditioned wet exchanger was measured out using a cut-down syringe and placed in a conical flask. 50 mL of the conditioned simulate was then added and the loaded flasks were placed in a shaker water bath which was thermostatted to 25 °C. 1 mL samples of the simulate were removed after 1, 2, 6, 24 and 36 hours. The samples were counted and the percentage removal(P) of the main nuclides was calculated as defined in equation 5.1. The caesium distribution coefficients were also calculated after a contact time of 24 and 30 hours as defined by equation 6.2. The mass of the exchanger used in each test was determined by measuring out an additional 0.5 mL of the wet exchanger which was dried at 110 °C and then weighed.

5.6.2 Results

The measured activity and the percentage removal are listed in Table 5.5 and Table 5.6 respectively for the following nuclides : Am-241, Ce-144, Cs-137, Cs-134, Sr-85, Np-237, Eu-154, Ru-106, Zr-95, Co-58, Cd-109, Zr-95, and Sb-124. The calculated caesium distribution coefficients are given in Table 5.6

The percentage removal at pH 2 and pH 8 are plotted for Cs-137 in Figure 5.5, Sr-85 in Figure 5.6, Am-241 in Figure 5.7, Np-237 in Figure 5.8, and Ru-106 in Figure 5.9

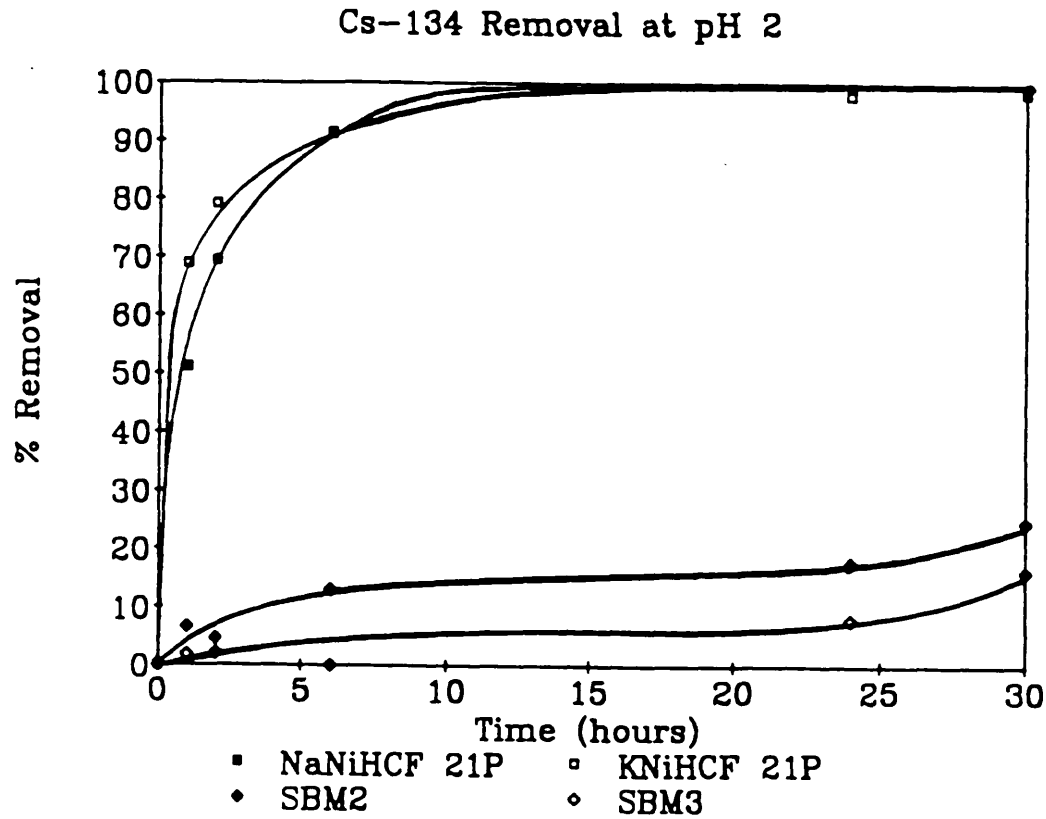
Table 5.5 Measured activity of solution from sorption tests with simulated waste

				Nuclides (activity in Becquerels)										
				Am-241	Ce-144	Cs-134	Cs-137	Eu-154	Np-237	Ru-106	Zr-95	Co-58	Cd-109	Sr-85	Sb-124
Initial spiked solution pH 2				118.00	303.90	1353.00	20550	361.90	535.50	1264.00	166.10	870.40	1945.00	34.74	599.80
Initial spiked solution pH 8				108.40	281.60	1303.00	19870	331.50	511.80	1164.00	144.70	782.20	1827.00	35.64	541.00
ION EX.	pH	TIME (Hours)	COUNT (hours)												
Na-Na-FC	2	1	1/2	117.70	315.00	662.00	10210	362.90	526.90	1222.00	166.00	837.90	1913.00	21.50	618.60
Na-Ni-FC	2	2	1/2	116.00	306.50	413.70	6150	372.60	551.80	1083.00	165.40	743.10	1991.00	15.21	569.40
Na-Ni-FC	2	6	1/2	119.30	301.50	115.50	1682	367.40	543.20	1103.00	161.50	756.20	1974.00	10.33	603.60
Na-Ni-FC	2	24	1	117.50	312.10	7.69	99.28	375.70	525.00	1060.00	151.10	727.00	1881.00	6.54	569.60
Na-Ni-FC	2	30	4	109.70	295.60	8.91	69.15	364.40	506.70	1046.00	159.70	717.30	1877.00	6.68	593.00
K-Ni-FC	2	1	1/2	90.31	265.20	420.40	6153	285.00	389.70	1260.00	126.80	863.90	1415.00	15.37	474.80
K-Ni-FC	2	2	1/2	68.07	261.10	283.50	4007	236.30	349.20	1114.00	109.40	764.30	1266.00	12.26	408.80
K-Ni-FC	2	6	1/2	49.74	210.70	118.10	1716	215.90	323.90	1103.00	105.90	770.40	1200.00	7.59	396.00
K-Ni-FC	2	24	1	34.15	199.70	26.63	190.70	181.30	256.50	1027.00	71.62	698.60	937.00	4.54	267.70
K-Ni-FC	2	30	4	28.56	167.20	21.30	115.70	168.10	226.70	886.80	69.86	608.20	843.70	4.62	261.10
2	2	1	1/2	105.00	300.50	1264.00	19480	349.20	567.90	1205.00	157.50	805.00	2103.00	34.53	588.60
2	2	2	1/2	115.90	281.80	1291.00	19420	376.00	507.10	1190.00	165.20	820.40	1927.00	32.32	617.60
2	2	6	1/2	120.20	290.90	1177.00	18400	366.10	550.50	1232.00	156.80	790.60	1999.00	31.83	586.10
2	2	24	1/2	115.10	324.70	1112.00	17560	361.70	505.30	1180.00	176.70	785.90	1783.00	30.29	607.20
2	2	30	4	100.00	265.70	1019.00	15940	333.50	468.60	1084.00	134.90	730.10	1732.00	27.00	501.70
3	2	1	1/2	114.70	304.50	1329.00	20230	363.40	508.00	1151.00	160.80	772.90	1994.00	35.13	600.90
3	2	2	1/2	118.10	317.90	1324.00	20300	359.10	525.30	1198.00	179.30	821.80	1961.00	33.91	670.20
3	2	6	1/2	115.50	348.50	1405.00	21030	371.30	516.60	1194.00	160.90	858.10	1778.00	33.87	549.20
3	2	24	1/2	116.80	370.00	1219.00	18930	375.00	570.70	1259.00	162.60	863.60	2073.00	33.18	607.60
3	2	30	4	103.20	271.70	1119.00	17180	341.80	485.20	1100.00	141.40	741.90	1749.00	28.65	528.60
Na-Ni-FC	8	1	1/2	107.10	276.70	464.30	7100	307.50	426.50	956.80	132.60	651.50	1636.00	13.32	479.00
Na-Ni-FC	8	2	1/2	84.83	209.10	317.80	4685	259.80	369.30	858.40	115.40	566.30	1323.00	11.14	431.30
Na-Ni-FC	8	6	1/2	71.95	204.00	132.90	1788	213.40	311.00	612.80	93.26	420.30	1129.00	7.16	348.70
Na-Ni-FC	8	24	1	26.52	69.43	39.40	426	73.17	109.70	116.90	32.33	154.00	415.30	2.85	122.20
Na-NI-FC	8	30	4	13.42	36.99	28.10	292	42.35	55.49	75.92	16.86	105.40	208.70	2.42	63.03
K-Ni-FC	8	1	1/2	97.29	260.00	452.70	6614	292.60	437.60	1039.00	121.30	712.30	1624.00	18.97	453.60
K-Ni-FC	8	2	1/2	84.51	220.50	320.80	4794	265.10	372.00	909.30	129.90	619.90	1312.00	14.17	485.60
K-Ni-FC	8	6	1/2	51.55	164.30	103.30	1396	183.10	256.60	633.90	86.40	434.80	935.60	6.85	331.00
K-Ni-FC	8	24	1	11.50	44.35	33.00	84.62	38.16	58.61	160.00	19.58	28.00	221.90	4.08	73.17
K-Ni-FC	8	30	4	4.94	14.89	13.00	35.84	16.83	27.15	74.00	11.78	11.00	113.10	2.89	44.02
2	8	1	1/2	75.48	218.90	1338.00	20400	226.10	377.44	869.30	116.20	619.20	1422.00	36.50	434.20
2	8	2	1/2	66.66	100.00	1278.00	19480	195.70	286.30	744.10	130.70	502.50	1040.00	NA	490.10
2	8	6	1/2	28.52	96.58	1278.00	19450	82.69	149.50	258.60	56.86	348.50	492.00	29.83	204.70
2	8	24	1/2	5.60	26.07	1262.00	19170	15.71	55.96	NA	9.31	NA	236.90	29.32	41.82
2	8	30	4	3.72	12.51	1164.00	17960	15.66	51.67	NA	14.14	21.00	186.20	28.68	36.44
3	8	1	1/2	64.27	151.80	1105.00	16510	188.00	263.30	886.10	93.05	587.50	956.10	26.01	347.80
3	8	2	1/2	55.59	160.50	1073.00	16040	198.00	293.60	863.70	99.01	602.70	1066.00	26.29	355.60
3	8	6	1/2	53.43	114.50	805.10	12220	156.90	235.00	843.00	80.77	578.80	1037.00	22.29	301.90
3	8	24	1	15.16	47.30	451.00	6967	43.45	80.40	299.80	18.42	370.00	320.30	11.83	74.67
3	8	30	4	9.14	26.78	399.50	5987	30.17	52.68	254.70	16.65	309.30	220.70	10.27	57.51

Table 5.6 Percentage Removal of Radionuclides from Simulated Waste

ION-EX	pH	TIME (hours)	Am-241	Ce-144	Cs-134	Cs-137	Eu-154	Np-237	Ru-106	Zr-95	Co-58	Cd-109	Sr-85	Sb-124
Na-Na-FC	2	1	0.25	-3.65	51.07	50.32	-0.28	1.61	3.32	0.06	3.73	1.65	38.11	-3.13
Na-Ni-FC	2	2	1.69	-0.86	69.42	70.07	-2.96	-3.04	14.32	0.42	14.63	-2.37	56.22	5.07
Na-Ni-FC	2	6	-1.10	0.79	91.46	91.82	-1.52	-1.44	12.74	2.77	13.12	-1.49	70.26	-0.63
Na-Ni-FC	2	24	0.42	-2.70	99.43	99.52	-3.81	1.96	16.14	9.03	16.48	3.29	81.17	5.04
Na-Ni-FC	2	30	7.03	2.73	99.34	99.66	-0.69	5.38	17.25	3.85	17.59	3.50	80.77	1.13
K-Ni-FC	2	1	23.47	12.73	68.93	70.06	21.25	27.23	0.32	23.66	0.75	27.25	55.76	20.84
K-Ni-FC	2	2	42.31	14.08	79.05	80.50	34.71	34.79	11.87	34.14	12.19	34.91	64.71	31.84
K-Ni-FC	2	6	57.85	30.67	91.27	91.65	40.34	39.51	12.74	36.24	11.49	38.30	78.15	33.98
K-Ni-FC	2	24	71.06	34.29	98.03	99.07	49.90	52.10	18.75	56.88	19.74	51.83	86.93	55.37
K-Ni-FC	2	30	75.80	44.98	98.43	99.44	53.55	57.67	29.84	57.94	30.12	56.62	86.70	56.47
2	2	1	11.02	1.12	6.58	5.21	3.51	-6.05	4.67	5.18	7.51	-8.12	0.60	1.87
2	2	2	1.78	7.27	4.58	5.50	-3.90	5.30	5.85	0.54	5.74	0.93	6.97	-2.97
2	2	6	-1.86	4.28	13.01	10.46	-1.16	-2.80	2.53	5.60	9.17	-2.78	8.38	2.28
2	2	24	2.46	-6.84	17.81	14.55	0.06	5.64	6.65	-6.38	9.71	8.33	12.81	-1.23
2	2	30	15.25	12.57	24.69	22.43	7.85	12.49	14.24	18.78	16.12	10.95	22.28	16.36
3	2	1	2.80	-0.20	1.77	1.56	-0.41	5.14	8.94	3.19	11.20	-2.52	-1.12	-0.18
3	2	2	-0.08	-4.61	2.14	1.22	0.77	1.90	5.22	-7.95	5.58	-0.82	2.39	4.97
3	2	6	2.12	-14.68	-3.84	-2.34	-2.60	3.53	5.54	3.13	1.41	8.59	2.50	8.44
3	2	24	1.02	-21.75	9.90	7.88	-3.62	-6.57	0.40	2.11	0.78	-6.58	4.49	-1.30
3	2	30	12.54	10.60	17.29	16.40	5.55	9.39	12.97	14.87	14.76	10.08	17.53	11.87
Na-Ni-FC	8	1	1.20	1.74	64.37	64.27	7.24	16.67	17.80	8.36	16.78	10.45	62.63	11.46
Na-Ni-FC	8	2	21.74	25.75	75.61	76.42	21.63	27.84	26.25	20.25	27.67	27.59	68.74	20.28
Na-Ni-FC	8	6	33.63	27.56	89.80	91.00	35.63	39.23	47.35	35.55	46.31	38.20	79.91	35.55
Na-Ni-FC	8	24	75.54	75.34	96.98	97.86	77.93	78.57	89.96	77.66	80.33	77.27	91.99	77.41
Na-NI-FC	8	30	87.62	86.86	97.84	98.53	87.22	89.16	93.48	88.35	86.54	88.58	93.21	88.35
K-Ni-FC	8	1	10.25	7.67	65.26	66.71	11.73	14.50	10.74	16.17	9.02	11.11	46.77	16.16
K-Ni-FC	8	2	22.04	21.70	75.38	75.87	20.03	27.32	21.88	10.23	20.82	28.19	60.24	10.24
K-Ni-FC	8	6	52.44	41.65	92.07	92.97	44.77	49.86	45.54	40.29	44.46	48.79	80.79	38.82
K-Ni-FC	8	24	89.39	84.25	97.47	99.57	88.49	88.55	86.25	86.47	96.42	87.85	88.56	86.48
K-Ni-FC	8	30	95.44	94.71	99.00	99.82	94.92	94.70	93.64	91.86	98.59	93.81	91.90	91.86
2	8	1	30.37	22.27	-2.69	-2.67	31.79	26.25	25.32	19.70	20.91	22.17	0.39	19.74
2	8	2	38.51	64.49	1.92	1.96	40.97	44.06	36.07	9.68	35.82	43.08	NA	9.41
2	8	6	73.69	65.70	1.92	2.11	75.06	70.79	77.78	60.70	55.49	73.07	16.30	62.16
2	8	24	94.83	90.74	3.15	3.52	95.26	89.07	100.00	93.57	100.00	87.03	17.73	92.27
2	8	30	96.57	95.56	10.67	9.61	95.28	89.90	81.10	90.23	97.32	89.81	19.53	93.26
3	8	1	40.71	46.09	15.20	16.91	43.29	48.55	23.87	35.69	24.96	47.67	27.02	35.71
3	8	2	48.72	43.00	17.65	19.28	40.27	42.63	25.80	31.58	23.02	41.65	26.23	34.27
3	8	6	50.71	59.34	38.21	38.50	52.67	54.08	27.58	44.18	26.07	43.24	37.46	44.20
3	8	24	86.01	83.20	65.39	64.94	86.89	84.29	74.24	87.27	52.74	82.47	66.81	86.20
3	8	30	91.56	90.49	69.34	69.87	90.90	89.71	78.12	88.49	60.49	87.92	71.18	89.37

Figure 5.5 Sorption from a simulated waste solution - Cs-134 removal



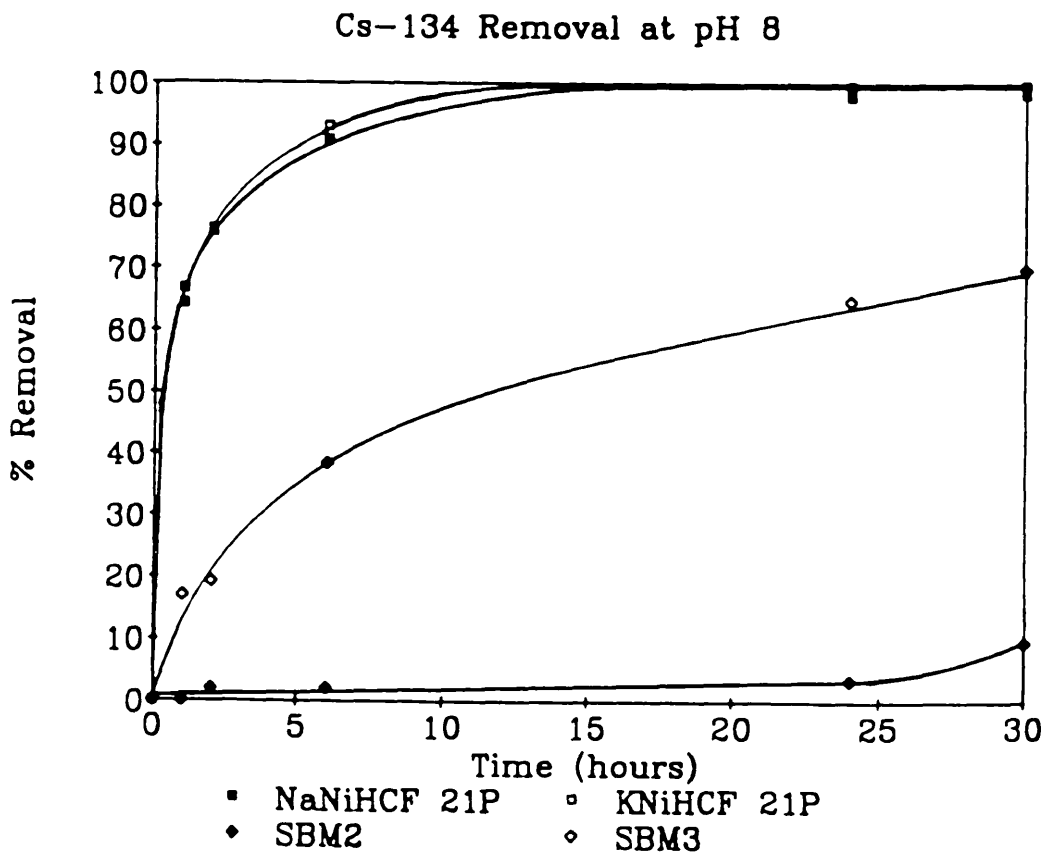
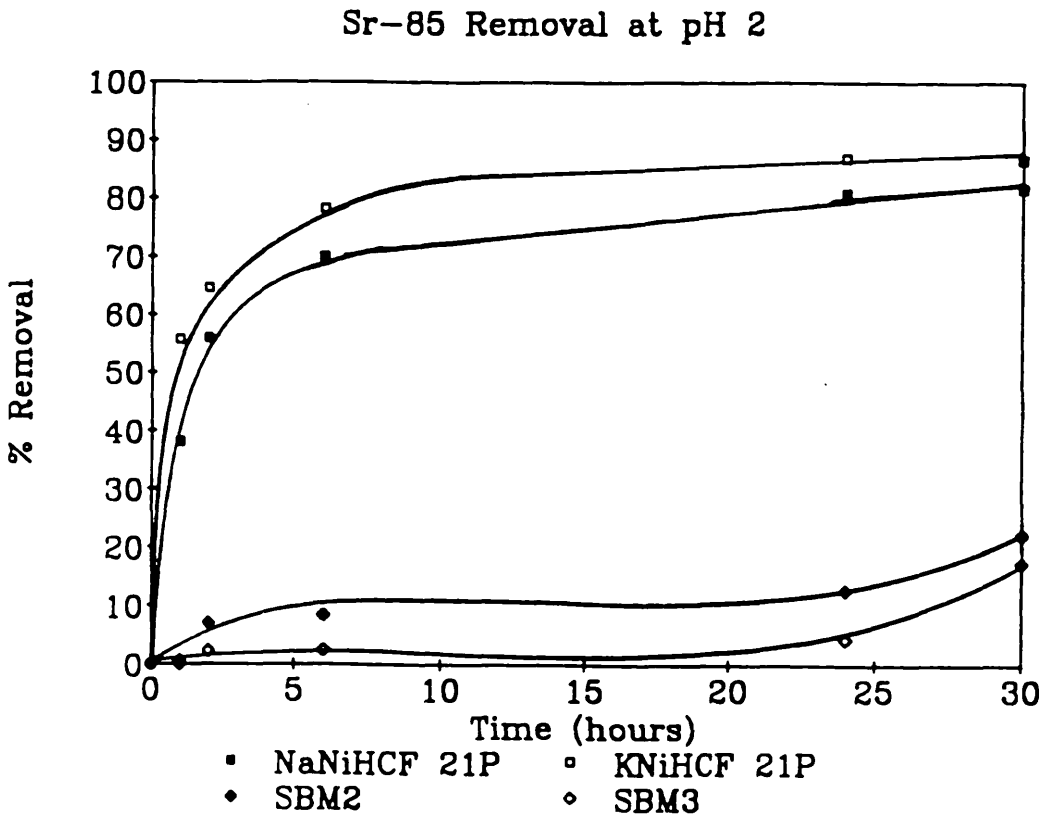


Figure 5.6 Sorption from a simulated waste solution - Sr-85 removal



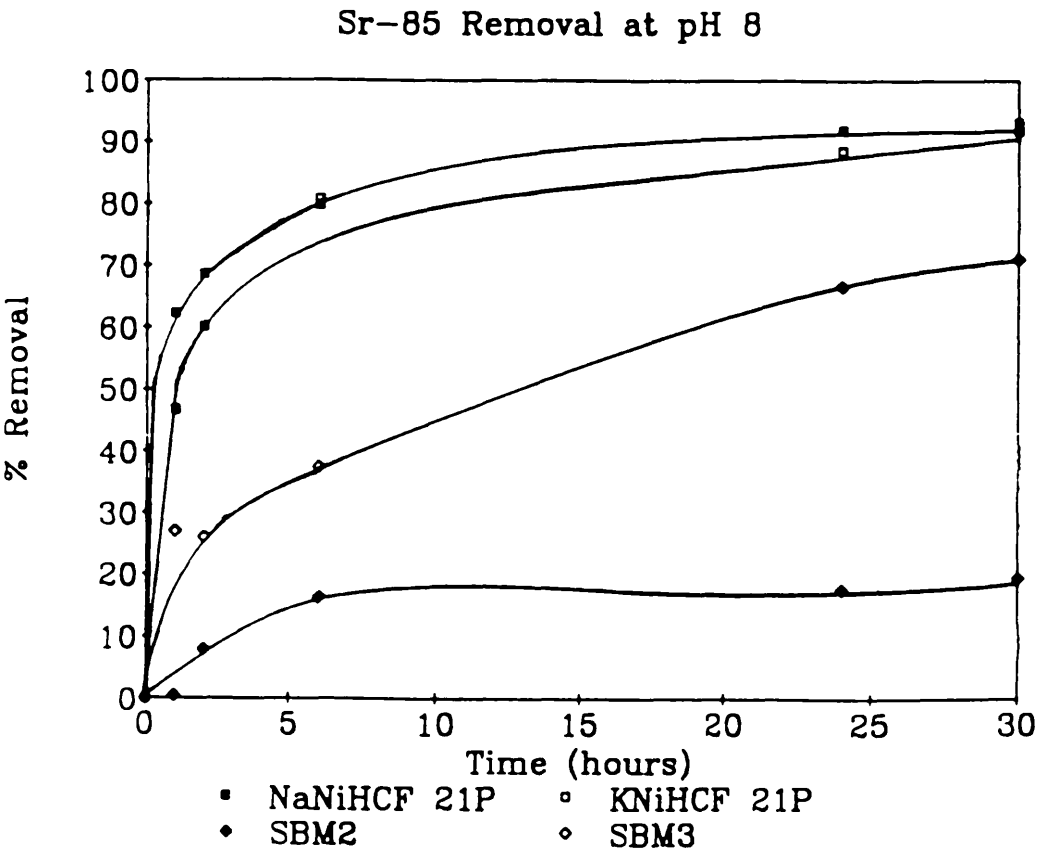
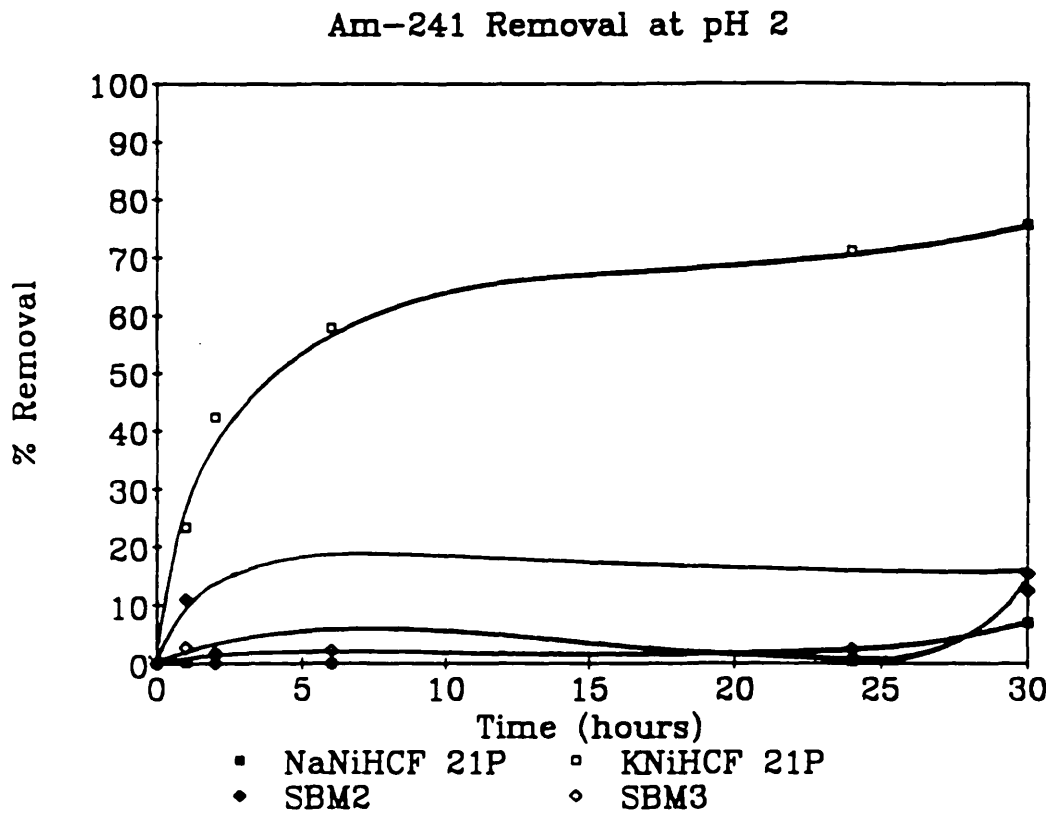


Figure 5.7 Sorption from a simulated waste solution - Am-241 removal



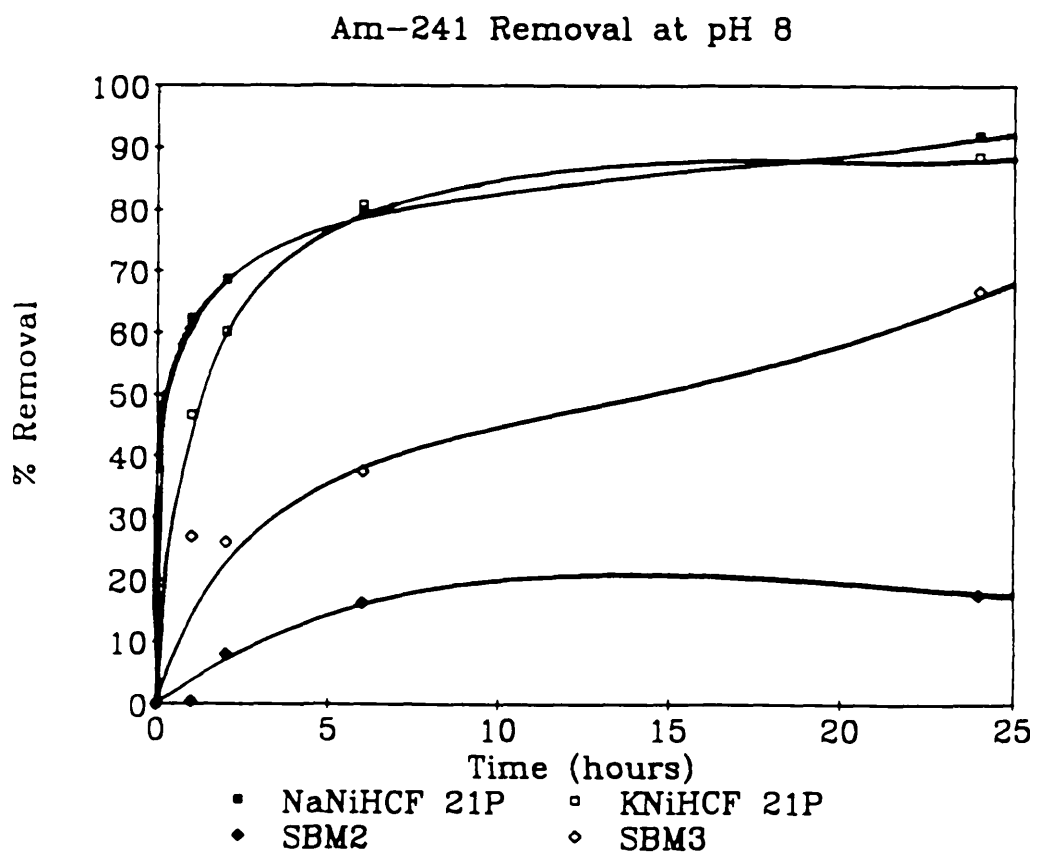
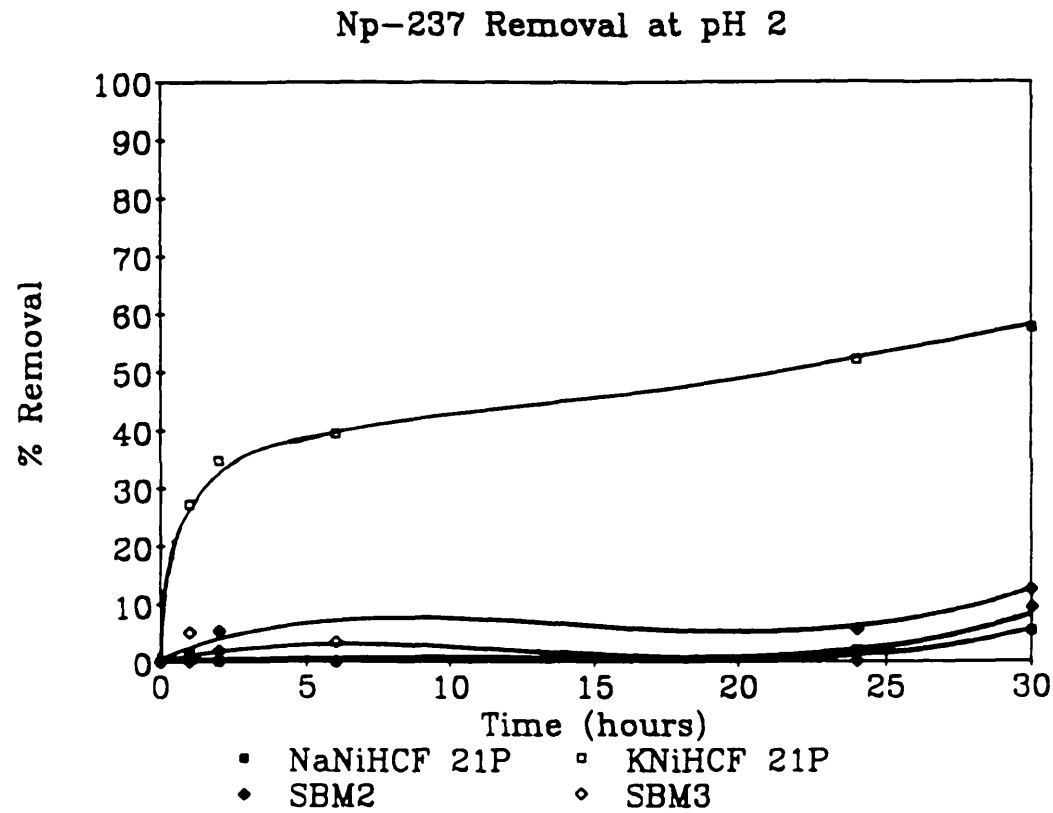


Figure 5.8 Sorption from a simulated waste solution - Np-237 removal



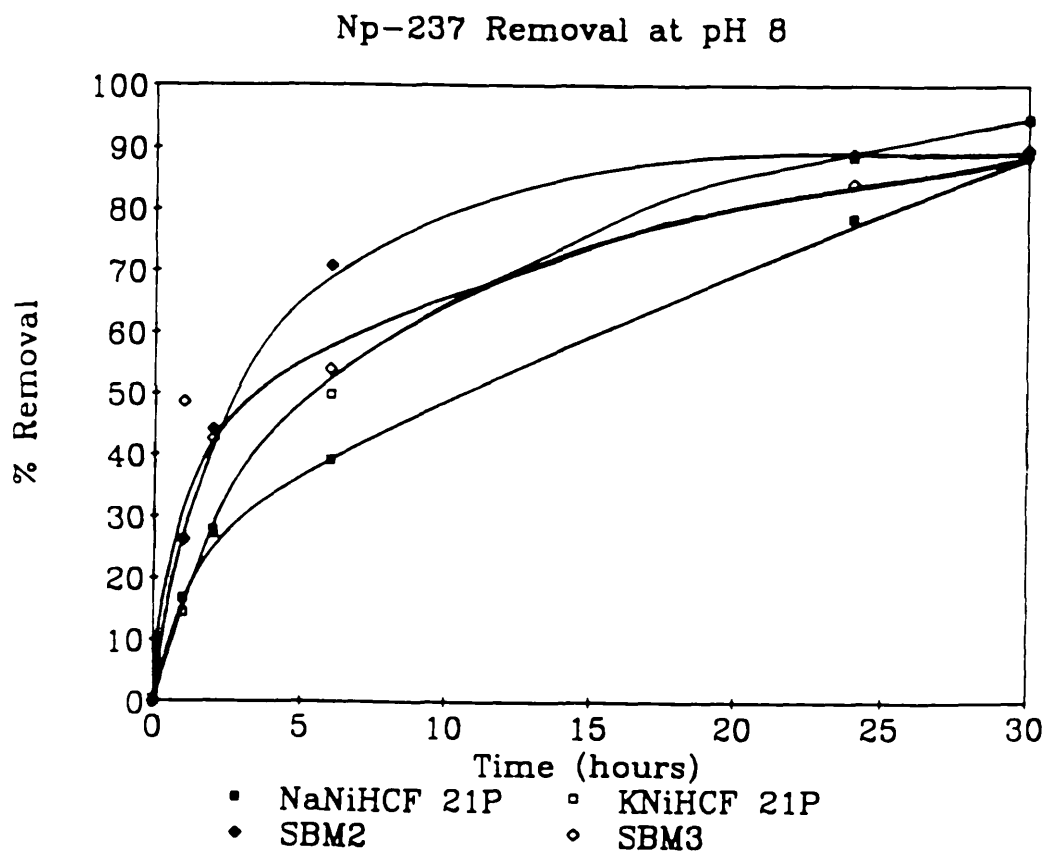


Figure 5.9 Sorption from a simulated waste solution - Ru-106 removal

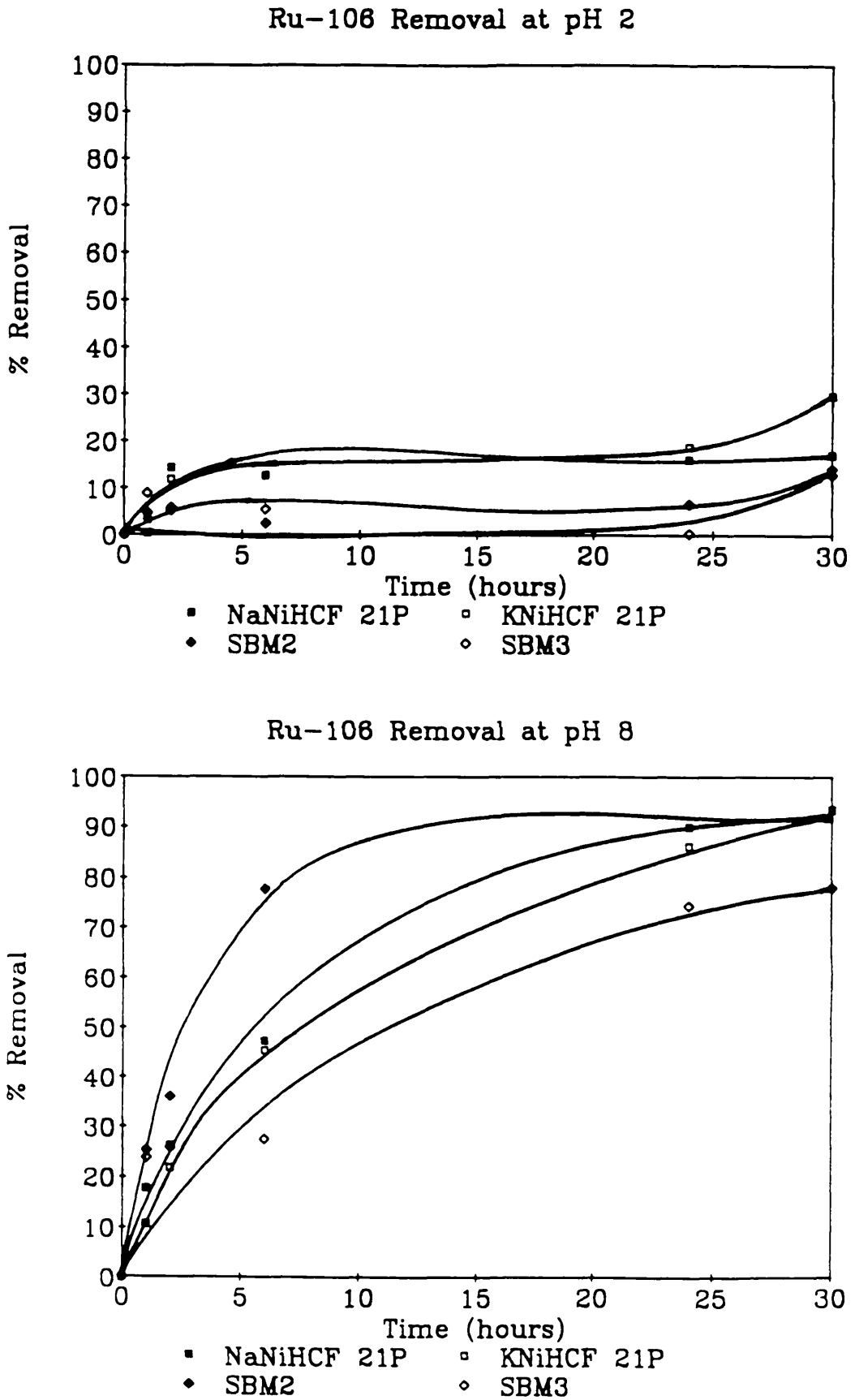


Table 5.7 Caesium distribution coefficients from tests with simulated waste

0.5 mL exchanger (Batch 21: 600-1000 microns) contacted with 50 mL of the simulated waste solution.

0.5 mL of NaNiHCF $\simeq$ 0.35 g *

0.5 mL of KNiHCF $\simeq$ 0.34 g *

pH	Contact Time (hours)	Caesium Distribution Coefficient (R_d)	
		NaNiHCF (mL/g)	KNiHCF (mL/g)
2	24	29420	15700
2	30	42280	25970
8	24	6340	32482
8	30	9820	76950

* Determined by measuring out an additional sample of the exchanger which was dried(110 °C) and then weighed.

5.6.3 Discussion

At pH 2, both NaNiHCF and KNiHCF removed 99.5 % of the caesium and over 80 % of the strontium, while there was no appreciable uptake of the other nuclides. The retention of a wide range of radionuclides by nickel hexacyanoferrate(supplied by Applied Research, Belgium) was measured by Neskovic et al.(142). Significantly, they found that there was removal of a wide range of nuclides and also cadmium, and no removal of either cerium, strontium and ruthenium. Their measurements were made in 1N acids which means that the results cannot be compared directly with the present work.

Both the silica based materials did not significantly remove any of the measured nuclides at pH 2.

At pH 8, both NaNiHCF and KNiHCF selectively removed 99 % of the caesium with approximately 90 % removal of all the other measured nuclides. The silica based materials also removed about 90 % of all the nuclides with the exception of the caesium and strontium. Neither of these was removed by SBM2 and the removal of both was about 70 % by SBM1. These results suggest that the uptake of caesium and strontium onto the hexacyanoferrates(II) is due to adsorption whereas the uptake of the other nuclides is probably due to the deposition of insoluble hydrolysis products, and is therefore independent of the functionality of the exchanger. This is also suggested by comparing the faster kinetics of the caesium and strontium uptake at pH 8 with those of the other nuclides.

Some measurements of the distribution coefficients for caesium and some other radionuclides with nickel hexacyanoferrate have also been given by Kawamura et al.(87). There was large caesium removal in both neutral and acidic conditions, limited removal of iron and removal of cobalt only in 4M HNO_3. Only very limited removal of zirconium was found.

The kinetics of caesium uptake onto NaNiHCF and KNiHCF appear to be slower than those reported by Phillips et al.(143) for the NaCuHCF. This could be accounted for by the smaller particle size of the NaCuHCF which was 100-500 microns whereas in the present work both the KNiHCF and NaNiHCF were granular with the relatively large size of 600-1000 microns.

The caesium distribution coefficients, R_d, after a contact time of 30 hours are significantly larger than those after 24 hours indicating that equilibrium had not yet been reached. The R_d values are all larger (above 5000), however the values for NaNiHCF at pH 8 are not as high as the other values. This may be due to a more stable granular form of the NaNiHCF at pH 8 which would result in slower kinetics. These R_d values, and the values given in Section 5.3 for sorption from only a caesium solution, are of the order 10^4, although a more accurate comparison cannot be made due to the relatively large counting errors. It is expected that the

caesium R_d values would be less when other nuclides are also in the solution due to interference effects. A reduction in the caesium distribution coefficients in the presence of high concentrations of cerium, strontium and ruthenium was also observed by Kawamura et al.(87)

CHAPTER 6

THE SORPTION OF RADIOCAESIUM BY NaNiHCF IN A PACKED COLUMN AND THE PREDICTION OF BREAKTHROUGH CURVES

6.1 Introduction

The column performance of some of the prepared samples of sodium nickel hexacyanoferrate (NaNiHCF) for the removal of caesium from aqueous solution was investigated. The experimental breakthrough curves were obtained in small-scale packed columns using an automated counting system.

The curves were fitted to a mathematical model which involved the solution of the material balance and kinetic equations. A comparison was made between the numerical solution obtained using a Freundlich type isotherm and the analytical solution which is possible when the isotherm is assumed to be rectangular.

6.2 Experimental methods

6.2.1 Column set-up

The sorption of caesium in a packed bed of NaNiHCF was investigated using the experimental rig shown in Fig. 6.1. In each test 1 or 2 g of the exchanger was placed in a glass column of 1 cm diameter, where it was supported by a sintered glass filter. The adsorber was gently fluidised by back washing with 1 M $NaNO_3$ which served to remove trapped air bubbles and also to fully wet the adsorber.

Feed solutions were prepared using 100, 500 or 1000 mg/L caesium as inactive $CsNO_3$, and 1 M $NaNO_3$. Tracer caesium-134 (0.605 MeV γ emitter) was used which allowed efficient and convenient analysis of caesium in the samples by gamma scintillation counting. It was calculated that the ambient tracer caesium concentration in the solutions was negligible.

An estimate of the volume of feed and the time required to reach breakthrough was made from the measured batch capacity of the adsorber and the concentration of caesium in the feed. With the flowrates used (0.075 and 0.21 m^3 m^{-2} h^{-1}) it was found that periods in excess of 24 hours would be required. A constant speed peristaltic pump was used for the feed which was found to give a constant flow over these required periods.

6.2.2 Set-up of counting equipment for analysis of the column effluent

A method of automatically counting the column effluent was designed, as shown in Fig. 6.2, in order to run the tests over long periods. The effluent was passed through a coil which was attached to an intrinsic germanium detector that was connected to a Canberra Series 35 multichannel analyser (MCA). The analyser was programmed to repeatedly count the effluent over a fixed period of time and provide a printout of the data.

The sample coil was filled through an empty column to ensure an accurate count of the feed solution. Independent samples of the feed and column effluent were collected to check for the build up of caesium on the surface of the sample coil, or the carrying over of fines, and counted separately to check the ratio of the caesium concentrations.

The response of the counting system was tested with a step change in the feed which was passed through an empty column. The flowrate of the feed was 17.1 mL/h, and the system was set up to take 5 minute counts over the period of the step change. The response to the step change is shown in Figure 6.3. From the step change, an estimate was made of the dead volume below the packed bed and of the associated tubing before the sampling coil on the detector. This dead volume was accounted for in the total effluent volume for the time at which the effluent concentration was measured.

Figure 6.1 Column test rig

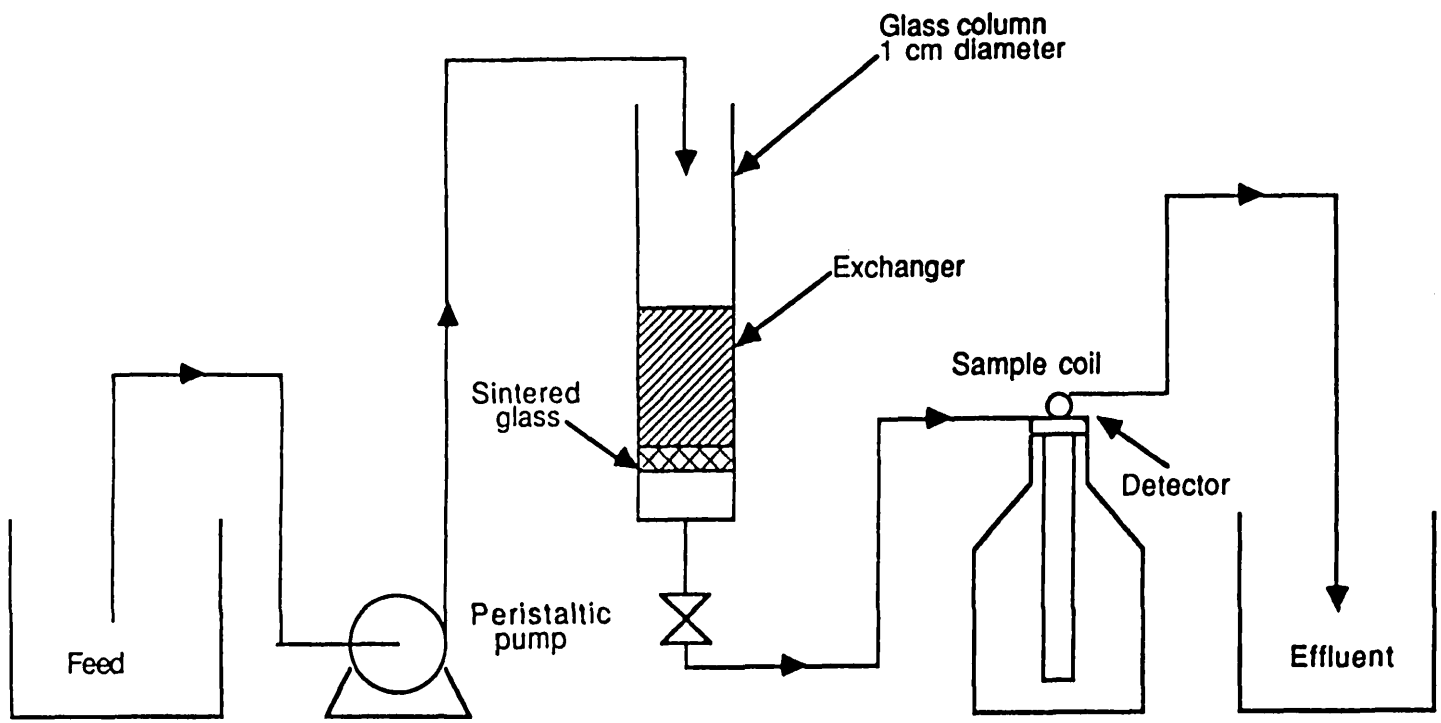


Figure 6.2 Arrangement of counting equipment for column tests

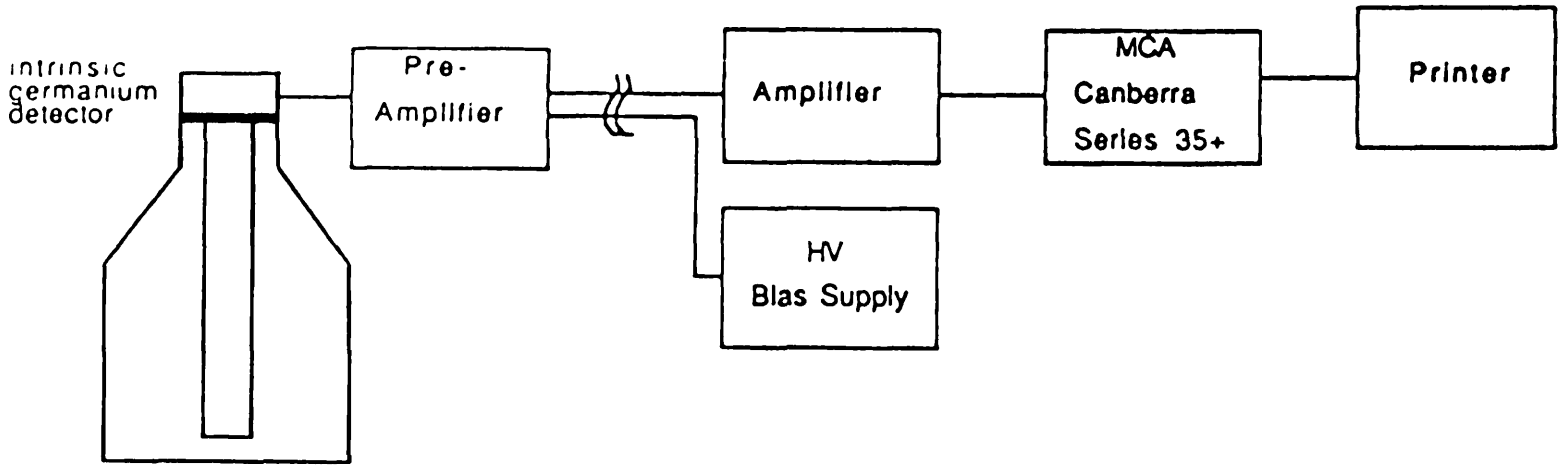
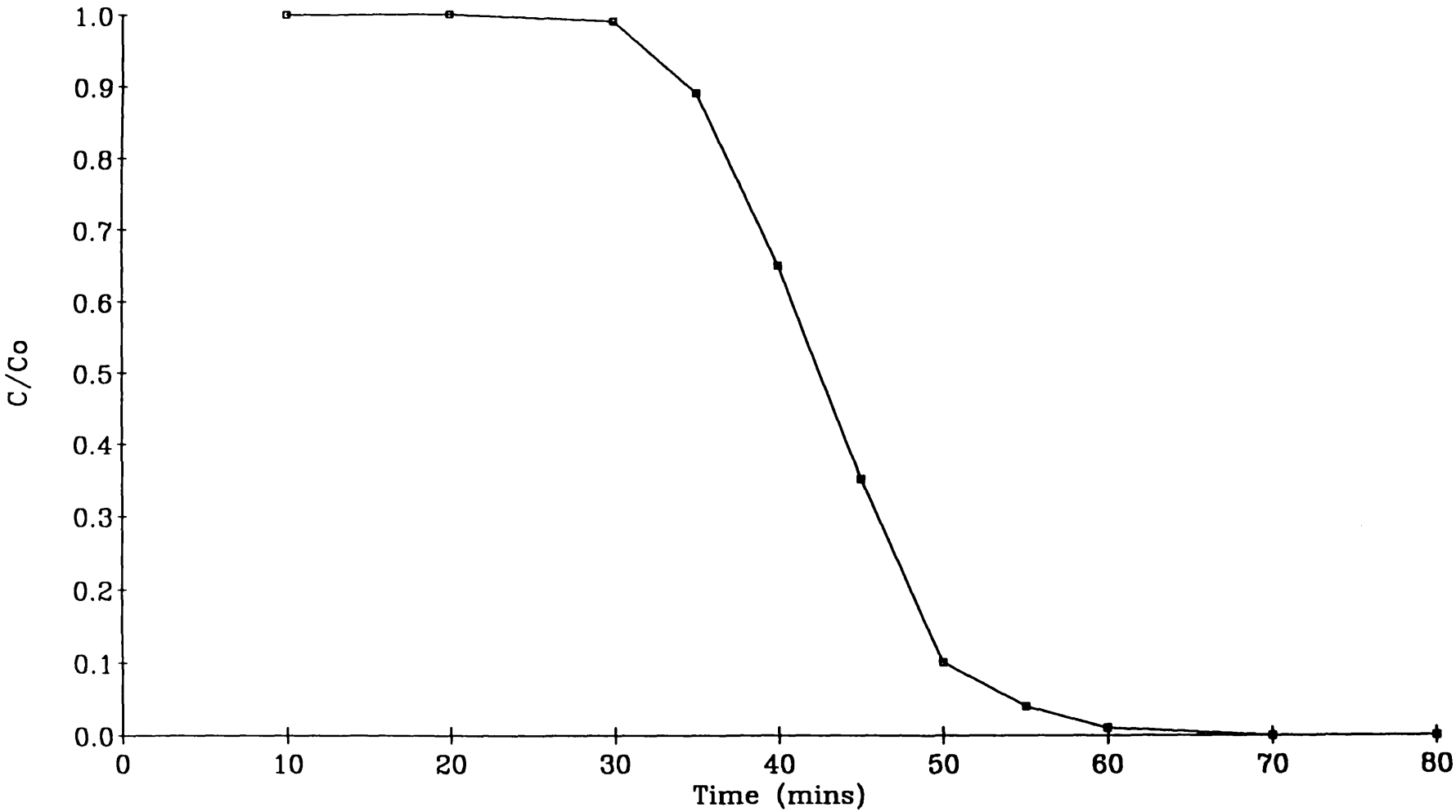


Figure 6.3 Response of the counting equipment to a step change in an empty column



6.2.4 Calculation of working capacity

The working capacity, q_0 (mg/g), of the adsorber was calculated as the average caesium loading per dry mass of the adsorber, m, at the end of a column test as detailed in Section 5.2.2. The capacity can be calculated directly from the area above the breakthrough curve, A_{btc}. When the breakthrough curve is plotted as the dimensionless concentration of the fluid, x, against the number of void bed volumes of feed, BV, the area above the curve is dimensionless and is related to capacity by equation 6.1.

$$q_0 = \frac{A_{btc}\, c_0\, z\, \pi\, d_c^2\, e}{4\, m} \tag{6.1}$$

The capacity measured from the breakthrough curve was also checked by mass balance from the total volume of the column effluent, V_{te}, and its caesium concentration, c_{te}, according to equation 6.2.

$$q_0 = \frac{V_{te}\,(c_0 - c_{te})}{m} \tag{6.2}$$

6.2.4 Determination of bed voidage

The voidage of the packed bed was measured directly using 1 g of the adsorber, which was wetted and then loaded as a slurry into a small glass column which had a sintered glass bottom. The bed was allowed to settle and then the solution level was lowered carefully to that of the adsorber. The column was centrifuged to remove the interstitial solution and a value of the bed voidage(e) calculated from the volume of fluid removed.

6.2.5 Prediction of mass transfer mechanism

A detailed discussion of the mass transfer mechanisms involved in ion exchange and sorption process is given in the standard texts, particularly those by Helfferich(20,144), Ruthven(135) and Vermeulen(145). The rate of sorption is

usually controlled by either liquid film diffusion, diffusion through the particle, or the rate of reaction. In intermediate cases, it can be found that a combination of resistances have significant effects and consequently, each needs to be considered individually. A comprehensive treatment of six standard models used for adsorption processes has been given recently by Do and Rice(146) who suggest that two key parameters can be used to select the appropriate model.

The best method of distinguishing between particle and film diffusion is the interruption test which can be applied to column tests, although it is more often used in kinetic tests. The sorption test is stopped by removing the particles from solution for a short period of time. On reimmersion only particle diffusion control will give a sorption rate higher than that at the moment of interruption. The increased rate is due to internal concentration gradients having time to level out. An example of the use of the interruption is given by Lee(33,86) in a study of the mechanism of caesium sorption onto KCuHCF. In column tests, the interruption test can be simply applied by interrupting the flow of the feed solution for a period of time, and then restarting it again. Similarly, if a column test which has reached complete breakthrough is stopped and left for a period of time, it may be found that caesium is again removed on restarting the feed. This was carried out in column test 9.

An additional criterion which may be used to distinguish between particle and film diffusion is the effect of the solution concentration on the sorption rate and the shape of the breakthough curve as described by Hall et al.(147). The sorption rate will beindependent of the solution concentration if particle diffusion is controlling, while for film diffusion, the rate will be proportional to the concentration(20). Column tests 12 and 13 were carried out under identical conditons with the exception of the feed concentration, and provide an additional indication of the sorption mechanism.

6.3 Prediction of column performance

6.3.1 The development of a suitable mathematical model

The prediction of the onset of breakthrough and the shape of the breakthrough curve are of fundamental importance in the design and scale-up of an adsorption column. A considerable amount of literature is available on the prediction of breakthrough curves and the effect of different mass transfer mechanisms and equilibrium relationships. An extensive review of the different cases is given by Ruthven(135) and Vermeulen(145). In general, a solution of the mass and heat balances coupled with an adsorption rate expression is required to obtain the breakthrough curve.

For the sorption of trace quantities, it can be assumed that the column is isothermal and the breakthrough curve obtained by the simultaneous solution of a differential mass balance and a sorption rate equation. Assuming plug flow through the column and that there is negligible axial dispersion, the usual form of the differential mass balance is given by:-

$$u \frac{\partial c}{\partial z} + \frac{\partial c}{\partial t} + \left(\frac{1-e}{e}\right) \rho_p \frac{\partial q}{\partial t} = 0 \qquad (6.3)$$

The form of the sorption rate equation and definition of a suitable mass transfer coefficient are dependent on the mechanism of mass transfer and a representative driving force. From the general shape of the breakthrough curves and results from the tests described in Section 6.2.5, it was proposed that the sorption of caesium by NaNiHCF is controlled by particle diffusion within the range of conditions used. Using a pseudo mass transfer coefficient, k, and applying the Glueckauf and Coates(148) approximation of a linear driving force across a solid film, the rate of sorption may be represented by:-

$$\frac{\partial q}{\partial t} = k (q^* - q) \qquad (6.4)$$

The value of k is a function of the particle diameter, diffusivity and a correction factor for the linear driving force. An expression relating k to the particle phase diffusivity is given by Glueckauf(149).

An alternative approximation to the linear driving force is the quadratic driving force of Vermeulen(141), who found that it provided a better fit for data. Cooper(150) found that this quadratic approximation gave much better agreement to the exact solution for slow particle diffusion in spheres with an irreversible equilibrium. However, use of the quadratic driving force considerably complicates the solution, and it is generally found that use of the linear driving force can provide an adequate fit of data(151,152).Battrum and Thomas(153) compared the use of the linear and quadratic driving forces to model the adsorption of CO_2 by activated carbon with a favourable isotherm, and found that the solutions were very similar with both providing good fits of experimental data. Another example of the use of the linear driving force approximation is given by Chiang and Hwang(154) in a moving zone collocation method for the simulation of long adsorption columns. A linear driving force is also widely used with an overall mass transfer coefficient in cases when both external and internal mass transfer resistances are significant. This approach was used by Sowerby and Crittenden(155) to simplify the solution of a more complex vapour phase adsorption and desorption model.

The value of q^*, the solid phase concentration in equilibrium with x, is obtained from the sorption isotherm. For NaNiHCF, the caesium sorption isotherm has already been described in detail in Section 5.4 where it was fitted by a Freundlich expression. By restricting this to a specified concentration range, the expression is usually put into a dimensionless form:-

$$y^* = x^b \tag{6.5}$$

By defining the usual time(τ) and bed(ξ) parameters, Equations 6.3 and 6.4

may also be transformed into dimensionless form as follows:-

$$\frac{\partial x}{\partial \xi} + \frac{\partial y}{\partial \tau} = 0 \tag{6.6}$$

$$\frac{\partial y}{\partial \tau} = (y^* - y) \tag{6.7}$$

Where:-

$$\tau = k\left(t - \frac{z}{u}\right) \tag{6.8}$$

and $$\xi = \frac{k\rho_p q_o z}{c_o u}\left(\frac{1-e}{e}\right) \tag{6.9}$$

For an initially unreacted bed to which a feed of concentration c_o is introduced at time t=0, the initial and boundary conditions are:-

I.C. $t = 0$: $\tau = -k\frac{z}{u}$ $x = y = 0$ at all z

B.C. $t > 0$: $x = 1$ at $z = 0$

The solution of Equations 6.5, 6.6 and 6.7 require a numerical solution due to the non-linearity of the Freundlich equation. An implicit finite difference method was used in the present work which was based on the algorithm given by Kyte(151) as detailed in Section 6.3.2.

The non-linearity may be removed if the isotherm is extremely favourable by assuming that the adsorption is irreversible which would be described by a rectangular isotherm (ie. b=0). Equation (6.5) may then be replaced by:-

$$\begin{aligned} y^* &= 0 \quad \text{for } x = 0 \\ y^* &= 1 \quad \text{for } x > 0 \end{aligned} \tag{6.10}$$

The applicability of using a rectangular isotherm to represent a favourable ion exchange system has been discussed by Vermeulen(141). Prediction of the breakthrough curve is obtained by an analytical solution of equations 6.6, 6.7, and 6.10 which was developed by Cooper(150), as detailed in Section 6.3.3. The accuracy of the numerical solution can also be checked with the analytical solution at the limit of b=0.

6.3.2 Numerical solution with a Freundlich type isotherm

For the prediction of the breakthrough curve with a Freundlich type isotherm, a simulateous solution is required for equations 6.5, 6.6 and 6.7. By substituting for $\frac{\partial y}{\partial \tau}$ in equation 6.6 using equation 6.7, and also eliminating y* using equation 6.5, the solution is reduced to a pair of coupled non-linear partial differential equations:-

$$\frac{\partial x}{\partial \xi} = -(x^b - y) \tag{6.11}$$

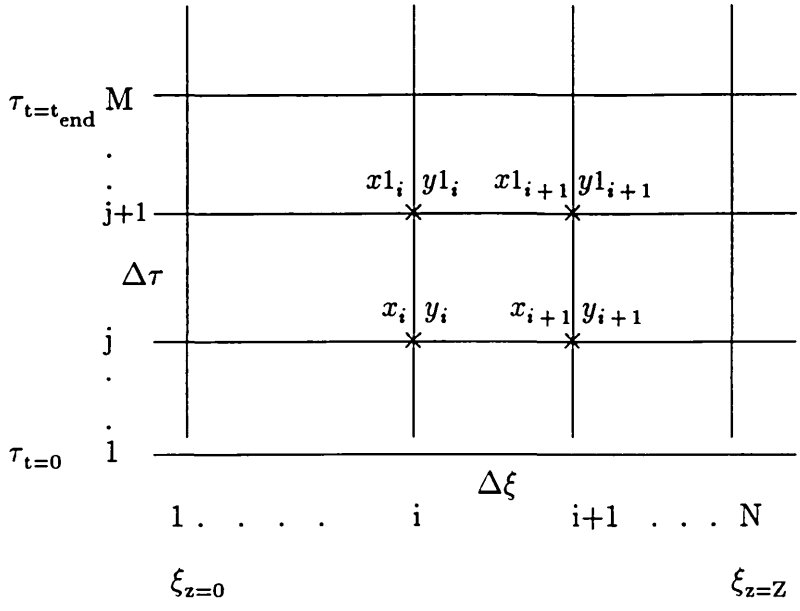
$$\frac{\partial y}{\partial \tau} = (x^b - y) \tag{6.12}$$

Equations 6.11 and 6.12 can be readily solved using a fully implicit method similar to the method used by Kyte(15 1). The method used by Kyte was used to solve a pair of equations when external mass transfer was controlling, as opposed to solid film control in the present model, and so some modifications to the basic method were required. Using the mesh points shown in Figure 6.4, the two equations may be put into finite difference forms:-

$$x_{i+1,j+1} = x_{i,j+1} - \frac{\Delta\xi}{2}\left\{(x^b - y)_{i,j+1} + (x^b - y)_{i+1,j+1}\right\} \tag{6.13}$$

$$y_{i,j+1} = y_{i,j} + \frac{\Delta\tau}{2}\left\{(x^b - y)_{i,j+1} + (x^b - y)_{i,j}\right\} \tag{6.14}$$

Figure 6.4 Mesh used in the numerical solution using implicit method



In the numerical solution it is convenient to reduce the variables x and y to one dimensional arrays by introducing the variables $x1_i$ and $y1_i$ corresponding to $x_{i,j+1}$ and $y_{i,j+1}$. The term $(x^b - y)_{i,j}$ was put into a subroutine (FUN) which was called for different values of the x_i, y_i, $x1_i$ and $y1_i$. Equations 6.13 and 6.14 are then transformed into the following equations which were used in the program:-

$$x1_{i+1} = x1_i - \frac{\Delta\xi}{2}\left\{\mathrm{FUN}(x1_{i,}, y1_i) + \mathrm{FUN}(x1_{i+1,}, y1_{i+1})\right\} \tag{6.15}$$

$$y1_i = y_i + \frac{\Delta\tau}{2}\left\{\mathrm{FUN}(x1_i \quad , y1_i) + \mathrm{FUN}(x_i, y_i)\right\} \tag{6.16}$$

The algorithm used in the fortran program Freund for the solution of equations 6.15 and 6.16 is outlined in the following points:-

i) Initial values of x_i and y_i were set by the initial conditions.

ii) The values of x_i and y_i were used as initial estimates of $x1_i$ and $y1_i$. At the first step, an intial estimate of 0.5 was used.

iii) The values of x_i and y_i at the start of an iteration were saved as $x1old_i$ and $y1old_i$.

iv) The values of $x1_{i+1}$ were calculated using equation 6.15 for i=1 to n − 1, or until a value of $x1_{1+1}$ was less than 10^{-4}, in which case nend =i+1.

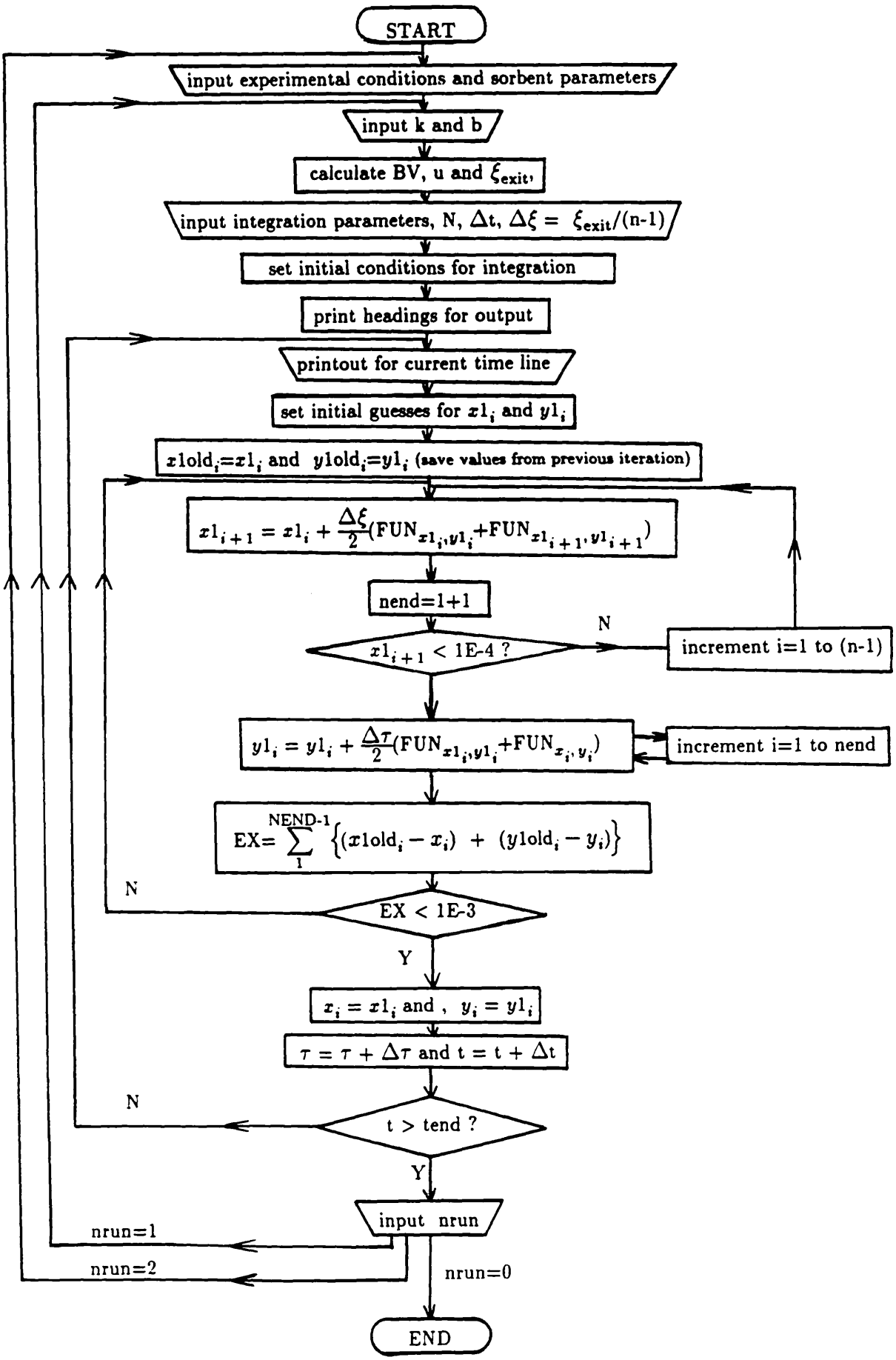
v) The calculated values of $x1_i$ were then used to calculate values of $y1_i$ using equation 6.16 for i=1 to nend.

vi) Steps iii, iv and v were repeated until converegence had been achieved.

vii) The calculation continued with step ii for a new time step

A detailed flow diagram for the fortran program FREUND is shown in Figure 6.5, and a full listing given in Appendix B. The program was compiled using Ryan McFarland Fortran on a 286-12 IBM compatible personal computer which was fitted with an Intel 287 maths coprocessor. The printout from a run using the data for column test 12 is shown in Figure 6.11 which is included in the results(Section 6.4). The run time for this case was about 1 minute.

Figure 6.5 Flow diagram of program FREUND.FOR



6.3.3 Analytical solution with an assumed rectangular isotherm

Prediction of the breakthrough curve is obtained by an analytical solution of equations 6.6, 6.7, and 6.10 which was developed by Cooper (150). The model was also used by Yoshida and Ruthven(152) who presented the solution in following form:-

$1+\tau < \xi$ $\quad y = x = 0$ (unreacted bed) (6.17)

$\xi < 1$ $\quad y = 1\text{- } e^{-\tau} \quad x = 1 - \xi e^{-\tau}$ (initial formation of pattern) (6.18)

$1 \leq \xi \leq 1 + \tau$ $\quad y = x = 1 - e^{\xi-\tau-1}$ (constant pattern) (6.19)

More recently, Yoshida et al.(156,157) compared the form of this solution with that obtained for the case of an external liquid film controlling, and also developed a combined solution for cases when both the internal and external films were significant. The essential difference between the solutions for internal solid film control and for liquid film control is the shape of the breakthrough curve at breakthrough. In the case of the solid film controlling the breakthough is sharp with a rapid increase in the exit concentration of the fluid, while for external fluid film controlling, the breakthrough is not clearly defined with a slow increase in the exit concentration.

The use of the analytical solution allows the model to be fitted directly to the experimental breakthrough curve using the measured uptake and a value for the pseudo mass transfer coefficient k.

The analytical model also provides an explicit expression for the value of the time parameter, τ_b at the onset of breakthrough:-

$$\tau_b = \xi - 1 \tag{6.20}$$

The corresponding value of the actual time, t_b, for breakthrough is given from rearranging the definition of τ, equation 6.8:-

$$t_b = \frac{\tau_b}{k} + \frac{z}{u} \qquad (6.21)$$

The analytical solution may be conveniently put into a Lotus spreadsheet which allows the convenient format for the input of experimental data and output of the predicted breakthrough curve. The experimental data can also be put into the same spreadsheet allowing the user to fit a value of the pseudo mass transfer coefficient interactively by viewing a graph of the predicted breakthrough curve together with experimental data. The equations used in the spreadsheet are shown in Figure 6.6, and the following procedure was used to fit the model to experimental data:-

i) The following experimental parameters are entered:-

test number and description of sample		
column height	Z	cm
column diameter	d_c	cm
bed voidage	e	-
feed concentration	c_0	mg/mL
feed flowrate	Q	mL/h
measured uptake of solid	q_0	mg/g
mass of solid	m	g

ii) The experimental breakthrough curve is entered in block F30:53 as a function of time, which is entered in block A30:53. For convenience an appropriate time increment is entered in E26.

iii) The following intermediate parameters are calculated in the spreadsheet:-

geometric bed volume	BV_g	$\frac{Z\, d_c^2\, \pi}{4}$	mL

volume ratio solid:void		(1-e)/e	-
interstitial velocity	u	$\frac{4\,Q}{\pi\, d_c^2\, e}$	cm/h
particle density	ρ_p	$\frac{m}{((1\text{-}e)BV)}$	g/mL
bed parameter at exit	ξ_{ex}	$\frac{k\rho_p q_o Z}{c_o u}\left(\frac{1-e}{e}\right)$	-
time parameter at breakthrough	τ_b	$\xi_{ex} - 1$	-
time at breakthrough	t_b	$\frac{\tau_b}{k} + \frac{z}{u}$	h

iv) The predicted breakthrough curve is calculated using the following parameters which are calculated for a t.

time parameter	τ	$k\left(t + \frac{Z}{u}\right)$	-
volume of solution fed	V	Q t	mL
no. void bed volumes fed	BV_v	$\frac{V}{BV_g\, e}$	mL
exit concentration	c	$1\text{-}\ e^{\xi_{ex}\text{-}\tau\text{-}1}$	mg/mL

iv) Iterate the value of k checking the predicted breakthrough curve with the experimental data by visual observation of a graph of the curves.

The printout of the spread sheet with the data for column test 12 is shown in Figure 6.10 which is included with the results in the next Section.

Figure 6.6 Equations used in Lotus spreadsheet to give analytical solution

	A	B	C	D	E
1	Column Test No.	12			
2	**********	**********			
3	Model :-	solid film, linear kinetics			
4					
5	column height		2.4	cm	
6	geometry	diameter	1	cm	
7		geometric BV	=C5*C6^2*3.1416/4	cm^3	
8		bed voidage	0.42		
9		(1-e)/e	=(1-C8)/C8		
10					
11	Feed	Co	0.5	mg/mL	
12		flow	5.65	mL/hour	
13		interstil.vel.	=(C12*4/(3.1416*C6^2*C8))		
14					
15	Exchanger	NJ1 B3	250-420	microns	
16		qo	83	mg/g	
17		mass	1	g	
18		ro	=(C17/((1-C8)*C7))	g/cm^3	
19					
20	mass trans.coeff.		0.34	h-1	
21					
22	Bed length parameter		=(C20*C16*C5*C18*C9/(C11*C13))		
23					
24	Tau breakthrough		=(C22-1)	time	=(C24/C20)+(C5/C13)
25					
26	tau increment		=(E26*C20)	time	0.5
27					
28	time (hours)	tau	volume mL	BV	C/Co
29	**********	**********	**********	*********	*********
30	10	=($C$20*(A30-($C$5/$C$13)))	=(A30*$C$12)	=C30/($C$8*$C$7)	0
31	20	=($C$20*(A31-($C$5/$C$13)))	=(A31*$C$12)	=C31/($C$8*$C$7)	0
32	25	=($C$20*(A32-($C$5/$C$13)))	=(A32*$C$12)	=C32/($C$8*$C$7)	0
33	=(A32+$E$26)	=($C$20*(A33-($C$5/$C$13)))	=(A33*$C$12)	=C33/($C$8*$C$7)	0
34	=(A33+$E$26)	=($C$20*(A34-($C$5/$C$13)))	=(A34*$C$12)	=C34/($C$8*$C$7)	0
35	26.6	=($C$20*(A35-($C$5/$C$13)))	=(A35*$C$12)	=C35/($C$8*$C$7)	
36	=(A35+$E$26)	=($C$20*(A36-($C$5/$C$13)))	=(A36*$C$12)	=C36/($C$8*$C$7)	=1-(EXP($C$22-B36-1))
37	=(A36+$E$26)	=($C$20*(A37-($C$5/$C$13)))	=(A37*$C$12)	=C37/($C$8*$C$7)	=1-(EXP($C$22-B37-1))
38	=(A37+$E$26)	=($C$20*(A38-($C$5/$C$13)))	=(A38*$C$12)	=C38/($C$8*$C$7)	=1-(EXP($C$22-B38-1))
39	=(A38+$E$26)	=($C$20*(A39-($C$5/$C$13)))	=(A39*$C$12)	=C39/($C$8*$C$7)	=1-(EXP($C$22-B39-1))
40	=(A39+$E$26)	=($C$20*(A40-($C$5/$C$13)))	=(A40*$C$12)	=C40/($C$8*$C$7)	=1-(EXP($C$22-B40-1))

6.4 Results

The full experimental details of each of the column tests is given in Table 6.1. In the tests a variety of the prepared products were used, some of which were heated in the mother liquor during the preparation as detailed in the table. The parameters which were varied were the feed solution, flowrate, packed height and the feed concentration.

Table 6.1 Experimental details of column tests

No.	sample	size micron	ppt. heated in Mother Liq.(80°C)	C_o mg/L	q_o mg/g	flow mL/h	BVH	Z cm	geometric BV	capacity mg/g(dry) area	effl.
1	NJ1 A1	250-420	2 hr	1000	98	17.1	9.9	2.2	1.73	100	-
2	NJ1 A1	150-250	2 hr	1000	98	17.1	11.1	2.0	1.54	100	-
3	NJ1 A2	250-420	2 hr	1000	100	17.1	10.4	2.1	1.65	100	-
5	NJ3 A1	250-420	2 hr	500	98	17.1	4.4	4.9	3.85	88	-
6	NJ3 B2	250-420	2 hr	500	81	17.1	9.9	2.2	1.73	81	-
8	NJ3 A1	250-420	2 hr	500	84	19.8	5.7	4.4	3.45	80	78
9	NJ3 A1	250-420	2 hr	500	84	22.3	11.8	2.4	1.88	83	76
10	NJ3 A1	250-420	2 hr	500	84	70.2	37	2.4	1.88	78	76
11	NJ1 A3	250-420	2 hr	100	94	19.8	10.5	2.4	1.88	72	-
12	NJ1 B3	250-420	2 hr	500	85	5.65	3.0	2.4	1.88	83	-
13	NJ3 B3	250-420	2 hr	1000	85	5.65	3.0	2.4	1.88	84	86
14	NJ3 B3	250-420	2 hr	1000	85	3.21	6.04	2.4	1.88	78	77
15	NJ3 A3	600-1000	2 hr	1000	92	5.6	9.45	1.8	1.41	94	92
16	NJ5 A1	250-420	no	1000	174	16.8	11.9	1.8	1.41	162	173
18	NJ5 A2	250-420	no	1000	174	5.87	2.2	3.4	2.67	174	176
19	NJ7 A2	250-420	no	1000	161	5.1	6.65	1.9	1.49	161	172
20	NJ7 B3	250-420	no	1000	134	18.3	10.9	3.8	3.98	122	129
21	NJ7 B1	250-420	no	1000	133	18.3	5.47	1.9	1.49	117	109

Typical experimental breakthrough curves for three of the column tests(12, 16 and 18) are shown in Figures 6.7, 6.8 and 6.9. In these breakthrough curves the dimensionless solution concentration at the column exit is plotted against the number of void bed volumes of solution passed through the column. In test 12, the sample was heated in the mother liquor during the preparation while for column tests 16 and 18 the samples were not heated.

In order to fit the models to the experimental curves, the working capacity of the adsorber was first calculated as described above. A value for the pseudo mass transfer coefficient was initially obtained by directly fitting the analytical model as described in Section 6.3.3. A printout of the spreadsheet with the data used for column test 12 is shown in Figure 6.10. The value of the pseudo mass transfer coefficient was then varied slightly to achieve the best fit with the numerical model incorporating the Freundlich isotherm. The output from program FREUND with the predicted breakthrough curve for column 12 is shown in Figure 6.11. The predicted breakthrough curves for tests 12, 16 and 18 are shown together with the experimental curves in Figures 6.7, 6.8 and 6.9.

Figure 6.7 Breakthrough curve for column test 12

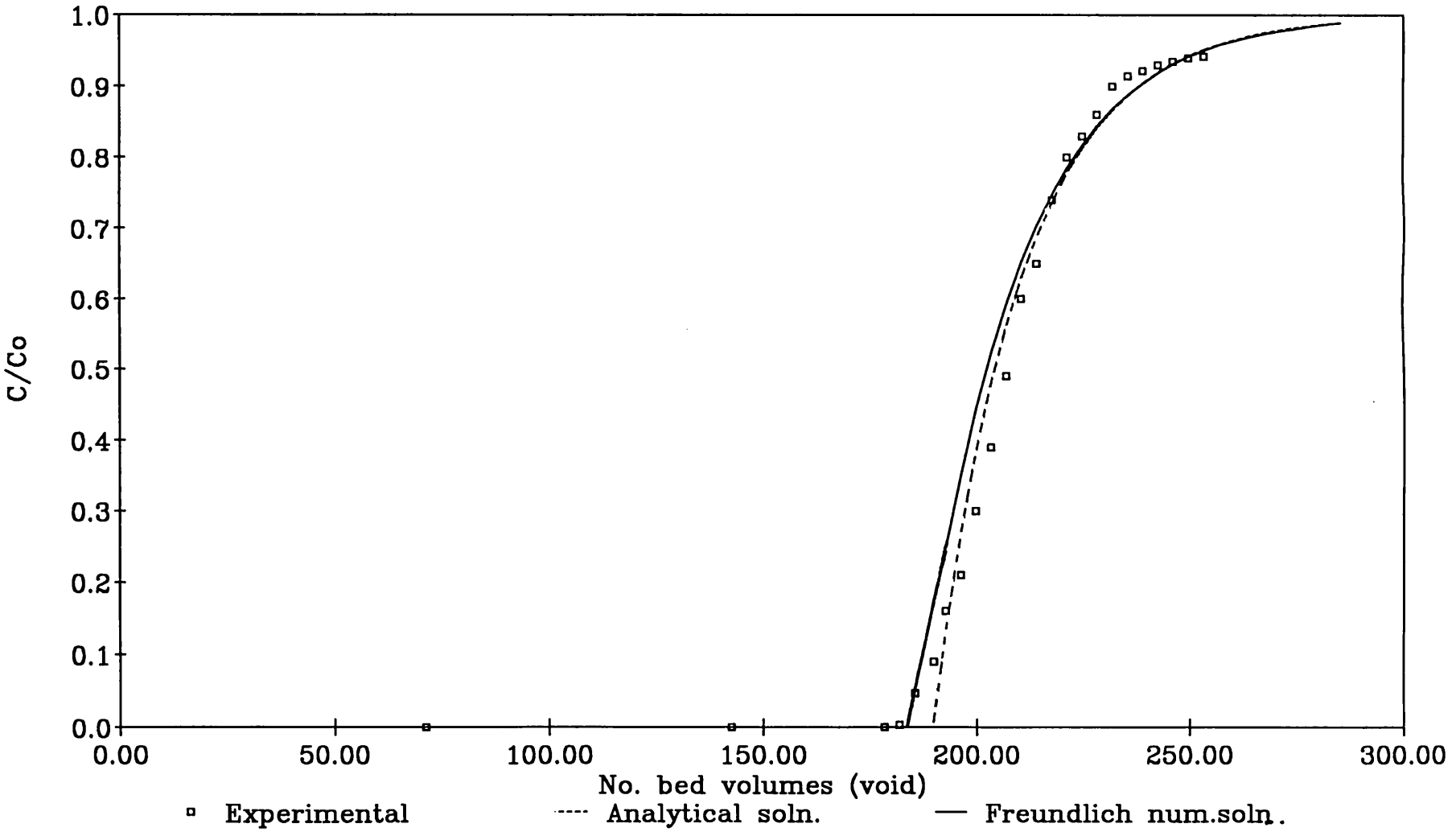


Figure 6.8 Breakthrough curve for column test 16

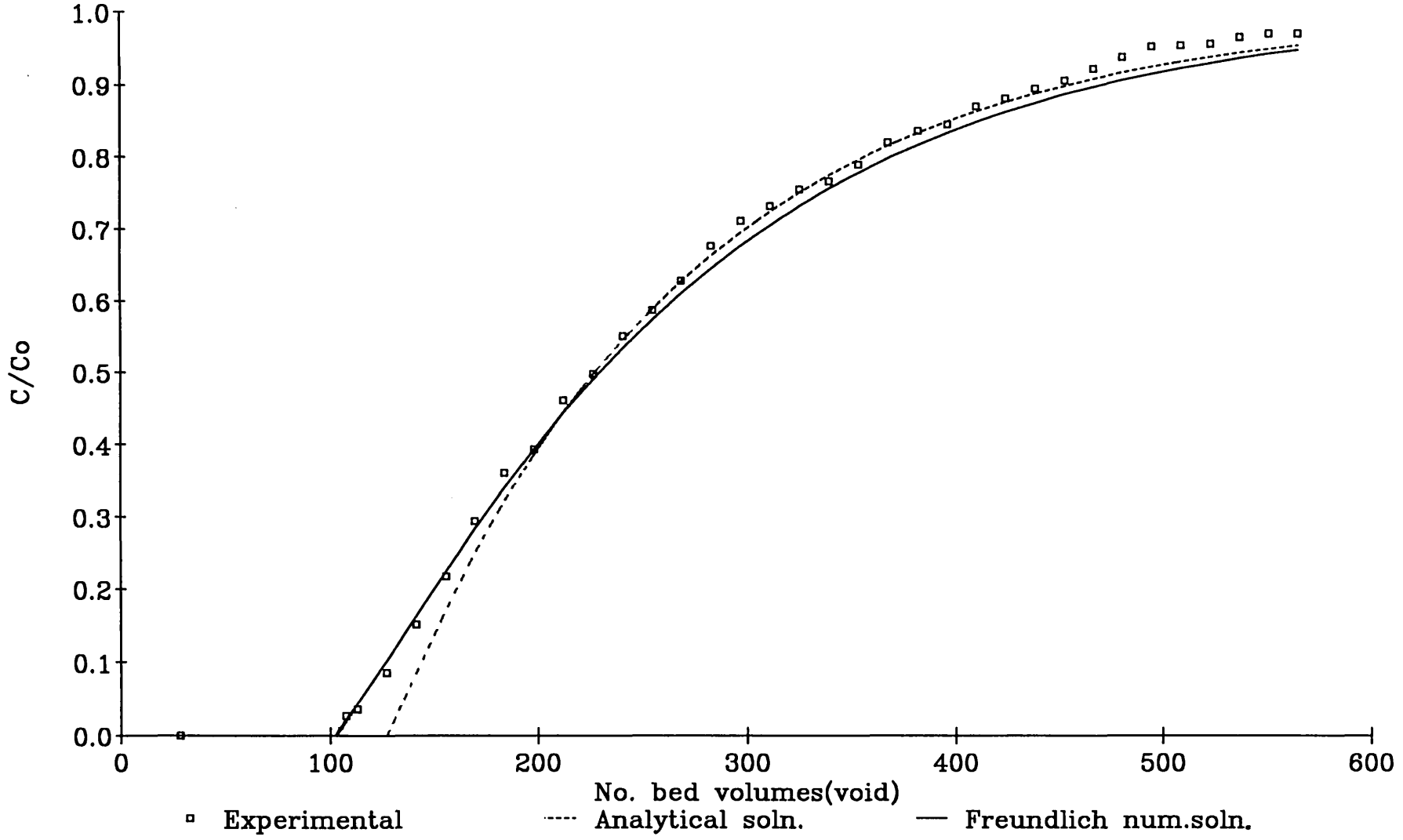


Figure 6.9 Breakthrough curve for column test 18

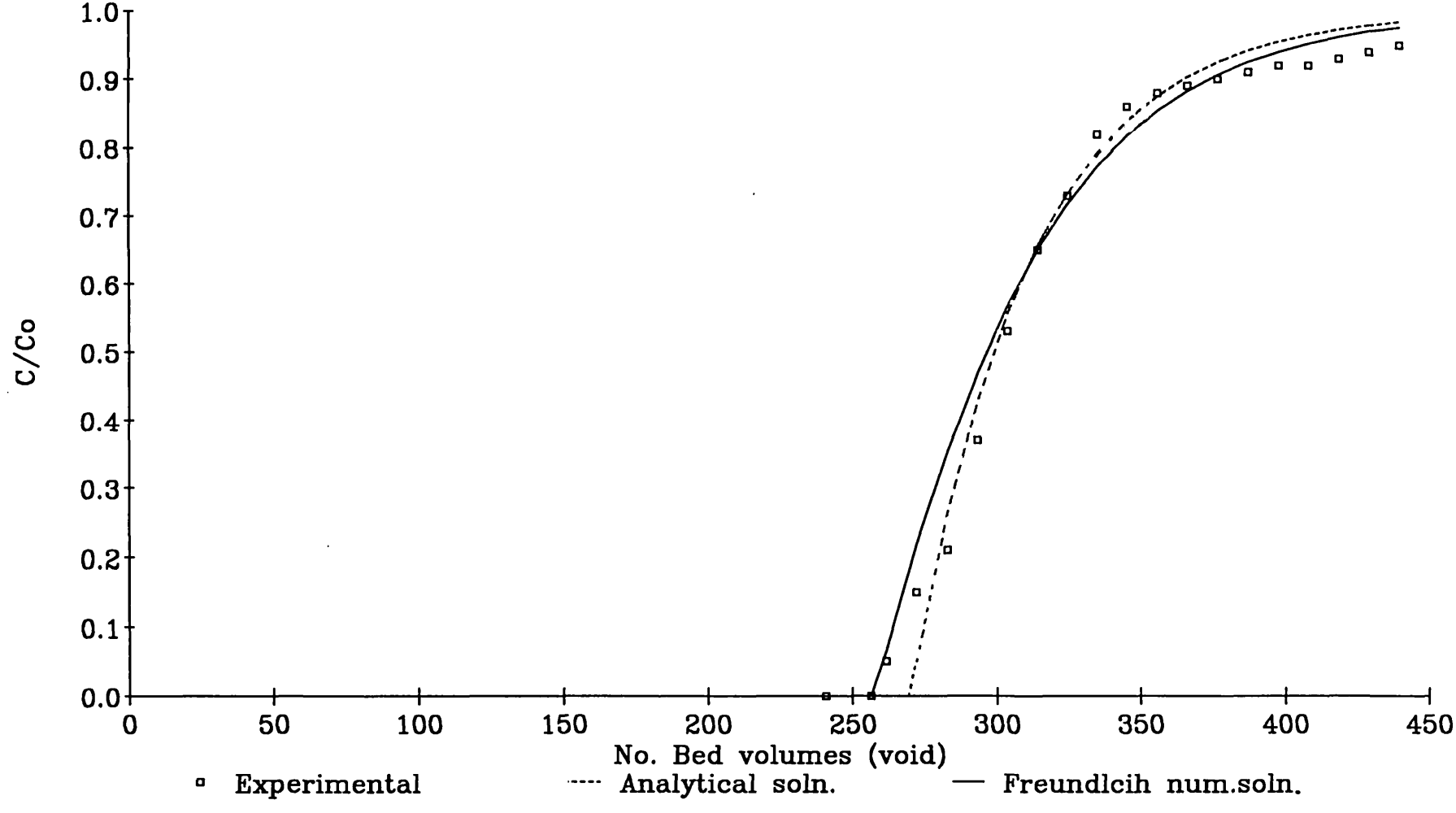


Figure 6.10 Lotus spreadsheet to give analytical solution for column test 12

	A	B	C	D	E	F
1	Column Test No.	12				
2	**********					
3	Model :-	solid film, linear kinetics				
4						
5	column height		2.4	cm		
6	geometry	diameter	1	cm		
7		geometric BV	1.885	cm^3		
8		bed voidage	0.42			
9		(1-e)/e	1.38			
10						
11	Feed	Co	0.5	mg/mL		
12		flow	5.65	mL/hour		
13		interstil.vel.	17.128			
14						
15	Exchanger	NJ1 B3	250-420	microns		
16		qo	83	mg/g		
17		mass	1	g		
18		ro	0.915	g/cm^3		
19						
20	mass trans.coeff.		0.34	h-1		
21						
22	Bed length parameter		9.989			
23						
24	Tau breakthrough		8.989	time	26.58	hours
25						
26	tau increment		0.17	time	0.5	
27						exp. data
28	time (hour	tau	volume mL	BV	C/Co	C/Co
29	**********					*********
30	10	3.35	56.50	71.37	0	0
31	20	6.75	113.00	142.73	0	0
32	25	8.45	141.25	178.42	0	0
33	25.5	8.62	144.08	181.99	0	0.003
34	26	8.79	146.90	185.55		0.046
35	26.6	9.00	150.29	189.84	0.0070	0.09
36	27	9.13	152.55	192.69	0.1332	0.16
37	27.5	9.30	155.38	196.26	0.2687	0.21
38	28	9.47	158.20	199.83	0.3831	0.3
39	28.5	9.64	161.03	203.40	0.4795	0.39
40	29	9.81	163.85	206.96	0.5609	0.49
41	29.5	9.98	166.68	210.53	0.6295	0.6
42	30	10.15	169.50	214.10	0.6874	0.65
43	30.5	10.32	172.33	217.67	0.7363	0.74
44	31	10.49	175.15	221.24	0.7775	0.8
45	31.5	10.66	177.98	224.81	0.8123	0.83
46	32	10.83	180.80	228.37	0.8417	0.86
47	32.5	11.00	183.63	231.94	0.8664	0.9
48	33	11.17	186.45	235.51	0.8873	0.915
49	33.5	11.34	189.28	239.08	0.9049	0.922
50	34	11.51	192.10	242.65	0.9198	0.93
51	34.5	11.68	194.93	246.22	0.9323	0.935
52	35	11.85	197.75	249.78	0.9429	0.94
53	35.5	12.02	200.58	253.35	0.9518	0.942
54	36	12.19	203.40	256.92	0.9594	
55	36.5	12.36	206.23	260.49	0.9657	
56	37	12.53	209.05	264.06	0.9711	
57	37.5	12.70	211.88	267.63	0.9756	
58	38	12.87	214.70	271.19	0.9794	

Figure 6.11 Printout of Fortran program FREUND.FOR

Numerical solution for column test 12

```
COLUMN NO.  12 SAMPLE
      H (CM)    D (CM)     B V (ML)     E
      2.40       1.00       1.88       0.42
   CO (MG/ML)  QO (MG/G) ROP (G/ML)    Q (ML/H)
      0.50       83.00       0.92          5.65

SOLID FILM, LINEAR    DRIVING FORCE, FREUNDLICH ISOTHERM

MASS TRANSFER COEFFICIENT  0.380 H-1
FREUNDLICH COEFFICIENT     0.13

FOR INTEGRATION  N =  50  DT = 0.1000

NIT   TIME(H)  TAU    VOL (BV)    XO     YO     X      Y

  0     0.0  -0.05      0.0      1.000 0.001 0.001 0.001
  5     1.0   0.33      3.0      1.000 0.317 0.001 0.001
  5     2.0   0.71      6.0      1.000 0.533 0.001 0.001
  5     3.0   1.09      9.0      1.000 0.681 0.001 0.001
  7     4.0   1.47     12.0      1.000 0.782 0.001 0.001
  5     5.0   1.85     15.0      1.000 0.851 0.001 0.001
  5     6.0   2.23     18.0      1.000 0.898 0.001 0.001
  6     7.0   2.61     21.0      1.000 0.930 0.001 0.001
  5     8.0   2.99     24.0      1.000 0.952 0.001 0.001
  5     9.0   3.37     27.0      1.000 0.967 0.001 0.001
  6    10.0   3.75     30.0      1.000 0.978 0.001 0.001
  5    11.0   4.13     33.0      1.000 0.985 0.001 0.001
  5    12.0   4.51     36.0      1.000 0.990 0.001 0.001
  6    13.0   4.89     39.0      1.000 0.993 0.001 0.001
  5    14.0   5.27     42.0      1.000 0.995 0.001 0.001
  5    15.0   5.65     45.0      1.000 0.997 0.001 0.001
  6    16.0   6.03     48.0      1.000 0.998 0.001 0.001
  5    17.0   6.41     51.0      1.000 0.998 0.001 0.001
  5    18.0   6.79     54.0      1.000 0.999 0.001 0.001
  6    19.0   7.17     57.0      1.000 0.999 0.001 0.001
  7    20.0   7.55     59.9      1.000 1.000 0.001 0.001
  5    21.0   7.93     62.9      1.000 1.000 0.001 0.001
  6    22.0   8.31     65.9      1.000 1.000 0.001 0.001
  7    23.0   8.69     68.9      1.000 1.000 0.001 0.001
  5    24.0   9.07     71.9      1.000 1.000 0.001 0.001
  6    25.0   9.45     74.9      1.000 1.000 0.001 0.001
  5    26.0   9.83     77.9      1.000 1.000 0.008 0.033
  5    27.0  10.21     80.9      1.000 1.000 0.234 0.251
  4    28.0  10.59     83.9      1.000 1.000 0.435 0.447
  4    29.0  10.97     86.9      1.000 1.000 0.587 0.596
  4    30.0  11.35     89.9      1.000 1.000 0.700 0.706
  4    31.0  11.73     92.9      1.000 1.000 0.783 0.787
  4    32.0  12.11     95.9      1.000 1.000 0.843 0.846
  4    33.0  12.49     98.9      1.000 1.000 0.887 0.889
  4    34.0  12.87    101.9      1.000 1.000 0.919 0.920
  3    35.0  13.25    104.9      1.000 1.000 0.941 0.942
  3    36.0  13.63    107.9      1.000 1.000 0.958 0.959
  3    37.0  14.01    110.9      1.000 1.000 0.970 0.970
  3    38.0  14.39    113.9      1.000 1.000 0.978 0.979
  3    39.0  14.77    116.9      1.000 1.000 0.984 0.985
  3    40.0  15.15    119.9      1.000 1.000 0.989 0.989
```

In order to investigate the effect of the column height independently, two column tests were carried out with the same parameters except for the height. In column Test 20, 2 g of the sample was used while in Test 21, 1 g was used. To show the similarity in the shape of the breakthrough curves, the curves expressed in terms of the number of void bed volumes of feed are shown in Figure 6.12 and the same curves are shown in Figure 6.13 expressed in terms of the actual volume of feed. In both figures the predicted breakthrough curves are shown which were calculated using the analytical solution with the assumed rectangular isotherm.

In order to gain an understanding of the mass transfer mechanism taking place some column tests were carried out using the tests described in Section 6.2.5. In column test 9, the test was stoppped after complete breakthrough had been reached and then was restarted 24 hours later in order to observe whether subsequent sorption of caesium took place. The full breakthrough curve for test 9 with the restart after the interruption is shown in Figure 6.14. Tests 12 and 13 were carried out under identical conditions, except that in test 12 the feed concentrations was 0.5 g Cs/L, while in test 13 the concentration was 1.0 g Cs/L. The experimental breakthrough curves for these two tests together with the predicted analytical solution with an assumed rectangular isotherm are shown in Figure 6.15

The full experimental details and the values of q_0 and k which were used in the prediction of the breakthrough curves for the column tests which were modelled are given in Tables 6.2 and 6.3

Figure 6.12 Breakthrough curves for column tests 20 and 21 (on basis of BV)

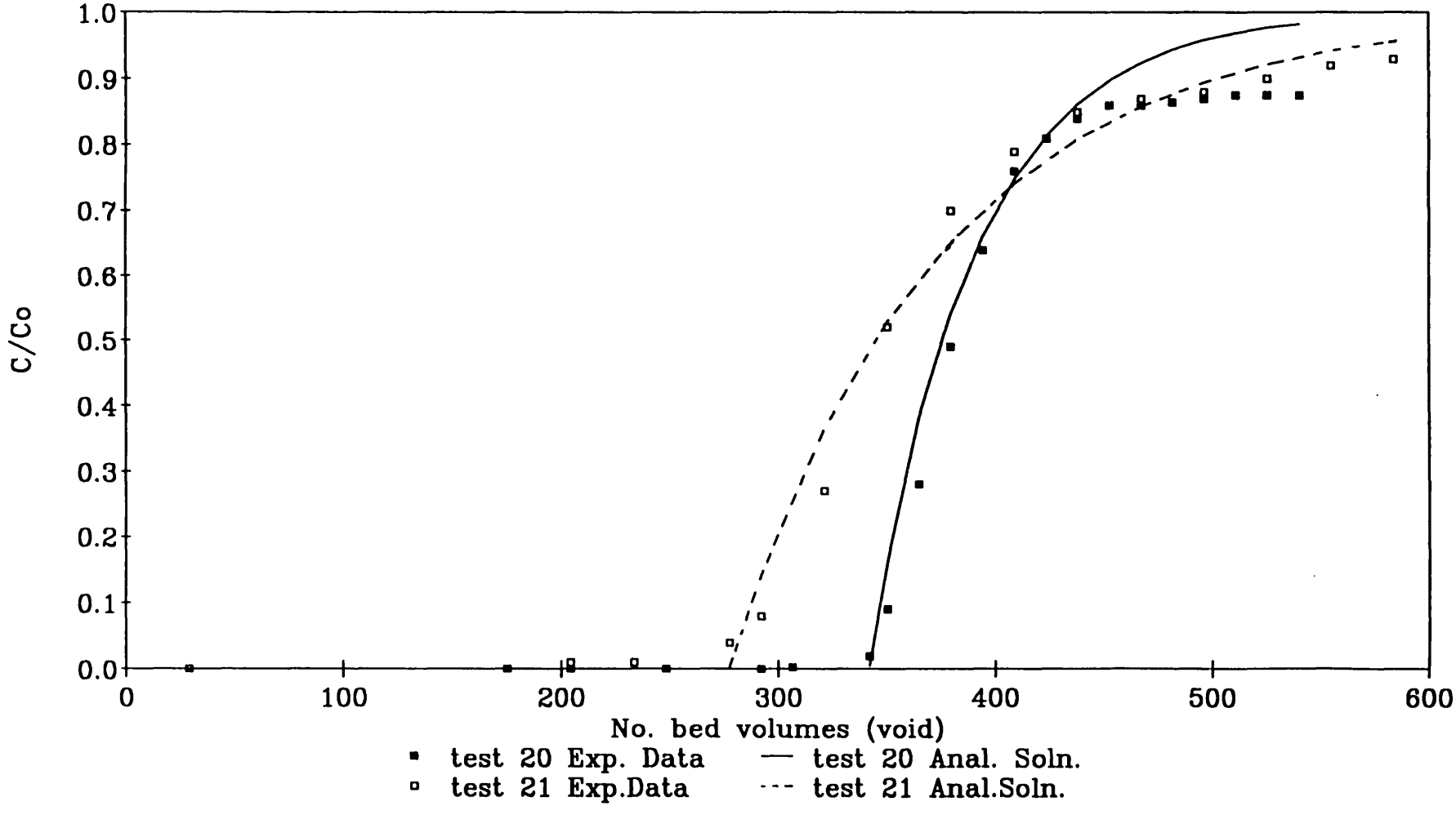


Figure 6.13 Breakthrough curves for column tests 20 and 21 (on basis of feed volume)

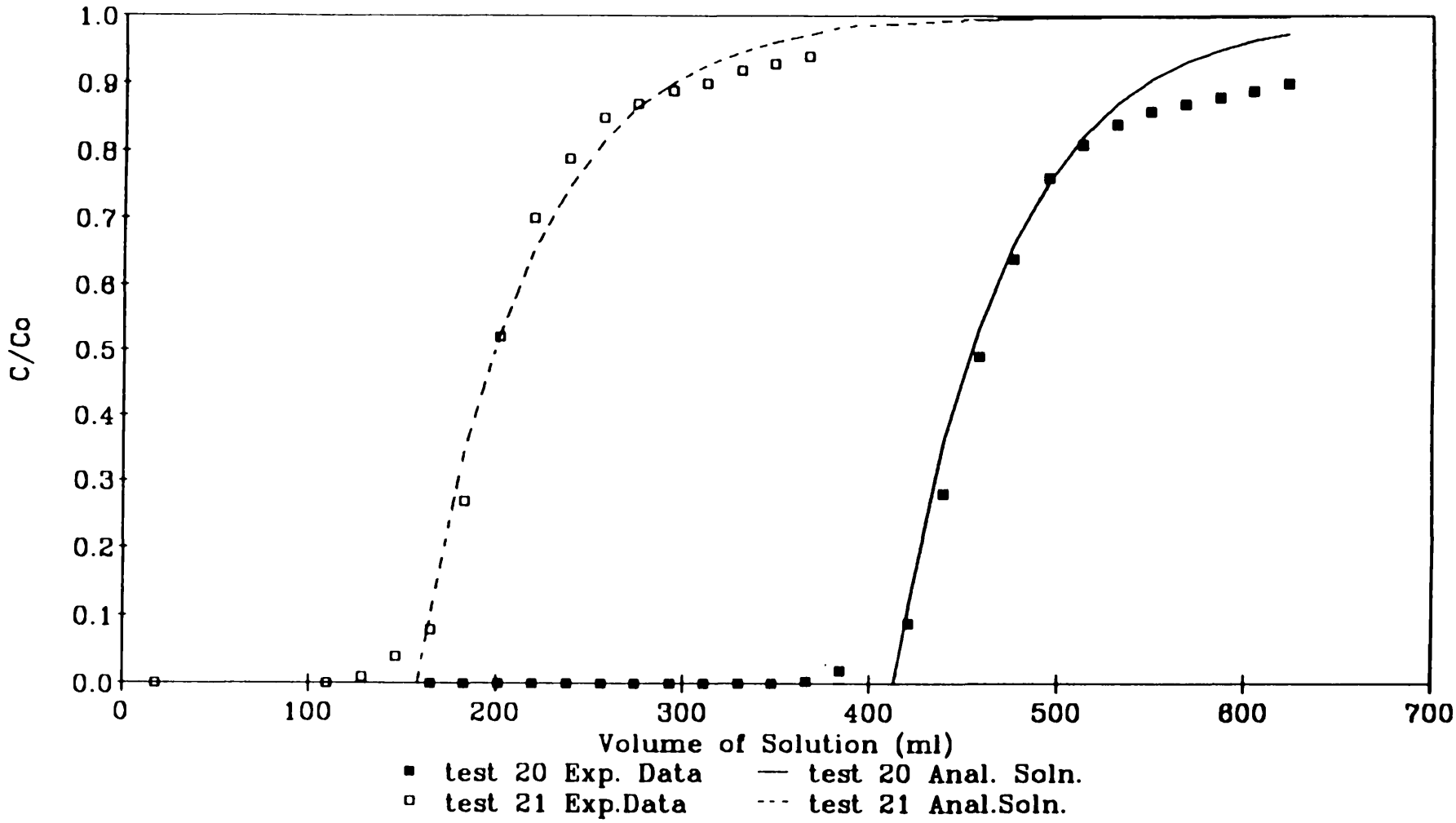


Figure 6.14 Breakthrough curve for column test 9
showing a restart after an interuption of 24 hours

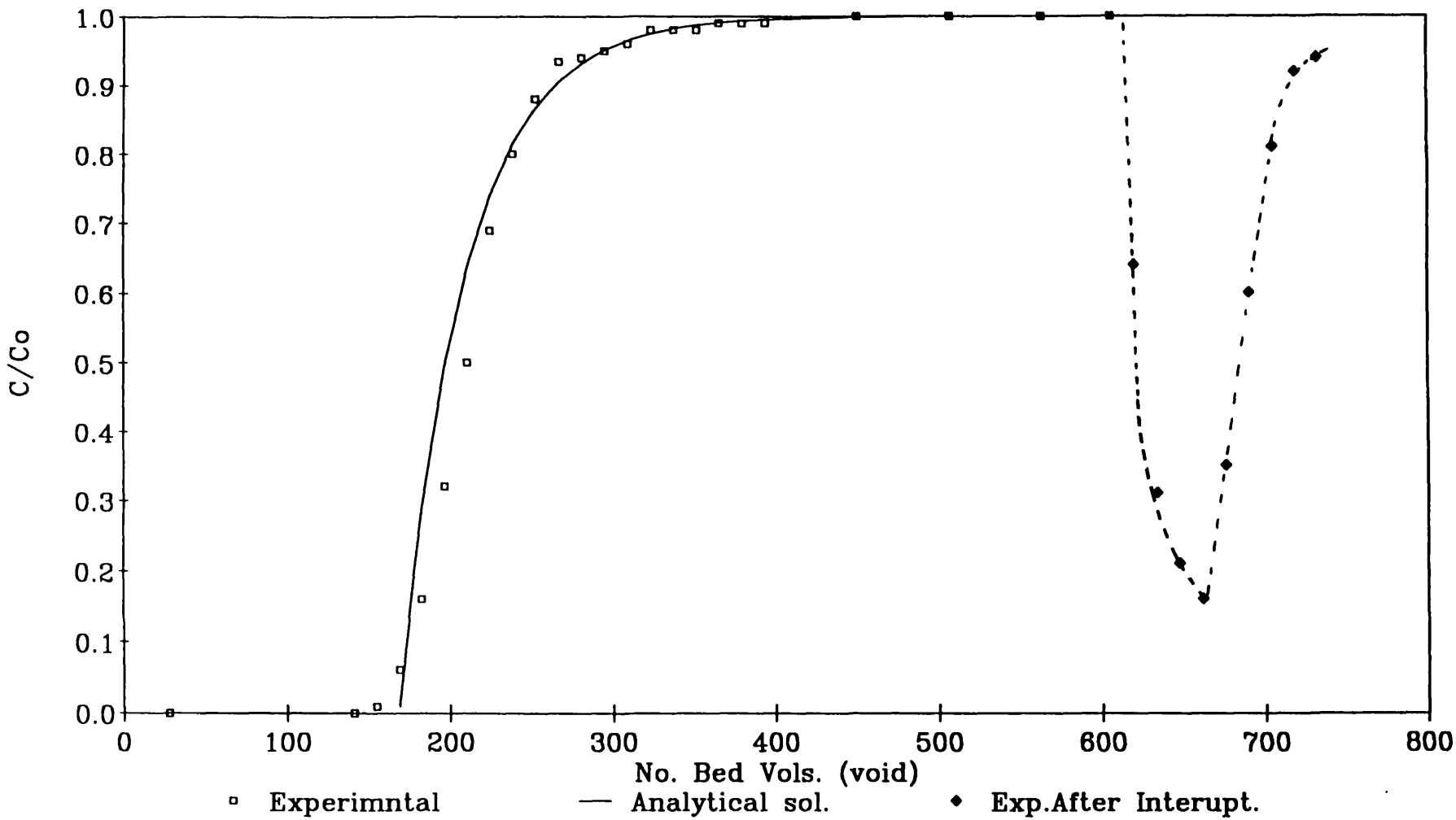


Figure 6.15 Breakthrough curve for column tests 12 and 13

To show the effect of feed concentration with all other parameters constant

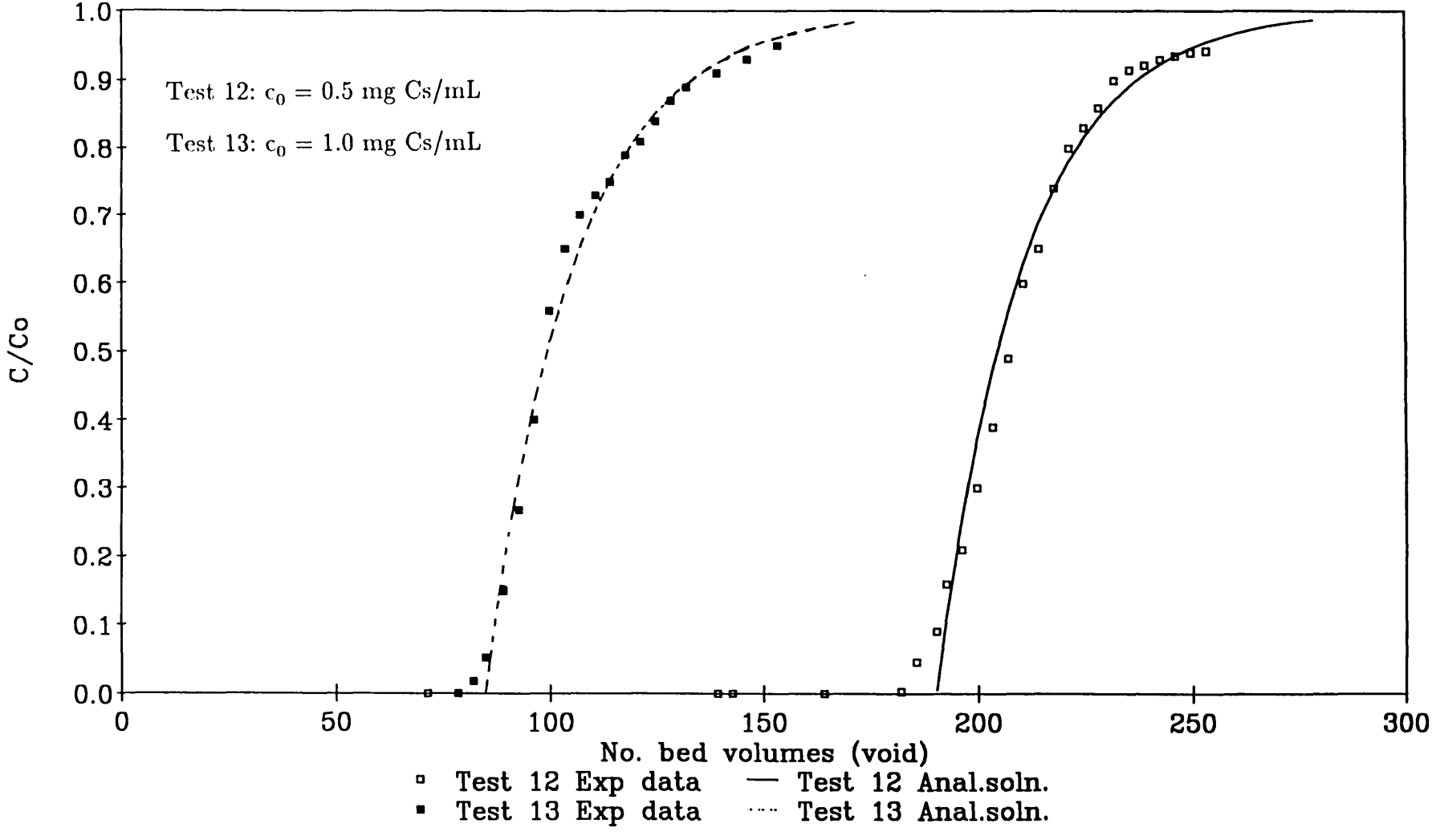


Table 6.2 Details of column tests which were modelled as examples

Test No.	9	12	13	16	18	20	21	
Column height	2.4	2.4	2.4	1.8	3.4	3.8	1.9	cm
Column diameter	1.0	1.0	1.0	1.0	1.0	1.0	1.0	cm
Bed voidage	0.42	0.42	0.42	0.42	0.42	0.42	0.42	-
Feed caesium conc.	500	500	1000	1000	1000	1000	1000	mg/L
Flowrate	22.3	5.65	5.65	16.8	5.9	18.3	18.3	mL/h
Mass of adsorber	1.0	1.0	1.0	1.0	2.0	2.0	1000	g(dry)
Density of adsorber	0.915	0.915	0.915	1.22	1.29	1.16	1.17	g(dry)/mL
Bed volume(void)	0.79	0.79	0.79	0.59	1.12	1.25	0.63	mL

Table 6.3 Parameters used to fit models

Test No.	9	12	13	16	18	20	21	
Working capacity of adsorber								
From area above curve	83	83	84	160	174	122	117	mgCs/g(dry)
From bulk effluent	75	81	86	165	172	129	120	mgCs/g(dry)
Fitted values of pseudo mass transfer coefficient								
Analytical solution	0.67	0.34	0.34	0.2	0.127	0.32	.315	h^{-1}
Numerical solution	NC	0.38	NC	0.24	0.15	NC	NC	h^{-1}
(NC= Not Calculated)								

6.5 Discussion

The general shape of the breakthrough curves obtained from the experimental column tests were good with no caesium detected in the effluent up to the breakthrough point which was characterised by a sharp rise in the caesium concentration. These sharp curves which were obtained, with both samples that were heated during the preparation and those which were not heated, are characteristic of a favourable isotherm with particle diffusion control. The measured capacities were in good agreement with those obtained from the batch tests described in Section 5.4.

The similarity in the shape of the breakthrough curves for tests 20 and 21 with different bed heights show that entry effects are not a major factor in the small scale tests. The curves follow the predicted pattern with the analytical solutions based on the number of bed volumes of feed and also the total feed volume. The two tests gave the same shaped curve when plotted against the feed volume while in the plot against the number of bed volumes, a difference was observed in the shape due to different bed volumes in the two tests.

The restart of test 9 (Figure 6.14) after an interruption and the effect of the fluid phase concentration on the shape of the breakthrough curves in tests 12 and 13 (Figure 6.15) provide further indications of the mass transfer mechanism as described in Section 6.2.5. In test 9, there is increased adsorption of caesium after the interruption, and in tests 12 and 13 the shapes of the breakthrough curves are very similar, indicating that the rate of adsorption is controlled by particle diffusion as already suggested by the general shape of the breakthrough curves.

The plots of the breakthrough curves show that both the numerical solution with the Freundlich isotherm and the analytical solution with assumed rectangular isotherm provide satisfactory fits of the experimental data. The value of the pseudo mass transfer coefficient was higher in test 9, when the flowrate was higher, than those in tests 12 and 13 when similar samples were used. In each of the tests, slightly lower value of the pseudo mass transfer coefficient were used for the

rectangular isotherm.

The accuracy of the models needs to be assessed by consideration of the fit along the shape of the curve and also by the occurrence of breakthrough. It was observed that both models seem to predict the shape of the curves adequately, although it was found that the use of the Freundlich isotherm predicts the occurrence of breakthrough more accurately.

All of the experimental breakthrough curves showed a slightly premature breakthrough which gave the characteristic 'S' shape to early part of the curves. In general, it is difficult to elucidate whether this is due to the deviation of the isotherm from the rectangular form, or to external mass transfer at low solute concentrations(20,135). In the present work, neither of the models predicts the premature breakthrough which suggests that the shape of the isotherm is not responsible, and it is therefore due to a change in the mass transfer mechanism. This is commonly observed in sorption processes and was found by Lee(33) for the case of the sorption of caesium by NaCuHCF. The more general model given by Yoshida et al.(156) can be used to include both film and intraparticle diffusion, although the solution is complicated by the need to determine values for a diffusional resistance parameter, δ. In the present work, the models used can be considered suitable as only slight deviations are observed, although for the prediction of performance with lower feed concentrations (eg. 10 mg/L Cs), consideration should be given to using the more general model.

Additionally, axial dispersion was not taken into account in the present models which could lead to a broadening of the curves which would account for the slightly premature breakthrough. According to Ruthven(135) the initial breakthrough time is more sensitive to the mass transfer resistance than to axial dispersion, whereas the situation is reversed in the saturation region. As the models used in the present work provide a good fit for the curves in the saturation region it can be deduced that axial dispersion is not important.

CHAPTER 7

CONCLUSIONS

Sodium nickel hexacyanoferrate (NaNiHCF) is a suitable material for the selective sorption of radiocaesium and is known to have advantages over the use of other complex hexacyanoferrates. These advantages include a high selectivity for caesium over a wide range of pH (2-10) and in the presence of high concentration of competing ions.

A freeze-thaw method was developed to prepare the NaNiHCF in a granular form using a ratio of Ni:$Fe(CN)_6$ = 1.3 and washing with 1 M $NaNO_3$. The conditions under which the prepared precipitates are frozen are crucial in obtaining a product with a good granular form suitable for use in a packed column. The use of insulation to slow down the rate of freezing was found to be the most significant factor for granulation to take place. It is therefore suggested that the freezing rate is controlled by the rate at which the heat of fusion can be removed from the samples rather than by the rate of either nucleation or crystal growth. It is also necessary that the freezing process is fully complete.

From a detailed analysis during the preparative steps and of the final products, it has been confirmed that NaNiHCF does not have a definite stoichiometric formula and is probably best represented by the general formula $Na_{2x}Ni_{2-x}Fe(CN)_6$ which was given by Loos Nescovic et al.(5).

It was found that heating the prepared precipitates of NaNiHCF in the mother liquor has an important effect on the release of nickel into solution and also the sorption properties of the final product. The capacities measured in both batch and column tests for the samples which were heated were in the range 80-90 mg Cs/g (0.6-0.68 meq./g) and for the samples which were not heated, 170-180 mg Cs/g (1.28-1.35 meq./g). For both products the adsorption isotherm was found to

be very favourable and could be fitted by a Freundlich type expression.

The product NaNiHCF is selective for caesium over a wide range of pH but is only completely stable in the range pH 4 to pH 10. Below pH 4 it is found that nickel is released from the product into solution, while above pH 10 decomposition of the product takes place.

It has been shown that the use of NaNiHCF in a packed column is very effective for the selective sorption of caesium from salt solutions. The experimental breakthrough curves show that no caesium was detected in the effluent up to the breakthrough point which was observed by a sharp rise in the caesium concentration.

The curves were fitted to a model which assumed that the sorption was controlled by a linear driving force across a solid film. The model was solved numerically using the Freundlich isotherm, and also by using an analytical solution with an assumed rectangular isotherm.

It was found that both models could be fitted to the experimental data using the measured parameters and an appropriate value for the pseudo mass transfer coefficient. The use of these models will enable the effect of the solution flowrate, feed concentration, and bed height on the column performance to be predicted with some precision.

CHAPTER 8

RECOMMENDATIONS FOR FUTURE WORK

Having studied the factors required to make a consistent granular product of NaNiHCF on a laboratory scale, a method for the preparation on a larger scale should now be developed. In particular, attention should be paid to the geometry and rate of heat transfer during the freeze-thaw method, as these were vital to obtaining a high yield of granules with a size suitable for column use.

The present work has indicated significant changes in the properties of the product when the precipitates were heated in the mother liquor which were not investigated at a fundamental level. Structural analysis of the products and a detailed study of the caesium sorption mechanism would give some indications of the nature of these differences, and indicate which product may be preferred.

The models which were developed to predict the experimental breakthrough curves with particle diffusion controlling were found to provide very good fits with the range of caesium concentrations used. For column tests with significantly lower caesium feed concentrations, it is likely that film diffusion may become more significant and would therefore need to be included in the model. Using lower caesium concentrations(5 or 10 mg/L) in column tests would considerably complicate the measurement of breakthrough curves due to the much longer time periods required, and the significantly higher activity which would be loaded onto the columns.

The ability of hexacyanoferrates to selectively remove caesium over a wide range of pH is now well proven, although limited knowledge is available on the removal of other ions. There is now a great need to remove other toxic metals, such as Hg, Cd and Co, and the applicability of using hexacyanoferrates should be assessed in direct comparison with other adsorbents, such as activated carbons.

CHAPTER 9

NOMENCLATURE

a	pore radius	$\mathring{A}$
A_0	radioactive count of initial solution	counts s^{-1}
A_t	radioactive count of solution after time t	counts s^{-1}
A_{btc}	area above breakthrough curve	-
a	constant in Freundlich expression	mL g^{-1}
b	Freundlich coefficient	-
c	solution concentration	mg mL^{-1}
c_0	feed solution concentration	mg mL^{-1}
c_{te}	concentration of total effluent in column test	mg L^{-1}
d_c	diameter of column	cm
e	bed voidage	-
i	increment for step along length of bed	-
j	increment for time step	-
k	psuedo mass transfer coefficient (solid film)	h^{-1}
m	mass of exchanger	g
P	percentage removal of nuclides in batch tests	%
p	pressure	N m^{-2}
q	solid phase concentration	mg g^{-1} (dry)
q_0	solid phase concentration in equilibrium with c_o	mg g^{-1} (dry)
q^*	solid phase concentration in equilibrium with c	mg g^{-1} (dry)
Q	volumetric flowrate	mLh^{-1}
R_d	distribution coefficient in batch tests	mL g^{-1}
t	time	h
t_{end}	time at end of column test	h
u	interstitial velocity	cm h^{-1}

V	volume of solution	mL
V_{te}	volume of total effluent in column test	mL
z	distance through bed	cm
Z	length of bed	cm
ρ_p	particle density (dry mass/volume of absorber)	g cm^{-1}
σ	surface tension	N cm^{-1}
θ	contact angle	°

Dimensionless terms

x	solution concentration	$\frac{c}{c_o}$
y	solid phase concentration	$\frac{q}{q_o}$
y^*	solid phase concentration in equilibrium with x	$\frac{q^*}{q_o}$
τ	time parameter	$k\left(t - \frac{z}{u}\right)$
ξ	bed length parameter	$\frac{k\rho_p q_o z}{c_o u}\left(\frac{1-e}{e}\right)$

CHAPTER 10

REFERENCES

1. Nuclear power and fuel cycle, status and trends
   IAEA meeting, Vienna, 1988

2. World Nuclear Industry Handbook 1991
   Nuclear Engineering International

3. Marshall, W. C.
   Nuclear Technology International, 1988, 15-19

4. Cole, H. A.
   Understanding Nuclear Power, Gower Technical Press, 1988

5. Davies, L. M.
   IAEA meeting, Vienna, 1988, p55

6. Bennett, B.
   The Chemical Engineer, June 1985, 25-38

7. Duncan, A. G. and Brown, S.
   Nuclear Energy 21(3) 1982 161-166

8. Carley-Macauly, K. W.
   I. Chem. Eng. Symposium Series No.77 233-278

9. Hooper, E.W.; Phillips B.A.; Dagnall S.P.; Monckton N.P.
   AERE-R 11088 (1984)

10. Kourim, V.; Vojtech, O
    Atomic Energy Review Vol 12 No.2, 1974 pp 215-273

11. Ginniff, M. E.; Monckton, N. P.
    Nuclear Technology International, 1988 139-142

12. Jones, S. R.
Energy Production Processes, I. Chem. E. meeting
12th-14th April, 1988, London. pp 271-279

13. Cross, J. E.; Hooper, E.
Ion Exchange Conference, Cambridge, 1988. Ed. M. Streat. pp 457-467

14. Jenkins, I. L.
Hydrometallurgy, 5 1979, 1-13

15. Jenkins, I. L.
Solvent Extraction and Ion Exchange, 2(1), 1-27 (1984)

16. Howden, M.
I. Chem. E. Symposium Series No. 77

17. Howden, M.
Ion Exchange for Industry, Cambridge, 1984. Ed. M. Streat. pp 66-73
(Pub. Ellis Harwood)

18. Heathfield, W.; Howden, M.
Nuclear Technology International, 1988, 149-151

19. Kunin, R.
Ion Exchange Resins, John Wiley 2e, 1963

20. Helfferich, F.
Ion Exchange, McGraw-Hill, 1962

21. Dorfner, K.
Ion Exchangers, Properties and Applications, Ann Arbor Science Pub. Inc. 1972

22. Amphlett, C. B.
Inorganic Ion Exchangers, Elsevier Publishing Company, 1964

23. Thomson, H.S.
J. Roy. Agr. Soc. Engl. 11 (1850) 68

24. Way, J. F.
J. Roy. Agr. Soc. Engl. 11 (1850) 313; 13 (1852) 123

25. Gans R.
Jahrb. Preuss. Geol. Landesanstalt (Berlin), 26 (1905) 179

26. Calmon, C
The Chemical Engineer, November 17, 1980

27. Dyer, A.; Jemil, M.
Ion Exchange for Industry, Ed. Streat, SCI 1988, pp 494-503

28. Maroccheilli, A.; Pietrelli, L.; Casaccia, C.
Sovent Extraction and Ion Exchange 7(1), 159-172 (1989)

29. Robinson, S.; Begovich, J.; Brown, C.; Cambell, D.; Collins, D.
AIChe Symposium Series No.259 vol. 83

30. Faubel, W.; Ali, A.
Radiochimica Acta 40, 49-56 (1986)

31. Pekarek, V.; Vesely, V.
Talanta 19, 1245-1283 (1972)

32. Lowenschuss, H.
Radioactive Waste Manag. 2(4), 327-341 (1982)

33. Lee, E.F.T.
Ph.D. thesis, Imperial College, London, (1981)

34. Loos-Neskovic, C.; Federoff, M.; Garnier, E.; Gravereau, P.
Talanta 31(12), 1133-1147 (1984)

35. Vol'khin, V.V.; Zil'berman M.V.; Kolesova S.A.; Shul'ga E.A.
J. Appl. Chem. USSR 48, 52 (1975)

36. Vol'khin, V.V.
Inorganic Materials 15(6), 1086-1091 (1979)

37. Dolezal, J.; Kourim, V.
Radiochem. Radioanal. Let. 1(5), 295-303 (1969)

38. Dolezal, J.; Stejskal,; Kourim, V.
J. Radioanal Cnem. 21, 363-369 (1974)

39. Bellomo, A.; De Marco, D.; Casale, A.
Talanta 19, 1236-1240 (1972)

40. Hendrickson, W.F.; Riel, G.K.
Health Physics 28, 17-21 (1975)

41. Krylov, V.N.; Gedeonov, L.I.; Rakov, N.A.; Trofimov, A.M.
Soviet Radiochem. 15(5), 660-664 (1973)

42. Prout, W.E.; Russell E.R.; Groh, H.J.
J. Inog. Nucl. Chem. 27, 473-479 (1965)

43. Shahbandeh, R.
Ph.D. Thesis, Imperial College, London. (1980)

44. Kolesova, S.A.; Vol'khin, V.V.
Inorg. Mater. 2(6), 946-950 (1966)

45. Koshcheeva, E.A.; Vol'khin, V.V.
Russ. J. Inorg. Chem. 12(10), 1455-1457 (1967)

46. Vol'khin, V.V.; Kolesova, S.A.
Zh. Prikl. Khim. 40, 342-345 (1967)

47. Vol'khin, V.V.; Koshcheeva, E.A.
Inorg. Mater. 4(6), 803-807 (1968)

48. Vol'khin, V.V.; Shul'ga, E.A.; Zil'berman M.V.
Inorg. Chem. 7(1), 69 (1971)

49. Shul'ga, E.A.; Vol'khin, V.V.
Inorg. Mater. 7(2), 262-265 (1971)

50. Egorova, N.V.; Krylov, V.N.; Pitalev, V.G.; Stepanov, A.V.
Soviet Radiochem. 20(5), 633-639 (1978)

51. Sharygin, L.M.; Pospelov, A.A.; Chukhlantsev V.G.
Soviet. Radiochem. 7(6), 747-750 (1965)

52. Sharygin, L.M.; Pospelov, A.A.; Chakhlantsev V.G.
Soviet. Radiochem. 11(5), 550-553 (1969)

53. Roginskii, S. Z.
Soviet Radiochem. 2(4), 181-188 (1960)

54. Kawamura, F.; Motojima, K.
Nucl. Technol. 58(2), 242 (1982)

55. Baranovskii, V.N.; Viza, Y.; Katykhin, G.S.; Nikitin, M.K.;
Soviet Radiochem. 19(6), 654-656 (1967)

56. Konecny, C.; Caletka, R.
J. Radioanal. Chem. 14, 255-266 (1973)

57. Terada, K.; Hayakawa, H.; Swada, K.; Kiba, T.
Talanta 17, 955 (1970)

58. Narbutt, J.; Sivinski, J.; Bartos, B.; Bilewicz, A.
J. Rad. Nucl. Chem. 10(1), 41-49 (1986)

59. Watari, K.; Imai, K.; Izawa, M.
J. Nucl. Sci. and Technol. 6, 522 (1969)

60. Kozlova, G.A.; Vol'khin, V.V.; Zil'berman, M.V.
J. Appl. Chem. USSR 52, 1340-1342 (1979)

61. Dave, T.N.; Indusaker, V.K.
J. Chem. Tech. Biotechnol. 36, 31-37 (1986)

62. Roginskii, S.Z.; Attshuler, O.V.; Yanovskii, M.I.;Malinina, E.I.; Morokovets, A.E.
Radiokhimiya 2(4), 431-437 (1960)

63. Stejskal, J.; Soukup, J.; Dolezal, J.; Kourim, V.
J. Radioanal. Chem. 21, 371 (1974)

64. Kourim, V.; Rais, J.; Millon, B.
J. Inorg. Nucl. Chem. 26, 1111 (1964)

65. Nott, B.R.
Water Chem. and Corr. Problems in Nuclear Power Plants, Proc. Int. Symp.
IAEA-SM-264/32 Vienna (Pub. 1983)

66. Baran, V.; Caletka, R.; Tympl, M.; Urbanek, V.;
J. Radioanal. Chem. 24, 353-359 (1975)

67. Ullrich, J.; Tympl, M.; Pekarek, V.; Vesely, V.
J. Radioanal. Chem. 24, 361-368 (1975)

68. Caletka, R.; Tympl, M.
J. Radioanal. Chem. 30, 155-172 (1976)

69. Sharygin, L.M.; Galkin, V.M.; Shtin, A.P.
Inorg. Mater. 15(11), 1614 (1978)

70. Sharygin, L.M.; Moiseev, V.E.; Kuzmina, R.V.; Egorov, Y.V.;Pyshkin, V.P.;
Kurushkin, S.P.; Galkin, V.M.
Soviet Radiochem. 28(3), 326 (1987)

71. Vizachii, A.G.; Moiseev, V.E.; Sharygin, L.M.
Inorg. Mater. 22(3), 396 (1986)

72. Zouad, S.; Loos-Neskovic, C.; Federoff, M.
Int. Conf. Nucl. Fuel Reproc. & Waste Manag. Recon 87, (Aug.1987)

73. Malik, W.U.; Srivastava, S.K.; Bhandari, V.M.; Kumar, S.
J. Inorg. Nucl. Chem. 38, 342 (1976)

74. Saraswat, I.P.; Srivastava, S.K.; Sharma, A.K.
J. Coll. and Interface Sci. 84(1), 163 (1981)

75. Saraswat, I.P.; Suresh, K.; Srivastava, S.K.; Sharma, A.K.
Can. J. Chem. 57, 1214 (1979)

76. Saraswat, I.P.; Suresh, K.; Venma. S.K.; Sharma, A.K.
Can. J. Chem. 58, 2250 (1980)

77. Malik, W.U.; Srivastava, S.K.; Singh, R.P.; Kumar, S.
J. Radioanal. Chem. 36, 469 (1977)

78. Saraswat, I.P.; Srivastava, S.K.; Sharma, A.K.
J. Inorg. Nucl. Chem. 43, 1653 (1981)

79. Jain, A.K.; Agrawal, S.; Singh, R.P.
J. Radioanal. Chem. 60(1), 111 (1980)

80. Jain, A.K.; Agrawal, 8.; Singh, R.P.
Anal. Chem. 52, 1364 (1980)

81. Nagy, J.; Madi, I.
Isotopenpraxis 20(3), 101-105 (1984)

82. Lehto, J.; Harjula, R.; Wallace, J.
J. Radioanal. Nucl. Chem. Articles, 111(2), 297-304 (1987)

83. Boni, A.L.
Analyt. Chem. 38, 89 (1966)

84. Arino, H.; Kramer, H.H.
Int. J. Appl. Rad. & Isotopes 24, 197 (1973)

85. Lehto, J.; Harjula, R;
Solv. Ext. and Ion Ex. 5(2), 343 (1987)

86. Lee, E.F.T.; Streat, M.
J. Chem. Tech. & Biotechnol. 33A, 333-338 (1983)

87. Kawamura, S.; Shibata, S.; Kurotaki, K.; Takeshita, H.
Anal. Chim. Acta 102, 225-228 (1978)

88. Shahbandeh, R.; Streat, M.
J. Chem. Tech. Biotechnol. 32, 580-585 (1982)

89. Bennett, B.A.; Shahbandeh, R.; Streat, M.
J. Chem. Tech. Biotechnol. 32, 586-593 (1982)

90. Lee, E.F.T.; Streat, M.
J. Chem. Tech. Biotechnol. 33A, 80-86 (1983)

91. Lee, E.F.T.; Streat, M.
J. Chem. Tech. Biotechnol. 33A, 87-96 (1983)

92. Shul'ga, E.A.; Vol'khin, V.V.; Zolotavin, V.L.; Kalugina, N.N.
J. Appl. Chem. USSR 45, 2588 (1972)

93. Watari, K; Imai, K.; Izawa, M.
J. Nucl. Sci. Techn. 4(4), 190 (1967)

94. Jain, A.K.; Singh, R.P.; Bala, C.
J. Radioanal. Chem. 75(1-2), 85-89 (1982)

95. Ganzerli Valentini, M.T.; Stella, R.; Cola, M.
J. Radioanal. Nucl. Chem. 102(1), 99 (1986)

96. Des Ligneris, J.
These Docteur-Ingenieur, Claremont-Ferramd. (1969)

97. Pottier, F; Chauvert, P.
Coloq. Hisp.-Fr. Trat. Combust. Irradiados Quim Plutonio, 2nd (1969), 253-278 (pub.1971)

98. Kawamura, S.; Shibata, S.; Kurotaki,K.
Anal. Chim. Acta. 81, 91-97 (1976)

99. Zilber'man, M.V.; Vol'khin, V.V,; Kozlova, G.A.
Soviet Radiochem. 26(5), 559-562 (1984)

100. Loos-Neskovic, C.; Fedoroff, M;
Ann. Chim. Fr. 9, 609-624 (1984)

101. Fedoroff, M.; Loos-Neskovic, C.
Mater. Tech. Fr. 357 (1982)

102 Loos-Neskovic, C.; Fedoroff, M.
Solvent Extraction and Ion Exchange, 7(1), 131-158 (1989)

103 Loos-Neskovic, C.; Fedoroff, M.
French Patent 84-12139 (1984)

104. Qureshi, M.; Varsheny, K.G.; Israili, A.H.
J. Chromatogr. 59, 141 (1971)

105. Gill, J.S.; Tandon, S,N.
J. Inorg. Nucl. Chem. 34, 3885-3892 (1972)

106. Gill, J.S.; Tandon, S.N.
Int. J. App. Rad. and Isop. 25, 31-33 (1974)

107. Lieser, K.H.; Bastian, J.; Hecker, A.B.H.; Hild, W.
J. Inorg. Nucl. Chem. 29, 815-825 (1967)

108. Bastian, J; Lieser, K.H.
J. Inorg. Nucl. Chem. 29, 827-832 (1967)

109. Kourim, V.; Lazicek, M.; Dolezal,J;
J. Radioanal. Chem. 21, 355-362 (1974)

110. Narbutt, J.; Bilewicz, A.; Gniazdowski-Laren, E.
Water Chem. and Corr. Problems in Nuclear Power Plants, Proc. Int. Symp.
IAEA-SM-264/31, Vienna, 287 (Pub. 1983)

111. Bilewicz, A.; Narbutt, J.
Isotopenpraxis 20(4), 141-142 (1984)

112. Caletka, R.; Konecny, C.
J. Radioanal. Chem. 30, 119-129 (1976)

113 Krylov, V. N.
Radiokhimiya vol. 30 No.5 (1988) 644-649

114. Ganzerli Valentini, M.T.; Meloni, S.; Maxia, V.
J. Inorg. Chem. 34, 1427 (1972)

115. Cola, M; Ganzerli Valentini, M.T.
Inorg. Nucl. Chem. Letters 8, 5 (1972)

116. Ganzzerli Valentini, M.T.; Maxia, V.; Meloni, S.; Rolier, M.A.
Gazzetta Chemica Italiana, 103, 205 (1973)

117. Vlasselaer, S.; D'Olieslager, W.; D'hont, M.
J. Inorg. Nucl. Chem. 38, 327-330 (1976)

118. Vlasselaer, S.; D'Olieslager, W.; D'hont, M.
J. Radioanal. Chem. 35, 211-222 (1977)

119. Kourim, V.; Rais, J.; Stejskal, J.
J. Inorg. Nucl. Chem. 26, 1761-1764 (1964)

120. Kawamura, S.; Kurotaki, K.; Izawa, M.
Bull. Chem. Soc. Jap. 42, 3003 (1969)

121. Gill, J.S.; Tandon, S.N.
J. Radioanal. Chem. 13, 391 (1973)

122. Kawamura, S.; Shibata, S.; Kurotaki, K.
Anal. Chim. Acta. 56, 405 (1971)

123. Sharygin, L.M.; Moiseev, V.E.; Galkin, V.M.; Kuzmina, R.V.; Pyshkin, V.P.; Boguslavskii, V.B.; Gutorova, T.I. Soviet Radiochem. 26(5), 575 (1984)

124. Smyth, M.
Industrial Chemistry Division, UKAEA, Harwell - Private communication,

125. Knight
The Freezing of supercooled liquids, Van Nostrand, 1967

126. Dorsey, N.E.
Trans. Am. Phil. Soc., 38, 301 (1948)

127. Wollhöver, K.; Körber, Ch.; Scheiwe, M.W.; Hartmann, U.
Int. J. Heat and Mass Transfer vol. 28, no.4 pp 761-769 (1985)

128. Grange, B. W.; Viskanta, R.; Stevenson, W. H.
Int. J. Heat and Mass Transfer vol. 19 pp 373-384 (1976)

129. Kingery, W.D.; Goodnow, W.H.
Ice and Snow Properties, Processes and applications, Conf, MIT Feb 12-16, 1962, ed. W.D. Kinge, MIT Press 1963

130. Vogel, V. A,
Macro and Semimicro Qualitative Inorganic Analysis
4th Ed. Longmans (1965)

131. Brunauer, S.; Emmett, P.H.; Teller, E.
J. Am. Chem Soc. 60, 309 (1938)

132. Gregg, S. J. and Sing, K. S. W.
Adsorption, surface area and porosity, 2e, Academic Press (1982)

133. Smith, J.M.
Chemical Engineering Kinetics, 3e McGraw Hill (1981)

134. Ritter, H. L.; Drake, L. C.
Ind. Eng. Chem., Anal. Ed. 17, 787 (1945)

135. Ruthven, D.M.
Principles of Adsorption and Adsorption Processes, Wiley, New York (1984)

136. Vermeulen, T.
Advances in Chemical Engineering 2(1958) 147, Separation by Adsorption methods

137. Brunauer, S; Emmett, P.H.; Deming, W. E.; Teller, E.
J. Am. Chem Soc. 62, 1723 (1940)

138. Freundlich, H.
Colloid and Capilliary Chemistry, Methuen 1926

139. Kobble, R. A.; Corringan, T. E.
Ind. Eng. Chem. 44, 383 (1952)

140. Sipps, R.
J. Chem. Phys. 18, 1024 (1950)

141. Vermeulen, T.
Ind. Eng. Chem. 45 1664 (1953)

142 Neskovic-Loos, C.; Fedoroff, M. and Revel, G.
J. Radioanal. Chem. 30 533-545 (1976)

143. Phillips, B.; Hooper, E.W.; Dagnall, S.P.; Monkton, N.P.
Study of the behaviour of Inorganic Ion Exchangers in the Treatement of MA Wastes
Part 1. AERE - G2872, DoE/RW/84.153

144. Helfferich, F.
Ion Exchange Kinetics; Ion Exchange - A Series of Advances. Ed. Marinsky, J. A.
Edward Arnold Ltd. (1966)

145. Vermeulen, T.; Douglas LeVan M.; Hiester, N. K.; Klein, M. S.
Chemical Engineers' Handbook, Section 16 Adsorption and Ion Exchange,
6e McGraw-Hill, ed Perry, R.H. and Green D. W. (1984)

146. Do, D. D.; Rice, R.G.
Chem Eng. Sci. 42 No. 10 2269-2284 (1987)

147. Hall, K. R.; Eagleton, L. C.; Acrivos, A.; Vermuelen, T.
Ind. Eng. Chem. Fund. 5 No. 2, 212-223 (1966)

148. Glueckauf E.; Coates J.E.
J. Chem. Soc. 1315 (1947)

149. Glueckauf, E.
Trans. Faraday Soc. 51, 1540 (1955)

150 Cooper, R.S.
Ind. Eng. Chem. Fund. 4 308 (1965)

151. Kyte, W.S.
Chem. Eng. Sci. 28 1853-1856, (1973)

152. Yoshida, H.; Ruthven, D.M.
Chem. Eng. Sci. 38 (6) 877-884 (1983)

153 Battrum, M.; Thomas, W. J.
Trans. I. Chem. E. vol 69, part A, 119-129 (1991)

154 Chiang, A. S. T.; Hwang, G. W.
Computers Chem. Engng. vol. 13, No. 3 pp 281-290 (1989)

155 Sowerby, B.; Crittenden, B. D.
Trans. I. Chem. E. vol 69, part A, 3-13 (1991)

156. Yoshida, H.; Kataoka, T.; Ruthven, D.M.;
Chem. Eng. Sci. 39(10) 1489-1497 (1984)

157. Yoshida, H.; Kataoka, T.; Ruthven, D.M.;
Chem. Eng. Sci. 43 (7) 1647-1655 (1988)

Appendix A

Listing of BBC Basic program for controlled frezzer unit

```
10    REM TEMPERATURE CONTROL FOR 4 CHANNEL FREEZER UNIT
20    REM ********************************************
30    REM PROGRAMME WRITTEN BY DAVID JACOBI
40    REM ********************************************
50    REM EXPLANATIONS OF SYMBOLS
60    REM BOOLD=OLD TEMPERATURE VALUE
70    REM DIFA =DIFFERENTIAL CONSTANT
80    REM INFA =INTEGRAL CONSTANT
90    REM PROCTIME=CALCULATION OF SAMPLING INTERVAL
100   REM PROCPID=CALCULATION OF PID FEED BACK
110   REM PF = PROPORTIONAL CONSTANT
120   REM Q = PRESENT TEMP-DESIRED TEMP
130   REM RATE= 0-255 AMOUNT OF POWER APPLIED
140   REM SLOPE IS THE FIRST RATE OF TEMP DECREASE
150   REM TAD=PRESENT TEMPERATURE
160   REM TEM DESIRED TEMPERATURE
170   REM TDIFA=DIFFERENTIAL CONSTANT DIV.BY TIME INTERVAL
180   REM TIM=SAMPLING TIME INTERVAL
190   REM TIMA=TIM/100 TO MAKE IT IN SEC
200   REM TINFA=INTEGAL CONSTANT DIV. BY TIME INTERVAL
210   REM TINT= INTEGRAL FEEDBACK FACTOR
220   REM TITA=TIME ON THE PLATO
230   REM TOLD=TIME AT THE END OF THE SLOPE
240   REM ****************************
250   REM DEFINITION OF ARRAYS
260   REM ****************************
270   REM
280   DIM SLOPE(4),TINT(4),TAM(4),SLOP(4),TIMC
290   DIM YS(4),TEM(4),LANG(4),MC(4),MM
300   DIM Q(4),DIFF(4),RATE(4),PROP(4),TAD
310   DIM W(4),X(4),Y(4)
320   REM ****************************
330   REM CALIBRATION OF TEMP SENSORS
340   REM ****************************
350   MM(1)=5.49E-4:MC(1)=-5.1
360   MM(2)=5.49E-4:MC(2)=0.2
370   MM(3)=5.49E-4:MC(3)=0.0
380   MM(4)=5.49E-4:MC(4)=-1.7
390   REM ****************************
400   REM SETTING INITIAL VALUES
410   REM ****************************
420   NTIM=O
430   UD=O
440   TA=O:N=O:BOOLD=O
450   FOR C=1 TO 4
460   SLOPE(C)=O:TINT(C)=O:TAM(C)=O:TIMC(C)=O
470   NEXT C
480   TITA=O
490   ZEIT=O
500   REM HEATERS INITIALLY SWITCHED OFF
510   ?&FCC0=0
520   ?&FCC1=0
530   ?&FCC2=0
540   ?&FCC3=0
550   REM ****************************
```

```
560     REM INPUT CONTROL SETTINGS
570     REM ****************************
580     CLS
590     INPUT"HOW MANY CHANNELS ?"NOC
600     REM ****************************
610     MODE 4
620     FOR C=1 TO NOC
630     PRINT TAB(10,11)"PRESS FOR CHAN"C
640     PRINT TAB(10,13)"1=NO SLOPE"
650     PRINT TAB(10,15)"2=ONE SLOPE"
660     PRINT TAB(10,17)"3=TWO SLOPES"
670     PRINT TAB(10,19)"4 FOR INSTRUCTIONS"
680     PRINT TAB(10,6) "CONTROLLED FREEZER UNIT"
690     PRINT TAB(10,7) "**********************"
700     PRINT TAB(15,26)"-----------------"
710     INPUT K: IF K=1 THEN PROCVAZO
720     IF K=2 THEN PROCVLAZO
730     IF UD>O THEN GOTO 820
740     NEXT C
750     INPUT"CHANNEL TO BE PLOTTED"PC
760     CLS
770     REM INPUT CONTROLLER SETTINGS
780     PROCINCON
790     ******************************
800     REM BEGIN TEMPERATURE CONTROL
810     ******************************
820     PROCOTO
830     REM ****************************
840     REM DEFINE PROCVAZO
850     REM INPUT CONSTANT SET TEMPERATURE
860     REM ****************************
870     DEF PROCVAZO
880     CLS
890     YS(C)=O
900     PRINT "FOR CHAN",C
910     INPUT"ENTER TEMPERATURE "TEM(C)
920     TEM(C)=ABS(TEM(C))
930     CLS
940     ENDPROC
950     REM ****************************
960     REM DEFINE PROCVLAZO
970     REM INPUT TEMPERATURES WITH SLOPE
980     REM ****************************
990     DEF PROCVLAZO
1000    CLS
1010    YS(C)=1
1020    INPUT"INITIAL TEMPERATURE?"TAM(C)
1030    INPUT"DESIRED TEMPERATURE? "TEM(C)
1040    TAM(C)=ABS(TAM(C))
1050    TEM(C)=ABS(TEM(C))
1060    INPUT "RATE OF CHANGE IN DEG.C./HR?"SLOPE(C)
1070    SLOP(C)=SLOPE(C)/3600
1080    REM IF ADVAL(1)=0 THEN GOTO 850
1090    CLS
1100    ENDPROC
1110    REM ****************************
1120    REM DEFINE PROCINCON
1130    REM INPUT CONTROLLER SETTINGS
1140    REM PROP, DIFF AND INT TIMES
1150    REM ****************************
1160    DEF PROCINCON
```

```
1170    INPUT "PROPORTIONAL FACTOR? "PF
1180    INPUT "DIFFERENTIAL FACTOR? "DIFA
1190    INPUT "INTEGRAL FACTOR?    "INFA
1200    TIM=100
1210    TINFA=INFA/TIM
1220    TDIFA=DIFA/TIM
1230    IF UD>O THEN GOTO 1270
1240    CLS
1250    ENDPROC
1260    REM*****************************
1270    DEF PROCOTO
1280    REM MAIN LOOP SUBROUTINE
1290    REM CALL ROUTINES FOR CLOCK, CONTROL AND UPDATING SCREEN
1300    REM ***************************
1310    TA=0
1320    TIME=0
1330    CLS
1340    PROCDRAW
1350    PROCTIME
1360    FOR C=1 TO NOC
1370    PROCMOTO
1380    PROCMETA
1390    IF C=PC THEN PROCPLOT
1400    PROCUPDATE
1410    IF INKEY(-82)THEN PROCCHANGE
1420    NEXT C
1430    IF N>1300 THEN GOTO 1340
1440    GOTO 1350
1450    ENDPROC
1460    REM ***************************
1470    DEF PROCTIME
1480    REM SETS TIME INDEPENDENTLY FOR EACH CHANNEL
1490    REM ***************************
1500    TIM=200
1510    NTIM=2/3600
1520    TA=TIM+TA
1530    IF TIME>TA GOTO 1550
1540    GOTO 1530
1550    FOR D=1 TO NOC
1560    TIMC(D)=TIMC(D)+NTIM
1570    NEXT D
1580    ENDPROC
1590    REM *************************
1600    DEF PROCMOTO
1610    REM READS MEASURED TEMPS AND SETS HEATER OUTPUTS USING PID CONTROL.
1620    REM *************************
1630    TAD(C)=ADVAL(C)
1640    TAD(C)=MM(C)*TAD(C)+MC(C)
1650    IF YS(C)=0 THEN GOTO 1690
1660    TAM(C)=TAM(C)+SLOP(C)
1670    Q(C)=TAD(C)-TAM(C)
1680    GOTO 1700
1690    Q(C)=TAD(C)-TEM(C)
1700    PROP(C)=Q(C)*PF
1710    TINT(C)=(PROP(C)/TINFA)+TINT(C)
1720    IF TINT(C)>5O THEN TINT(C)=50
1730    IF TINT(C)<-50 THEN TINT(C)=-50
1740    BOOLD=PROP(C)
1750    DIFF(C)=(BOOLD-TAB(C))*PF*TDIFA
1760    RATE(C)=INT(TINT(C)+DIFF(C)+PROP(C))
1770    IF RATE(C)<0 THEN RATE(C)=0
```

```
1780    IF RATE(C)>200 THEN RATE(C)=200
1790    ?&FCC0=RATE(l)
1800    ?&FCC1=RATE(2)
1810    ?&FCC2=RATE(3)
1820    ?&FCC3=RATE(4)
1830    ENDPROC
1840    REM ***************************
1850    DEF PROCMETA
1860    REM CHECK TEMPS FOR END OF SLOPE
1870    REM ***************************
1880    IF ABS(TAM(C))>ABS(TEM(C)) THEN YS(C)=0
1890    ENDPROC
1900    REM ***************************
1910    DEF PROCUPDATE
1920    REM UPDATES OUTPUT TO SCREEN
1910    DEF PROCUPDATE
1920    REM UPDATES OUTPUT TO SCREEN
1930    REM ***************************
1940    VDU 23,1,0;0;0;0;
1950    @%=&20106
1960    FOR U=1 TO 4
1970    W(U)=5
1980    X(U)=ll
1990    Y(U)=17
2000    IF TAD(U)>9.95 THEN GOTO 2030
2010    W(U)=6
2020    PRINT TAB(5,(U+2)) " "
2030     IF TEM(U)>9.95 THEN GOTO 2060
2040    X(U)=12
2050    PRINT TAB(ll,(U+2))" "
2060    IF TAM(U)>9.95 THEN GOTO 2090
2070    Y(U)=18
2080    PRINT TAB(17,(U+2))" "
2090    NEXT U
2100    PRINT TAB(1,1)"CH. MTEM   TEM   TAM    TIME (HOURS)"
2110    PRINT TAB(2,3)"1";TAB(W(1),3)TAD(1);TAB(X(1),3)TEM(1);TAB(Y(1),3)TAM(1)
2120    PRINT TAB(2,4)"2";TAB(W(2),4)TAD(2);TAB(X(2),4)TEM(2);TAB(Y(2),4)TAM(2)
2130    PRINT TAB(2,5)"3";TAB(W(3),5)TAD(3);TAB(x(3),5)TEM(3);TAB(Y(3),5)TAM(3)
2140    PRINT TAB(2,6)"4";TAB(W(4),6)TAD(4);TAB(X(4),6)TEM(4);TAB(Y(4),6)TAM(4)
2150    @%=&20206
2160    PRINT TAB(23,3)INT(TIMC(1))
2170    PRINT TAB(23,4)TIMC
2180    PRINT TAB(23,5)TIM
2200    @%=&00001
2210    PRINT TAB(24,8) "FOR CHANNEL ",INT(PC)
2220    @%=&00005
2230    PRINT TAB(24,10)"RATE = "(INT(RATE(PC)))
2240    PRINT TAB(24,11)"PRO  = "(INT(PROP(PC)))
2250    PRINT TAB(24,12)"INT  = "(INT(TINT(PC)))
2260    PRINT TAB(24,13)"DIF  = "(INT(DIFF(PC)))
2270    ENDPROC
2280    REM ***************************
2290    DEF PROCDRAW
2300    REM DRAWS AXIS FOR PLOT
2310    REM ***************************
2320    N=0
2330    MOVE 2,5
2340    DRAW 2,800
2350    MOVE 2,500
2360    DRAW 1500,500
2370    PRINT TAB(4,29)"TO CHANGE SETTINGS OR STOP PRESS  S"
```

```
2380    MOVE 2,500
2390    ENDPROC
2400    REM ****************************
2410    DEF PROCPLOT
2420    REM PLOTS ERROR FROM SET TEMPS
2430    REM ****************************
2440    N=N+1
2450    M=250
2460    IF Q(PC)<1 THEN M=150
2470    Z=Q(PC)*M+500
2480    DRAW N,Z
2490    IF N>1300 THEN CLS
2500    ENDPROC
2510    REM ****************************
2520    DEF PROCCHANGE
2530    REM ALLOWS CHANGE IN SETTINGS
2540    ?&FCC0=0
2550    ?&FCC1=0
2560    ?&FCC2=0
2570    ?&FCC3=0
2580    VDU 23,1,1;0;0;0;
2590    PRINT TAB(2,24)"ENTER -"
2600    PRINT TAB(4,26)"1 TO SET NEW TEMP                "
2610    PRINT TAB(4,27)"2 TO SET CONTROL PARAMETERS      "
2620    PRINT TAB(4,28)"3 TO PLOT DIFFERENT CHAN.        "
2630    PRINT TAB(4,29)"4 TO STOP                        "
2640    INPUT UD
2650    IF UD=4 THEN END
2660    IF UD=3 THEN GOTO 2760
2670    IF UD=2 THEN PROCINCON
2680    IF UD=1 THEN GOTO 2700
2690    GOTO 2640
2700    CLS
2710    PRINT TAB(2,25)"ENTER CHANNEL NUMBER             "
2720    INPUT C
2730    TIMC(C)=0
2740    CLS
2750    GOTO 630
2760    INPUT"ENTER CHAN, NO."PC
2770    GOTO 1270
2780    ENDPROC
```

Appendix B

Listing of Fortran program 'FREUND'

```
C     PROGRAM TO PREDICT COLUMN PERFORMANCE OF NANIHCF
C     PARTICLE FILM CONTROL WITH LINEAR DRIVING FORCE AND FREUNDLICH ISOTHERM
C     ASSUMED UNIFORM VELOCITY PROFILE, NO DISPERSION AND ISOTHERMAL
C
      PROGRAM FREUND
      REAL H,K,L
      CHARACTER SAMP*25,KTYPE*9
      DIMENSION X(300),Y(300),X1(300),Y1(300),X1OLD(300),Y1OLD(300)
      EXTERNAL FUN
      PI=3.14159
 5    PRINT *,' ENTER NCOL., H(CM), D(CM), Q(ML/H), E'
      READ *,NCOL,L,D,Q,E
      PRINT *,' ENTER SAMPLE,CO(MG/L), QO(MG/G), ROP(G/ML),'
      READ *,SAMP,CO,QO,ROP
C
C     ENTER K AND B, RERUN OPTION REPEATS FROM HERE WITH ABOVE COL. PARAMS.
C
 6    PRINT *,' ENTER MASS TRANSFER COEF., AND FREUDLICH COEF.,B'
      READ *,K,B
C
C     CALCULATE BED VOLUME, INTERSTIAL VEL. AND BED PARAM. AT L
C
      BV=PI*D*D*L/4
      U=Q*4/(PI*D*D*E)
      XI=ROP*QO*K*L*(1-E)/(CO*E*U)
C
C     ENTER LENGTH AND TIME INCREMENTS, AND TIME FOR INTERGRATION
C
      PRINT *,' ENTER N, TIME STEP AND PRINT INT. AND FINAL TIME(HRS)'
      READ *,N,DT,PRINT,TEND
      PRINT *,' ENTER OUTPUT FILE NUMBER AND NODE TO BE PRINTED'
      READ *,NOUT,NOD
      DTAU=K*DT
      DXI=XI/(N-1)
C
C     SET INITIAL CONDITIONS
C
      DO 8 I=1,N
      X(I)=0.001
      Y(I)=0.001
 8    CONTINUE
      X(1)=1.0
      PRNEX=0-(DT/2)
      T=0
      TAU=K*(0-(L/U))
      VOL=0
      NIT=0
      NSTEP=1
C
C     PRINT OUT HEADINGS
C
      WRITE(NOUT,500) NCOL,SAMP
      WRITE(NOUT,510) L,D,BV,E
      WRITE(NOUT,520) CO,QO,ROP,Q
      WRITE(NOUT,530) K
```

```
      WRITE(NOUT,535) B
      WRITE(NOUT,540) N,DT
      WRITE(NOUT,550)
500   FORMAT(/,' COLUMN NO. ',I3,' SAMPLE ',A)
510   FORMAT(/,'      H (CM)   D (CM)    B V (ML)    E',/1X,4F10.2)
520   FORMAT(/,'    CO (MG/ML)  QO (MG/G)   ROP (G/ML)  Q (ML/H)',/,1X,4F10.2)
530   FORMAT(/,' MASS TRANSFER COEFFICIENT ',F6.3,' H-1')
535   FORMAT('FREUNDLICH COEFFICIENT         ',F6.3)
540   FORMAT(,' FOR INTEGRATION  N = ',I3,'  DT = ',F6.4,//)
550   FORMAT(/' NIT   TIME(H)  TAU   VOL (BV)   XO    YO    X     Y',/)
C
C     PRINT OUT CURRENT TIME LINE
C
 10   IF(T.LT.PRNEX) GOTO 11
      WRITE(NOUT,570) NIT,T,TAU,VOL,X(1),Y(1),X(NOD),Y(NOD)
      WRITE(6,570) NIT,T,TAU,VOL,X(1),X(NOD),Y(NOD)
570   FORMAT(1X,I3,F7.1,F7.2,F7.1,4X,4F6.3)
      PRNEX=PRNEX+PRINT
C
C     CALCULATE VALUES OVER NEW TIME STEP X1,Y1 FROM PRESENT VALUES X,Y'
C
 11   NIT=0
C     INITIAL GUESS FOR NEW TIME LINE
C     IF(NSTEP.GT.1)GOTO 13
C     DO 12 I=1,N
C
C     X1(I)=0.5
 12   Y1(I)=0.5
C     X1(1)=1
C     NSTEP=2
C     GOTO15
      DO 14 I=1,N
      X1(I)=X(I)
 14   Y1(I)=Y(I)
C
C     NEW ITERATION FOR X1 AND Y1
C
 15   ERR=0.
      NIT=NIT+1
C     SAVE VALUES OF X1 AND Y1 FROM PREVIOUS ITERATION
      DO 16  I=1,N
      X1OLD(I)=X1(I)
 16   Y1OLD(I)=Y1(I)
C
C     CALCULATE VALUES OF X1(I+1) = X(I+1,J+1,K+1)
C
      DO 32 I=1,(N-1)
      NEND=I+1
      FUNO=FUN(X1(I),Y1(I),B)
      FUN1=FUN(X1(I+1),Y1(I+1),B)
      X1(I+1)=X1(I)-(DXI*(FUNO+FUN1)/2)
 32   IF(X1(I+1).LT.1E-4) GOTO 33
 33   CONTINUE
C
C     CALCULATE VALUES OF Y1(I) =Y(I,J+1,K+1)
C
      DO 34 I=1,NEND
      FUNO=FUN(X1(I),Y1(I),B)
      FUN1=FUN(X(I),Y(I),B)
      Y1(I)=Y(I)+(DTAU*0.5*(FUNO+FUN1))
 34   CONTINUE
```

```
      IF(N.EQ.NEND) GOTO 38
      DO 36 I=NEND,N
      X1(I)=0.001
      Y1(I)=0.001
 36   CONTINUE
 38   DO 40 I=1,(NEND-1)
      EX=X1OLD(I)-X1(I)
      EY=Y1OLD(I)-Y1(I)
      ERR=ERR+ABS(EX)+ABS(EY)
 40   CONTINUE
      IF(ERR.LT.1E-3) GOTO 50
      IF(NIT.GT.50) GOTO 450
      GOTO 15
C     CONVERGENCE ACHIEVED
 50   CONTINUE
C     SET VALUES OF X AND Y FOR NEW TIME STEP
      DO 55 I=1,N
      X(I)=X1(I)
      Y(I)=Y1(I)
 55   CONTINUE
      TAU=TAU+DTAU
      T=T+DT
      VOL=T*Q/BV
      IF(T.GT.TEND) GOTO 200
      GOTO 10
200   PRINT *,' TO CONTINUE ENTER NEW TIME, ELSE 0'
      READ *,TEND1
      IF(TEND1.LT..1) GOTO 460
      TEND=TEND1
400   GOTO 10
450   PRINT *,' NO. ITERARATIONS EXCEEDED'
460   PRINT *,' TO RERUN ENTER 1, NEW RUN 2, STOP 0'
      READ *,NRUN
      IF(NRUN.EQ.1) GOTO 6
      IF(NRUN.EQ.2) GOTO 5
      END
      FUNCTION FUN(X,Y,B)
      REAL X,Y
      IF(X.LT.1E-10) GOTO 800
      FUN=(X**B)-Y
      RETURN
700   FUN=500
      RETURN
800   FUN=0
      RETURN
      END
```

Appendix C

Paper

Jacobi, D. L. and Streat, M.

Sorption of caesium by sodium nickel hexacyanoferrate(II): column performance and prediction of breakthrough curves.

I. Chem. E. Sym. Series No. 119 (Extraction '90) 107-118, 1990

SORPTION OF CAESIUM BY SODIUM NICKEL HEXACYANOFERRATE(II): COLUMN PERFORMANCE AND PREDICTION OF BREAKTHROUGH CURVES

D.L.Jacobi* and M.Streat**

The column performance of sodium nickel hexacyanoferrate(II) (NaNiHCF) for the removal of caesium from aqueous solution was investigated. Experimental breakthrough curves were determined using prepared samples of NaNiHCF in small glass columns with continuous analysis of the effluent solution. The adsorption isotherm was also determined experimentally and found to be extremely favourable, fitting a Freundlich type expression.
The experimental breakthrough curves were fitted to a mathematical model which was solved numerically using the Freundlich isotherm and also analytically when the isotherm was assumed to be rectangular. It was found that both models allowed a good fit of the experimental data and therefore enabled the effect of flowrate, bed height and caesium concentration on the breakthrough volume to be predicted with some precision.

INTRODUCTION

The use of complex hexacyanoferrates (HCFs) for the removal of caesium from radioactive waste streams is now a well established procedure in the nuclear industry. These complexes are highly selective for caesium ions in high salt content solutions and possess excellent thermal and radiation stability. A wide variety of HCFs have been prepared using different transition metals as reviewed by Lowenschuss (1), Hooper *et al.* (2) and Loos-Neskovic *et al.* (3). In general HCFs are made by mixing a salt of the transition metal with a ferrocyanide solution to give a finely divided precipitate which has to be granulated for packed column use. In the above reviews, the nickel complex in particular is noted for its exceptionally high affinity for caesium in comparison to other transition metals such as copper, cobalt, zinc and manganese.

The column performance of sodium nickel hexacyanoferrate(II) for the removal of caesium from aqueous solution, using samples prepared at Imperial College, is described in this paper. The adsorption isotherm was determined from a series of batch tests and experimental breakthrough curves obtained using small glass columns.

The curves were fitted to a mathematical model which involved the solution of the material balance and kinetic equations. A comparison was made between the numerical solution obtained using a Freundlich type isotherm and the analytical solution which is possible when the isotherm is assumed to be rectangular.

* British Gas, LRS, Michael Road, Fulham SW6 2AD

** Department of Chemical Engineering, Loughborough University of Technology, Leicestershire, LE11 3TU

EXPERIMENTAL METHODS

Preparation of Materials

Samples of NaNiHCF in a granular form were prepared by the authors at Imperial College using a freeze-thaw method which was based on earlier work by Vol'khin *et al.* (4,5). $NiSO_4$ and $Na_4Fe(CN)_6$ were mixed with a ratio of Ni:Fe = 1.3 to give a finely divided precipitate which was then washed. By freezing and thawing the precipitate under controlled conditions a granular material was formed which could be easily filtered. The product was then dried and the fraction with a particle size of 250-420 microns was used in the column tests.

Column Performance

The sorption of caesium in a packed bed of NaNiHCF was investigated using the experimental rig shown in Fig. 1. In each test 1 or 2 g of the exchanger was placed in a glass column of 1 cm diameter where it was supported by a sintered glass filter. The adsorber was gently fluidised by back washing with 1 M $NaNO_3$ which served to remove trapped air bubbles and also to fully wet the adsorber.

Feed solutions were prepared using 500 or 1000 ppm caesium as inactive $CsNO_3$ in 1M $NaNO_3$. Tracer caesium-134 (γ emitter - 0.605 MeV) was used which allowed efficient and convenient analysis of caesium in the samples by gamma scintillation counting. It was calculated that the tracer caesium concentration in the solutions was negligible. A constant speed peristaltic pump was used for the feed which was found to give a constant flow over the long operating periods that were required.

From an initial calculation based on the batch capacity of the adsorber and the concentration of caesium in the feed, an estimate was made of the volume of feed required and the time taken to reach breakthrough. With the flowrates used (0.075 and 0.21 $m^3\ m^{-2}h^{-1}$) it was found that periods in excess of 24 hours would be required. In order to run the tests over these long periods a method of automatically counting the column effluent was designed as shown in Fig.2. The effluent was passed through a coil which was attached to an intrinsic germanium detector that was connected to a Canberra Series 35 multichannel analyser (MCA). The analyser was programmed to repeatedly count the effluent over a fixed period of time and provide a printout of the data.

In order to obtain an accurate count of the feed solution, the sample coil was filled through an empty column. To check for the build up of caesium on the surface of the sample coil or the carrying over of fines, independent samples of the feed and column effluent were collected in phials and counted separately to check the ratio of the caesium concentrations.

Calculation of Working Capacity

The working capacity q_o(mg/g), of the adsorber was calculated as the average caesium loading per dry mass of the adsorber at the end of a column test. The capacity was calculated from the area above the breakthrough curve, and was also checked by mass balance from the caesium concentration and total volume of the column effluent.

Determination of Adsorption Isotherm from Batch Tests

The adsorption isotherm for NaNiHCF was determined in a series of batch contact tests. In each test a known mass of the adsorber was contacted with a volume of feed solution. The samples were shaken over a period of 72 hours which was assumed sufficient for equilibrium to be reached. The caesium concentration of the solution (c) was determined by counting and the solid phase concentration (q*) determined by mass balance. The solid phase concentrations were expressed as mg Cs per g of dry mass of exchanger.

Determination of bed voidage

The voidage of the packed bed was measured directly using 1 g of the adsorber which was wetted and then loaded as a slurry into a small glass column which had a sintered glass bottom. The bed was allowed to settle and then the solution level was lowered carefully to that of the adsorber. The column was centrifuged to remove the interstitial solution and the value of the bed voidage (e) calculated from the weight of fluid removed.

PREDICTION OF COLUMN PERFORMANCE

The prediction of the onset of breakthrough and the shape of the breakthrough curve are of fundamental importance in the design and scale-up of an adsorption column. A considerable amount of literature is available on the prediction of the breakthrough curves and the effect of different mass transfer mechanisms and equilibrium relationships. An extensive review of the different cases is given by Ruthven (6). In general, a solution of the mass and heat balances, coupled with an adsorption rate expression, is required to obtain the breakthrough curve.

For the sorption of trace quantities, it can be assumed that the column is isothermal and the breakthrough curve can be obtained by the simultaneous solution of a differential mass balance and a sorption rate equation. Assuming plug flow through the column and that there is negligible axial dispersion, the usual form of the differential mass balance is given by:-

$$u\frac{\partial c}{\partial z} + \frac{\partial c}{\partial t} + \left(\frac{1-e}{e}\right)\rho_p\frac{\partial q}{\partial t} = 0 \qquad (1)$$

The form of the sorption rate equation and definition of a suitable mass transfer coefficient are dependent on the mechanism of mass transfer and a representative driving force. From kinetic tests carried out by the authors (7), it is proposed that the sorption of caesium by NaNiHCF is controlled by particle diffusion within the range of conditions used. Using a pseudo mass transfer coefficient, k, and applying the Glueckauf and Coates (8) approximation of a linear driving force across a solid film, the rate of sorption may be represented by :-

$$\frac{\partial q}{\partial t} = k(q^* - q) \qquad (2)$$

The value of k is a function of the particle diameter, diffusivity and a correction factor for the linear driving force. The value of q*, the solid phase concentration in equilibrium is obtained from the isotherm which, for the sorption of caesium by NaNiHCF, was found to be a Freundlich type expression:-

$$q^* = a\,c^b \qquad (3)$$

A limitation of using a Freundlich expression is that the isotherm is open ended, with no account being made for the saturation of the adsorber. This may be avoided by restricting the expression to a specified concentration range and expressing the isotherm in dimensionless form:-

$$y^* = x^b \tag{4}$$

Equations (1) and (2) may also be transformed into dimensionless form by defining the usual time and bed parameters as follows:-

$$\frac{\partial x}{\partial \xi} + \frac{\partial y}{\partial \tau} = 0 \tag{5}$$

$$\frac{\partial y}{\partial \tau} = (y^* - y) \tag{6}$$

For an initially unreacted bed, to which a feed of concentration c_o is introduced at a time $t = 0$, the initial and boundary conditions are:-

$$I.C. \quad t=0: \quad \tau = -k\frac{z}{u} \quad x = y = 0 \quad all \quad z$$

$$B.C. \quad t>0: \quad x = 1 \quad at \quad z = 0$$

The solution of equations (4), (5) and (6) requires a numerical solution due to the non-linearity of the Freundlich equation. An implicit finite difference method was used in the present work, which was based on the algorithm described by Kyte (9).

The non-linearity may be removed, if the isotherm is extremely favourable by assuming that the adsorption is irreversible, which would be described by a rectangular isotherm (i.e. b=0). Equation (4) may then be replaced by:-

$$y^* = 0 \quad for \quad x = 0$$

$$y^* = 1 \quad for \quad x > 0 \tag{7}$$

The applicability of using a rectangular isotherm to represent a favourable ion exchange system has been discussed by Vermeulen (10). Prediction of the breakthrough curve is obtained by an analytical solution of equations (5), (6) and (7) which was developed by Cooper (11). The solution falls into three cases:-

$1 + \tau < \xi$	$y = x = 0$	*(unreacted bed)*
$\xi < 1$	$y = 1 - e^{-\tau} \quad x = 1 - \xi e^{-\tau}$	*(initial formation of pattern)*
$1 < \xi < 1 + \tau$	$y = x = 1 - e^{\xi - \tau - 1}$	*(constant pattern)*

More recently, Ruthven and Yoshida (12-14) have used this analytical solution and have compared the form of this solution with that obtained for the case of liquid film controlling. The use of the analytical solution allows the model to be fitted directly to the experimental breakthrough curve, and also leads to a greater understanding of the shape of the curve. The accuracy of the numerical method was also checked with the analytical solution at the limit of $b = 0$.

RESULTS

The experimentally determined isotherm for sorption of caesium from 1 M $NaNO_3$ onto NaNiHCF is shown in dimensionless form in Fig. 3. The isotherm was fitted with a Freundlich type expression, $y = x^{0.248}$ which was valid for concentrations at which the adsorber was not saturated.

The experimental details of two of the column tests carried out are listed in Table 1.

The differences between the two tests are the solution flowrate and packed bed height. The experimental breakthrough curves are shown in Figs. 4 and 6 with the fitted analytical solutions and also in Figs. 5 and 7 with fitted numerical solutions. In these breakthrough curves the dimensionless solution concentration at the column exit is plotted against the number of void bed volumes of solution passed through the column.

In order to fit the models to the experimental curves, the working capacity of the adsorber was first calculated as described above. A value for the pseudo mass transfer coefficient was initially obtained by directly fitting the analytical model and then this value varied slightly to achieve the best fit with the numerical model. The values of q_o and k which were used in the solutions are listed in Table 2.

DISCUSSION

The general shape of the breakthrough curves obtained from the experimental column tests was good, with no caesium detected in the effluent up to the breakthrough point which was characterised by a sharp rise in the caesium concentration. The effect of the solution flowrate and bed height is clearly seen, with the breakthrough point occurring after about 100 bed volumes in Test A and only after about 250 bed volumes in Test B. The general shape of the breakthrough curve is also much sharper in the case of Test B, which may account for the slight increase in the working capacity.

The plots of the breakthrough curves shown in Fig 4 - 7 show that, in general, both the numerical solution with the Freundlich isotherm and the analytical solution with assumed rectangular isotherm provide adequate fits of the experimental data. The values of the pseudo mass transfer coefficients that were used were higher in Test A when the flowrate was higher, and in both tests a slightly lower value was used for the rectangular isotherm.

The accuracy of the models needs to be assessed by consideration of the fit along the shape of the curve and also by the occurrence of breakthrough. It is observed that both models seem to predict the shape of the curves adequately although it is found that with the use of the Freundlich isotherm the occurrence of breakthrough is more accurately predicted. It is generally not clear if the slightly premature breakthrough observed is due to the form of the isotherm or to axial dispersion. Axial dispersion was not taken into account in the models. A change in the mass transfer mechanism at low caesium concentrations may also occur and this could affect the occurrence of breakthrough.

CONCLUSIONS

It has been shown that the use of NaNiHCF in a packed column is very effective for the selective sorption of caesium from salt solutions. The adsorption was found to be very favourable and can be fitted with a Freundlich type expression.

The experimental breakthrough curves show that no caesium was detected in the effluent up to the breakthrough point, which was observed by a sharp rise in the caesium concentration.

The curves were fitted to a model which assumed that the sorption was controlled by a linear driving force across a solid film. The model was solved numerically using the Freundlich isotherm, and also by an analytical solution using an assumed rectangular isotherm.

It was found that both models could be fitted to the experimental data using the measured parameters and an appropriate value for the pseudo mass transfer coefficient. The use of these models will enable the effect of the solution flowrate, feed concentration, and bed height on the column performance to be predicted with some precision.

SYMBOLS USED

a	=	constant in Freundlich expression (ml/g)
b	=	Freundlich coefficient
c	=	solution concentration (mg/ml)
c_o	=	feed solution concentration (mg/ml)
k	=	mass transfer coefficient (solid film) (h^{-1})
q	=	solid phase concentration (mg/g[dry])
q_o	=	solid phase concentration in equilibrium with c_o (mg/g[dry])
q*	=	solid phase concentration in equilibrium with c (mg/g[dry])
u	=	interstitial velocity (cm/h)
z	=	distance through bed (cm)
e	=	bed voidage
ρ_p	=	particle density (dry mass/volume of adsorber) (g/cm^3)

Dimensionless terms

x	=	solution concentration (c/c_o)
y	=	solid phase concentration (q/qo)

y^* = solid phase concentration in equilibrium with x (q^*/q_o)

τ = time parameter $\left[k\left(t-\frac{z}{u}\right)\right]$

ξ = bed length parameter $\left[\frac{k\rho_p q_o z}{c_o u}\left(\frac{1-e}{e}\right)\right]$

REFERENCES

1. Lowenschuss, H., 1982, Radioactive Waste Management, 9(4), 327-341
2. Hooper, E.W., Phillips, B.A., Dagnall, S.P., Monkton, N.P., 1984, AERE-R11088
3. Loos-Neskovic, C., Federoff, M., Garnier, E., Gravereau, P., 1984, Talanta, 31(12), 1133-1147
4. Vol'khin, V.V., Kolesova, S.A., 1967, Zh. Prikl. Khim., 40, 342-345
5. Vol'kin, V.V., Koshcheeva, E.A., 1968, Inorganic Materials, 4(6), 803-807
6. Ruthven, D.M., 1984, Principles of Adsorption and Adsorption Processes, Wiley, New York
7. Jacobi, D.L., Unpublished work.
8. Glueckauf, E., Coates, J.E., 1947, J. Chem. Soc., 1315
9. Kyte, W.S., 1973, Chem. Eng. Sci., 28, 1853-1856
10. Vermeulen, T., 1953, Ind. Eng. Chem., 45, 1664
11. Cooper, R.S., 1965, Ind. Eng. Fund., 4, 308
12. Yoshida, H., Ruthven, D.M., 1983, Chem. Eng. Sci., 38(6), 877-884
13. Yoshida, H., Kataoka, T., Ruthven, D.M., Chem. Eng. Sci., 39(10), 1489-1497
14. Yoshida, H., Kataoka, T. Ruthven, D.M., 1988, Chem. Eng. Sci., 43(7), 1647-1655

ACKNOWLEDGEMENT

One of us (DLJ) wishes to acknowledge the award of a research studentship from the UKAEA. The work described in this paper was carried out as part of a research contract with the UKAEA, Harwell Laboratory, and was sponsored by the Department of the Environment.

TABLE 1 - Experimental Details of Column Tests

	A	B	
Column height	1.8	3.4	cm
Column diameter	1.0	1.0	cm
Bed voidage	0.42	0.42	-
Feed caesium concentration	1.0	1.0	mg/ml
Flowrate	16.8	5.9	ml/h
Mass of adsorber	1.0	2.0	g(dry)
Particle density of adsorber	1.22	1.29	g(dry)/ml
Bed volume (void)	0.59	1.12	ml

TABLE 2 - Parameters used to fit Models

	A	B	
Working capacity of adsorber			
From area above curve	160	174	mgCs/g(dry)
From bulk effluent	165	172	mgCs/g(dry)
Fitted values of pseudo mass transfer coefficient			
Analytical solution	0.20	0.127	h^{-1}
Numerical solution	0.24	0.15	h^{-1}

Figure 1. Column Test Rig

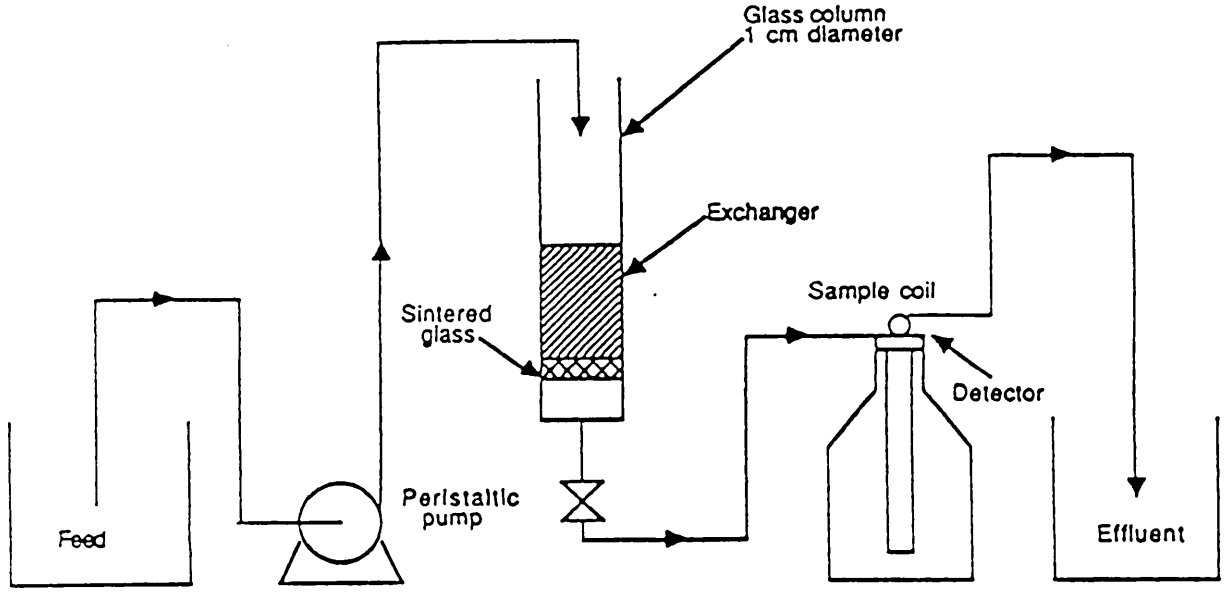


Figure 2. Arrangement of Counting Equipment for Column Tests

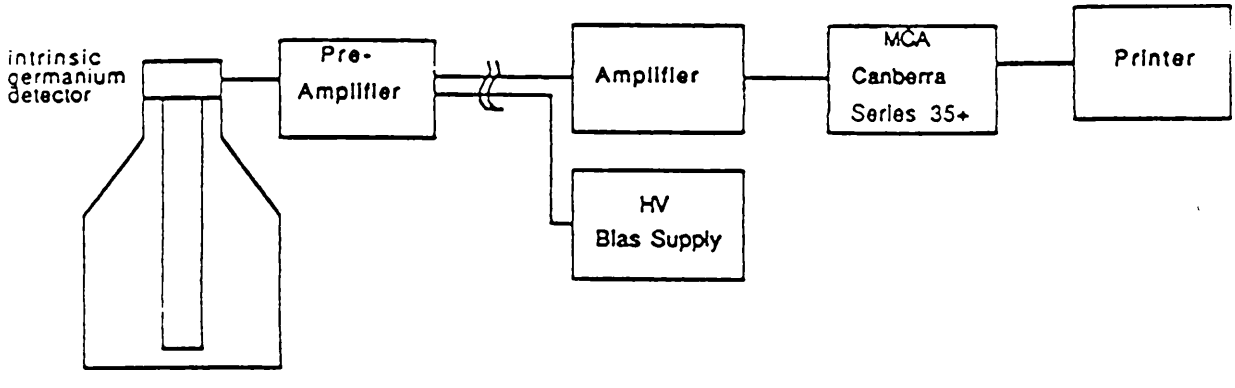
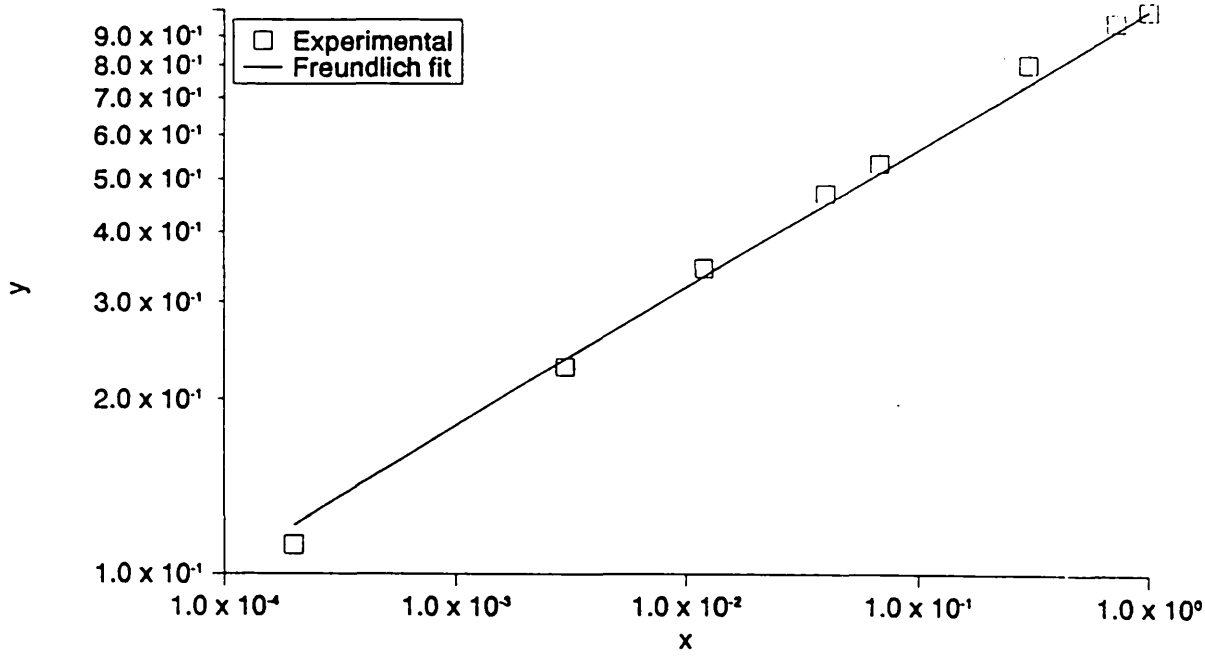
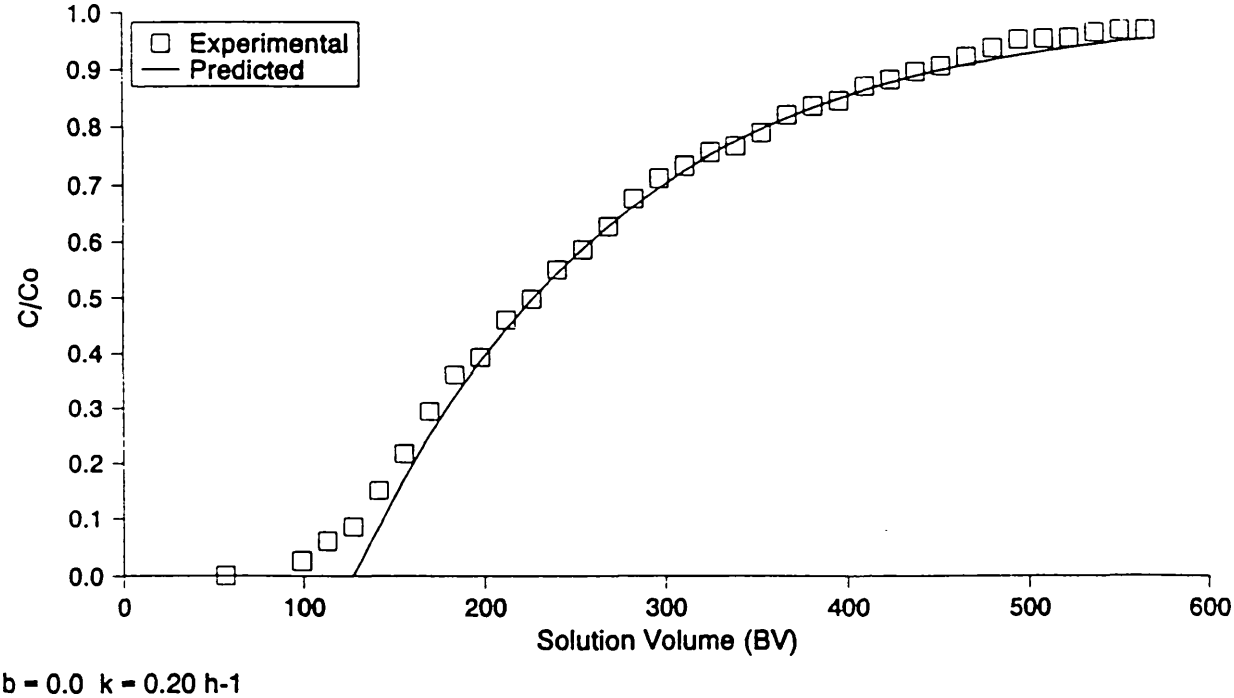


Figure 3. Adsorption Isotherm for NaNiHCF



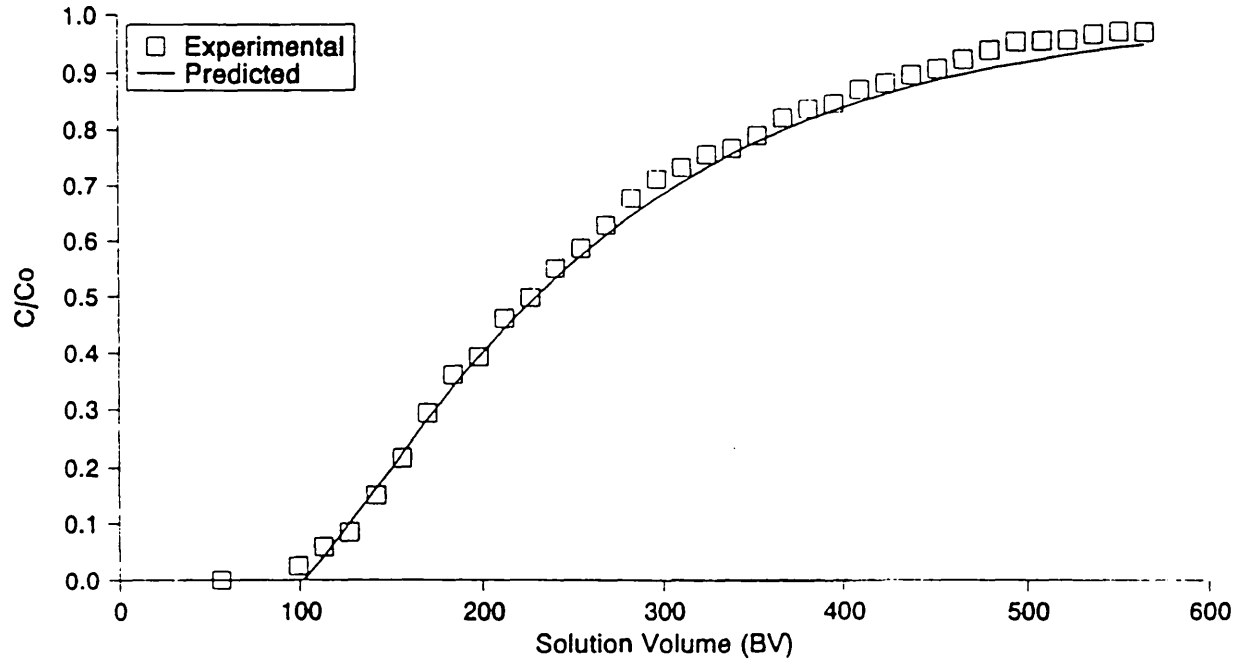
Freundlich fit with b=0.248

Figure 4. Breakthrough curve for Test A Fitted with Analytical Solution



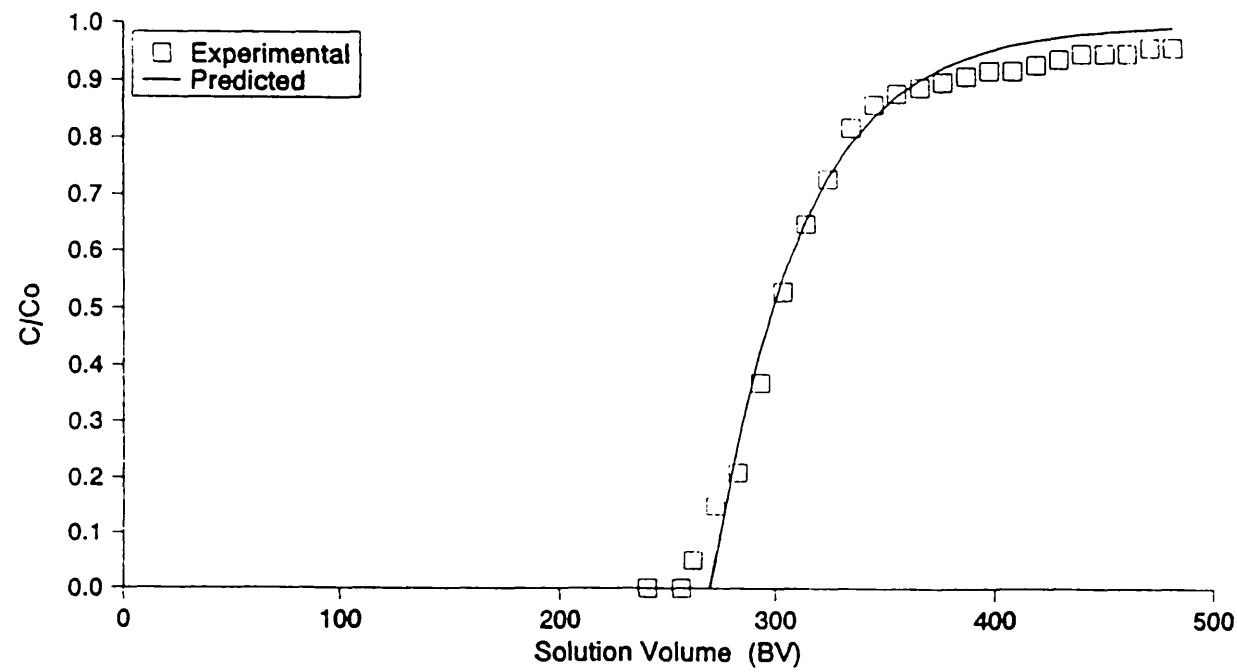
b = 0.0 k = 0.20 h-1

Figure 5. Breakthrough Curve for Test A
Fitted with Numerical solution



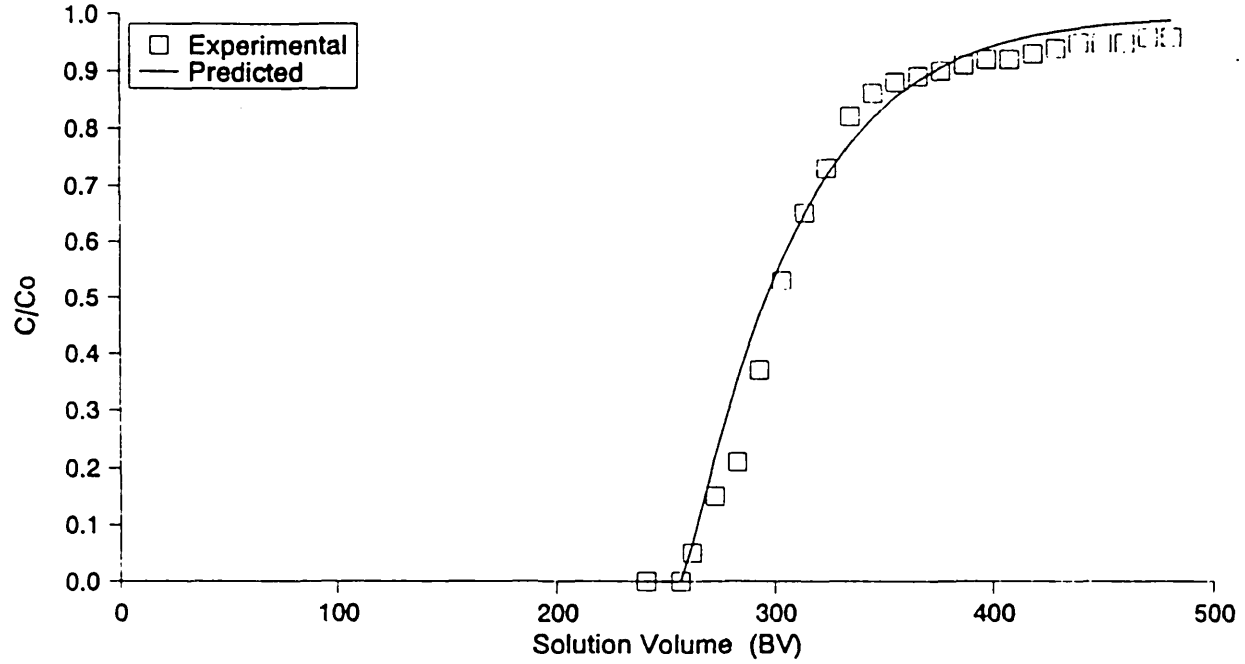
b = 0.248 k = 0.24 h-1

Figure 6. Breakthrough Curve for Test B
Fitted with Analytical Solution



b = 0.0 k = 0.127 h-1

Figure 7. Breakthrough Curve for Test B
Fitted with Numerical Solution



b = 0.248 k = 0.15 h-1